EVALUATION AND IMPROVEMENT OF LIQUID PROPELLANT ROCKET CHUGGING ANALYSIS TECHNIQUES: FINAL REPORT PART II

A STUDY OF LOW FREQUENCY COMBUSTION INSTABILITY IN ROCKET ENGINE PREBURNERS USING A HETEROGENEOUS STIRRED TANK REACTOR MODEL

PREPARED BY

Timothy A. Bartrand

and presented as a thesis for the Master of Science Degree
The University of Tennessee, Knoxville
August, 1987

Work supported by NASA GRANT NAG8-542
Principal Investigator: Paul E. George, II

EVALUATION AND IMPROVEMENT OF LIQUID PROPELLANT ROCKET CHUGGING ANALYSIS TECHNIQUES: FINAL REPORT PART II

A STUDY OF LOW FREQUENCY COMBUSTION INSTABILITY IN ROCKET ENGINE PREBURNERS USING A HETEROGENEOUS STIRRED TANK REACTOR MODEL

PREPARED BY

Timothy A. Bartrand

and presented as a thesis for the Master of Science Degree
The University of Tennessee, Knoxville
August, 1987

Work supported by NASA GRANT NAG8-542
Principal Investigator: Paul E. George, II

ACKNOWLEDGEMENTS

I gratefully acknowledge the help that my advisor, Dr. P.E. George, has given me in research and the preparation of this thesis. His insights and the time he has spent helping me are greatly appreciated.

I also thank NASA, Marshall Space Flight Center, Huntsville, AL, for funding this research and Dave Seymour, of Marshal Space Flight Center, for the information he provided me on the space shuttle main engine shutdown.

ABSTRACT

During the shutdown of the space shuttle main engine, oxygen flow is shut off from the fuel preburner and helium is used to push the residual oxygen (between the oxidizer valve and the preburner combustion chamber) into the combustion chamber. During this process a low frequency combustion instability, or chug, occurs. This chug has resulted in damage to the engine's augmented spark igniter due to backflow of the contents of the preburner combustion chamber into the oxidizer feed system.

To determine possible causes and fixes for the chug, the fuel preburner was modelled as a heterogeneous stirred tank combustion chamber, a variable mass flow rate oxidizer feed system, a constant mass flow rate fuel feed system and an exit turbine. Within the combustion chamber gases were assumed perfectly mixed. To account for liquid in the combustion chamber, a uniform droplet distribution was assumed to exist in the chamber, with the mean droplet diameter determined from an empirical relation. A computer program was written to integrate the resulting differential equations.

Because chamber contents were assumed perfectly mixed, the fuel preburner model erroneously predicted that combustion would not take place during shutdown. The combustion rate model was modified to assume that all liquid oxygen that vaporized instantaneously combusted with fuel. Using this combustion model, the effect of engine parameters on chamber pressure oscillations during the SSME shutdown was calculated. These studies showed that decreasing the

pressure downstream of the preburner's exit turbine, decreasing the fuel temperature, increasing the helium temperature and decreasing the length of the line connecting the helium storage tank to the helium check valve all had adverse effects on engine stability.

TABLE OF CONTENTS

LIST OF TABLES

LIST OF FIGURES

LIST OF ABBREVIATIONS AND SYMBOLS

ABBREVIATIONS

CS : Control Surface

CV : Control Volume

FPOV : Fuel Preburner Oxidizer Valve

LOX : Liquid Oxygen

SSME : Space Shuttle Main Engine

STR : Stirred Tank Reactor

TSTR : Transient Stirred Tank Reactor

VARIABLES

A : Area (m^2)

a_1, a_2, a_3 : Constants (dimensionless)

b : Constant (dimensionless)

C : Reaction Rate Coefficient (dimensionless)

c^* : Characteristic Propellant Velocity (m/s)

c_{dm} : Constant for finding mean droplet diameter (dimensionless)

c_{ftp} : Constant for finding mass flow rate through the exit turbine (dimensionless)

c_p : Molar Specific Heat at Constant Pressure (J/kgmole·K)

D : Diameter (m)

E : Total Energy (Joules)

F : Force (N)

F_f : The Force on a Pipe due to Friction (N)

f : Constant Used to Find F_f (m^{-1})

ΔH : Latent Heat of Vaporization (Joules)

h : Molar Enthalpy (J/kgmole)

k : Thermal Conductivity (W/m·K)

L : Pipe Length (m)

L^* : Characteristic Combustion Chamber Length (m)

l : Length (m)

M : Molecular Weight (kg/kgmole)

M_g : Mass of Product Gases in the Combustion Chamber (kg)

$\dot{m}$: Mass Flow Rate (kg/s)

N_j : Constant Exponent in a Reaction Rate Expression (dimensionless)

NN : Number of Nodes in the Oxidizer Feed System

NP : Number of Pipes in the Oxidizer Feed System

NRXN : Number of Elementary Chemical Reactions

NS : Number of Species in the Combustion Chamber

NSTRM : Number of Inlet Streams to the Combustion Chamber

n : Unit Vector

O/F : Ratio of the Oxidier and Fuel Mass Flow Rates (dimensionless)

P : Pressure (Pa)

ΔP : Pressure Drop from the Storage Tank to the Combustion Chamber (Pa)

PHG : Hot Gas Pressure (Downstream of the Preburner Turbine) (Pa)

$\dot{Q}$: Heat Transfer Rate out of the Combustion Chamber (J/s)

q : Volumetric Flow Rate (m^3/s)

R : Gas Constant (J/kg·K)

R_g : Universal Gas Constant (J/kgmole·K)

Re : Reynolds Number (dimensionless)

r : Radius (m)

T : Temperature (K)

ΔT : Temperature Difference Between a Droplet and the Surrounding Gases (K)

t : Time (sec)

u : Molar Internal Energy (J/kgmole)

V : Volume (m^3)

v : Velocity (m/s)

α : Burning Rate Parameter, $c_p \Delta T/\Delta H$ (dimensionless)

β : Density of Liquid in the Combustion Chamber (kg/m^3)

ε_{ss} : Convergence Criterion (kgmoles/kg)

Γ_i : Volumetric Rate of Production of Species i ($kgmoles/m^3 \cdot s$)

Γ_j : Volumetric Rate of Elementary Reaction j ($kgmoles/m^3 \cdot s$)

Θ : Combustion Time Delay (sec)

Θ_g : Insensitive Combustion Time Delay (sec)

Θ_m : Mixing Time (sec)

Θ_v : Vaporization Time (sec)

λ_n, ω_n : Eigenvalues

μ_g : Viscosity of the Gases In the Combustion Chamber (N·s/m)

ϕ : Droplet Age in the Combustion Chamber (sec)

ρ : Density (kg/m^3)

σ : Mole Number (kgmoles/kg)

τ : Sensitive Time Lag (sec)

Ω : Vaporization Rate (kg/s)

ω_v : Vaporization Rate per Droplet (kg/s/droplet)

SUBSCRIPTS

b : Burned

c : Combustion Chamber

e : Exit Flow

f : Fuel

i : Species i, Inlet Flow

j : Reaction j, Stream j

k : Pipe Node k

m : Mixing

o,ox : Oxidizer

t : Tank

v : Volumetric

1 : Upstream

2 : Downstream

SUPERSCRIPTS

' : Forward Reaction

" : Reverse Reaction

* : Inlet

CHAPTER I

INTRODUCTION

For start-up and normal operation, the Space Shuttle Main Engine (SSME) fuel preburner maintains stable operation. During shutdown, however, both in ground test firings and actual use, the fuel and oxidizer preburners frequently undergo low frequency combustion instability, or chug. The chug is manifest as pressure oscillations in the preburners and their feed systems. These oscillations have resulted in undesirable turbopump bearing loads and have damaged the augmented spark igniter oxidizer supply piping due to backflow of fuel and oxidizer from the preburner combustion chamber into the feed system. This study is concerned with modelling the SSME fuel preburner and predicting its behavior during chug.

Following is an overview of the SSME and fuel preburner, an account of the engine shutdown process and a description of the model to be used.

1.1 THE SSME AND FUEL PREBURNER

Figure 1.1 shows a schematic of the SSME. Liquid hydrogen, stored at 19 K (34°R) and 0.21 MPa (30 psia), and liquid oxygen, stored at 90 K (164°R) and 0.69 MPa (100 psia), are the engine's propellants. Both the hydrogen and the oxygen enter the engine via low pressure pumps. These raise the pressure of the propellants to prevent cavitation in the subsequent pumps. After leaving the low

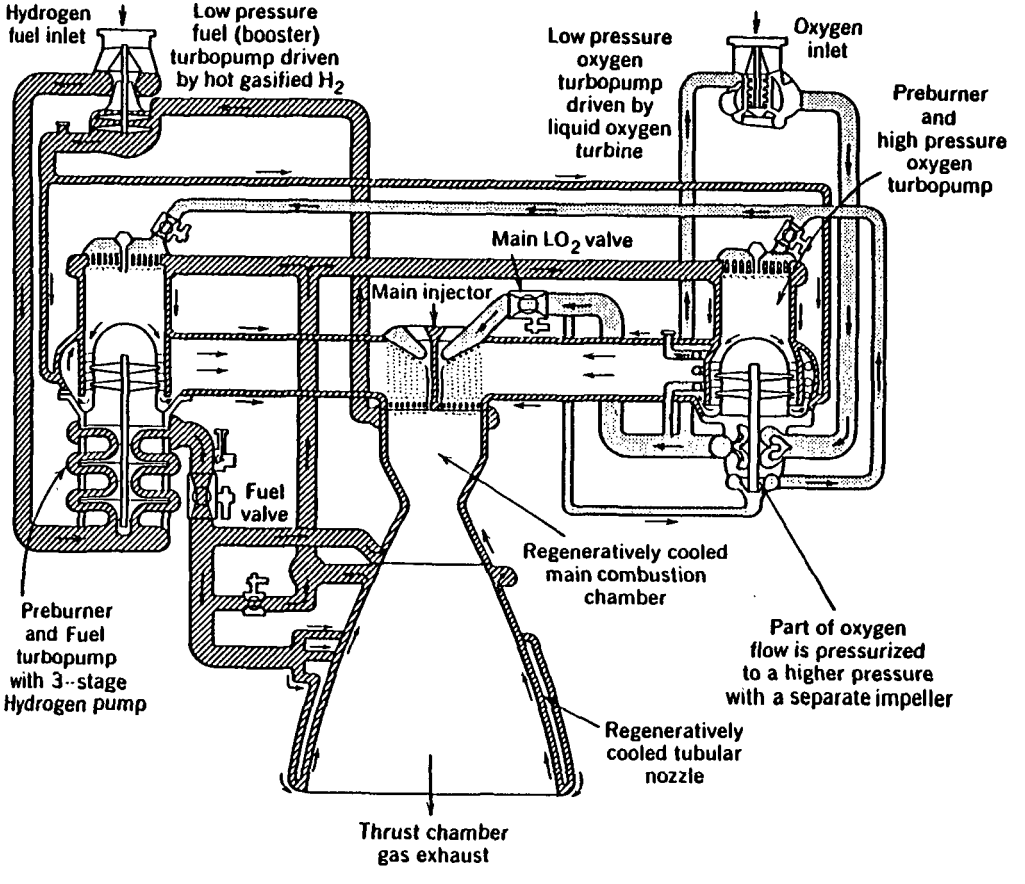

Figure 1.1: Space Shuttle Main Engine Propellant Flow Schematic
(From Sutton, 1986)

pressure pumps, the hydrogen and oxygen are pumped to high pressures by the turbopumps driven by the exit flow of the fuel and oxidizer preburners. At full power level the hydrogen leaves the fuel turbopump at 48.25 MPa (7000 psia) and the oxidizer leaves the oxidizer turbopump at 30.33 MPa (4400 psia).

Most of the oxygen (86% at full power level) flows directly to the main combustion chamber. The remainder flows to the two preburners. Upon leaving the high pressure pump, 76% (at full power level) of the hydrogen flows directly to the preburners. The remainder flows through the engine, cooling the preburner combustion chambers, the main combustion chamber and the nozzle.

The oxidizer and fuel preburners serve two purposes in the SSME: to drive the turbines which supply power to the high pressure pumps and to preheat the hydrogen for combustion in the main combustion chamber. At full power level, the fuel preburner operates at around 1090 K (1960°R) and 39.01 MPa (5660 psia) and the oxidizer preburner operates at around 830 K (1500°R) and 38.60 MPa (5600 psia). During the fuel preburner chug, the pressure in the fuel preburner varies around 4.48 MPa (650 psia). Actual average chamber temperature data is not available, but the Marshall Space Flight Center SSME transient model predicts mean temperatures between 440 K and 800 K (800°R and 1400°R) during the chug.

Injection of liquid oxygen and supercritical hydrogen into the fuel preburner is accomplished by means of 264 coaxial injectors. To cool the plate, hydrogen also is injected through small orifices

across the face plate. At full power level, just before injection, the hydrogen is at about 160 K (284°R) and 43.08 MPa (6250 psia) and the oxygen is at about 120 K (214°R) and 48.4 MPa (7020 psia).

At full power level, the fuel preburner operates at an equivalence ratio ((fuel/oxidizer)/(fuel/oxidizer)$_{stoichiometric}$) of about 8. Mass flow rates of hydrogen and oxygen into the fuel preburner are 36.4 kg/s (80 lb/s) and 37.7 kg/s (83 lb/s), respectively. Hot gases from the preburners exit the preburner combustion chambers through turbines and enters the main combustion chamber via the hot gas manifold and the main injection plate. In the main combustion chamber the products from the two preburners are burned with oxygen. The equivalence ratio in the main combustion chamber is about 1.33.

1.2 SSME SHUTDOWN AND THE FUEL PREBURNER CHUG

When the SSME shuts down, it is important that combustion ceases in the preburners and that oxidation does not begin in the feed system, so a helium purge is used to push oxygen from the feed system and preburners and assure that the system is above the rich limits of combustion of hydrogen with oxygen. It is during the helium purge that the fuel preburner chug takes place. Figure 1.2 shows the fuel preburner manifold. The helium purge orifice is a small pipe that links the helium supply piping to the pipes that reach the helium check valves. The helium check valves restrain the

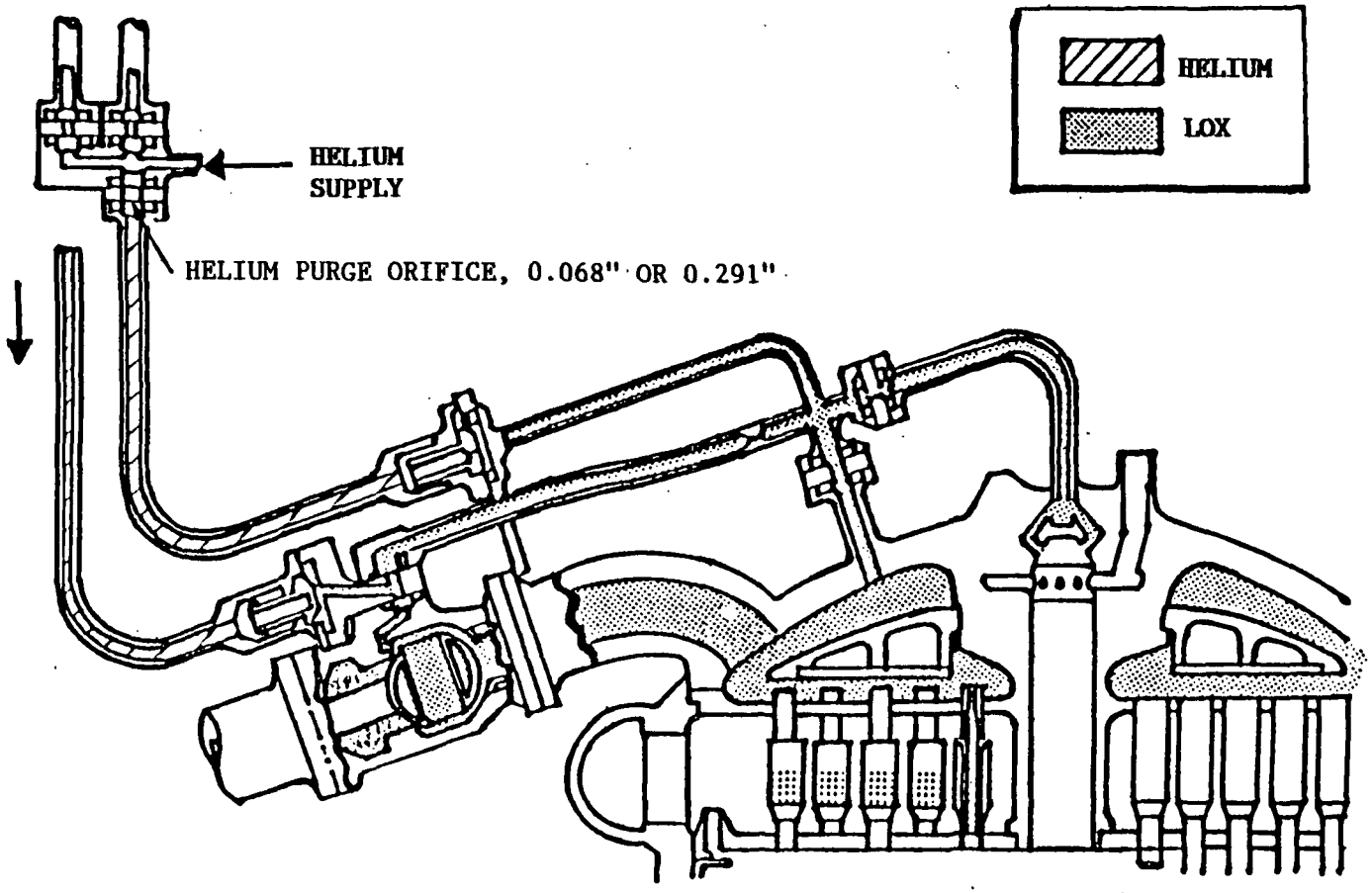

Figure 1.2: Fuel Preburner Manifold and Feed System Schematic
(From Rockwell International Corp., Rocketdyne Div.)

helium until the pressure downstream of the valves drops below 5.17 MPa (750 psia).

Shutdown is accomplished and controlled by the closing of the oxidizer preburner oxidizer valve, the fuel preburner oxidizer valve, the main oxidizer valve and the main fuel valve and the opening of the helium purge check valves. Table 1.1 (adapted from George, 1984) gives the valve sequence and the resulting events during the SSME shutdown. Two points should be noted from Table 1.1. First, before chugging begins in the fuelside preburner, both the fuelside preburner oxidizer valve and the main oxidizer valve are closed; the fuelside preburner is isolated from the oxidizer feed system. Second, no valve openings or closings coincide with the onset or ending of chug. These points are further discussed in Chapter II.

When the fuelside preburner chug begins is dependent on the power level from which the engine is cut off and the diameter of the helium purge orifice. Pressure traces for typical fuelside preburner chugs for SSME test firings are found in Figure 1.3. These traces are plots of the deviation of the chamber pressure from the mean chamber pressure versus time. The traces were filtered to show only frequencies between 50 and 200 Hz. Figure 1.3 (a) is a pressure trace for a small helium purge orifice diameter (0.17 cm [0.068 inches]) and Figure 1.3 (b) is a trace for a large helium purge orifice diameter (0.74 cm [0.291 inches]). Using the small helium purge orifice resulted in a short chug whose amplitude is about 2.89

Table 1.1: Sequence of Events During the SSME Shutdown

TIME AFTER CUTOFF (SEC)	EVENT
1.4	OXIDIZER PREBURNER OXIDIZER VALVE SEALS CLOSE OXIDIZER PREBURNER PRESSURE DROPS SMOOTHLY FROM 800 PSIA TO 500 PSIA
1.8	HELIUM CHECK VALVES OPEN, PUSHING OXIDIZER FROM THE OXIDIZER PREBURNER MANIFOLD INTO COMBUSTION CHAMBER OXIDIZER PREBURNER CHAMBER PRESSURE RISES TO 750 PSIA AND STABILIZES. HELIUM FLOW SUBSIDES AFTER THE INITIAL SPIKE
2.2	FUEL PREBURNER OXIDIZER VALVE SEALS CLOSE HELIUM FLOW RATE IMMEDIATELY RISES MAIN OXIDIZER VALVE CLOSES (AFTER THE FUEL PREBURNER OXIDIZER VALVE)
2.3	HELIUM FLOW STABILIZES, AS DO THE FUEL PREBURNER AND OXIDIZER PREBURNER CHAMBER PRESSURES FOR THE SMALL ORIFICE TESTS HELIUM FLOW RATE CONTINUES TO INCREASE FOR THE LARGE ORIFICE TESTS
2.3 - 2.5	CHUGGING BEGINS IN THE FUELSIDE PREBURNER; LARGE AMPLITUDE FOR THE LARGE ORIFICE AND SMALL AMPLITUDE FOR THE SMALL ORIFICE LOW LEVEL CHUGGING MAY ALSO BEGIN IN THE OXIDIZER PREBURNER
2.5	LARGE AMPLITUDE CHUG BEGINS FOR THE SMALL HELIUM PURGE ORIFICE TESTS A TEMPORARY REDUCTION IN THE AMPLITUDE OF THE THE FUELSIDE PREBURNER CHUG OCCURS DURING THE LARGE ORIFICE TESTS
3.0	CHUGGING ENDS
3.7	THE MAIN FUEL VALVE CLOSES

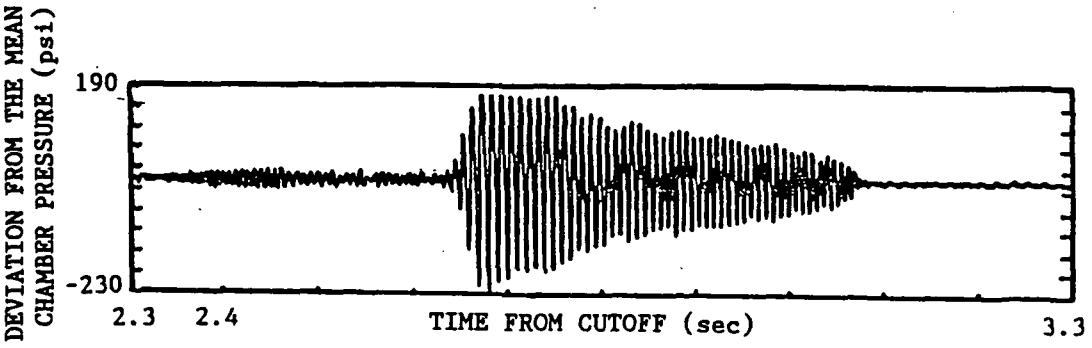

(a) Helium Purge Orifice = 0.068"

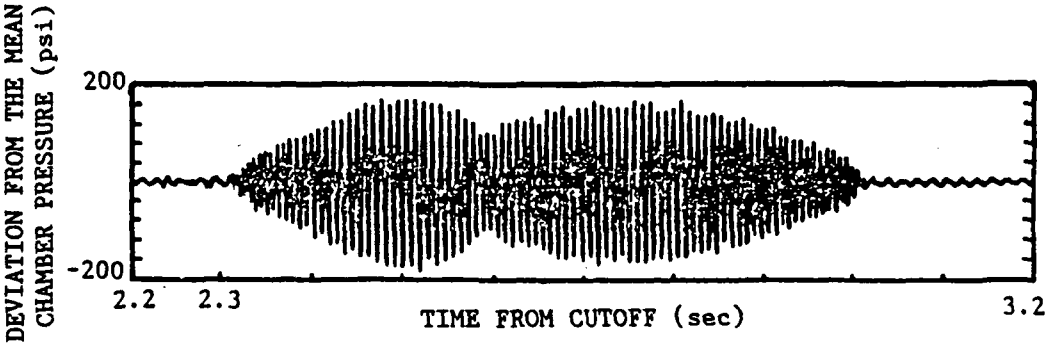

(b) Helium Purge Orifice = 0.291"

Figure 1.3: Pressure Traces for the SSME Fuel Preburner Chug (From George, 1984)

(Pressure Traces Were Filtered to Show Only Frequencies Between 50 and 200 Hz)

MPa (420 psi). Using the large orifice resulted in a longer but less severe chug. About three seconds after cutoff the chug ends and the chamber pressure and temperature decrease smoothly. The main fuel valve closes after the purge is complete.

Because the chug takes place after the fuel preburner and its piping are isolated from the oxidizer feed system and before the main fuel valve is closed, George (1984) concluded that the chug was not directly related to or triggered by valve openings and closings and that it was associated with the oxidizer purge process. As helium replaces oxygen in the oxidizer feed system, the fluid in the pipes becomes more compressible and propellant feed rates to the preburners become more sensitive to chamber pressure. This effect is described in greater detail in Chapter II.

1.3 MODELLING THE SSME FUEL PREBURNER AND FEED SYSTEM

Because of high mass flow rates, very reactive propellants, high chamber pressure and the fact that combustion takes place on many diffusion flames surrounding droplets throughout the combustion chamber, combustion in a liquid propellant rocket engine can be considered to take place homogeneously through the combustion chamber (Summerfield, 1951). Consequently, the present study modelled the fuelside preburner combustion chamber as a stirred tank reactor; contents are considered well mixed and properties are considered uniform throughout the chamber. Liquid droplets were distributed evenly through the combustion chamber and all had the

same characteristic diameter. The heterogeneous stirred tank reactor is more fully described in Chapter III.

The governing equations for the combustion chamber were derived from the conservation of mass applied to the liquid in the combustion chamber, the conservation of mass applied to the gases in the combustion chamber, the conservation of species, the conservation of energy and the perfect gas law. Auxiliary relations used to obtain terms in the governing equations included empirical expressions for average droplet diameter, droplet evaporation rate, thermodynamic properties for the gases in the combustion chamber and elementary reaction rates. Exhaust mass flow rate from the preburner was given as a function of the ratio of the pressure downstream of the exit turbine to the combustion chamber pressure. At each time, combustion chamber pressure, temperature, density (excluding liquid mass, which is assumed to occupy negligible volume), liquid density (kg of liquid per unit volume of the combustion chamber) and mole number of each species (kgmoles of the species per total mass (kg) in the combustion chamber) were calculated.

In the feed system the effects of the compressibility of helium were important, as was the feed system geometry, so a multiple pipe, multiple node feed system containing distinct liquid and gaseous phases was used to predict the transient feed system behavior. Governing equations for the feed system included the conservation of momentum along each pipe and the conservation of mass at each node. Time dependent variables were the fluid velocity in each pipe, the

liquid/vapor interface position in each pipe and the density at each node.

The combustion chamber and feed system governing equations were solved numerically on a digital computer, integrating over time. Since the equations are stiff (i.e., characterized by widely differing time constants for the dependent variables (Pratt and Radhakrishnan, 1986)) steps were taken to make the equations solvable without using an excess of computer time. In addition to using an integration routine written for solving systems of stiff differential equations, a steady state approximation was made for the concentrations of radicals and atoms in the combustion chamber to facilitate the solution of the governing equations.

Derivation and solution of the governing equations is given in Chapter III.

Success of this model is determined by its ability to predict a chug as encountered in the SSME fuel preburner during shutdown and its ability to vary engine parameters and find a way in which the fuel preburner chug can be lessened in severity or eliminated.

CHAPTER II

LITERATURE SURVEY

2.1 OVERVIEW OF DIFFERENT INSTANCES OF COMBUSTION INSTABILITY, THEIR CAUSES AND EFFECTS.

The phenomenon of combustion instability exists to some degree in all combustion processes. The sputtering of a match, the crackling of a log on a fire and the flickering of a candle are all everyday examples of combustion instability. Such early scientists as Rayleigh and Farraday noted pressure oscillations as sound waves generated during the burning of substances in a tube. Rayleigh (1945) described these oscillations as

> ... vibrations maintained by heat, the heat being communicated to the mass of air confined in the sounding tube at a place where, in the course of vibration, the pressure varies.

He concluded that "In consequence of the variable pressure within the resonator, the issue of gas, and therefore, the development of heat, varies during vibration." This is an apt description of the processes involved in a periodic combustion instability.

Combustion instability can be classified in a number of different ways. First, it can be either periodic or random. An example of a periodic instability is a pressure wave travelling around a combustion chamber due to varying combustion rates. Spikes or pops (spontaneous explosions) in rocket combustion chambers are examples of random instability. Second, combustion instabilities are

either chamber, system or intrinsic instabilities (Williams, 1985). Chamber instabilities involve only the processes that occur within a combustion chamber, while system instabilities involve interaction between processes occurring in a combustion chamber with processes occurring elsewhere in the system, such as in propellant feed lines or at the combustion chamber exit. An intrinsic instability involves only the combustion process and occurs whether or not there is a combustion chamber. Finally, periodic combustion instability can be classified according to its frequency. In rocket motor combustion instability, there exist three fairly distinct instability frequency ranges. High frequency instabilities (normally greater than 1000 Hz) are chamber instabilities involving longitudinal, transverse or radial waves within the rocket combustion chamber. Low frequency instabilities (normally less than 300 Hz) are system instabilities which couple changes in the propellant feed rate with changes in combustion rate in the combustion chamber. Intermediate frequency instabilities (frequencies between 300 Hz and 1000 Hz) involve aspects of both system and chamber instabilities: waves propagate within the combustion chamber and also within the feed system.

Periodic combustion instability is observed in ramjet engines and solid rocket engines as well as in monopropellant and bipropellant liquid rocket engines. Low frequency combustion instability in ramjet engines is a result of vortices in the combustion chamber and is very dependent upon chamber geometry (Yang and Culick, 1986). There are a number of parallels between liquid

rocket and solid rocket engine low frequency combustion instabilities. Schoyer (1986) describes the physical processes involved in solid rocket chugging as follows:

> The basic idea is that due to oscillatory combustion there is a fluctuating heat transfer into the propellant which superimposes an oscillation on the steady state profile in the pyrolizing propellant. Because the solid propellant depends on the (fluctuating) surface temperature, the pyrolysis rate will also vary, causing a fluctuating mass flow into the combustion chamber. If this fluctuating mass flow is more or less in phase with the pressure fluctuations, the two effects may enhance each other (causing resonance) and lead to oscillatory combustion.

Just as heat transfer and pyrolysis provide gaseous reactants in the burning of solid propellants, heat transfer and vaporization provide the gaseous reactants in the burning of liquid propellants. Combustion in solid and liquid rockets differs in two important ways. First, combustion can be considered to take place on a single planar flame front in a solid rocket combustion chamber, whereas combustion in a liquid propellant combustion chamber involves many diffusion flames that surround droplets. Second, the liquid propellant feed rates must also be considered for a liquid rocket engine.

As mentioned above, liquid rocket engines can undergo low, intermediate and high frequency combustion instability. The physical manifestations of these include noise, pressure and temperature oscillations in the combustion chamber (longitudinal, radial and transverse), changes or even reversals in the mass flow rate of the feed system, increased rates of heat transfer to engine components,

decreased engine performance and possibly severe vibrational loads on engine components.

For a liquid rocket engine, the most destructive type of combustion instability is high frequency instability, sometimes called screech, scream or acoustic instability. Screech can result in vibrational loads on rocket components and, more importantly, increased rates of heat transfer to chamber walls. Lawhead and Combs (1963) observed burnout of the injector face of a liquid rocket combustion chamber between 200 and 300 msec after the beginning of screech. Penner and Datner (1955) stated that performance might be improved by screech, although this would not offset the negative effects of screech.

During screech oscillations of pressure and temperature usually take place only within the combustion chamber of a rocket motor, although oscillations can also occur in the feed system. (Coultas,1972). Upon a perturbation, thermodynamic properties and chemical composition can change in a part of the combustion chamber, leading to a local change in the rate of combustion (Crocco et al., 1960). This change initiates a wave which propagates through the combustion chamber. The wave can be linear (discrete) or nonlinear (coupled with other waves) and radial, longitudinal or circumferential. The propellant feed system is usually not directly involved in the propagation of pressure and temperature waves, but is important in that it determines the amount and distribution of reactants in the combustion chamber. The mass flow rate in the feed

system does not oscillate during screech because oscillations in the chamber take place at a higher frequency than those to which the feed system can respond.

Among possible sustaining mechanisms for screech are the physical delays associated with the combustion process (atomization, vaporization and reaction rate), the sensitivity of the rate of combustion to pressure and temperature changes and the "explosion" of liquid droplets which are heated to temperatures above their critical temperatures (Coultas, 1972). Reardon, McBride and Smith (1966) showed that spatial nonuniformities in propellant injection rates across the injector were also, at times, responsible for screech. Their work was verified by experiment.

To prevent destructive high frequency combustion instability, liquid propellant rockets may need baffles or liners to cause combustion chamber conditions (pressure, temperature, distribution of propellants) to be more uniform or to change the resonant frequency of the engine (Williams, 1985). A change in the propellant spray field can also prevent destructive scream (Coultas, 1972). Both of these fixes involve local control of combustion rates.

Less common in liquid rocket motors, intermediate frequency instability, or buzz, involves waves in the propellant feed system as well as spatial combustion chamber pressure variations (Coultas, 1972). Buzz differs from screech in that it involves lower frequency disturbances and oscillations in the feed system. It differs from low frequency instability in that spatial variations in pressure,

temperature and chemical composition exist in the combustion chamber. Buzz causes structural loads on engine components and standing waves in the feed system pipes and may initiate high frequency instability.

Scream involves pressure and temperature waves that propagate in the combustion chamber as a result of spatially varying rates of combustion. Buzz is characterized by standing waves in the propellant feed system and spatial variations in combustion rate in the combustion chamber. In contrast to scream and buzz, combustion chamber pressure can be considered uniform during low frequency instability, or chug. In chug, aggregate oscillations in chamber pressure couple with oscillations in propellant feed rate, resulting in loss of performance, structural loads and possible failure of engine parts. The coupling of oscillations in chamber pressure and propellant feed rate is a result of the time delay between the injection of propellants into the combustion chamber and their combustion. Chugging in liquid bipropellant rocket engines is further described in section 2.2.

2.2 LOW FREQUENCY COMBUSTION INSTABILITY IN LIQUID BIPROPELLANT ROCKET ENGINES

Chugging in liquid bipropellant rocket engines is characterized by pulsations in the rate of propellant injection into the combustion chamber and variations in combustion chamber pressure (Penner and Datner, 1955). These pulsations are generally taken to be the result of the time lag that exists between the injection of

liquid propellants into the combustor and their conversion to hot product gases, as proposed by Summerfield (1951). Because of the inertia of the propellant mass in the feed lines, mass flow rates into a combustion chamber are not immediately responsive to changes in chamber pressure. Because of the combustion time lag, combustion chamber temperature, pressure and composition are not immediately responsive to changes in propellant mass flow. When response delays in the feed system and combustion system become coupled, large amplitude chugs can result. Figure 2.1 shows the coupling of the feed system and combustion chamber for a chugging rocket engine.

Because the conversion of low temperature propellants to high temperature products in a liquid bipropellant rocket engine is such a complex process, it would be difficult for a chug model to incorporate all facets of the process. An effort must be made to determine the most important parts of the process. In the SSME fuelside preburner, liquid oxygen and gaseous hydrogen combust. This involves injection of the hydrogen and oxygen, atomization and vaporization of the oxygen, mixing of the gaseous hydrogen and oxygen vapor and chemical reaction of the gaseous species. In his study of screech in liquid bipropellant rockets, Priem (1966) took atomization, vaporization and chemical reaction as the most important processes in combustion instability. In the current study, the author will also take these three processes to be the most important parts of the combustion process and neglect other parts such as gas phase mixing and wall catalyzed reactions. Atomization,

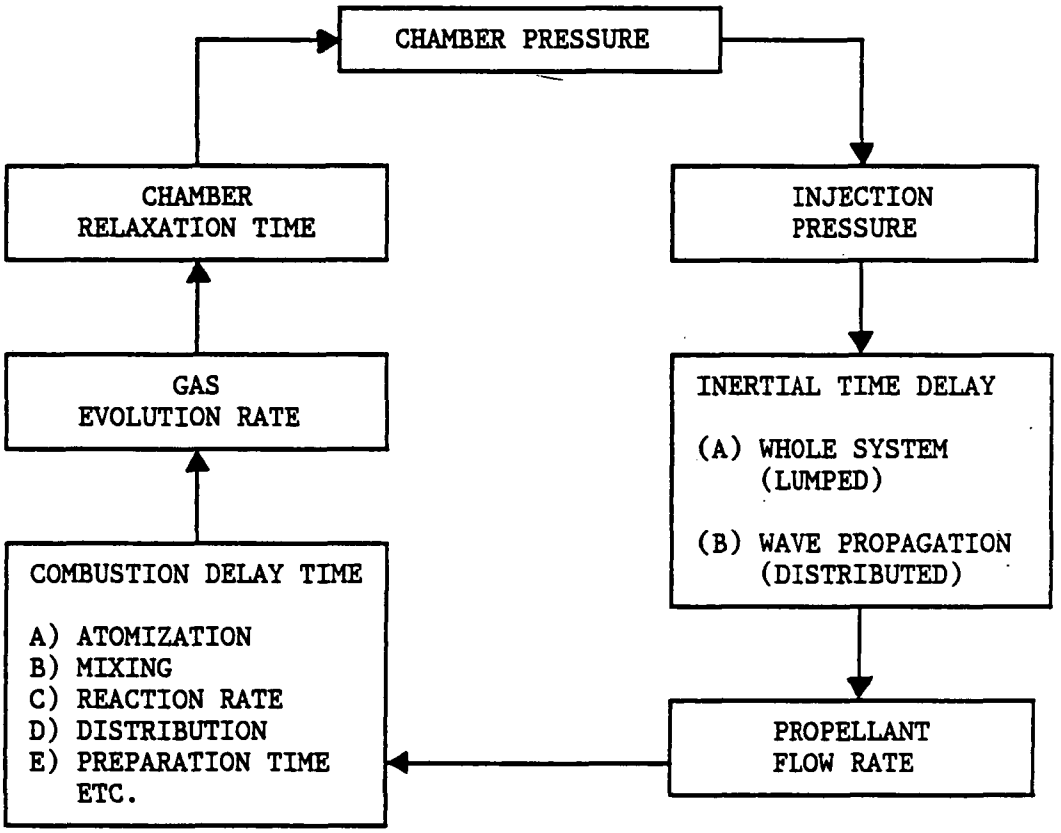

Figure 2.1: Processes Involved in Flow Fluctuation Instabilities
(From Penner and Datner, 1955)

vaporization and chemical reaction and their effect on chugging are briefly described below.

The atomization of a propellant stream is primarily dependent upon the way the stream is injected into the combustion chamber. Propellants can be premixed or distinct upon injection and injection can be accomplished by parallel jets, impinging streams or coaxial streams. After injection, streams may be deflected by a splashplate. The SSME fuelside preburner employs coaxial injectors. Coaxial injectors are primarily used when one of the injected fluids is gaseous and the other is a liquid, since they are well adapted to mixing a gaseous stream with a liquid one (Dykema, 1972).

During atomization, streams break into ligaments which break into droplets. Droplets can either evaporate, shatter or interact with each other. Priem (1966) said that atomization rate is proportional to the mass of unatomized liquid in the combustion chamber and a less strong function of chamber density and axial velocity of the liquid propellant upon injection. The mass of unatomized propellant in the combustion chamber at a given instant is a function of the injection rate previous to that time, so a change in injection rate of propellant will affect the atomization rate only after a time delay.

Spatial injection droplet distribution has been shown to have a great effect on screech (Reardon et al., 1966), but does not greatly affect chugging, since it is aggregate chamber pressure oscillations and not spatial pressure oscillations that are able to couple with

the feed system. Webber (1972) showed that gross changes (for example, not including any small droplets in the droplet distribution in the combustion chamber) in the estimation of droplet sizes in a chug model drastically changed his predicted pressure oscillation amplitudes and frequencies.

The vaporization rate for a liquid propellant in a rocket engine combustion chamber is dependent on the atomization process (droplet size and surface area), the heat transfer rate to the droplet and the rate at which propellant diffuses away from the droplet. To prevent chug, the part of the combustion time delay associated with vaporization should be made as short as possible. In the SSME fuelside preburner, coaxial injectors inject high speed hydrogen around a jet of liquid oxygen. The greater the speed of the hydrogen, the more shear on the liquid oxygen jet, the finer the atomization, the greater the vaporization rate and the shorter the vaporization delay time. Higher chamber temperatures also result in greater rates of vaporization of liquid propellants due to greater rates of heat transfer to droplets. Another way to increase the vaporization rate is to increase the temperature of the liquid propellant. For higher temperature liquid propellants, less energy must be transferred to the droplets to raise their temperature and vaporize them.

Chemical reaction rates, or equivalently, propellant combinations, can greatly influence combustion stability in a rocket engine, though often chemical reaction rate is taken as a less

important factor (Priem, 1966, and Reardon, 1972). Reaction rate can be important if it is sufficiently slow and makes up a significant fraction of the combustion time delay. Summerfield (1951) suggested that chug could be eliminated in some engines through the use of either more reactive propellants or some sort of catalysis.

A number of experimental investigations have been conducted to determine how rocket design parameters such as combustion chamber pressure, propellant combination, injector pressure drop, chamber length, number of injectors, feed system mass flow rates and propellant mixture ratio influence chugging. The results of two papers will be highlighted below.

Both Barrere and Moutet (1956) and Heidmann et al. (1967) noted that higher chamber pressure leads to higher frequency but lower amplitude pressure oscillations (Figures 2.2(a) and 2.2(b)). Temperature and pressure oscillations were roughly in phase during chug (Barrere and Moutet).

As characteristic chamber length (usually defined as the chamber volume divided by the area of the exit nozzle throat) is increased, the range of stable operating conditions is decreased (Heidmann et al.) while the frequency of pressure oscillations decreases (Barrere and Moutet). Chambers of the same characteristic length but different volumes were studied by Barrere and Moutet. Both chambers exhibited roughly the same pressure oscillation frequency, with the smaller chamber undergoing oscillations of slightly higher amplitudes.

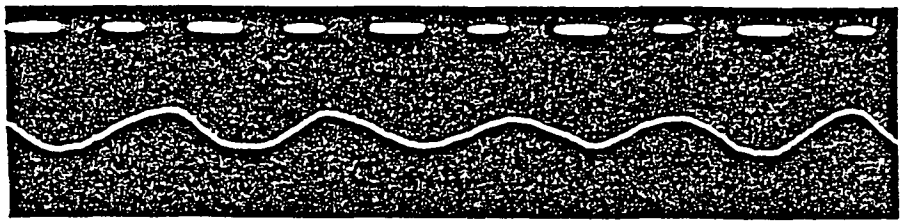

(a) Pressure Oscillations for an Average Chamber Pressure of 0.88 MPa

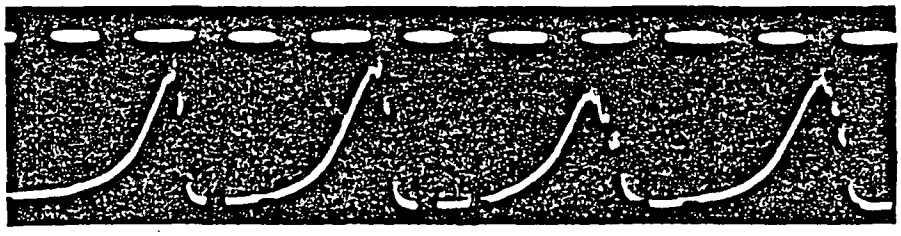

(b) Pressure Oscillations for an Average Chamber Pressure of 1.18 MPa

Figure 2.2: Effect of Chamber Pressure on Chug Amplitude and Frequency (Barrere and Moutet, 1956)

Increasing the number of jets (injectors) of a combustion chamber decreased the range of stable operating conditions (Heidmann et al.), presumably because of droplet and stream interactions driven by the pressure changes.

Changing the mixture ratio within a moderate range ($0.9 < m/m_s < 1.4$, where m is the fuel/oxidizer mixture ratio and m_s is the stoichiometric mixture ratio) had very little effect on chug frequencies for an engine whose propellants were nitric acid and furfurylic alcohol. The lowest amplitude pressure oscillations occurred for a stoichiometric mixture. This is due to a reduced combustion delay time, since collisions between appropriate molecules of reactants are most likely for a stoichiometric mixture.

2.3 CONTROLLING LOW FREQUENCY COMBUSTION INSTABILITY

Having described the processes involved in chugging, a number of methods for controlling chugging will be presented. First, combustion chamber geometry (characteristic length) can be changed. In many cases, as with the SSME, chug is encountered only after the engine has been built, so changing the chamber geometry is not a viable alternative. In addition, since chugging only occurs in the SSME during shutdown, extensive changes in chamber geometry is not merited.

Second, the pressure drop across the injectors can be increased. A larger pressure drop across the injectors means that a change in downstream (chamber) pressure will be a smaller fraction

of the upstream pressure (behind the injector) and will not effect feed system mass flow rates very much. Friction in the feed system and injectors damps oscillations in propellant flow. Any increase in the energy of the propellant stream will be reduced by the feed system and injector friction. Consequently, choosing an injector with much friction could result in a more stable engine. On the other hand, a greater pressure loss for the stream entering the combustion chamber would be the cost.

2.4 THE SSME FUELSIDE PREBURNER CHUG

There are a number of factors peculiar to the SSME fuelside preburner that contribute to the onset of chugging. First, as described in the introduction, the chug occurs during the SSME shutdown while helium progressively replaces liquid oxygen in the oxidizer feed system. The presence of helium in the oxidizer feed system makes the oxidizer mass flow rate more sensitive to changes in the chamber pressure than if there were no helium in the feed system. Gaseous helium is more compressible than liquid oxygen, so an increase in chamber pressure results in compression of the helium and a greater reduction in the oxidizer mass flow rate than if no helium were present. For a temperature and pressure near those at which the chug occurs (5.0 MPa and 100 K), the density and bulk modulus of oxygen are about 1000 kg/m^3 (62.4 lbm/ft^3) and 221 MPa (32,000 psia), respectively. For helium they are about 17 kg/m^3 (1.06 lbm/ft^3) and 12.4 MPa (1800 psia), respectively.

In the SSME fuelside preburner, liquid oxygen is burned at a low equivalence ratio (about 8.0 at rated power level) with hydrogen. Hydrogen has a very low critical temperature (33.3 K [60°R]) and pressure (1.29 MPa [188 psia]), so it enters the combustion chamber as a supercritical gas. The critical pressure of oxygen is about 5.09 MPa (738 psia), so during the SSME fuelside preburner chug, which takes place at pressures which vary around 4.83 MPa (700 psia), oxygen is a near critical liquid.

The conversion of gaseous hydrogen and oxygen to water vapor occurs as a chain reaction involving the radicals and atoms OH, O, H, HO_2 and H_2O_2 (Kuo, 1986). At high pressures, the radicals HO_2 and H_2O_2 dissociate and for high temperatures and high mass flow rates, reactions at the wall are not very important. Since the SSME fuelside preburner operates at high pressures, mass flow rates and temperatures, the following reactions can be considered to be the elementary steps in the overall conversion of H_2 and O_2 to water vapor:

$$H_2 + O_2 \rightarrow 2OH$$

$$H_2 + M \rightarrow 2H + M$$

$$OH + H_2 \rightarrow H_2O + H$$

$$H + O_2 \rightarrow OH + O$$

$$O + H_2 \rightarrow OH + H$$

$$H + H + M \rightarrow H_2 + M$$

$$H + O + M \rightarrow OH + M$$

$$O + O + M \rightarrow O_2 + M$$

$$H + OH + M \rightarrow H_2O + M$$

where M represents a third body, inert to the reaction . For a rocket engine combustion chamber, which operates at high temperatures and pressures, the atoms and radicals produced in the chain branching reactions will be consumed in the termination reaction nearly as soon as they are produced.

George (1984) observed during test firings of the SSME that using a 0.068 inch diameter helium purge orifice for the SSME fuelside preburner as opposed to a 0.291 inch orifice resulted in a 34% increase in maximum peak to peak amplitudes of pressure oscillations (from 335 psia) and a 38% decrease in chug duration (from 0.72 sec). Changing the purge orifice diameter did not substantially change the chug's center counted frequency (the average frequency at the chug's temporal center). The center counted frequency for the small and large orifices were 117 Hz and 117.5 Hz, respectively. Traces of pressure for small and large orifice engine test firings are shown in Figures 1.3(a) and 1.3(b) (page 8). Chug ending time was not affected by the change of the helium purge orifice diameter, but chug starting time was. Because of this, George ruled out oxygen depletion as the chug terminating mechanism. Helium flow rate and compressibility are evidently important in determining the character of the SSME fuelside preburner chug.

The only opening or closing of a valve that occurs near the chug's end is the closing of the main oxidizer valve. As described in Chapter I, during chug the fuelside preburner is isolated from

the oxidizer feed system, so valve openings and closings are probably not a concern in the SSME fuelside preburner chug. The valves that restrain the helium before the purge begins are poppet type valves that remain open even when the pressure drop across the valve is less than the cracking pressure (George, 1985). Therefore, helium purge valve clatter probably does contribute to the chug.

Because of the fuelside preburner turbine blade inertia, the exit mass flow rate does not respond immediately to a change in combustion chamber pressure. A relation for exit mass flow rate as a function of chamber pressure and temperature and pressure downstream of the turbine was given by Nguyen (1981) and is found in Chapter III.

Because of the above considerations, the model of the SSME fuelside preburner allows for the compressibility of helium in the piping system, a combustion time lag due to the atomization and vaporization times for oxygen and turbine blade inertia.

2.5 ROCKET ENGINE STABILITY PREDICTION MODELS

Most chug models have attempted to predict the domain of operating conditions within which a rocket engine can operate without undergoing destructive oscillations in pressure and temperature. By varying inputs such as combustion chamber pressure, injector pressure drop, combustion time delay or instability frequency to these models, stability boundaries for specific engines and general criteria for rocket engine stability can be found.

Figure 2.3 shows the rocket engine model used by Summerfield (1951). He related the rate of change of combustion chamber pressure with respect to time, t, at a given instant, to the propellant injection rate at a time t-Θ, using the equation:

$$\frac{dP_c}{dt} = \frac{R\,T_c}{V}\rho_c A_2 v_2(t-\Theta) - \frac{R\,T_c}{L^*c^*}\,P_c \qquad [2.2]$$

where T_c is the combustion chamber temperature (K), ρ_c is the combustion chamber density (kg/m^3), V is the combustion chamber volume (m^3), L* is the characteristic chamber length (m), c* is the characteristic propellant velocity (m/s), R is the gas constant for the gases in the combustion chamber (J/kg·K), A_2 is the area (m^2) at station 2 in Figure 2.3 and $v_2(t-\Theta)$ is the propellant velocity (m/s) at station 2 at time t-Θ. This implies that a mass of propellant injected into the combustion chamber occupies negligible volume and does not react at all until Θ seconds later when it is converted to products instantaneously. Θ is the combustion time delay and can be a function of chamber pressure, temperature and composition and of propellant composition and velocity. Characteristic chamber length, L*, is defined as the volume of the chamber divided by the average cross sectional area. Summerfield defined the characteristic propellant velocity, c*, as

$$c^* = f(\gamma)\sqrt{R\,T_c}$$

where γ is the ratio of the specific heats in the chamber .

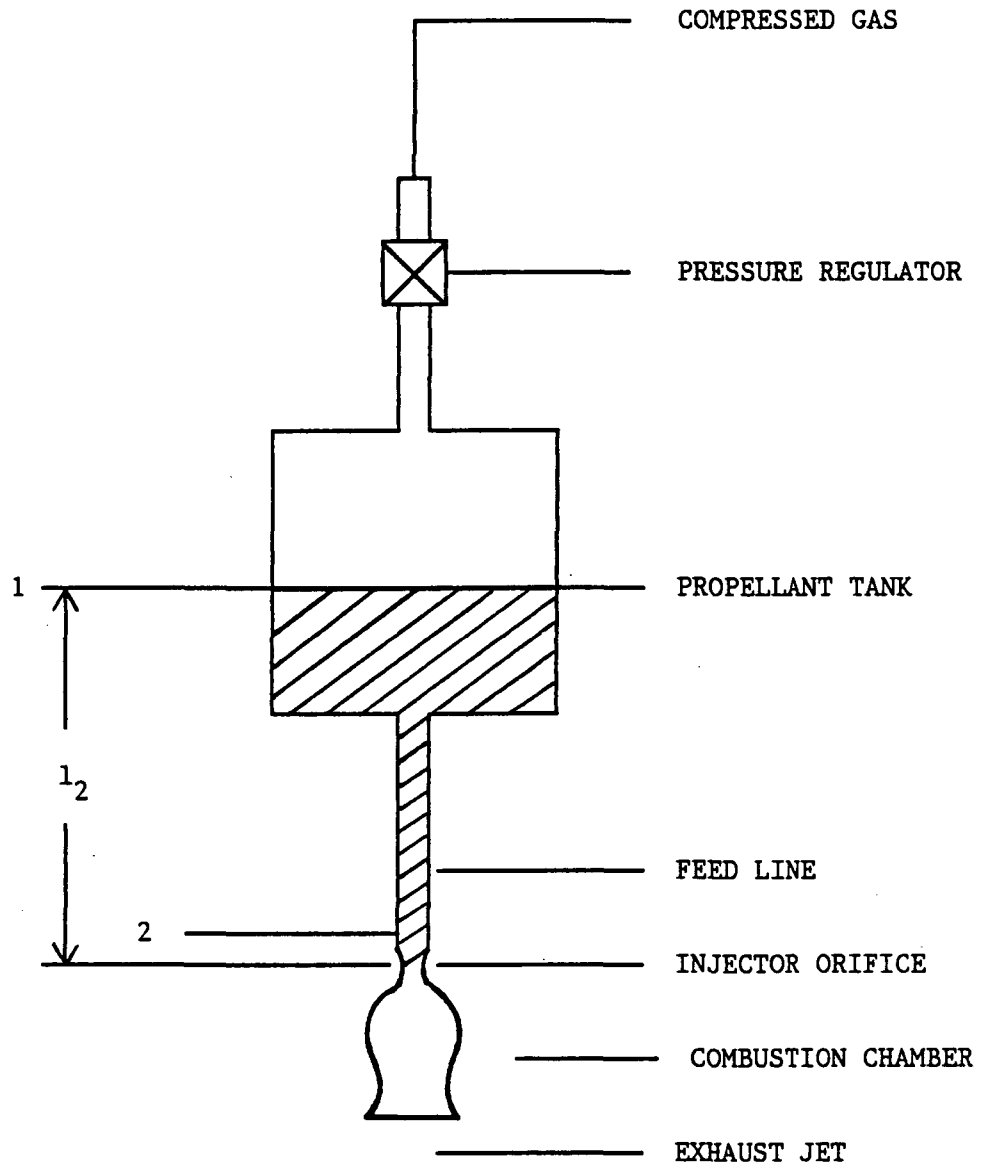

Figure: 2.3 Schematic of Summerfield's Liquid Propellant Rocket System (Summerfield, 1951)

Summerfield used conservation of energy for the control volume bounded by surfaces A_1 and A_2 along with continuity and equation [2.2]. Differentiating the result with respect to time and linearizing by saying that $v_2(t) - v_2(t-\Theta)$ is small, gave an equation of the form

$$u''(t) + A\,u'(t) + B\,u(t) + C\,u(t-\Theta) = 0 \qquad [2.3]$$

where $u = d(v_2)/dt$. Solutions of [2.3] are of the form

$$u = \Sigma\, U_n \exp((\lambda_n + \omega_n)t) \qquad [2.4]$$

Substituting [2.4] into [2.3], the values of λ_n and ω_n which satisfy [2.3] can be found.

Analyzing the eigenvalues of [2.3], Summerfield determined that the following condition must be met for a liquid rocket engine to be stable (i.e., to not undergo undamped pressure oscillations):

$$\frac{l_2}{P_c}\frac{\dot{m}}{A_2} + \frac{c^*L^*}{R\,T_c}\frac{2\,\Delta P}{P_c} > \Theta \qquad [2.5]$$

where ΔP is the pressure difference between the propellant storage tank and the combustion chamber (psi) and l_2 is the length of the propellant feed line (Figure 2.3).

Inequality [2.5] indicates that an unstable rocket engine can be made stable by

1. increasing the feed system pipes length,
2. increasing the propellant feed mass flow rate,

3. increasing the pressure drop from the storage tank to the combustion chamber,

4. decreasing the combustion chamber pressure or

5. increasing the characteristic chamber length.

Evaluation of [2.5] with the appropriate SSME fuelside preburner shutdown values (l_2 = 0.5 m [1.64 ft], $\dot{m}$ = 33.91 kg/s [74.8 lb/s], P_c = 4.825 MPa [700 psia], A_2 = 0.0025 m^2 [0.027 ft^2], c* = 60 m/s, [197 ft/s] [estimated from calculations by VanOverbeke and Claus, 1986], L* = 0.1 m [0.328 ft], R = 2080 J/kg·K [0.497 Btu/lbm·°R], ΔP = 0.345 MPa [50 psia] and T_c = 700 K [1260°R]) yields the stability criterion

$$\Theta < 0.0014 \text{ s}$$

(i.e., the combustion time delay must be less than 440 μs).

Crocco (1951) began his stability analysis for a monopropellant rocket engine using conservation of mass in the combustion chamber. Assuming, like Summerfield, that propellants have negligible volume until burned and that the mass burned over the time interval dt is equal to the mass of propellant injected over the time interval d(t-Θ), continuity for the combustion chamber can be written

$$\frac{dM_g}{dt} + \dot{m}_e(t) = \left(1 - \frac{d\Theta}{dt}\right) \dot{m}_i(t-\Theta) \qquad [2.6]$$

where $\dot{m}_e$ and $\dot{m}_i$ are the mass flow rates out of and into the combustion chamber and M_g is the mass of product gases in the combustion chamber.

Crocco divided the combustion delay time, Θ, into an insensitive part, Θ_g, which does not vary with small variations in chamber conditions and a sensitive part, τ .

$$\Theta = \Theta_g + \tau \qquad [2.7]$$

Θ_g can be given, for instance, by $L^*c^*/R \cdot T_c$. Crocco assumed that τ obeys the relation

$$\tau \, P_c^n = \text{const.} \qquad [2.8]$$

Using [2.8] and [2.7], Crocco nondimensionalized and linearized [2.6].

Applying the conservation of mass and momentum to the feed system, piping system behavior was seen to be dependent on three dimensionless groups: one involving the pressure drop across the injectors, the second involving the inertia of the propellant in the pipes and the third giving the relative elasticity of the pipes and the propellant within.

Using a version of [2.6] and the feed system equations, Crocco formulated a characteristic equation for a monopropellant rocket engine and found the stability boundaries that corresponded to various values of n in equation [2.8]. He concluded that using a varying time lag changed stability predictions, predicting a greater

range of stable operating conditions, but the changes were not great.

Using an annular section of a liquid bipropellant rocket engine combustion chamber, Priem determined the effect that atomization, vaporization and chemical kinetics had on screech. Though this model was for screech, the way that the combustion rate was modelled can be extended to a chug model.

Priem calculated combustion rate in three different ways. First, he assumed that chemical kinetics was the most important part of the combustion process. Atomization and vaporization times were assumed short enough that the propellants that were injected into the combustion chamber were immediately available for chemical reaction. In the second model vaporization was the controlling process. Atomization was considered very fast, so the liquid injected into the combustion chamber immediately assumed a given, nonvarying droplet distribution profile. Chemical reaction time was also considered negligible. Consequently, the combustion rate was equal to the vaporization rate. Finally, the times required for atomization and chemical reaction were considered very small and the combustion rate was set equal to the atomization rate.

Using conservation of mass, energy and axial momentum, Priem generated stability boundaries. The physical processes of vaporization and atomization were shown to be more important than chemical kinetics for screech. Stability was shown to be very

sensitive to the mass of unburned propellant in the combustion chamber. Priem confirmed his stability boundaries experimentally.

In a companion study to this one, Lim (1986) determined the stability boundaries of the SSME fuelside preburner during shutdown. Lim assumed

1. combustion chamber pressure is uniform and oscillates about a steady state value,
2. combustion chamber temperature is uniform,
3. the combustion delay time is the same for both propellants and
4. reaction rate is infinite and chemical kinetics can be ignored.

Like Summerfield, Lim assumed that the rate that propellants are burned is equal to their rate of injection at a previous time, $t-\theta$, where

$$\theta = \theta_v + \theta_m \qquad [2.9]$$

θ_v corresponds to vaporization time and θ_m to mixing time.

Conservation of mass was applied to the combustion chamber, leading to

$$\frac{d}{dt}(\rho_c V) = \dot{m}_{fb}(t-\theta) + \dot{m}_{ob}(t-\theta) - \dot{m}_e(t) \qquad [2.10]$$

where $\dot{m}_{fb}$ and $\dot{m}_{ob}$ are fuel and oxidizer burning rates, respectively (determined by conditions at time, $t-\theta$) and $\dot{m}_e$ is the chamber exit mass flow at time t. The system variables $\dot{m}_{fb}$, $\dot{m}_{ob}$, $\dot{m}_e$ and ρ_c were

expressed in terms of a steady state value plus a perturbation and substituted into [2.10] which was linearized. The resulting characteristic equation was solved and stability boundaries were generated.

In generating stability boundaries. Lim varied chamber pressure, fuel mass flow rate, oxidizer mass flow rate, fuel injection temperature and oxidizer injection temperature. Lim made the following conclusions from his stability boundaries.

1. The preburner system is generally more stable at lower chamber pressures.
2. For oxidizer and fuel temperatures of 40K, the system is inherently unstable. For oxidizer and fuel temperatures of 120 K, stability can be achieved only for P_c < 3.79 MPa (550 psia). Chugging could not be avoided for low fuel temperatures.
3. Fuel flow rates did not influence stability.
4. High oxidizer flow rates (or high helium purge rates) made the system stable.

2.6 STIRRED TANK REACTOR MODELS

A chemical reactor can be modelled as a batch reactor, a plug flow reactor or a stirred tank reactor (STR). In a batch reactor (Figure 2.4 (a)) reactants are fed into the reactor and left to react. After some time, the reactor is emptied. A plug flow reactor is shown in Figure 2.4 (b). Elements of fluid travel in an orderly

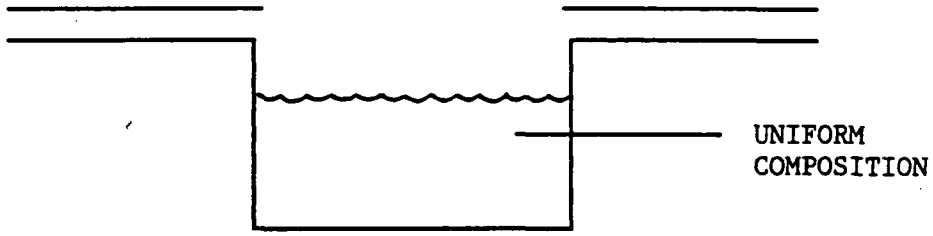

(a) Ideal Batch Reactor

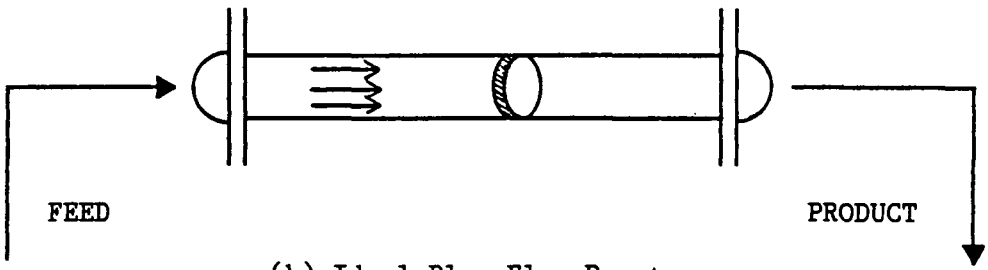

(b) Ideal Plug Flow Reactor

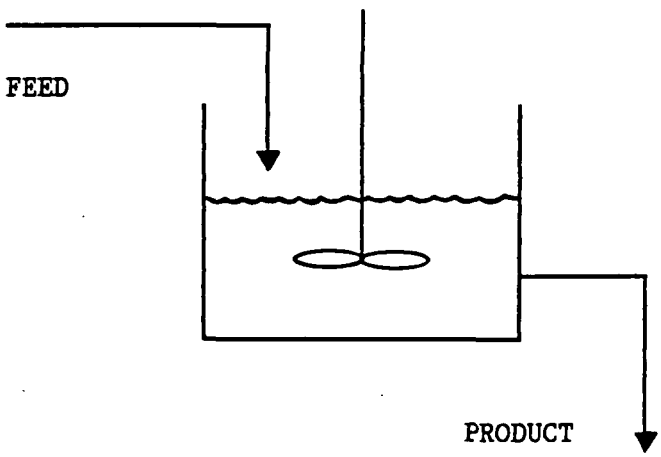

(c) Ideal STR

Figure 2.4: Ideal Chemical Reactors

way through the chamber with no element overtaking any other element (i.e., no mixing in the direction of the flow, but infinite radial mixing). A STR is a reactor for which contents are considered well mixed and properties of the contents are uniform throughout the combustion chamber (Figure 2.4 (c)). One ramification of the STR assumption is that some unburned reactants will always be present in the chamber outflow.

Webber (1972) used a heterogeneous STR to determine the transient behavior of a liquid rocket engine undergoing chug. His model included a simple feed system, injectors, a combustion chamber and a nozzle.

A lumped parameter approach was used for the feed system, resulting in the equation

$$\frac{dq}{dt} = \frac{P_t - P_c - (1/2)\, f \rho_c\, q|q|}{\rho \sum_{n}^{NP} (l_n/A_n)} \qquad [2.11]$$

where q is the volumetric flow rate (m^3/s) of the propellant, f is a coefficient chosen to approximate the sum of the turbulent line losses and the nozzle losses in the feed system (m^{-4}), l_n and A_n are the length (m) and area (m^2) of pipe n, respectively, P_t is the pressure in the propellant storage tank, P_c is the pressure in the combustion chamber and NP is the total number of pipes in the feed system.

Injector calculations included determination of the droplet size distribution and velocity upon injection. Relying heavily upon

empirical correlations, Webber found the droplet size distribution and velocities associated with a self-impinging doublet injector.

In the combustion chamber, the liquid and gaseous states were treated separately. Liquid propellants were divided into droplet size groups whose diameters and velocities were followed over time. Vaporization rate per droplet, ω_v (kg/sec per droplet), was given as

$$\omega_v = \left(\frac{\pi\, k}{c_p}\right) D\, (2 + 0.5\, Re^{0.5})\, \ln(1 + \alpha) \qquad [2.12]$$

where k is the droplet thermal conductivity (W/m·K), c_p is the specific heat of the vapor surrounding the droplet (J/kg·K) and D is the droplet diameter (m). α is the burning rate parameter, given as

$$\alpha = c_p \frac{\Delta T}{\Delta H} \qquad [2.13]$$

where c_p is the specific heat at constant pressure of the droplet (J/kg·K), ΔT is the temperature difference between the droplet and the surrounding gases (K) and ΔH is the droplet's latent heat of vaporization (J/kg). Re is the droplet Reynolds number, given as:

$$Re = \frac{\rho D\, |v_g - v_{in}|}{\mu_g} \qquad [2.14]$$

where v_g is the velocity of the gas in the chamber (m/s), v_{in} is the injection velocity and μ_g is the gas viscosity (N·s/m^2).

The gas state in the combustion chamber was considered well mixed and to be a perfect gas. Gas velocity was allowed to vary in the combustion chamber. Gas behavior was determined by conservation of mass in the combustion chamber, the perfect gas law and an expression for the expansion of gas through a choked nozzle.

Webber integrated his equations numerically using a fixed time step integration. The size of the time step was seen to be relatively unimportant. He was able to predict a 66 Hz chug whose maximum amplitude was about 200 psia for an average chamber pressure of 400 psia. From his study, Webber concluded that:

1. chug is sensitive to predicted temperature (he used empirical data to give chamber temperature as a function of stoichiometry) and
2. small variations in the droplet size distribution were not very important, but gross changes drastically changed the model's predictions.

Calculated frequencies were within 7% of experimental values and amplitudes were within 5%.

Courtney (1960) used a much simpler approach to determine combustion intensity (mass of propellant burned per volume per time in a combustion chamber) in a heterogeneous STR. He began with an assumed droplet size distribution and assumed steady state conditions and infinitely fast chemical kinetics. Droplet evaporation rate was given as:

$$\frac{dr}{d\phi} = -\frac{k}{2r} \qquad [2.15]$$

where k was assumed constant (but not explicitly given), r is the droplet radius and ϕ is the droplet age in the combustion chamber. Overall evaporation rate was determined by integrating [2.15] for $0 < r < r_{max}$. For a monodisperse spray, Courtney showed that combustion intensity is a strong function of droplet size; intensity increases rapidly with decreasing droplet size.

2.7 SUMMARY

Low frequency combustion instability in a liquid bipropellant rocket engine involves a coupling of oscillations in chamber pressure with oscillations in propellant flow rate. This coupling is possible because of the combustion time lag in the combustion chamber and the inertia of the propellant in the feed lines.

A number of models have predicted the domain of operating conditions in which a rocket engine will undergo stable operation. (Summerfield, Crocco, Lim and others). These models involve linearized equations from which either stability or instability of an engine can be predicted. In general, it has been shown from these models that higher propellant temperatures, lower chamber pressures and longer propellant feed lines lead to more stable rocket engines.

Other models have predicted either the steady state operation or transient behavior of rocket engines (Webber and Courtney). These

types of models generally involve nonlinear equations which are solved over time numerically for variables such as chamber pressure and temperature, droplet size distribution and combustion rate. The advantage of these models is that amplitudes and frequencies of oscillations in pressure, temperature and oxidizer mass flow rate can be calculated. These models have shown the STR model to be sufficient for modelling rocket engine combustion chambers undergoing chug.

The author has modelled the SSME fuelside preburner as a perfectly mixed reactor and has predicted its behavior during engine shutdown. Derivations of the governing equations for this model are found in Chapter III.

CHAPTER III

MODELLING THE SSME FUEL PREBURNER

The SSME fuel preburner is modelled as a multi-pipe, multi-node oxidizer feed system, a transient stirred tank reactor (TSTR) combustion chamber and an exit turbine, as shown in Figure 3.1. This approach is similar to that used by Webber (1972) and employs most of the same governing equations as those used by Pratt and Radhakrishnan (1986). Using a TSTR model allows the frequency and amplitude of oscillations in chamber pressure and oxidizer mass flow rate to be calculated. Using a multi-pipe, multi-node oxidizer feed system allows the position of a liquid/vapor interface in the feed system to be calculated at each integration time step.

The governing equations for the TSTR and oxidizer feed system are partially derived below and their solution is described. Full derivations are given in Appendix A.

The governing equations were solved on a digital computer. A program flowchart, listing and sample input and output files are found in Appendix B.

3.1 THE COMBUSTION CHAMBER

The TSTR model for the combustion chamber assumes that at any given time the combustion chamber can be considered a stirred tank reactor (properties and composition are uniform throughout the combustion chamber). With time, though, chamber composition and

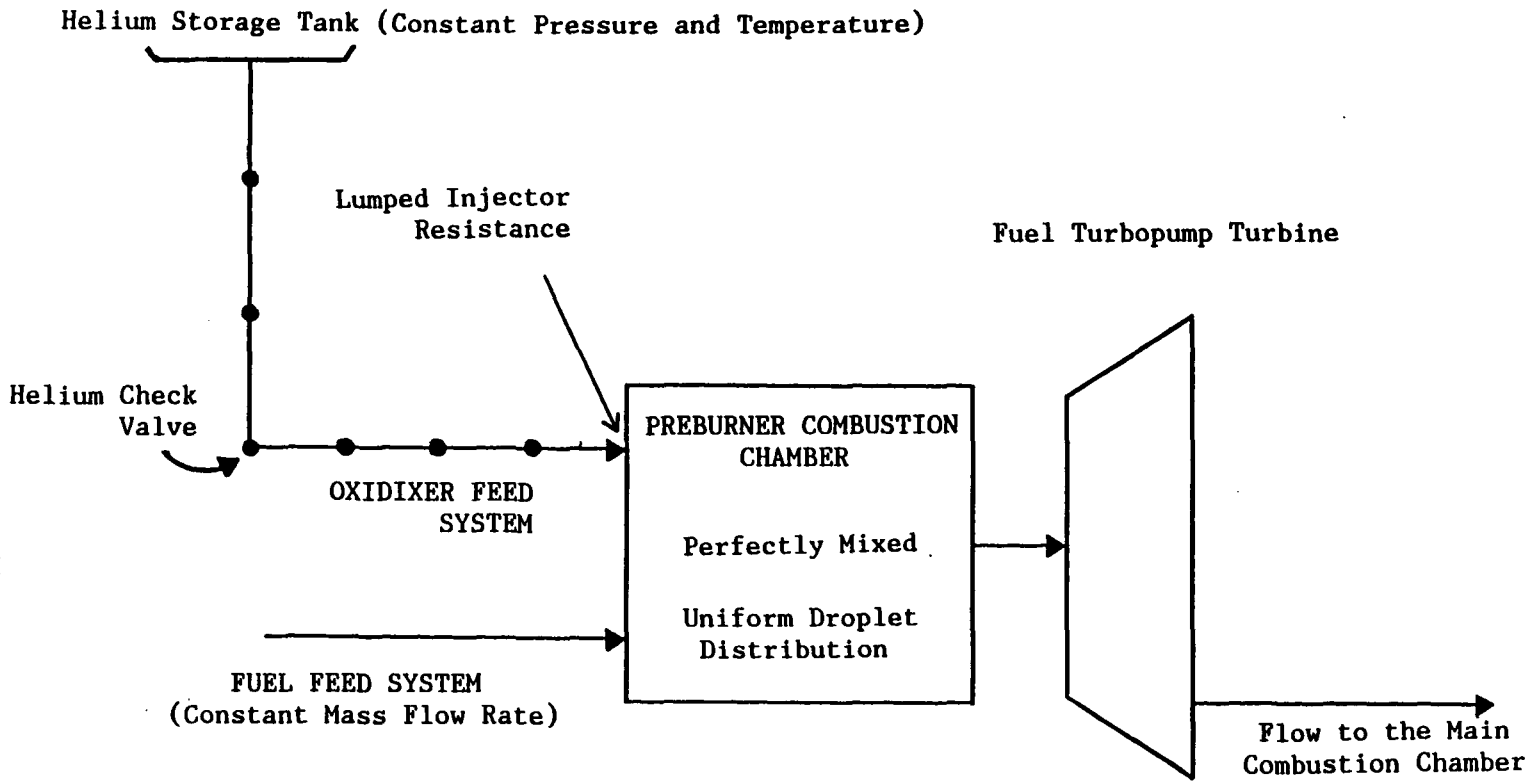

Figure 3.1: Schematic of the Fuelside Preburner Model

properties are allowed to vary. Using a TSTR to model a chugging rocket combustion chamber is justified, in that oscillations in the combustion chamber have long periods in comparison to the amount of time it takes a disturbance to travel through the combustion chamber. Also, it is aggregate, not local changes in pressure in the chamber that are able to couple with oscillations in the propellant feed rate to produce a low frequency system instability.

The TSTR model was used because it is simple, requiring a minimal number of calculations to determine the conditions at each time, because it can accommodate heterogeneous combustion and because a coupling of oscillations in feed system propellant flow with chamber pressure oscillations is possible.

Heterogeneous combustion of liquid oxygen with gaseous hydrogen occurs within the fuel preburner combustion chamber. This is accommodated by the TSTR model by the imposition of a uniform oxidizer droplet distribution throughout the combustion chamber. Droplets were assumed to all have the same diameter and an equal number of droplets are found in any part of the combustion chamber volume. The instantaneous average droplet diameter (D_m) was calculated using a relation given by Hersch and Rice (1967). For a coaxial injector with gaseous hydrogen injected through an anulus around a central stream of liquid oxygen,

$$D_m = c_{dm} \left(\frac{O}{F}\right) \sqrt{\frac{M_{H_2} A_{H_2}}{R_g \rho_j T_{H_2}} P_c} \qquad [3.1]$$

c_{dm} is a dimensionless constant equal to 0.485. (O/F) is the mass ratio of oxidizer flow to fuel flow, M_{H_2} is the molecular weight of hydrogen (kg/kgmole), A_{H_2} is the area of the anulus through which hydrogen is injected (m^2), R_g is the universal gas constant (J/kgmole·K), ρ_j is the density of the oxygen jet (kg/m^3), T_{H_2} is the temperature of the hydrogen on injection (K) and P_c is the chamber pressure (Pa). Equation [3.1] gives the mean droplet diameter of liquid oxygen droplets immediately after injection. In reality, the mean droplet diameter in the combustion chamber is less than that just after injection, however, equation [3.1] was used to give the mean droplet diameter throughout the chamber since no data were available for determination of the droplet distribution in the chamber. The effect that mean droplet diameter has on preburner operation is shown in Chapter IV.

The evaporation rate of a single droplet, ω_v (kg/sec/droplet), was given by Webber (1972) in equation [2.12]. For an average liquid density of β (mass of liquid per unit volume of the combustion chamber), the total vaporization rate, Ω (kg/s), including the contributions from all droplets, is

$$\Omega = \frac{6 \beta V}{\rho_l \pi D_m^3} \omega_v \qquad [3.2]$$

V is the combustion chamber volume (m^3).

Combustion rate was calculated in two different ways. First, all the oxygen that vaporized was assumed to combust immediately

with hydrogen to form water vapor. This implies that diffusion of oxygen vapor into the chamber contents and chemical reaction both occur instantaneously. Since oxygen is consumed as soon as it vaporizes, its rate of production by combustion Γ_{O_2} (kgmoles/s) is equal to negative its rate of production by vaporization:

$$\Gamma_{O_2} = - \frac{\Omega}{M_{O_2}} \qquad [3.3]$$

From conservation of atoms,

$$\Gamma_{H_2} = 2\ \Gamma_{O_2}$$
$$\Gamma_{H_2O} = - 2\ \Gamma_{O_2}$$

For the second combustion model, atomization was assumed infinitely fast. Oxygen vaporized according to [2.12] then instantaneously mixed with the gaseous species in the combustion chamber. The production of water vapor from hydrogen and oxygen occurred via a chain reaction involving nine elementary reactions and the species H_2, O_2, H_2O, H, O and OH.

To aid in the solution of the governing equations, the very reactive species H, O and OH were assumed to be consumed as soon as they were produced. In other words, their mole numbers, σ_i (kgmoles of species i per total mass in the combustion chamber) were constant at any time:

$$\frac{d\sigma_H}{dt} = \frac{d\sigma_O}{dt} = \frac{d\sigma_{OH}}{dt} = 0$$

This condition fixed the values of the σ_H, σ_O and σ_{OH} at each time step. A full derivation of reaction rate involving chemical kinetics is found in Appendix A.

The governing equations for the combustion chamber were derived from the conservation of mass for the gaseous and liquid contents of the combustion chamber, conservation of species, conservation of energy and the ideal gas relation.

Conservation of mass for the gaseous contents of the chamber is shown in Figure 3.2 and described analytically by equation [3.4].

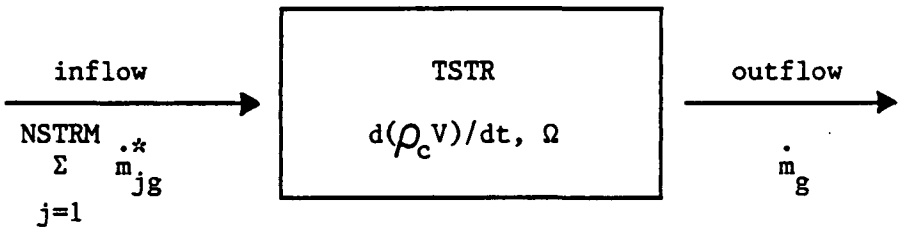

Figure 3.2: Conservation of Mass for the Gas Phase

$$\frac{d(\rho_c V)}{dt} = \left(\sum_{j=1}^{NSTRM} \dot{m}^*_{jg} \right) - \dot{m}_g + \Omega \qquad [3.4]$$

$\dot{m}_g$ is mass flow rate of gases out of the combustion chamber (kg/s),

ρ_c is combustion chamber density (kg/m^3), t is time (s), V is volume (m^3), NSTRM is the number of inlet streams to the TSTR, the subscript g denotes the gaseous state and superscript * denotes an inlet quantity.

Conservation of mass for the liquid contents of the chamber is shown in Figure 3.3 and described analytically by equation [3.5].

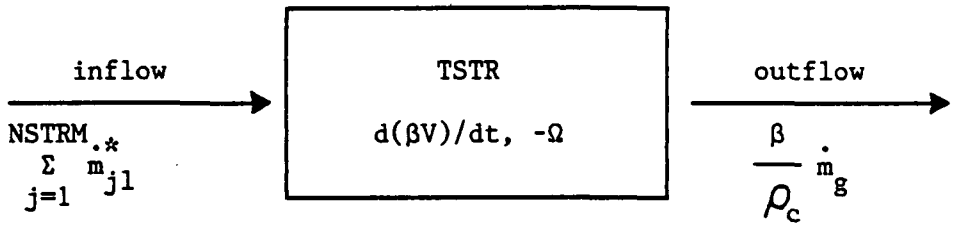

Figure 3.3: Conservation of Mass for the Liquid Phase

$$\frac{d(\beta V)}{dt} = \sum_{j=1}^{NSTRM} \dot{m}^*_{jl} - \Omega - \frac{\beta}{\rho_c}\dot{m}_g \qquad [3.5]$$

The subscript l denotes the liquid phase. Since the liquid density is uniform throughout the combustion chamber, the liquid outflow is given by $\beta\dot{m}_g/\rho_c$.

Conservation of species is shown in Figure 3.4 and described analytically by equation [3.6].

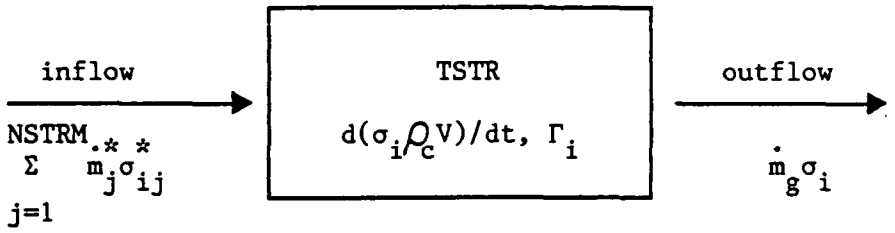

Figure 3.4: Conservation of Species

$$\frac{d(\sigma_i \rho_c V)}{dt} = \sum_{j=1}^{NSTRM} (\dot{m}_j^* \sigma_{ij}^*) - \dot{m}_g \sigma_i + \Gamma_i, \quad i=1,2,3,\ldots NS \qquad [3.6]$$

σ_i is the mole number of species i (kgmoles of i per kg in the combustion chamber), NS the number of species present in the combustion chamber and Γ_i the rate of production of species i by combustion (kgmoles/s).

Conservation of energy is shown in Figure 3.5 and described analytically by equation [3.7].

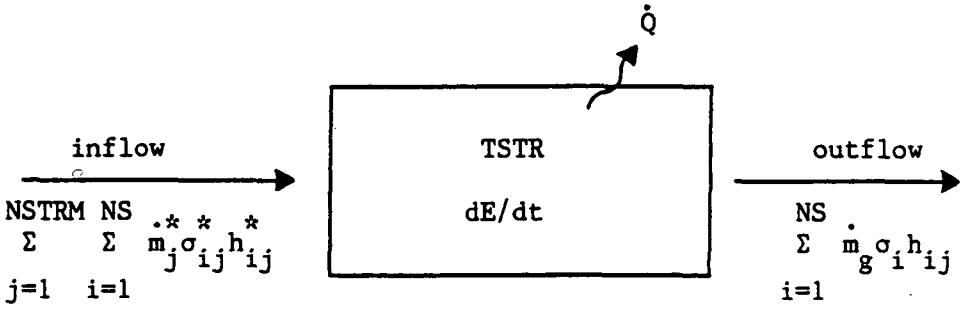

Figure 3.5: Conservation of Energy

$$\frac{dE}{dt} = \sum_{i=1}^{NS} \sum_{j=1}^{NSTRM} \dot{m}_j^* \sigma_{ij}^* h_{ij}^* - \sum_{i=1}^{NS} \dot{m}_g \sigma_i h_i - \dot{Q} \qquad [3.7]$$

E is the total (chemical plus sensible) energy (Joules) in the combustion chamber , h_i is the molar enthalpy of species i (J/kgmole) and $\dot{Q}$ is the heat transfer rate out of the combustion chamber (Joules/s).

Liquids in the chamber were assumed to occupy negligible volume. The volume occupied by liquid in the combustion chamber after a long time at a steady oxidizer mass flow rate of 5 kg/s and a chamber temperature of 1000K was calculated. At these conditions, the ratio of the volume occupied by liquid to the total chamber volume was 1 : 47,000. Gases were assumed to obey the ideal gas relation, which took the form

$$P_c = \rho_c \left(\sum_{i=1}^{NS} \sigma_i \right) R_g T_c \qquad [3.8]$$

$\sum_{i=1}^{NS} \sigma_i$ gives the average molecular weight of the chamber gases.

Equations [3.6], [3.7] and [3.8] were expressed in terms of the logarithmic variables ln T_c, ln P_c and ln σ_i, i=1,2,3,...NS. This prohibited negative values and facilitated integration by altering the time constants associated with these variables. In their final form, the conservation of mass for the liquid phase, the conservation of species, the conservation of energy and the ideal gas relation are

$$\frac{d\beta}{dt} = \left(\sum_{j=1}^{NSTRM} \dot{m}^{*}_{jlv}\right) - \Omega_v - \dot{m}_{gv}\frac{\beta}{\rho_c} \qquad [3.9]$$

$$\frac{d(\ln \sigma_i)}{dt} = \frac{1}{\rho_c \sigma_i}\sum_{j=1}^{NSTRM} \dot{m}^{*}_{jv}(\sigma^{*}_{ij} - \sigma_i) + \Gamma_{iv} \qquad [3.10]$$

$$i=1,2,3,\ldots NS$$

$$\frac{d(\ln T_c)}{dt} = \left[\sum_{i=1}^{NS}\sum_{j=1}^{NSTRM} \dot{m}^{*}_{jv}\sigma^{*}_{ij}h^{*}_{ij} - \sum_{i=1}^{NS} \dot{m}_{gv}\sigma_i h_i - \rho_c \sum_{i=1}^{NS} u_i(d\sigma_i/dt) - (d\rho_c/dt)\sum_{i=1}^{NS} \sigma_i u_i - \dot{Q}/V\right] \Big/ \left[T_c \rho_c \sum_{i=1}^{NS} \sigma_i (c_{pi} - R_g)\right] \qquad [3.11]$$

$$\frac{d(\ln P_c)}{dt} = \frac{d(\ln T_c)}{dt} + \frac{1}{\rho_c}\frac{d\rho_c}{dt} + \frac{1}{\left(\sum_{i=1}^{NS} \sigma_i\right)}\frac{d}{dt}\left(\sum_{i=1}^{NS} \sigma_i\right) \qquad [3.12]$$

The superscript v denotes a volumetric quantity ($1/m^3$), c_{pi} is the specific heat at constant pressure for species i (J/kgmole·K) and R_g is the universal gas constant (J/kgmole·K). The combustion chamber equations are derived in greater detail in Appendix A.

3.2 THE OXIDIZER FEED SYSTEM

Before shutdown begins, the fuel preburner oxidizer feed system is completely filled with liquid oxygen. During shutdown, gaseous

helium progressively replaces oxygen in the pipes. To create a feed system which was simple, yet responsive to changes in combustion chamber pressure and fluid compressibility in the pipes, the following assumptions were made.

1. Liquid oxygen is incompressible.
2. Helium behaves as a perfect gas.
3. Temperature is constant throughout the feed system.
4. Pipes have a characteristic cross sectional area; area is taken as constant throughout a given pipe.
5. There is no accumulation of mass at pipe nodes; the nodes have negligible volume
6. If a pipe contains both the liquid and the gas phases, a distinct interface exists between them.
7. Fluid velocity is constant within a given pipe (i.e., if there is an interface in the pipe, the liquid, the vapor and the interface are all assumed to be moving at the same velocity.
8. Flow resistance in a pipe is lumped at the pipe exit, so the flow resistance for a pipe containing a liquid/vapor interface is the same as that for a pipe which contains only liquid, until all of the liquid is expelled.

Time dependent variables in the feed system include the fluid velocity in each pipe, the density at each pipe node and the position of the liquid/vapor interface in each pipe.

Figure 3.6 shows a pipe containing a liquid/vapor interface.

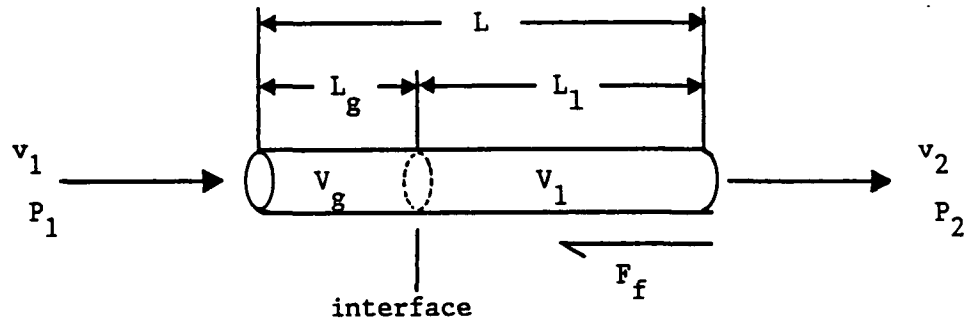

Figure 3.6: Schematic of a Pipe Containing a Liquid/Vapor Interface

V is volume (m^3), L is pipe length (m), v_1 and v_2 are upstream and downstream velocities (m/s), respectively, P_1 and P_2 are upstream and downstream pressures (Pa), respectively, A is pipe Area (m^2) and F_f accounts for turbulent and shear head losses in the pipe. Subscripts 1 and g denote the liquid and gas phases, respectively. Since pipe length is constant,

$$\frac{dL_g}{dt} = -\frac{dL_1}{dt} = v \qquad [3.13]$$

Conservation of momentum, expressed in integral form, is (White, 1979)

$$\Sigma F = \frac{\partial}{\partial t}\left(\iiint_{CV} \rho v dV\right) + \iint_{CS} \rho v(v \cdot n)\, dA \qquad [3.14]$$

ΣF is the sum of the longitudinal forces on the pipe. From Figure 3.6, one can see that

$$\Sigma F = (P_1 - P_2) A - F_f \qquad [3.15]$$

F_f is given as

$$F_f = f L \rho v^2 A \qquad [3.16]$$

where f is a constant (1/m) corresponding to the longitudinal force that either the gas or the liquid within the pipe is exerting on the pipe. Recall that if any liquid is in the pipe, it is as though there is only liquid in the pipe.

Using equations [3.13], [3.15] and [3.16], equation [3.14] can be written

$$L_g \frac{d\rho_g}{dt} + L_l \frac{d\rho_l}{dt} + \left(\frac{\rho_g L_g}{v} + \frac{\rho_l L_l}{v}\right) \frac{dv}{dt} = \frac{P_1 - P_2 - fL\rho v^2}{v} \qquad [3.17]$$

Equation [3.17] is applied to each pipe, leading to NP equations (NP is the number of pipes in the feed system).

Figure 3.7 shows a pipe node.

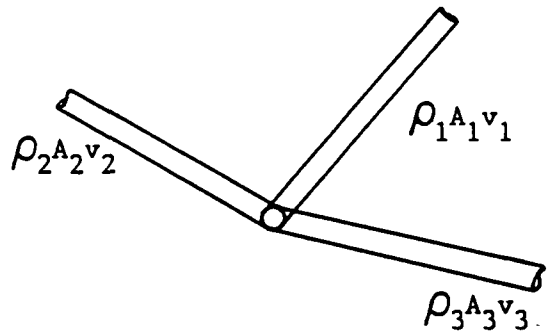

Figure 3.7: Schematic of a Pipe Node.

Since mass is not allowed to accumulate at the node, for NPN pipes connected at the node, conservation of mass for the node can be written

$$\sum_{n=1}^{NPN} (\rho_n A_n v_n) = 0 \qquad [3.18]$$

Equivalently,

$$\sum_{n=1}^{NPN} \frac{d}{dt} (\rho_n A_n v_n) = 0 \qquad [3.19]$$

Taking the derivative in [3.19] and assuming that the fluid in each pipe has the same density as the fluid in the others, equal to the density in the node, leads to

$$\frac{d\rho_n}{dt} \sum_{n=1}^{NPN} A_n v_n + \rho_n \sum_{n=1}^{NPN} A_n (dv_n/dt) = 0 \qquad [3.20]$$

[3.20] is applied to NN nodes, where NN is the number of nodes in the oxidizer feed system. The piping system equations are derived in greater detail in Appendix A.

Equations [3.17] and [3.20] constitute NN+NP equations in the NN unknown nodal densities and the NP unknown pipe velocities. This set of equations is linear and, at each time step, can be solved for dv_n/dt (n=1,2,3,... NP) and $d\rho_k/dt$ (k=1,2,3,... NN) .

3.3 THE EXIT TURBINE

Hot product gases pass through a turbine when exiting the fuel preburner. The mass flow rate of the gases through the turbine is a function of the pressure downstream of the turbine (PHG) and the inertia of the turbine blades, as well as the pressure in the combustion chamber. An equation which gives the mass flow rate through the turbine was given in the Dynamic Balance Model for the SSME (Nguyen, 1981) as

$$\dot{m} = c_{ftp} \left(\frac{P_c}{T_c}\right)^{0.5} \left[\left(\frac{PHG}{P_c}\right)^{1.43} - \left(\frac{PHG}{P_c}\right)^{1.71}\right]^{0.5} \qquad [3.21]$$

The parameter (c_{ftp}) is an empirical function of turbine geometry and speed. For this model, c_{ftp} is assumed to be constant during the short time duration of the chug. This implies that turbine speed decreases slowly.

3.4 SOLUTION OF THE GOVERNING EQUATIONS

Equations [3.9], [3.10], [3.11], [3.12], [3.17] and [3.20] were integrated numerically to give the values of T_c, P_c, σ_i (i=1,2,3,...NS), ρ_k (k=1,2,3,...NN), v_j (j=1,2,3,...NP) and L_g (position of the liquid/vapor interface in pipe j) (j=1,2,3,...NP) over time. The TSTR equations are nonlinear in the reaction rate expressions and the expression that give thermodynamic properties. Since the set of equations is also stiff (involving widely varying time constants), the IMSL math subroutine DGEAR was used to integrate the equations. DGEAR finds approximations to the solution of ordinary differential equations of the form

$$\vec{y}' = f(x,\vec{y})$$

for given initial conditions. The function $f(x,\vec{y})$ was calculated in a user supplied subroutine which was declared external in the main program and was accessed by DGEAR for each time step in the integration. A number of different integration methods were available in the DGEAR package. For most executions, the stiffness methods of Gear were used. Where possible, initial conditions were chosen to agree with experimental data. In other cases, when

experimental data were not available, "steady state" conditions were used as initial conditions. The selection of initial conditions is further discussed in Chapter IV.

Flow charts showing the solution process, a listing of program TRNCHG which was developed to solve the governing equations using DGEAR, a sample input file and sample output files are found in Appendix B.

CHAPTER IV

RESULTS

In Chapter III a Transient Stirred Tank Reactor (TSTR) model was proposed for predicting the transient behavior of the SSME fuelside preburner during the helium purge of the engine shutdown. Fuel feed rate is assumed constant, while the oxidizer feed system is modelled as a series of pipes and nodes and an injector resistance. The exiting fluid from the combustion chamber, containing gaseous products, gaseous reactants and liquid droplets, passes through an exit turbine.

A computer program, TRNCHG (Appendix B), was written to numerically integrate the resulting differential equations. From the results of TRNCHG it was possible to calculate the amplitude and frequency of oscillations in combustion chamber pressure and oxidizer mass flow rate. A number of engine parameters were varied to determine the role they play in the fuelside preburner chug and to demonstrate the reliability of TRNCHG. The parameters that were varied include the rate of heat transfer from the walls of the combustion chamber to the contents of the chamber, the mean droplet diameter, the fuel mass flow rate, the fuel temperature, the liquid oxygen (LOX) temperature, the temperature of the helium, and the length of the helium purge line (the pipe connecting the helium storage tank to the helium check valve (Figure 3.1, p. 43)) and the diameter of the helium purge line.

This chapter is a summary of the results of TRNCHG. All marked data points in the figures that follow were generated mathematically and were marked either to differentiate between curves on the same graph or to specify calculation points on curves drawn using few data points.

4.1 OPERATION OF THE FUELSIDE PREBURNER DURING THE SSME SHUTDOWN HELIUM PURGE

As described in Chapter I, during the SSME shutdown, gaseous helium pushes liquid oxygen from the oxidizer feed system of the fuelside preburner and into the combustion chamber. As outlined in Table 1.1 (page 7), just before the helium purge of the fuelside preburner begins, the fuelside preburner oxidizer valve (FPOV) is closed, so the velocity of the LOX in the preburner oxidizer feed system was set at 0.001 m/s (it was not set equal to zero because of the numerical difficulties arising from setting the velocity equal to zero). It is possible that a small amount of LOX enters the preburner combustion chamber between the time that the FPOV is closed and the valve that restrains the helium is opened. This is due to the heating and expansion of LOX in the pipe connecting the FPOV to the preburner manifold.

The pressure throughout the combustion chamber, oxidizer feed system and helium supply piping was assumed uniform and equal to the cracking pressure of the helium check valve, 5.17 MPa (750 psia).

The NASA SSME transient model predicts that the temperature in the fuelside preburner decreases at a rate of about 50 K/s (90°R/s) (Seymour, 1986) at the beginning of shutdown. Without any heat transfer from the chamber walls, TRNCHG predicts that the fuelside preburner temperature falls at a rate of 280,000 K/s when the helium check valves first open. Because the rate at which TRNCHG predicts the chamber temperature decays was too high, a rate of heat transfer to the chamber contents of 6.5×10^7 J/s (6.2×10^4 Btu/s) was selected for the TRNCHG helium purge simulation. This value was chosen because it made the initial temperature gradient predicted by TRNCHG closer to that predicted by the SSME transient model yet did not fix the chamber temperature. The selection of heat transfer rate will be further discussed in section 4.2.

At the beginning of the fuelside preburner helium purge, the pressure downstream of the exit turbine (PHG) is 2.41 MPa (350 psia). By the time the helium purge is over, PHG is 1.03 MPa (150 psia). The average value of PHG, 1.72 MPa (250 psia), was used for the helium purge simulation. The exit mass flow rate coefficient, c_{ftp}, was calculated using equation [3.21] (page 56). c_{ftp} was algebraically isolated and calculated by setting the initial exit mass flow rate equal to the fuel mass flow rate (which is constant during shutdown) and setting the chamber pressure equal to the initial chamber pressure, 5.17 MPa (750 psia). c_{ftp} was assumed constant during the short time duration of the chug.

No data on helium temperature in the helium line were available, so the temperature of the helium purge was set equal to the oxidizer temperature, 120 K (216°R).

A summary of inputs to TRNCHG for the SSME shutdown is given in Table 4.1.

Figure 4.1 shows TRNCHG's prediction for combustion chamber temperature during the helium purge. Time equal to zero corresponds to the time that the helium check valves are opened for this graph and all graphs generated for the SSME shutdown simulation. Chamber temperature falls until it reaches a fairly constant value, around 400 K (720°R). The steady value that the temperature reached was determined largely by the rate of heat transfer to the chamber contents. With no heat transfer, the steady state temperature is 188 K (338°R). Figure 4.1 includes only the first 25 msec of TRNCHG's predictions although the program was run until the helium/LOX interface in the oxidizer feed system reached the combustion chamber. Figure 4.2 is a plot of the mole number of oxygen vapor (kgmoles of oxygen vapor per mass (kg) in the combustion chamber) in the combustion chamber during shutdown versus time. The amount of oxygen vapor in the chamber rises sharply (from the program's minimum allowable value of 1.0×10^{-12} kgmoles/kg) to a steady value around 5×10^{-3} kgmoles/kg. The mole number of water vapor did not change significantly from the minimum allowable mole number.

Table 4.1: Inputs to TRNCHG for the SSME Shutdown Simulation

PARAMETER	VALUE AT THE BEGINNING OF THE SSME SHUTDOWN SIMULATION
Chamber Temperature	550 K (990°R)
Chamber Pressure	5.17 MPa (750 psia)
PHG	1.72 MPa (250 psia)
LOX Temperature	120 K (216°R)
Fuel Temperature	160 K (288°R)
Helium Temperature	120 K (216°R)
Fuel Mass Flow Rate	21.0 kg/s (46.3 lbm/s)
Heat Transfer Rate	6.5×10^7 J/s (6.2×10^4 Btu/s)
Pipe Length from the Helium Storage Tank to the Check Valve	1.5 m (4.9 ft)

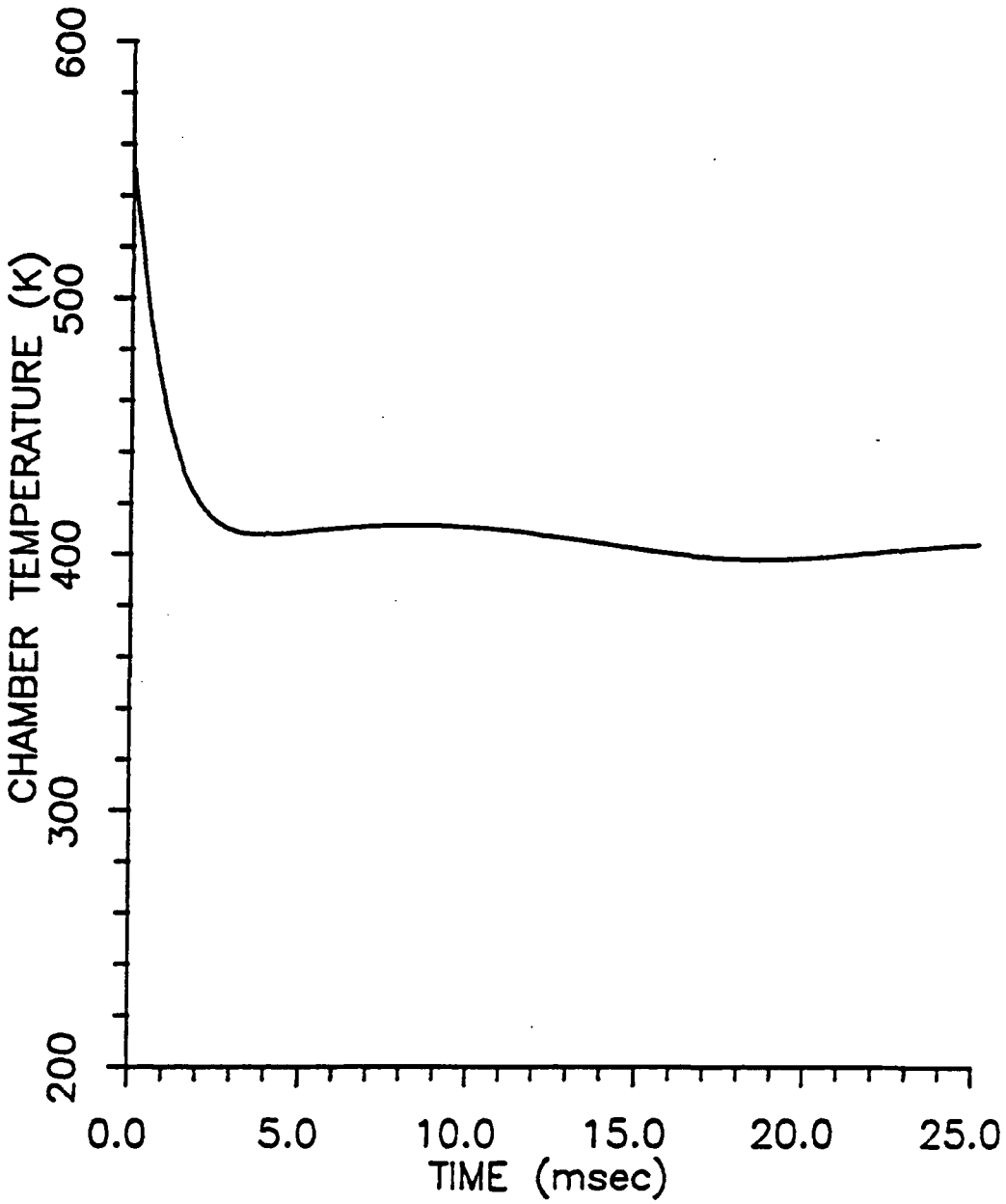

Figure 4.1: Temperature v. Time for SSME Shutdown

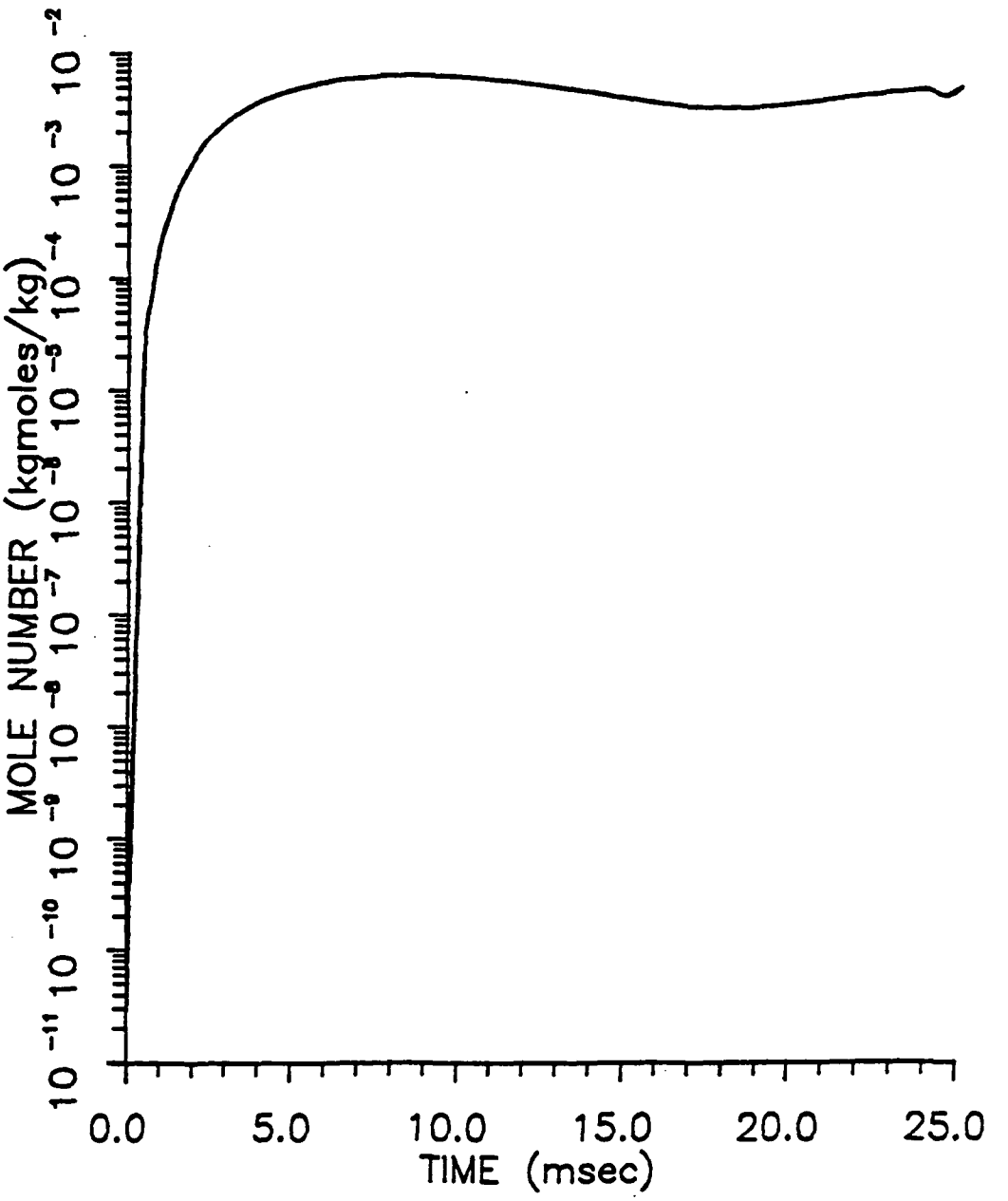

Figure 4.2: Mole Number of Oxygen Vapor in the Combustion Chamber v. Time for SSME Shutdown

As shown by Figures 4.1 and 4.2, TRNCHG predicts that ignition will not take place in the SSME fuelside preburner during the shutdown helium purge, contrary to the findings of test firings. There are two explanations for TRNCHG's incorrect prediction. First, using a TSTR model results in the overprediction of the equivalence ratio at which combustion takes place. In the heterogeneous stirred tank reactor, LOX vaporizes and the oxygen vapor is assumed to instantaneously mix with the gaseous contents of the combustion chamber. In actual droplet combustion, though, oxidizer and fuel burn on a diffusion flame surface around the droplet at a position where oxidizer and fuel meet in stoichiometric proportion. Thus, the TSTR model overpredicts the equivalence ratio at which combustion takes place; the mixture of gases is beyond the rich limits of combustion. Second, the kinetic mechanism and elementary reaction rate data used in TRNCHG may be inaccurate at the temperatures and pressures that are found in the preburner during the helium purge.

Since use of chemical kinetics in the calculation of combustion rate resulted in erroneous predictions, a second combustion model was used to predict preburner behavior during shutdown. All the LOX that was vaporized was assumed to immediately combust with hydrogen to form water vapor (i.e., chemical kinetics were assumed to be infinitely fast). Figure 4.3 shows TRNCHG's prediction of chamber pressure using this second combustion model and Figure 4.4 shows the predicted oxidizer mass flow rate. The symbols mark each third analytically generated data point. TRNCHG was allowed to run until

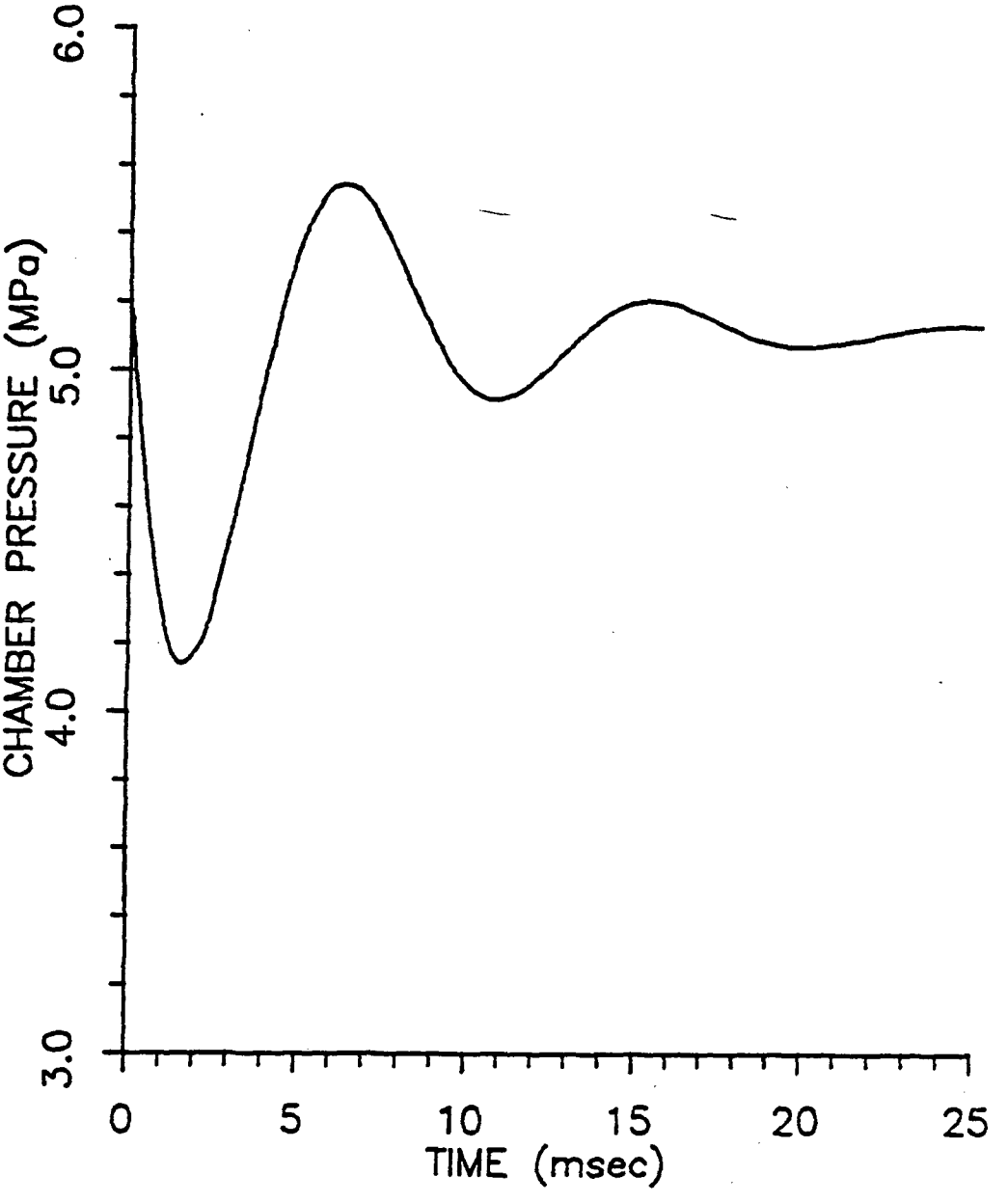

Figure 4.3: Chamber Pressure v. Time for the SSME Shutdown
(Infinitely Fast Chemical Kinetics)

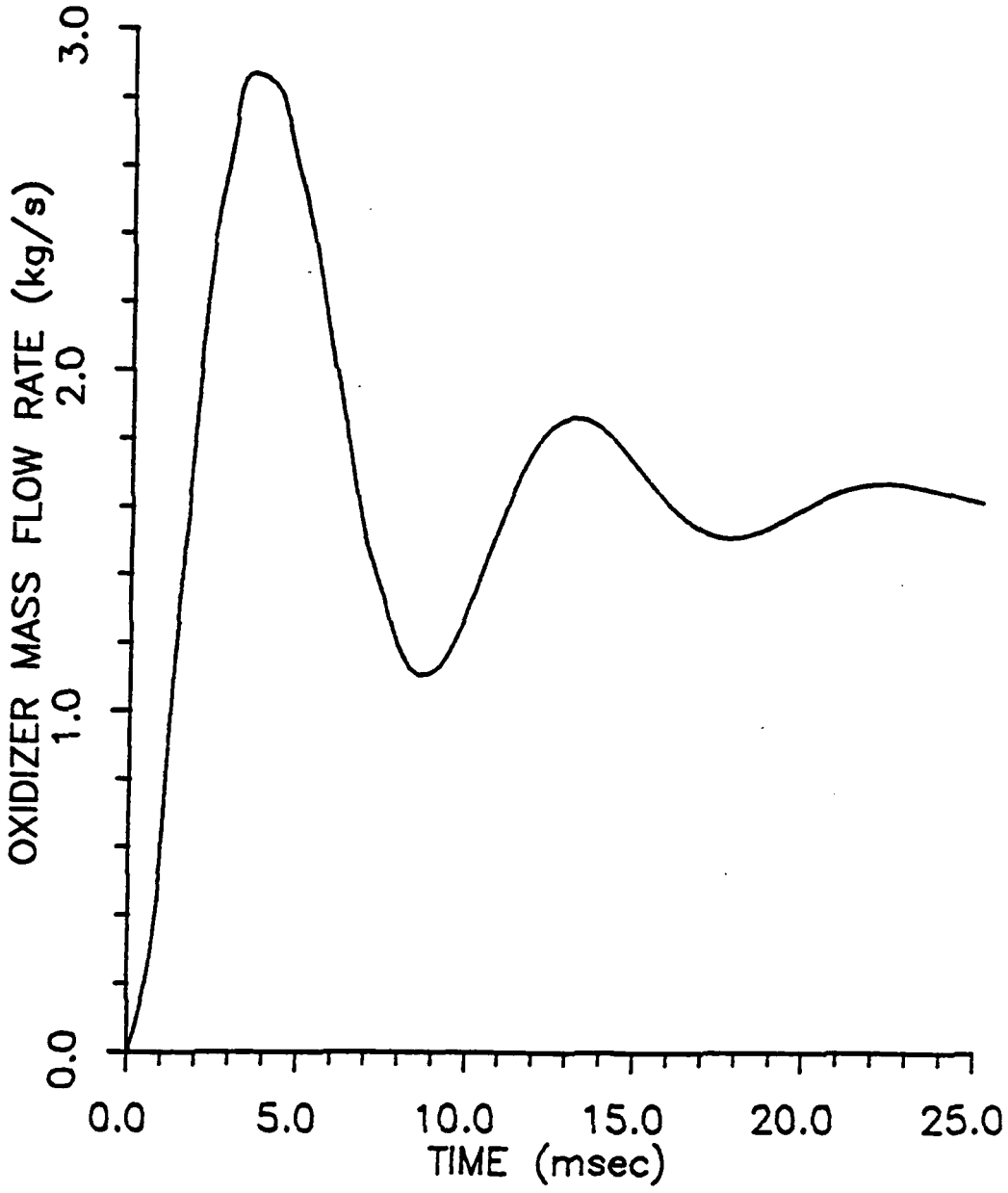

Figure 4.4: Oxidizer Mass Flow Rate v. Time for the SSME Shutdown (Infinitely Fast Chemical Kinetics)

the helium/LOX interface entered the combustion chamber, but only the first 25 msec of the run is shown in Figures 4.3 and 4.4, since no oscillations took place after that time. The initial peak to peak amplitude of the pressure oscillation is 1.4 MPa (200 psia) and the frequency of the oscillation is 111 Hz. The amplitude and frequency of pressure oscillations during an actual typical preburner chug are 2.41 MPa (350 psia) and 117 Hz, respectively. Oscillations in the chamber pressure and oxidizer mass flow rate are about 1/5 cycle more than 180° out of phase, due to the vaporization time delay.

To investigate the possibility that a disturbance in chamber pressure (for example, due to a change in the oxidizer preburner combustion chamber pressure) incites the fuelside preburner chug when the helium/LOX interface has progressed nearly to the combustion chamber, a perturbation was applied in TRNCHG at 50 msec. The system was perturbed by changing the constant, c_{dm}, in the expression for mean droplet diameter (equation [3.1], page 44). c_{dm} was changed from 0.485 to 20.0 at time equal to 50 msec. After 2.5 msec the value of c_{dm} was returned to 0.485. While c_{dm} was equal to 20.0, the vaporization rate decreased since the droplets were larger and the ratio of the surface area of liquid to the mass of liquid in the combustion chamber decreased. Because of the subsequent decrease in the evaporation rate of the LOX, liquid accumulated in the combustion chamber. When the value of c_{dm} was returned to 0.485, the accumulated liquid burned quickly and the chamber pressure rose sharply. The resulting chamber pressure

oscillations are shown in Figure 4.5. Once again, chamber pressure oscillations damped quickly.

Assuming infinitely fast chemical kinetics, TRNCHG did not predict sustained oscillations in chamber pressure. As described earlier, a number of the engine parameters used in this base case simulation of the SSME shutdown were selected as best guesses of the actual conditions that exist in the fuelside preburner during shutdown. To determine whether or not a change in engine parameters could incite a chug, engine parameters were varied, one at a time. In many cases a small change in an engine parameter had a large influence on preburner stability. Following is a summary of the predictions of TRNCHG when engine parameters were varied.

4.2 THE EFFECT OF HEAT TRANSFER RATE ON PREBURNER OPERATION

As discussed in section 4.1, in order for TRNCHG's prediction of initial temperature gradient to be equal to that predicted by the NASA SSME transient model, there must be heat transfer to the combustion chamber contents. Care had to be taken in choosing this rate of heat transfer, since data from which heat transfer rate could be calculated was not available and since heat transfer rate has such a large effect on the chamber temperature.

TRNCHG was executed using different rates of heat transfer and no oxidizer mass flow to find the temperature that the chamber contents would eventually reach. These steady state temperatures are

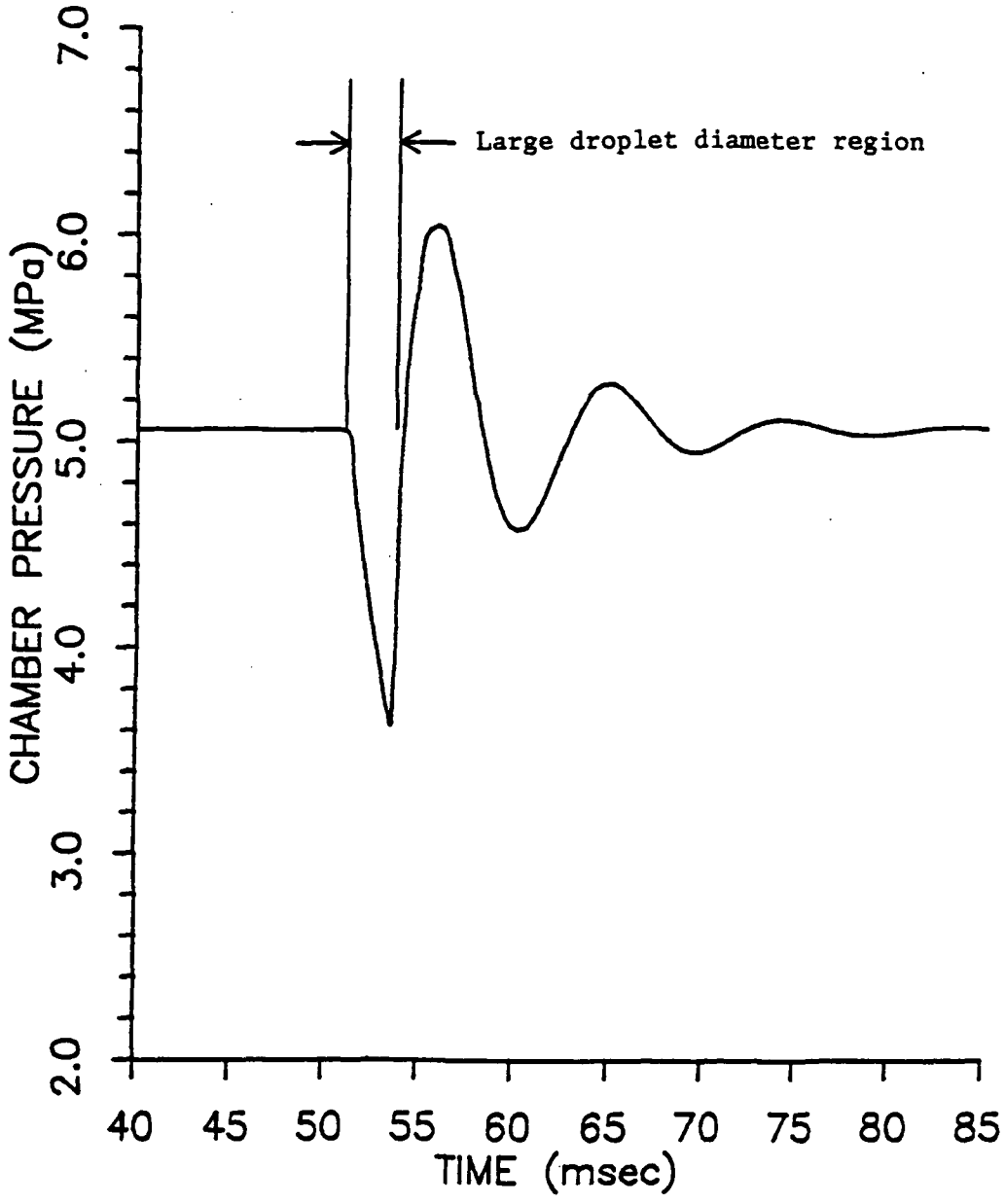

Figure 4.5: Preburner Response to a Perturbation During Shutdown (Infinitely Fast Chemical Kinetics)

plotted against heat transfer rate in Figure 4.6. High heat transfer rates have the effect of fixing chamber temperatures; even in the absence of combustion, the chamber temperature will never fall below the steady state temperature for a given heat transfer rate.

Figure 4.7 is a plot of chamber pressure versus time for heat transfer rates of 0 J/s, 7.5×10^7 J/s and 1.0×10^8 J/s. For higher heat transfer rates there is less oscillation in the chamber pressure than for the lower rates. Frequency of the oscillations remains the same for all the rates of heat transfer.

4.3 THE EFFECT OF DROPLET SIZE ON PREBURNER OPERATION

Mean droplet diameter proved very important in determining the operation of the fuelside preburner. to vary the mean droplet diameter, the constant, c_{dm}, in equation [4.1], was given the values 0.0485, 0.97, 1.94 and 3.88. These droplet coefficient values resulted in mean droplet diameters (averaged over the 25 msec shown in Figure 4.8) of 1.2 μm, 24.4μm, 63μm and 440μm, respectively. Note that changing c_{dm} changed the droplet diameter both directly and indirectly, since different values of c_{dm} lead to different values of average chamber pressure and oxidizer mass flow rate. Figure 4.8 shows predicted chamber pressure for the four values of the droplet coefficient and Figure 4.9 shows oxidizer mass flow rate. For c_{dm} below 1.0, pressure oscillations damp quickly. For c_{dm} greater than 1.0, oscillations become more sustained, until droplet size becomes

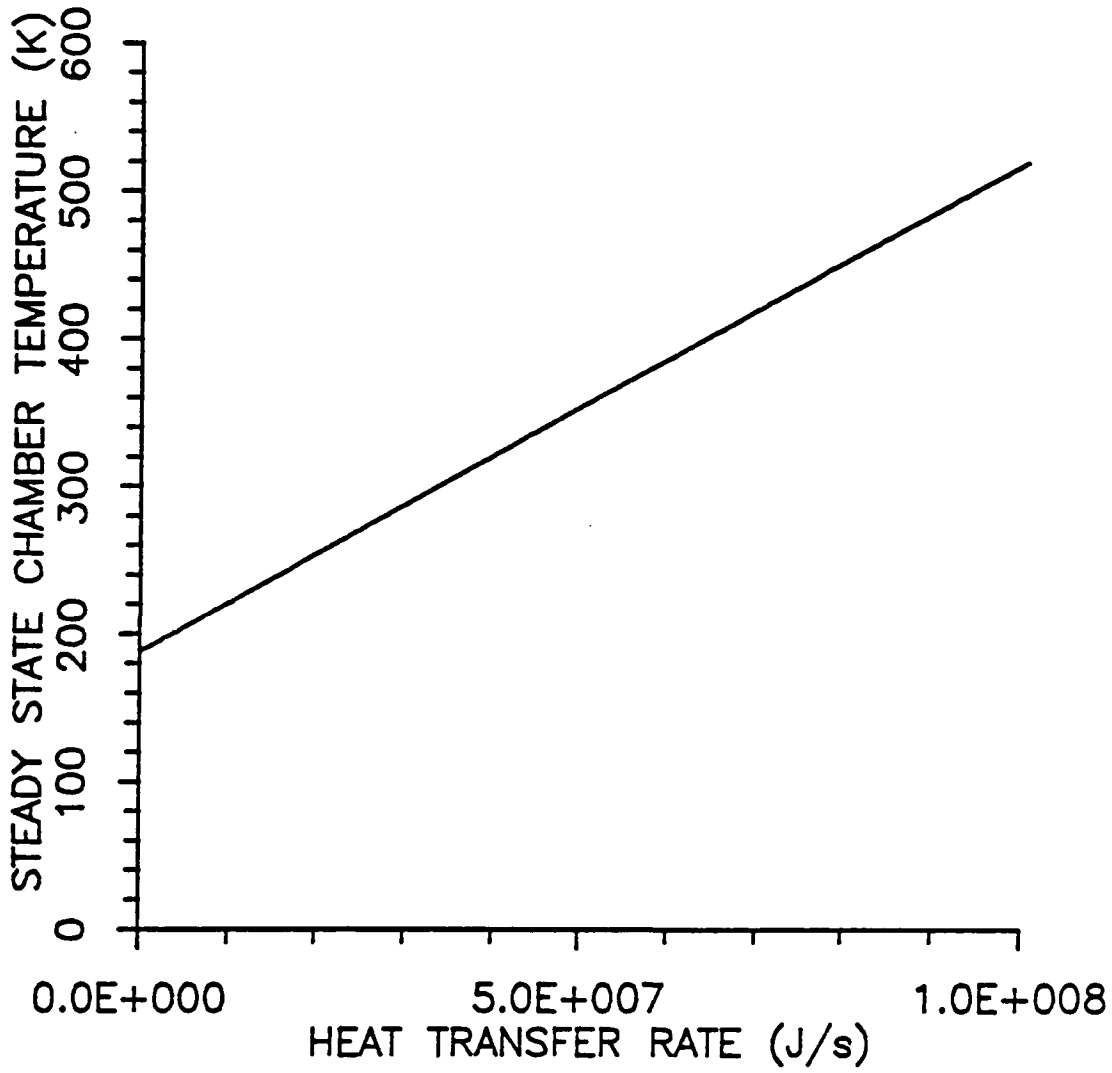

Figure 4.6: Steady State Temperature v. Heat Transfer Rate

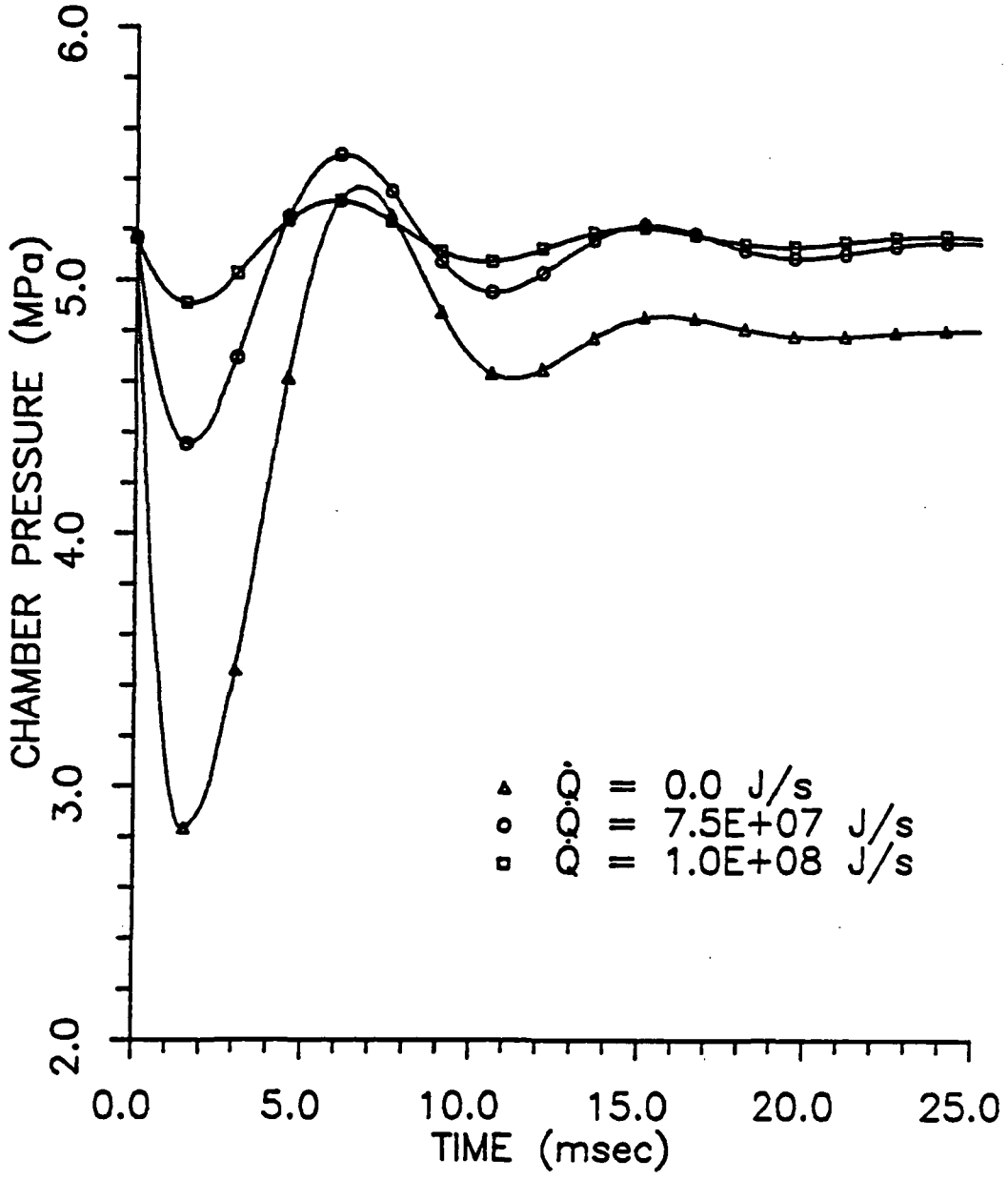

Figure 4.7: The Effect of Heat Transfer Rate on Chamber Pressure Oscillations

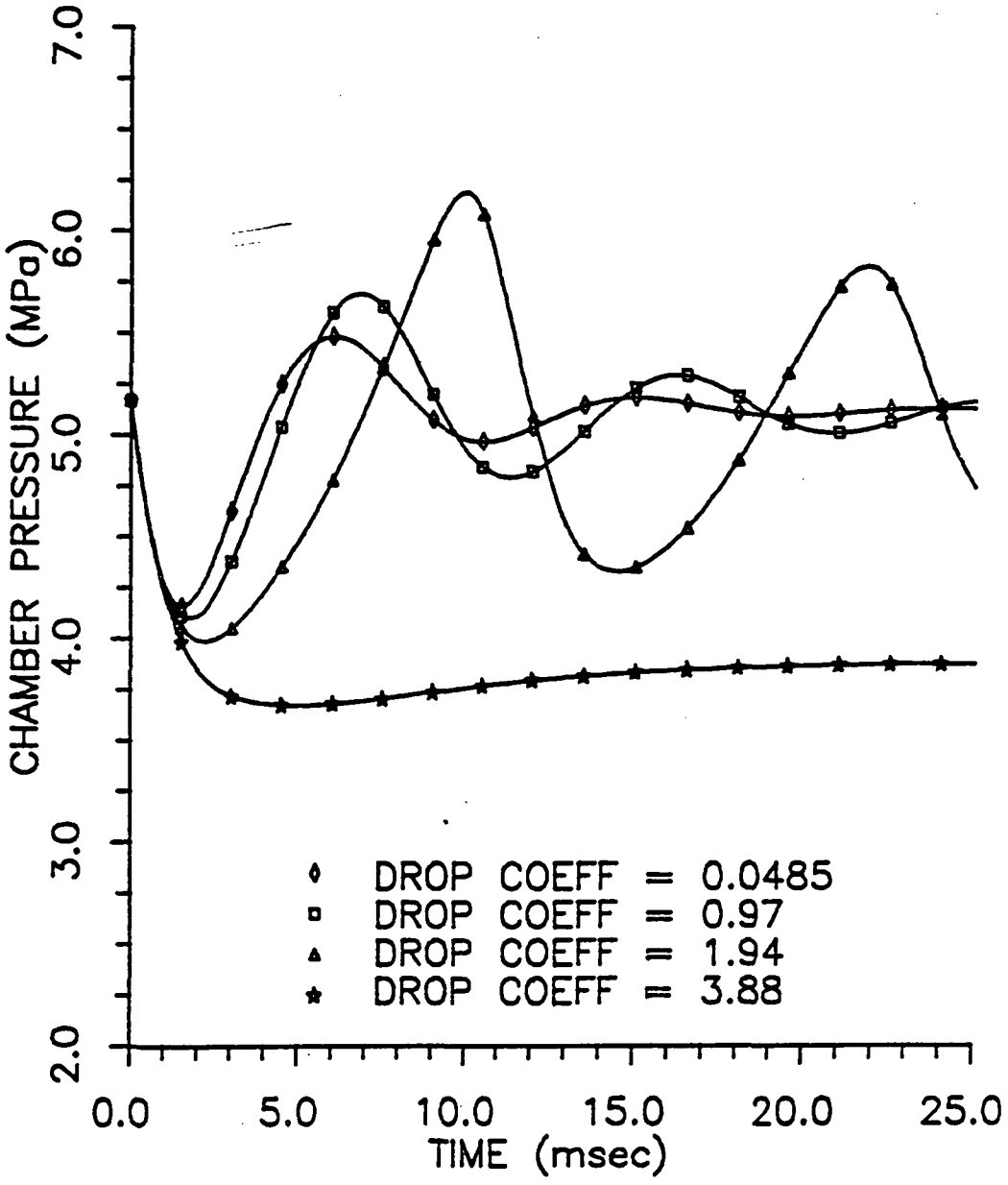

Figure 4.8: The Effect of Mean Droplet Diameter on Chamber Pressure Oscillations

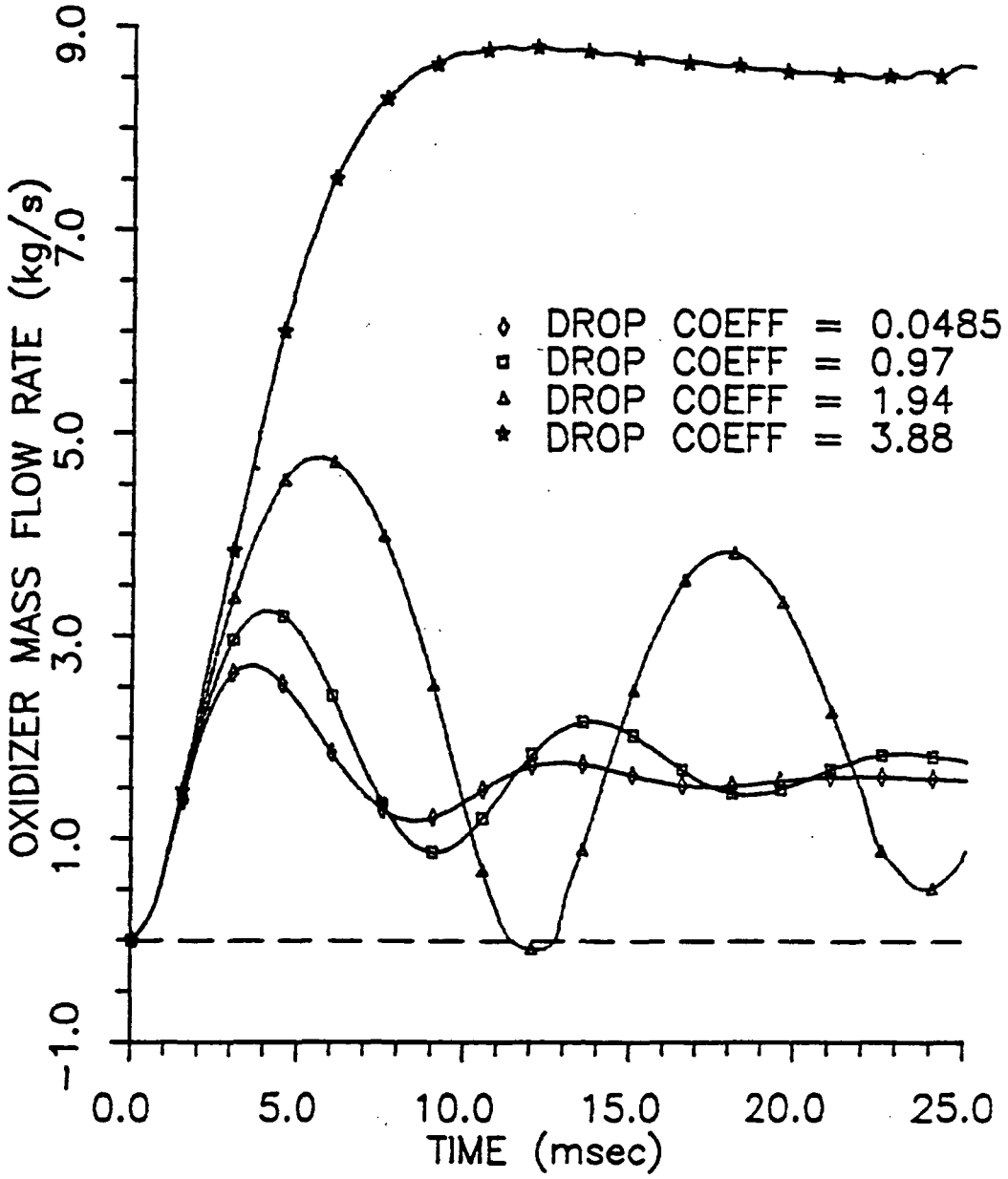

Figure 4.9: The Effect of Mean Droplet Diameter on Oxidizer Mass Flow Rate

so large that vaporization rate becomes very small (due to limited droplet surface area) and reaction blows off, as shown by the curve for c_{dm} = 3.88. For c_{dm} = 0.0485 the frequency of the pressure oscillation is 116 Hz. For c_{dm} = 1.97 the frequency is 83 Hz. For c_{dm} = 1.97 backflow of combustion chamber contents into the oxidizer feed system is predicted, as shown in Figure 4.9.

As seen in Figure 4.8, there is probably some critical mean droplet diameter (or equivalently, some critical combustion delay time) at which the fuelside preburner begins to undergo unstable operation. The critical diameter could be reached by changing the injector geometry or the fuel mass flow rate. The effect of fuel mass flow rate on the fuelside preburner is described in section 4.5. Since, in the absence of chemical kinetics, the value of c_{dm} determines the combustion time delay, c_{dm} could be raised to increase the combustion time delay and account for chemical kinetics. The exact amount that c_{dm} would have to be raised was not calculated by the author.

4.4 THE EFFECT OF THE OXIDIZER FEED SYSTEM ON PREBURNER OPERATION

TRNCHG was executed for LOX temperature equal to 90 K, 100 K, 120 K and 150 K (162°R, 180°R, 216°R and 270°R). All the other engine parameters were the same as those given in Table 4.1 (page 64). Decreasing the LOX temperature increases the LOX density and decreases the LOX vaporization rate in the combustion chamber.

Predicted chamber pressure is plotted against time in Figure 4.10. As predicted by Lim (1986), lower oxidizer temperatures resulted in less stable preburner operation (i.e., larger amplitude pressure oscillations that damped more slowly).

The frequency of chamber pressure oscillations is plotted against LOX temperature in Figure 4.11. As LOX temperature is decreased, oscillation frequency decreases slightly.

In this study, the term amplitude ratio refers to the ratio of the peak to peak amplitude of the second chamber pressure oscillation to the peak to peak amplitude of the first oscillation. It is used as a measure of the rate at which pressure oscillations damp out. Amplitude ratio is plotted against LOX temperature in Figure 4.12. The amplitude ratio rises linearly as LOX temperature is decreased from 150 K to 100 K. As LOX temperature is decreased below 100 K, the amplitude ratio increases more slowly.

4.5 THE EFFECT OF THE FUEL FEED SYSTEM ON PREBURNER OPERATION

Two fuel feed system parameters, the fuel temperature and the fuel mass flow rate, were varied in TRNCHG. As predicted by Lim (1986), lower fuel temperature led to sustained pressure oscillations. Contrary to Lim's predictions, fuel mass flow rate also influenced the preburner's stability.

TRNCHG was executed for fuel temperatures of 50 K, 100 K and 200 K (90°R, 180°R and 360°R). The resulting chamber pressure was

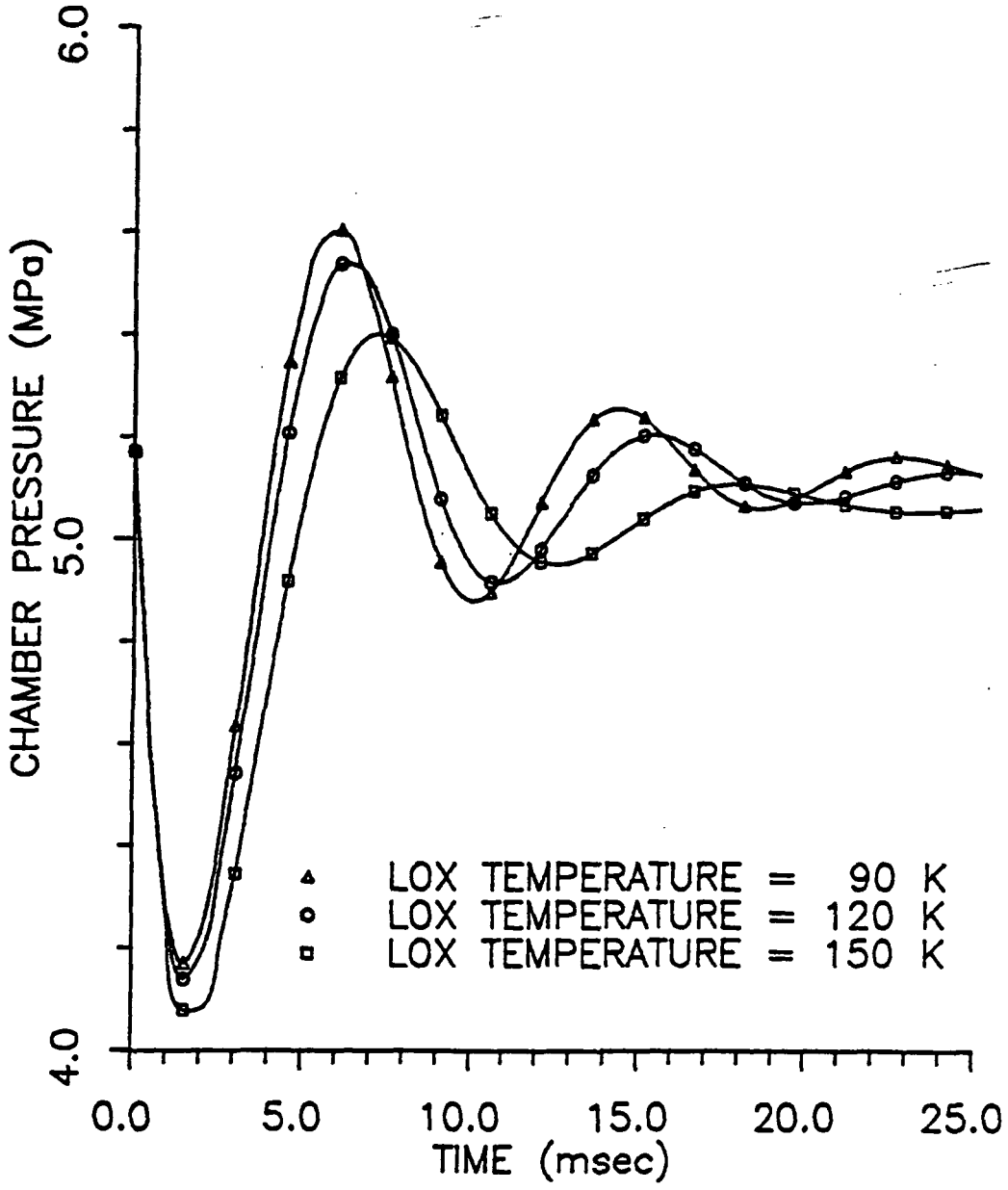

Figure 4.10: The Effect of Oxidizer Temperature on Chamber Pressure Oscillations

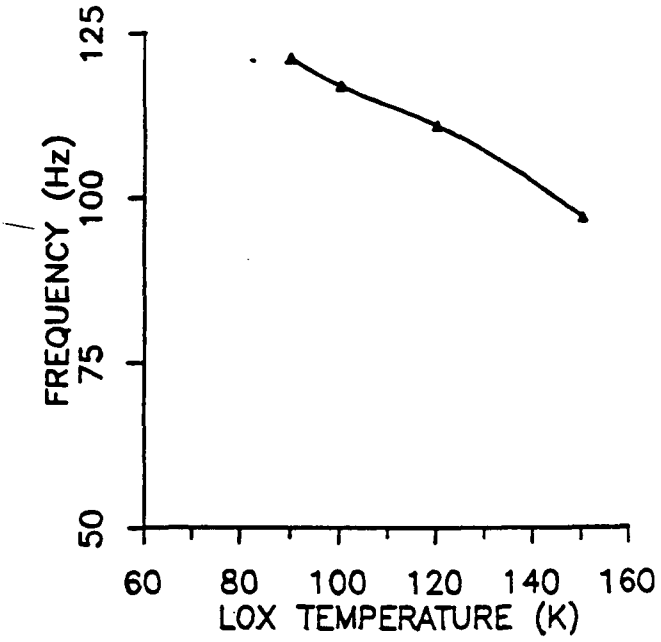

Figure 4.11: Pressure Oscillation Frequency v. LOX Temperature

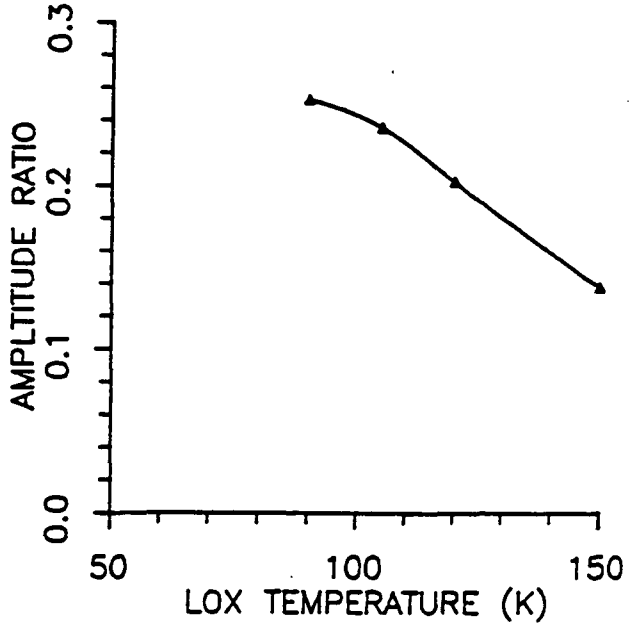

Figure 4.12: Amplitude Ratio v. LOX Temperature

plotted against time in Figure 4.13. Lower fuel temperatures resulted in more slowly damped pressure oscillations of greater amplitude and lower frequency. Oscillation frequency is plotted against fuel temperature in Figure 4.14. Frequency does not change much with temperature until the temperature becomes less than about 120 K, where frequency decreases rapidly as fuel temperature is decreased.

In Figure 4.15, chamber pressure was plotted against time for executions of TRNCHG using fuel mass flow rates of 12 kg/s, 18 kg/s and 25 kg/s. So that the results of these executions were not obscured by heat transfer rate to the chamber contents, the heat transfer rate was assumed to be 0.0 J/s for these runs. The fuel mass flow rate did not effect the pressure oscillation frequency, but did influence the rate at which the oscillations damped. The average oxidizer mass flow rate is plotted against the fuel mass flow rate in Figure 4.16.

The average oxidizer mass flow rate rises almost linearly with fuel mass flow rate. For high mass flow rates (greater combustion chamber throughput), more energy is needed to heat the fuel that does not participate in combustion and hot product gases are quickly swept from the combustion chamber. This leads to lower chamber pressures which lead to higher oxidizer mass flow rates.

As mentioned above, Lim (1986) predicted that fuel mass flow rate is not important in the fuelside preburner chug. The unexpected behavior of chamber pressure oscillations as mass flow rate is

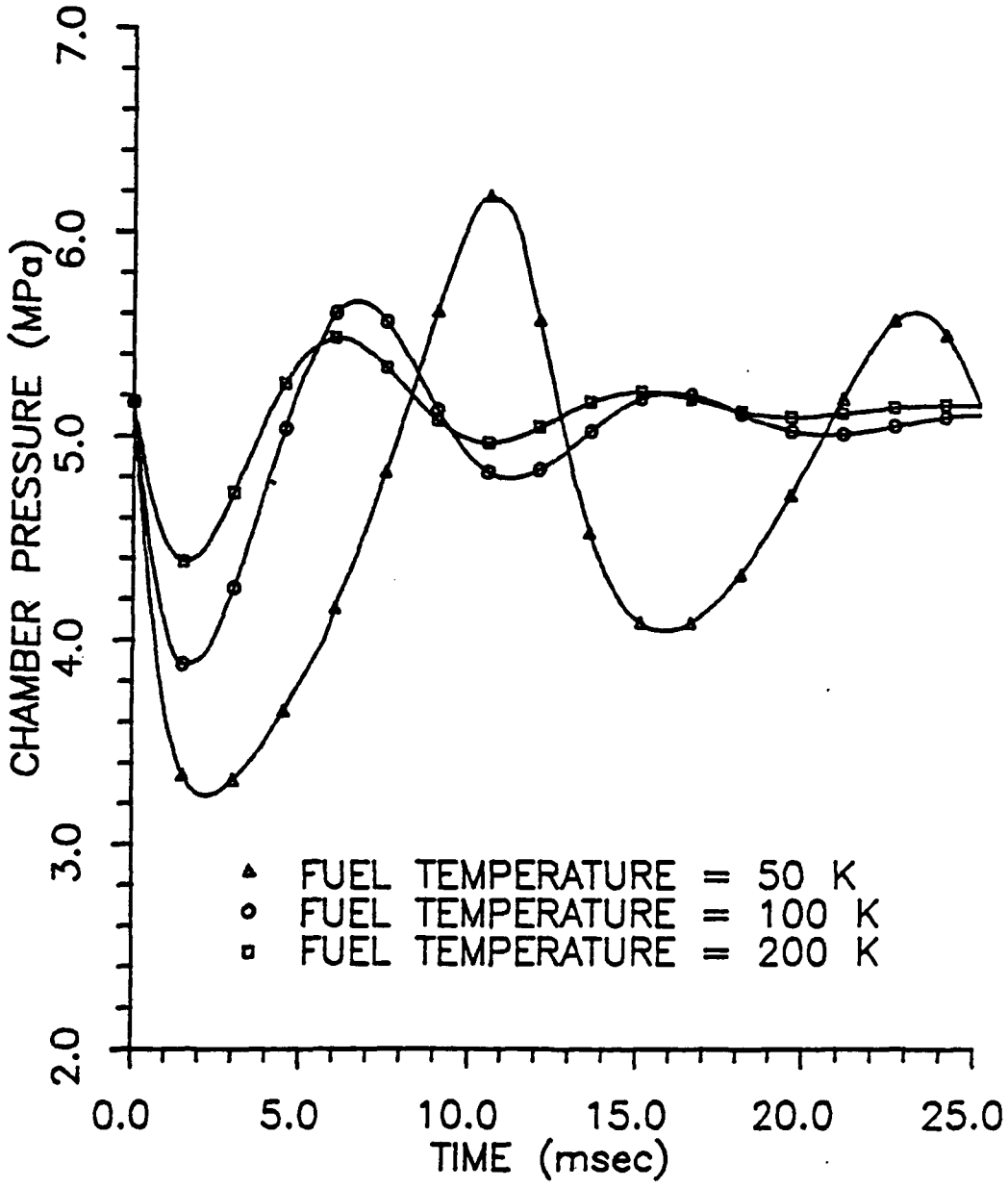

Figure 4.13: The Effect of Fuel Temperature on Chamber Pressure Oscillations

C - 2

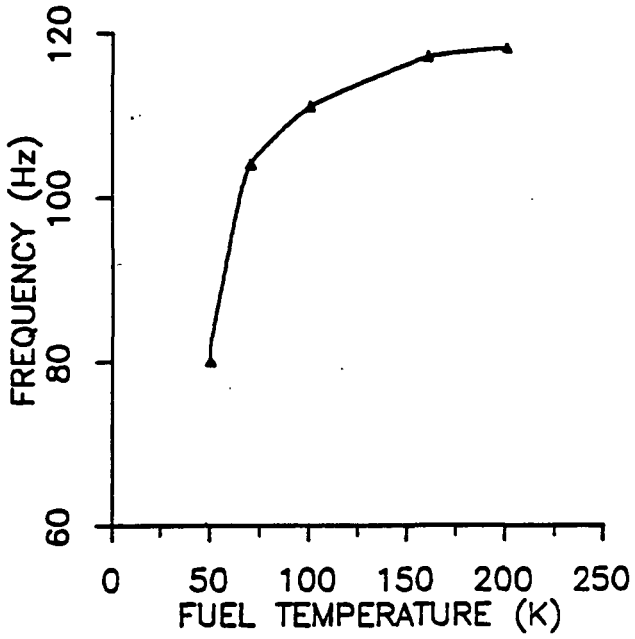

Figure 4.14: Pressure Oscillation Frequency v. Fuel Temperature

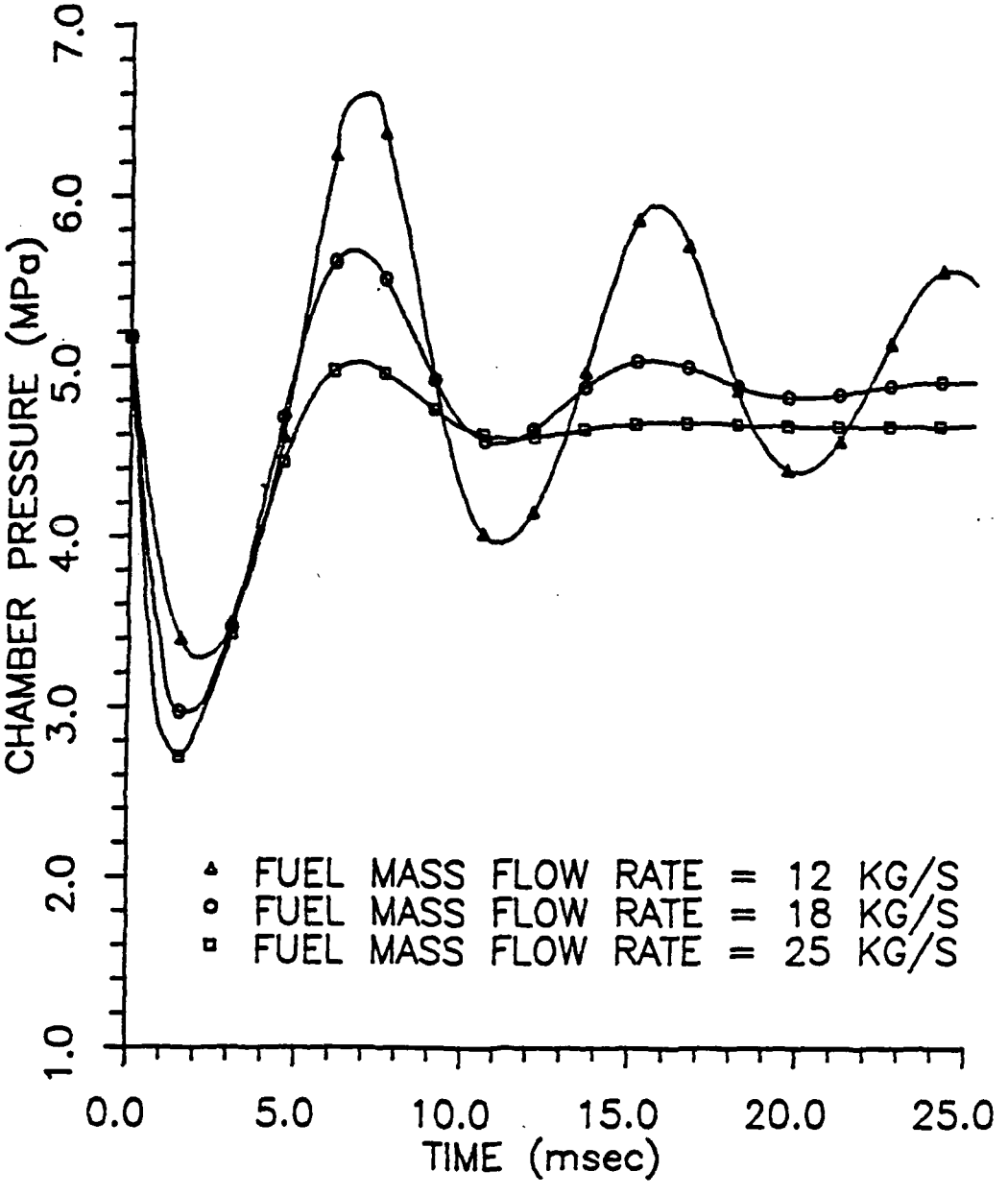

Figure 4.15: The Effect of Fuel Mass Flow Rate on Chamber Pressure Oscillations

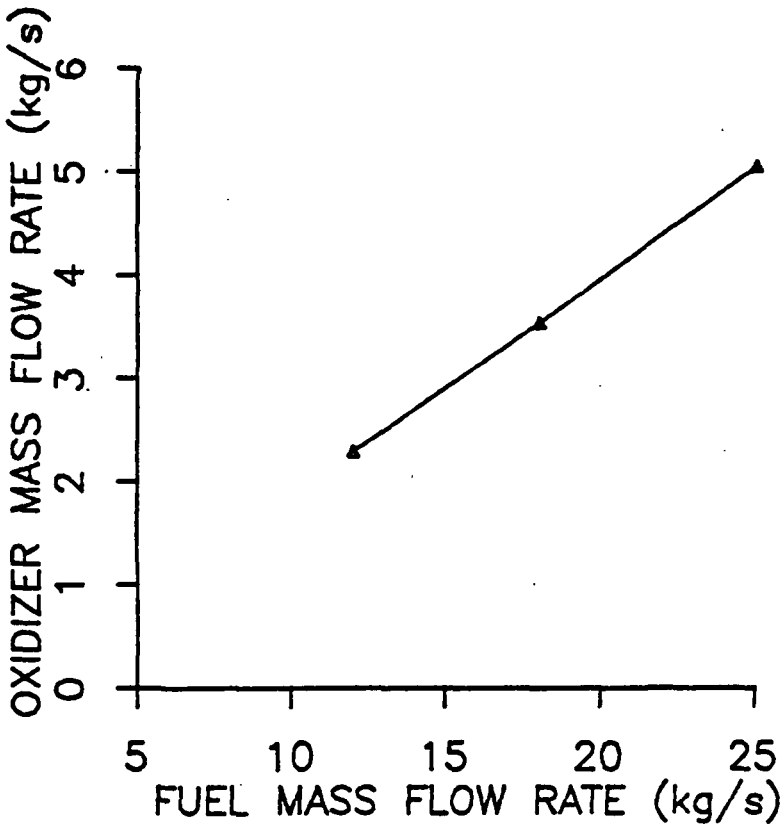

Figure 4.16: Oxidizer Mass Flow Rate v. Fuel Mass Flow Rate

changed is attributed to oscillations in chamber temperature. Recall that the fuelside preburner operates very fuel rich and that the incoming fuel is quite cold (160 K [288°R]). For a high fuel mass flow rates, much of the energy liberated by combustion raises the temperature of the hydrogen (most of which does not participate in chemical reactions) to the chamber temperature; there is not enough energy to raise the temperature much above the chamber temperature and sustain oscillations. For a lower mass flow rate, less energy is needed to heat the incoming hydrogen to the chamber temperature,so an oscillation in chamber temperature and an oscillation in chamber pressure can be sustained.

4.6 THE EFFECT OF THE EXIT TURBINE ON PREBURNER OPERATION

During shutdown, the pressure downstream of the exit turbine, PHG, falls from 2.41 MPa (350 psia) to 1.03 MPa (150 psia). It is possible that this change plays a part in inciting the fuel preburner chug. Figure 4.17 contains plots of chamber pressure versus time for PHG equal to 1.03 MPa, 1.72 MPa and 2.41 MPa. Frequency of the pressure oscillations is the same for all three values of PHG. The rate at which the oscillations are damped is smaller for lower values of PHG, as shown in Figure 4.18. Although changing the pressure downstream of the exit turbine did not produce chugging by itself, this change probably plays a part in the onset of chug.

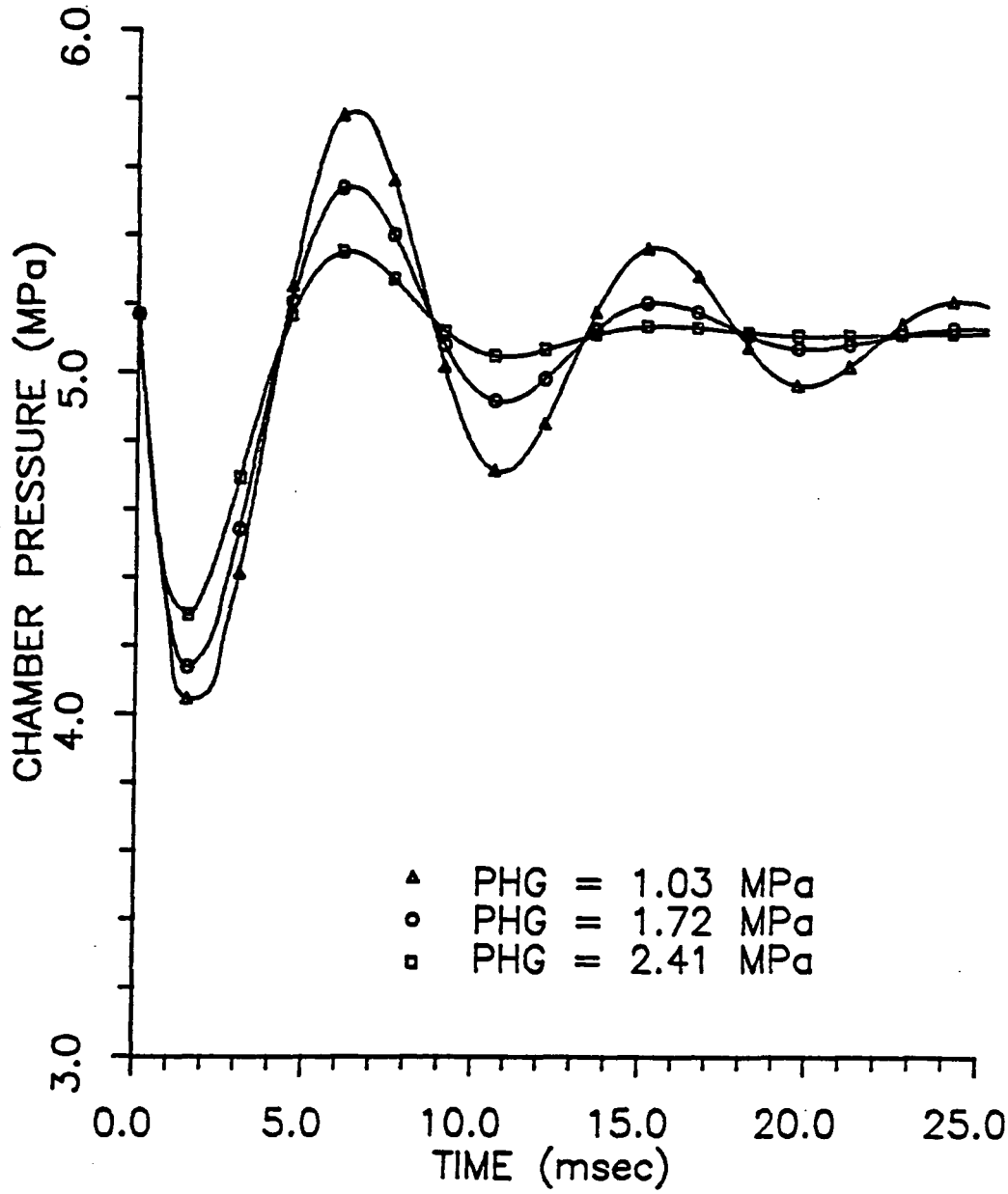

Figure 4.17: The Effect of the Pressure Downstream of the Exit Turbine on Chamber Pressure Oscillations

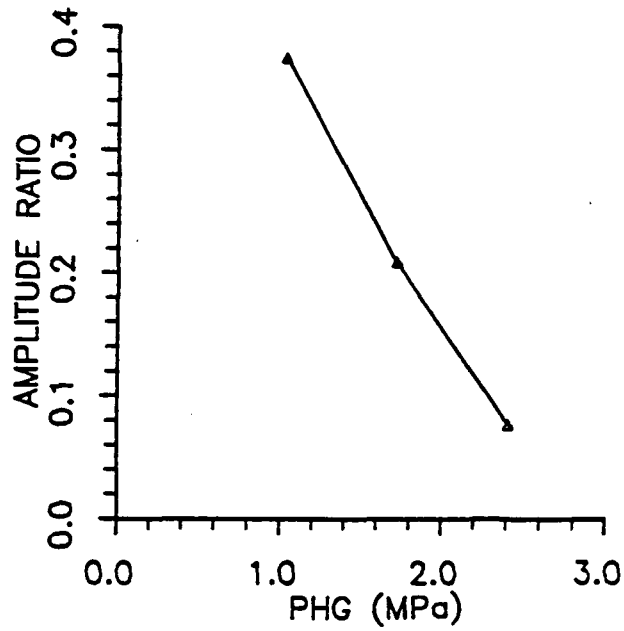

Figure 4.18: Amplitude Ratio v. Pressure Downstream of the Exit Turbine

4.7 THE EFFECT OF THE HELIUM PURGE ON PREBURNER OPERATION

At the onset of this research, it was thought that oscillations in helium density in the oxidizer feed system were at least partly responsible for the occurrence of the fuelside preburner chug. In section 4.1 it was shown that, even when the oxidizer feed system was almost completely filled with helium, a perturbation did not result in chug, so the presence of helium does not single-handedly bring about chug. To see what effect the presence of helium does have on fuel preburner operation, the temperature of the helium (assumed to be uniform and constant) and the helium purge line diameter and length were varied.

No data were available for the temperature of the helium at the helium check valve, so the temperature was initially assumed to be equal to the LOX temperature, 120 K (216°R). In Figure 4.19, chamber pressure is plotted against time for helium temperatures of 50 K, 150 K, 200 K and 300 K. Figure 4.20 shows the variation of the frequency of chamber pressure oscillations with helium temperature and Figure 4.21 shows the variation with helium temperature of the ratio of the peak to peak amplitudes of the second and first pressure oscillations. Higher helium temperatures lead to higher frequency pressure oscillations that damp more slowly. In the absence of helium, higher temperatures in the oxidizer feed system lead to more stable operation. Helium temperature reverses this

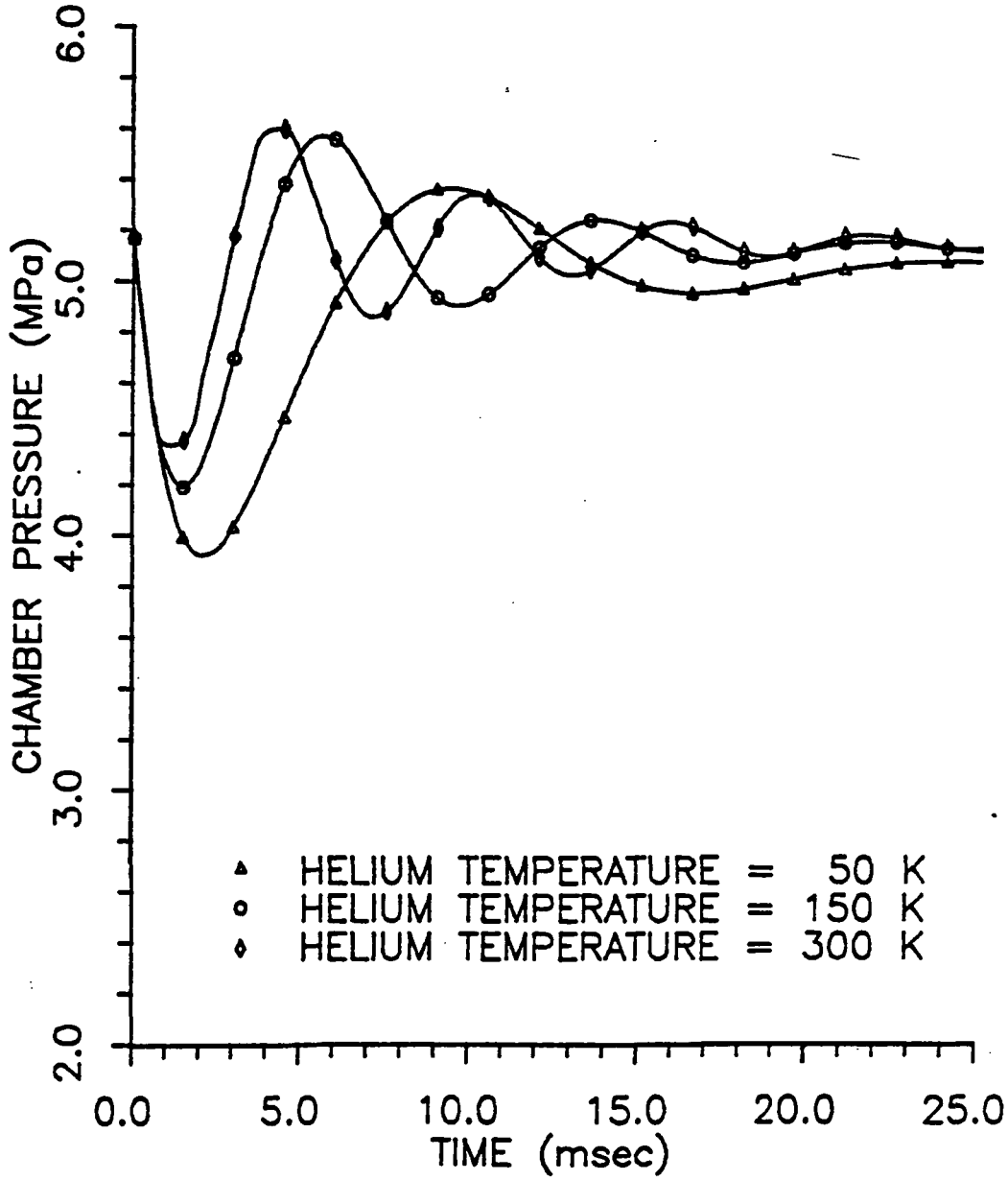

Figure 4.19: The Effect of Helium Temperature on Chamber Pressure Oscillations

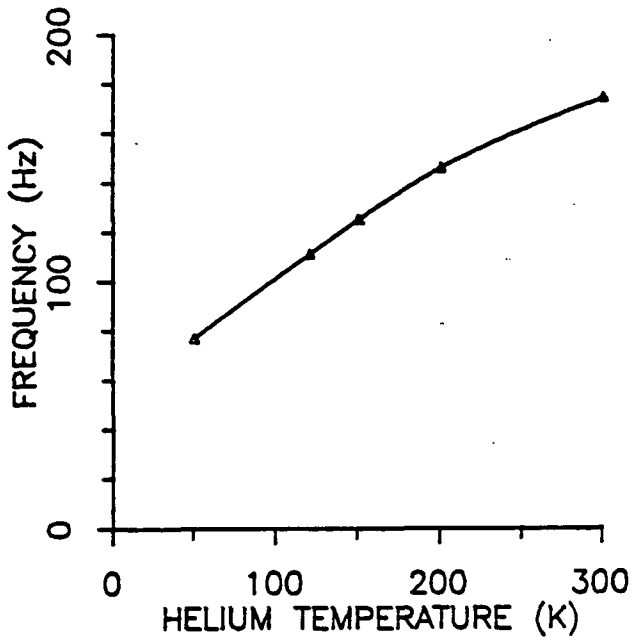

Figure 4.20: Pressure Oscillation Frequency v. Helium Temperature

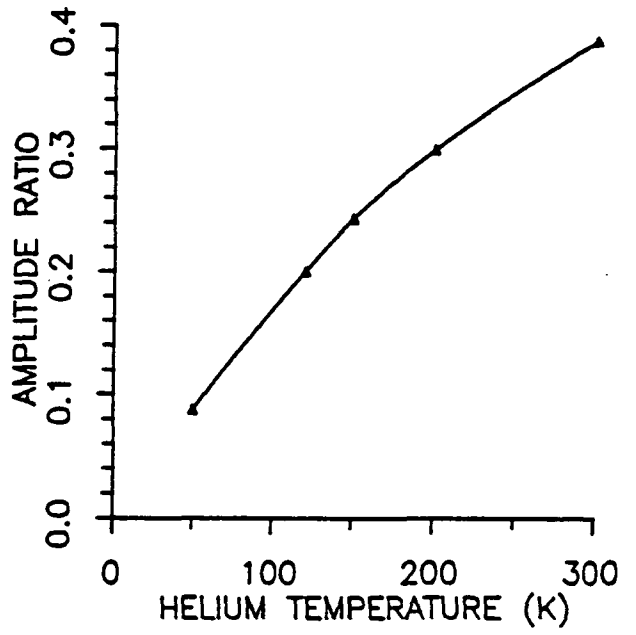

Figure 4.21: Amplitude Ratio v. Helium Temperature

trend. The presence of helium in the oxidizer feed system results in less stability for higher temperatures in the oxidizer feed system. The initial amplitude of pressure oscillations differed only slightly for the different helium temperatures.

As predicted by Summerfield (1951), shorter pipe lengths lead to chug. Figure 4.22 is a plot of chamber pressure versus time for the fuelside preburner for no helium purge line (i.e., for the helium tank mounted directly on the helium check valve). Execution of TRNCHG was halted after 8.3 msec because execution became very slow. For no helium line, the preburner undergoes undamped oscillations in chamber pressure and backflow of chamber contents into the oxidizer feed system.

Figure 4.23 is a plot of chamber pressure versus time for helium purge line lengths of 0.5 m and 2.0 m. Oscillation frequency and the ratio of the peak to peak amplitude of the second oscillation to that of the first are plotted against helium line length in Figures 4.24 and 4.25, respectively. Both the frequency and amplitude ratio rise sharply for helium line lengths below 0.5 m.

TRNCHG was executed using helium purge line diameters of 1.029 cm, 0.739 cm, 0.381 cm and 0.178 cm (0.4", 0.291", 0.381" and 0.15"). The resulting plots of chamber pressure versus time are found in Figure 4.26. For a helium purge line diameter of 0.178 cm, TRNCHG was unable to dependably calculate chamber pressure after about 5 msec because of numerical instability. The velocity of the

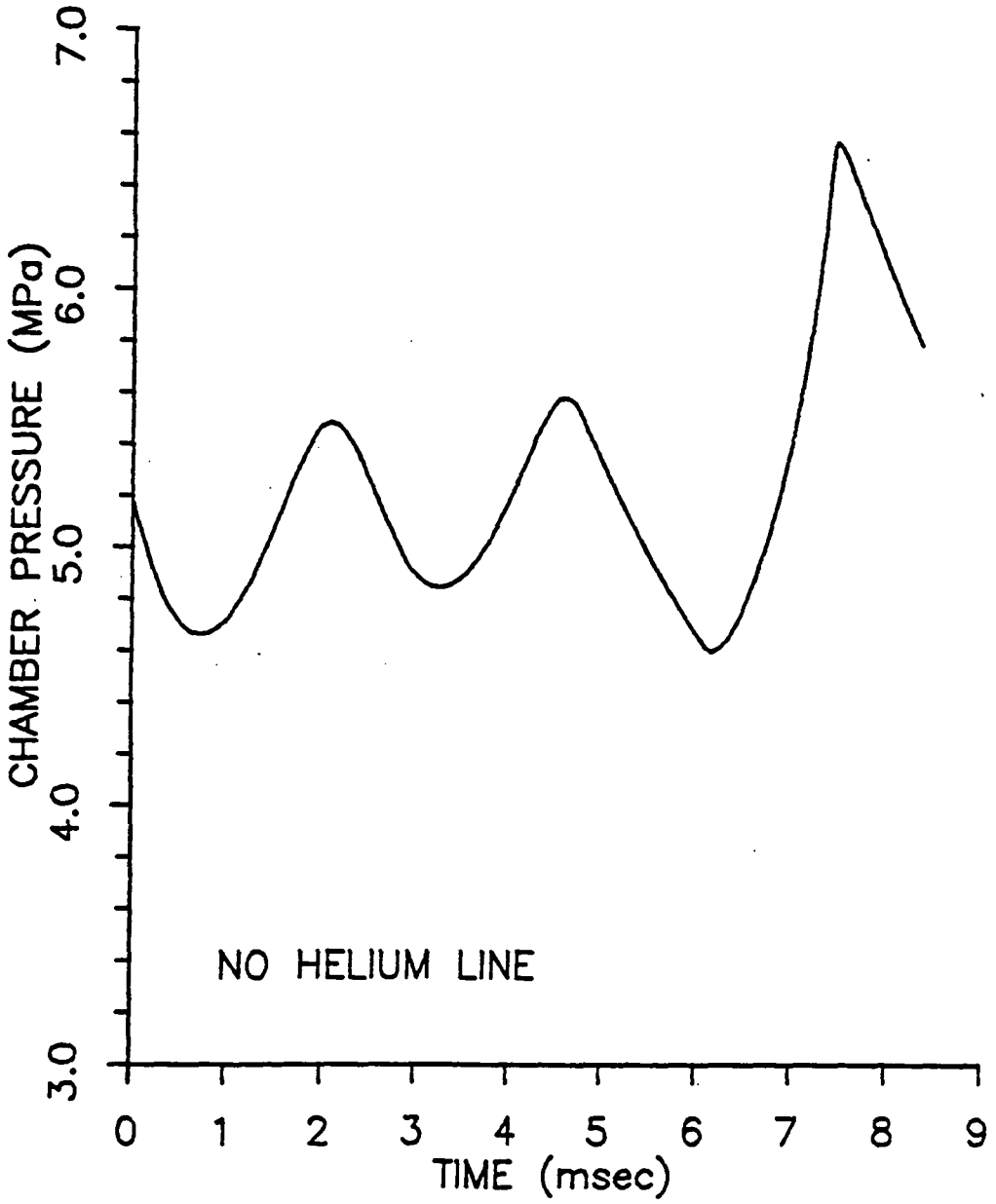

Figure 4.22: Chamber Pressure v. Time, No Helium Purge Line

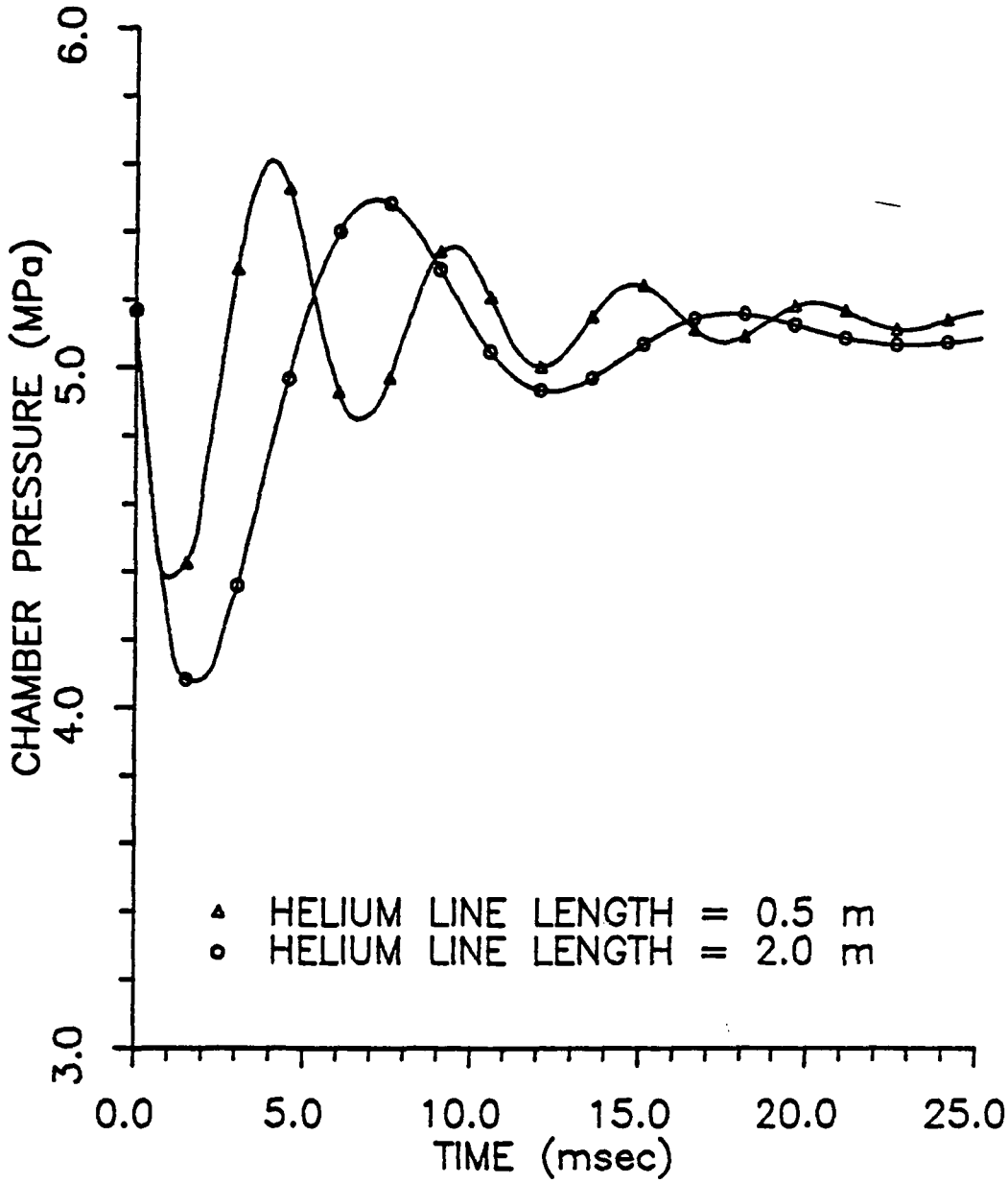

Figure 4.23: The Effect of Helium Line Length on Chamber Pressure Oscillations

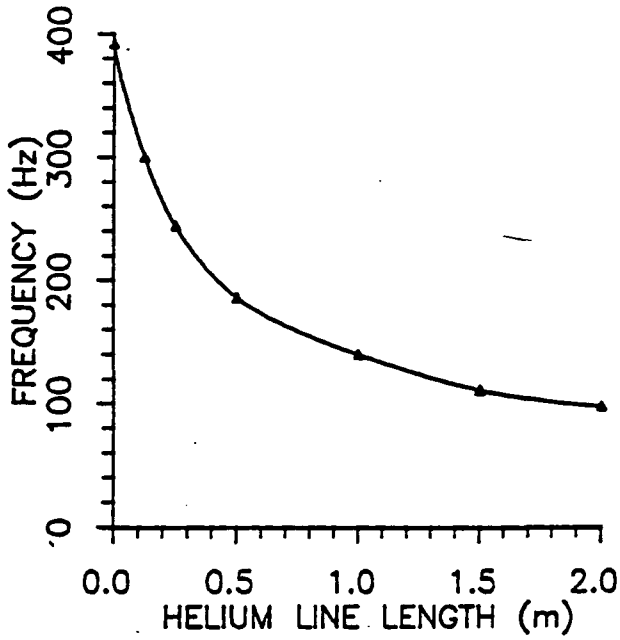

Figure 4.24: Pressure Oscillation Frequency v. Helium Line Length

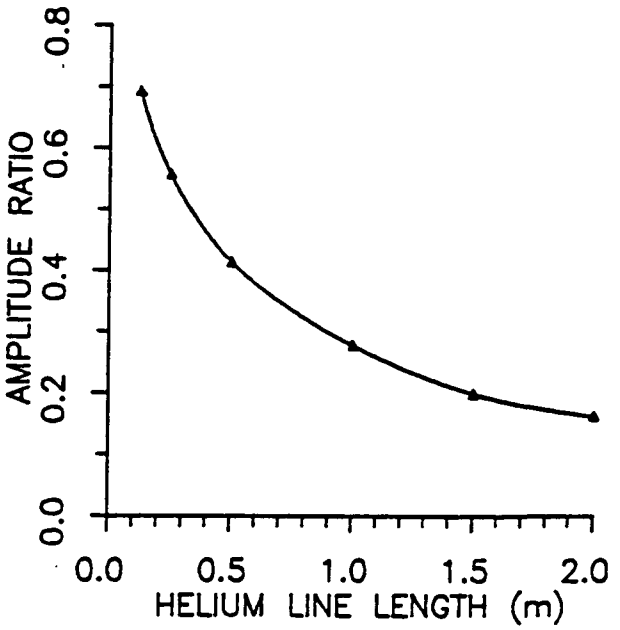

Figure 4.25: Amplitude Ratio v. Helium Line Length

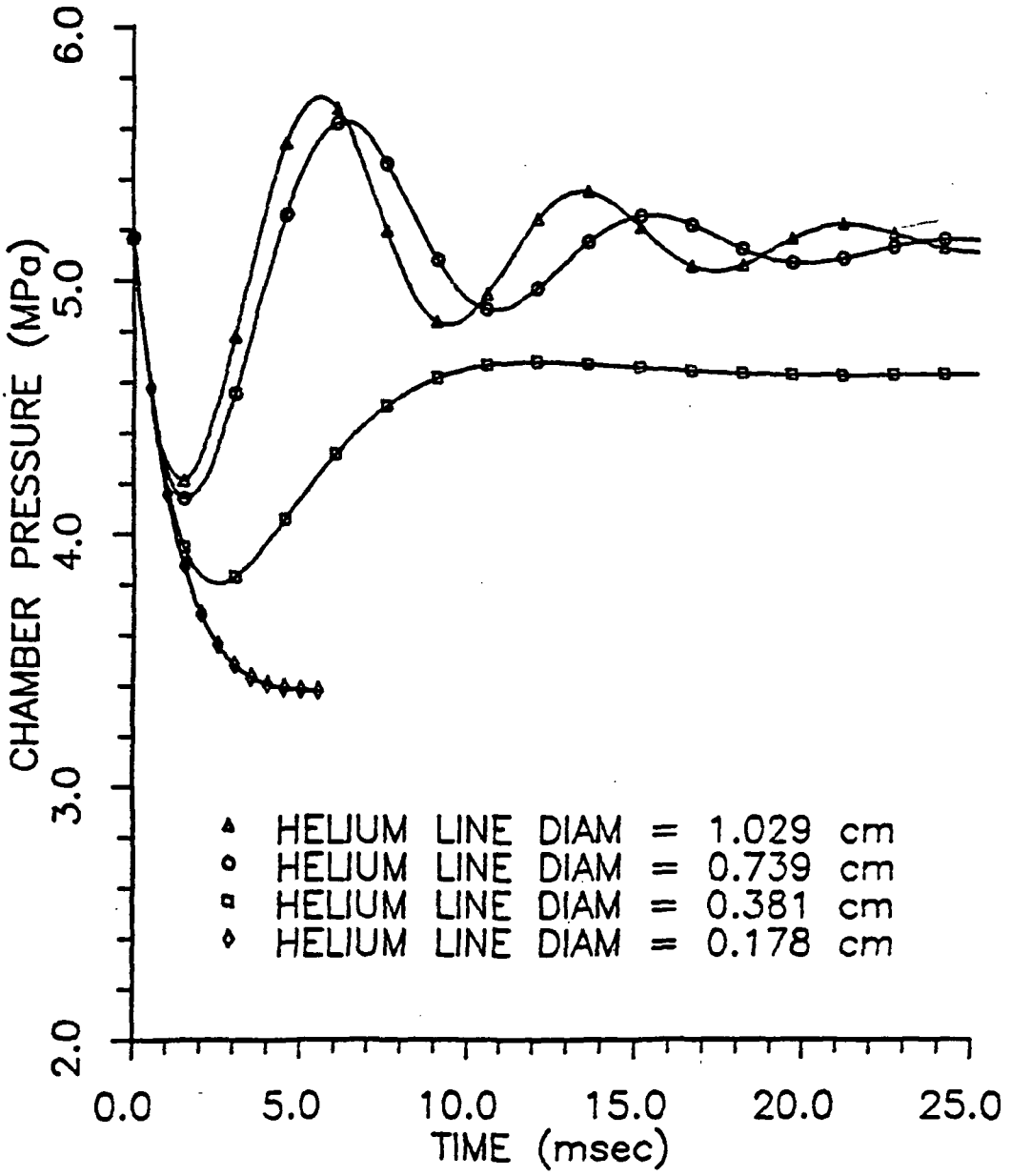

Figure 4.26: The Effect of Helium Line Diameter on Chamber Pressure Oscillations

fluid in the purge line began to undergo undamped high frequency numerical oscillations. To try to prevent numerical instability, the maximum error allowable in the IMSL integration routine, DGEAR, was reduced and the number of pipes in TRNCHG that represented the purge line was increased. Both of these changes resulted in slightly longer periods of numerical stability accompanied by considerably longer CPU times. The CPU time necessary for TRNCHG to give an accurate solution for a small diameter helium purge line was deemed too high and only the limited solution shown in Figure 4.26 was generated for a helium purge line diameter equal to 0.178 cm.

From Figure 4.26, one can see that a larger diameter helium purge line results in higher frequency chamber pressure oscillations of greater amplitude and which damp more slowly. The average chamber pressure decreases with decreases helium purge line diameter. For a given helium line length, the greater the volume of helium in the line, the less stable the preburner.

4.8 PREBURNER OPERATION AT FULL POWER LEVEL

TRNCHG was used to simulate fuelside preburner operation at full power level (with no helium purge) both to validate the program and to determine the part that chemical kinetics play in the preburner chug. Care had to be taken in choosing TRNCHG's initial conditions, since poor choices resulted in large derivatives and numeric overflows. Species mole numbers and the initial mass of

liquid in the combustion chamber were set equal to the values they would reach in a transient stirred tank reactor, after a long period of time, at constant chamber pressure, chamber temperature and oxidizer and fuel mass flow rates. The oxidizer mass flow rate was set equal to the oxidizer mass flow rate that would be reached in the pipes after a long period of time at constant upstream and chamber pressures. A summary of inputs to TRNCHG for the full power level simulation is given in Table 4.2

TRNCHG was first run assuming infinitely fast chemical kinetics and was then run taking chemical kinetics into account (as described in Chapter III and Appendix A). Chamber pressure for these runs is plotted against time in Figure 4.27. Just as in actual operation, the preburner does not undergo sustained chug at full power level. The initial pressure oscillations are due to the choice of the initial values of chamber pressure and chamber temperature. The presence of chemical kinetics has a pronounced effect on chamber pressure and temperature: pressure oscillations damp more slowly and the temperature and pressure that the combustion chamber reaches after a long time are lower when chemical kinetics are considered. The frequency of the pressure oscillations for the run involving kinetics is 164 Hz.

A perturbation was applied to the preburner, at full power level, with chemical kinetics included, to see if chug could be incited by a large disturbance. At 30 msec, the mean droplet diameter coefficient, c_{dm}, of equation [4.1], was reduced from 0.485

Table 4.2: Inputs to TRNCHG for Full Power Level

PARAMETER	VALUE AT THE BEGINNING OF THE FULL POWER LEVEL SIMULATION
Chamber Temperature	1106 K (1991°R)
Chamber Pressure	38.0 MPa (5500 psia)
Mass of Liquid in the Chamber	2.71×10^{-2} kg (5.01×10^{-2} lbm)
Oxidizer Mass Flow Rate	32.08 kg/s (70.72 lbm/s)
Fuel Mass Flow Rate	34.40 kg/s (75.84 lbm/s)
Pipe Length	0.12 m (0.39 ft)
Mass Fractions:	
He	0.0
H_2	5.40×10^{-1}
O_2	6.59×10^{-3}
H_2O	4.54×10^{-1}
H	5.76×10^{-6}
O	1.53×10^{-7}
OH	1.15×10^{-7}

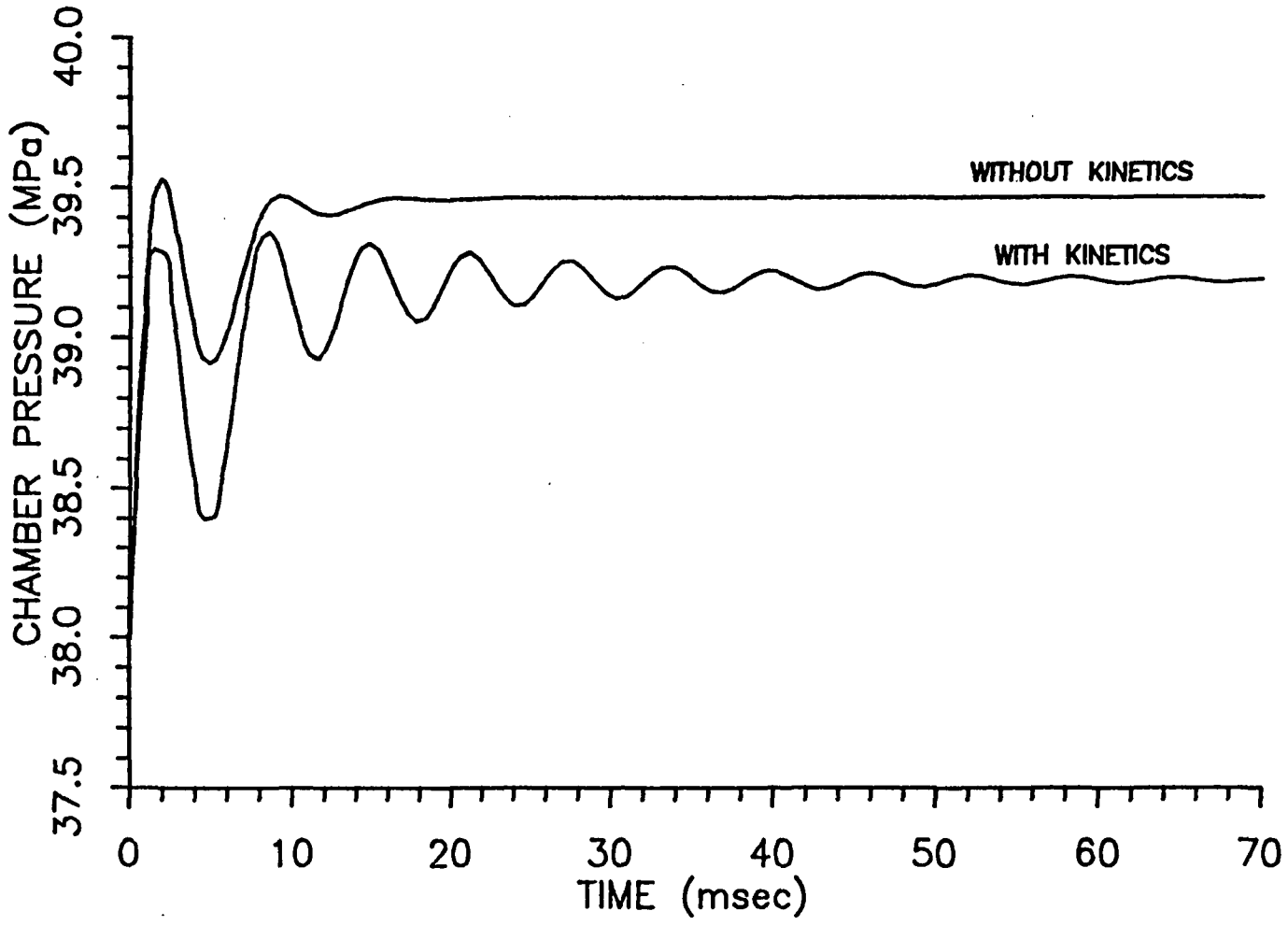

Figure 4.27: Chamber Pressure v. Time at Full Power Level

to 0.364 for 0.5 msec, and then returned to 0.485. The resulting chamber pressure oscillation is shown in Figure 4.28. Initially, when c_{dm} is reduced, the mean droplet size becomes smaller and more oxygen vaporizes and is available for combustion. During this time the pressure rises. Next, when the amount of liquid in the chamber and the injection rate of LOX into the chamber become small, the combustion rate and pressure fall. The oxidizer mass flow rate then increases and the oscillation in chamber pressure continues. Within seven cycles, the peak to peak amplitude of the pressure oscillations is damped to 16% of its original value.

4.9 CONDITIONS THAT RESULT IN INSTABILITY

Aside from reducing the helium line length to zero, it was not possible to incite chug by varying just one engine parameter, so it is a combination of engine parameters that cause the fuelside preburner chug. TRNCHG was run with various combinations of engine parameters. The purpose of these runs was not to determine the domain of engine parameters that give rise to chugging, but to demonstrate that TRNCHG can predict chug and to show that only small deviations from the engine parameters used for the SSME shutdown simulation can result in chug. Two runs that resulted in instability are described below.

Figure 4.29 is a plot of chamber pressure v. time for hydrogen temperature equal to 120K, helium temperature equal to 200 K, PHG equal to 1.03 MPa, fuel mass flow rate equal to 18 kg/s and mean

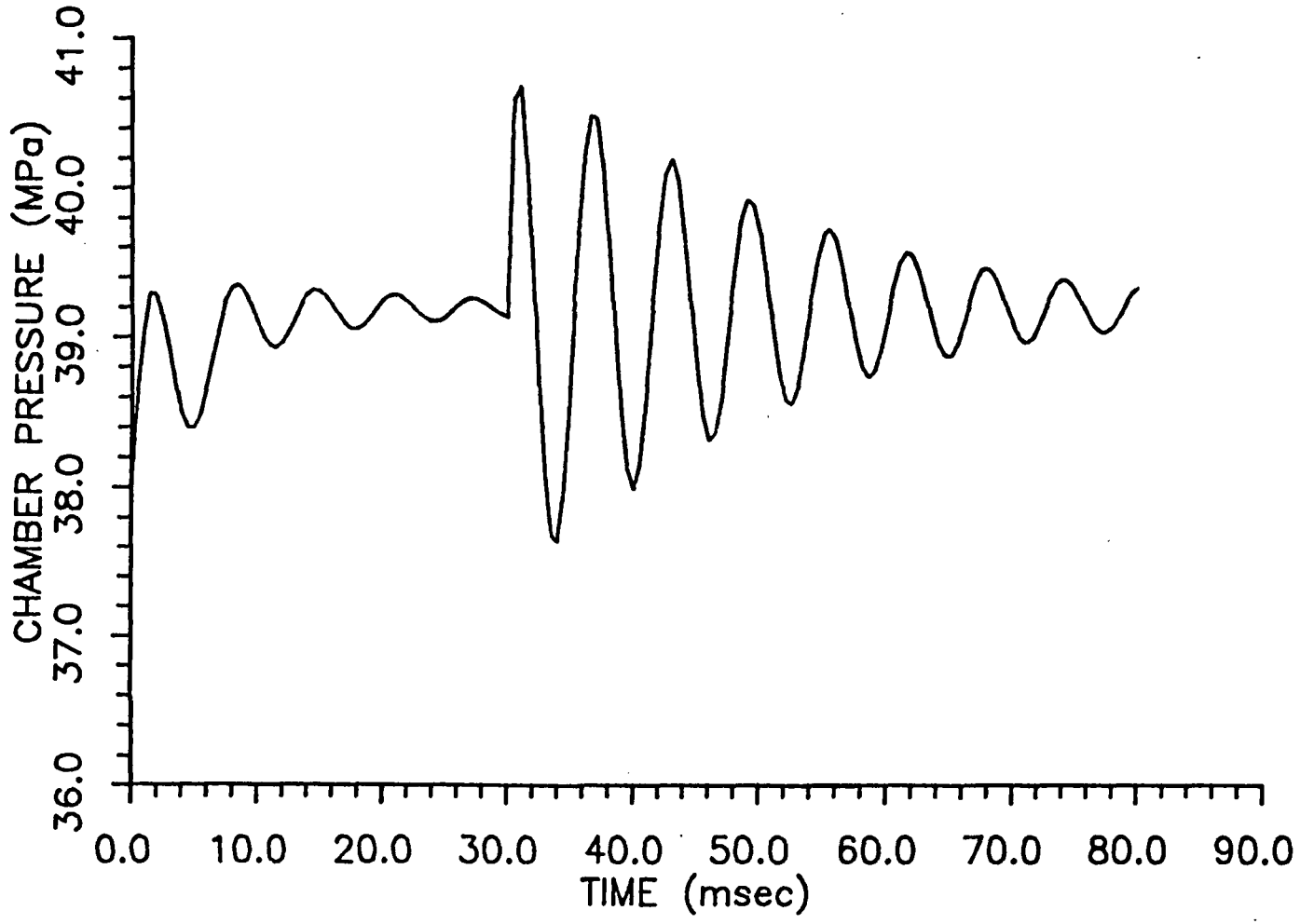

Figure 4.28: Preburner Response to a Perturbation at Full Power Level

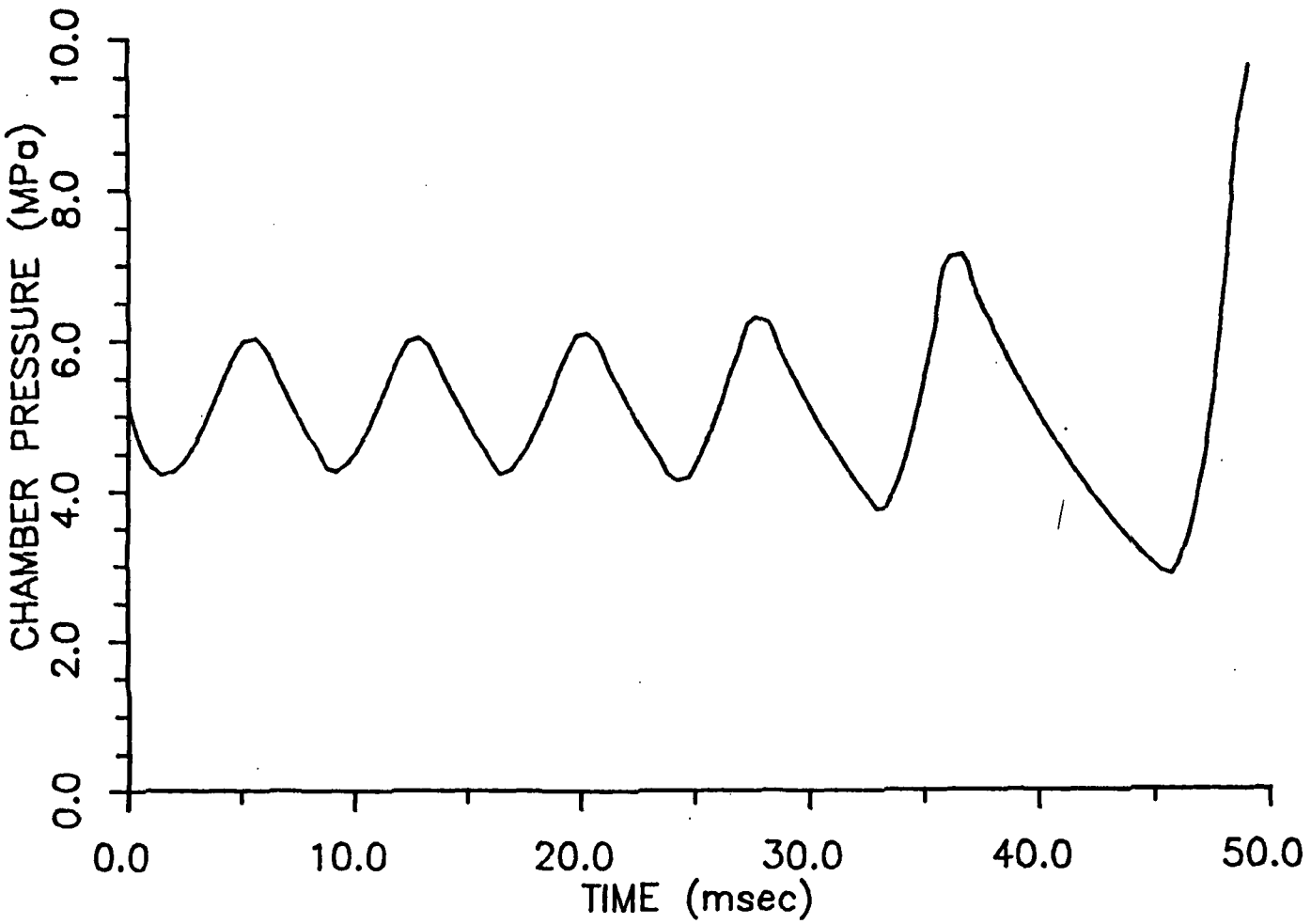

Figure 4.29: Unstable Preburner Operation (a)

droplet diameter coefficient equal to 0.585. All other engine parameters were the same as those listed in Table 4.1. Execution was halted after 49 msec because time for each integration step became too long. Using a mean droplet diameter of 0.485 and all other engine parameters the same as those described for Figure 4.29, TRNCHG predicted stable operation.

Figure 4.30 is a plot of chamber pressure versus time for hydrogen temperature equal to 70 K, fuel mass flow rate equal to 15 kg/s, heat transfer rate to the chamber contents equal to 8.5×10^7 J/s, PHG equal to 1.03 MPa and helium temperature equal to 200 K. All other engine parameters were the same as those listed in Table 4.1. This run was be made stable by lowering the helium temperature to 150 K.

4.10 SUMMARY OF RESULTS

The program TRNCHG, which was written to solve the governing equations derived in Chapter III for heterogeneous preburner operation, was supplied with the approximate conditions at the opening of the helium check valves and was executed. When chemical kinetics were allowed to proceed according to a chemical kinetic mechanism, the model erroneously predicted that ignition would not take place in the preburner. When chemical kinetics were assumed infinitely fast, the model predicted that a quickly damped pressure oscillation with a frequency of 111 Hz would take place immediately after the helium check valves were opened. An oscillation in

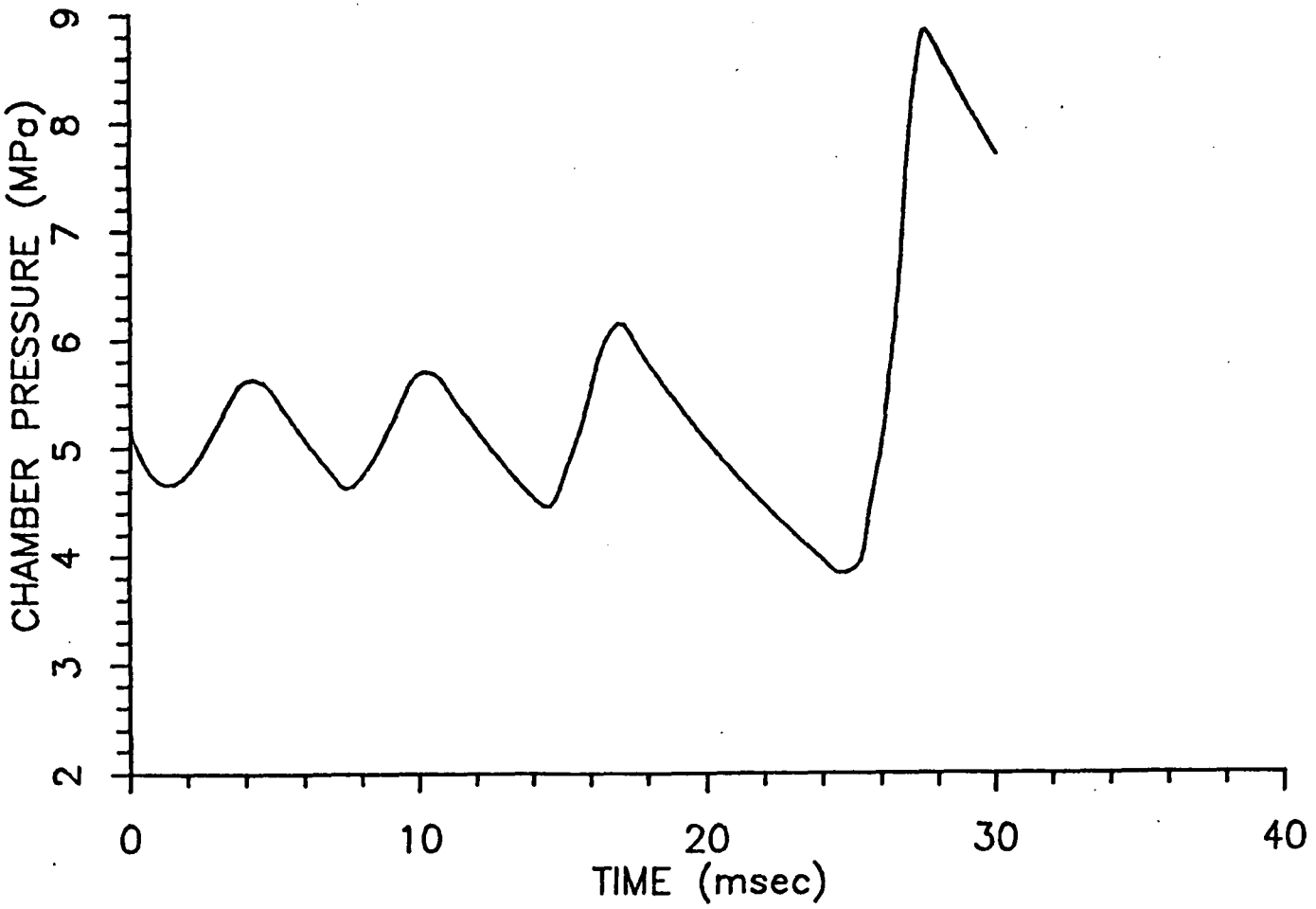

Figure 4.30: Unstable Preburner Operation (b)

oxidizer mass flow rate into the preburner combustion chamber was also predicted and it was about 1/5 cycle more than 180° out of phase with the pressure oscillation.

To determine their effect on engine stability, the following engine parameters were varied: heat transfer rate from the chamber walls, mean droplet diameter, oxidizer temperature, fuel temperature, fuel mass flow rate, pressure downstream of the fuel preburner exit turbine (fuel turbo-pump), helium temperature, helium line length and helium line diameter. It was found that small variations in a number of these parameters had a large effect on preburner operation. A summary of the effect that each of these parameters has on preburner operation is given in Table 4.3.

TRNCHG was also used to predict conditions in the fuel preburner at full power level. This was both to validate the model and to allow comparison of different reaction rate models. As expected, TRNCHG predicted stable operation at full power level. Assuming that rates of production of the species in the combustion chamber could be calculated using elementary reaction rates resulted in much more slowly damped oscillations in chamber pressure than assuming chemical kinetics were infinitely fast.

Finally, it was demonstrated that, after changing a small number of engine parameters by only a small amount, TRNCHG was able to predict unstable preburner operation.

Table 4.3: Summary of the Effects of Engine Parameters on Fuelside Preburner Operation

ENGINE PARAMETER BASE VALUE RANGE OF VALUES USED IN TRNCHG	EFFECT ON PREBURNER OPERATION
Heat Transfer Rate $Q = 6.5 \times 10^7$ J/s $0.0 \text{ J/s} < Q < 1.0 \times 10^8$ J/s	Heat transfer rate had a large effect on average chamber pressure and temperature, but very little effect on the rate at which pressure oscillations damped.
Mean Droplet Diameter Coefficient $c_{dm} = 0.485$ $0.0485 < c_{dm} < 3.88$	Higher values of c_{dm} lead to large amplitude pressure oscillations which damp more slowly and have lower frequencies. For some value of c_{dm} between 1.94 and 3.88, there is a critical value of c_{dm} for which the preburner is unstable. Above that value liquid droplets become too large and ignition does not occur.
LOX Temperature $T_{ox} = 120$ K $90 \text{ K} < T_{ox} < 150$ K	Lower oxidizer temperatures lead to higher frequency chamber pressure oscillations which damp relatively quickly. The amplitude ratio for $T_{ox} = 150$ K is 54.4% of that for $T_{ox} = 90$ K.
Fuel Temperature $T_{fuel} = 160$ K $50 \text{ K} < T_{fuel} < 200$ K	Below 120 K fuel temperature has a large effect on preburner stability. The frequency of chamber pressure oscillations for $T_{fuel} = 50$ K is 68% of that for $T_{fuel} = 150$ K. Oscillations damp more slowly and have greater amplitudes for lower fuel temperatures

Table 4.3: (continued)

ENGINE PARAMETER BASE VALUE RANGE OF VALUES USED IN TRNCHG	EFFECT ON PREBURNER OPERATION
Fuel Mass Flow Rate $\dot{m}_f$ = 21.0 kg/s $12.0 < \dot{m}_f < 25.0$	Decreasing the fuel mass flow rate caused chamber pressure oscillations to damp more slowly, but did not change the oscillation frequency. Higher fuel mass flow rates resulted in higher oxidizer mass flow rates.
Pressure Downstream of the Exit Turbine PHG = 1.72 MPa 1.03 MPa < PHG < 2.41 MPa	Decreasing the pressure downstream of the exit turbine resulted in more slowly damped chamber pressure oscillations, but did not change the frequency. The amplitude ratio for PHG = 1.03 MPa is 4.9 times that for PHG = 2.41 MPA
Helium Temperature T_{He} = 120 K 50 K < T_{He} < 300 K	Changing the helium temperature changed both the amplitude ratio and the oscillation frequency; Higher helium temperatures lead to higher frequency pressure oscillations that damped more slowly. The frequency at 200 K is 1.3 times that at 120 K. The amplitude ratio at 200 K is 1.5 times that at 120 K.
Helium Line Length L_{He} = 1.5 m 0.01 m < L_{He} < 2.0 m	If the helium storage tank were mounted directly on the helium check valves, the fuelside preburner would be unstable. Longer helium line lengths lead to more stable operation. Above 1.5 m, increasing the helium line length had only a small effect on oscillation frequency or amplitude ratio.

Table 4.3: (continued)

ENGINE PARAMETER BASE VALUE RANGE OF VALUES USED IN TRNCHG	EFFECT ON PREBURNER OPERATION
Helium Line Diameter D_{He} = 0.739 cm 0.173 cm < D_{He} < 1.029 cm	Large helium line diameters volumes of helium in the line) lead to higher chamber pressures and oscillations which have higher frequencies and damp more slowly. For the smallest helium line diameter, a full solution could not be generated because numerical instability was encountered.

CHAPTER V

CONCLUSIONS

The objectives of this study were to evaluate the validity of the TSTR model for modelling a rocket engine combustion chamber, to predict the amplitude and frequency of the SSME fuelside preburner shutdown chug and to determine the processes and engine parameters that give rise to the chug.

To meet the first two objectives the fuelside preburner was modelled as a heterogeneous TSTR combustion chamber, a variable mass flow rate oxidizer feed system, a constant mass flow rate fuel feed system and an exit turbine. A computer program, TRNCHG, was written to integrate the resulting differential equations numerically. For full power level simulations TRNCHG predicted stability and executed without difficulty. For SSME engine shutdown conditions, chemical kinetics were assumed infinitely fast and TRNCHG predicted quickly damped chamber pressure and oxidizer mass flow rate oscillations.

To meet the third objective, engine parameters which had been shown in literature to influence the stability of liquid rocket engine combustion were varied. This procedure was quite successful, showing that small changes in some engine parameters resulted in large changes in preburner operation and pointing out two engine parameters that have a larger role in the SSME fuelside preburner chug than predicted by Lim's (1986) linearized model.

Three questions are answered in this chapter: which engine parameters are the key parameters in the SSME fuelside preburner chug? how could the preburner model be extended or modified? and how well does the fuelside preburner model work?

5.1 KEY ENGINE PARAMETERS AND THEIR EFFECT ON PREBURNER STABILITY

As stated in Chapter IV, it is probably a combination of factors that result in the fuelside preburner chug. The most important factors and their influence on the preburner chug, as predicted by the program TRNCHG, are given below.

1. Mean droplet diameter. Mean droplet diameter is a function of injector geometry, chamber pressure and the ratio of the oxidizer and fuel mass flow rates. As mean droplet diameter is increased, pressure oscillations in the combustion chamber damp more slowly. This is due to an increase in the combustion delay time (or decrease in the vaporization rate) associated with large droplets. For a sufficiently large droplet diameter, reaction blows off.
2. Pressure downstream of the exit turbine (PHG). During engine shutdown, PHG falls from 2.41 MPa to 1.03 MPa (350 psia to 150 psia). Pressure oscillations were shown to damp more slowly for lower values of PHG.
3. Fuel temperature. As described in Chapter I, fuel cools the

main combustion chamber and nozzle before being injected into the fuelside preburner combustion chamber. During shutdown, the fuel mass flow rate to the combustion chamber is less than at full power level, but the main combustion chamber and nozzle are also cooler, so the temperature of the fuel injected into the fuelside preburner may be lower during shutdown. Lower fuel temperatures result in a less stable fuelside preburner. When the fuel temperature is reduced below 120 K, pressure oscillation frequency decreases rapidly and the oscillations become less damped.

4. Fuel mass flow rate. Contrary to the predictions of Lim (1986), lower fuel mass flow rates were predicted to cause oscillations in chamber pressure to damp out more slowly. There are two reasons for this. First, for lower fuel mass flow rates there is less cold fuel to heat to the chamber temperature and more energy is available (from combustion) to sustain pressure oscillations. Second, the mean droplet diameter is a function of the fuel mass flow rate: as fuel mass flow rate decreases, the mean droplet diameter increases. As shown in figure 4.10 (page 75), as mean droplet diameter is increased, preburner operation becomes less stable.
5. Helium temperature. Changing the Helium temperature did not substantially change the amplitude of pressure oscillations, but did influence their frequency. Frequencies of pressure

oscillations for helium temperatures of 120 K and 300 K were 111 Hz and 175 Hz, respectively.

6. Helium purge line geometry. The length and diameter of the pipe connecting the helium storage tank to the helium check valve both have a strong influence on the preburner's operation during shutdown. As predicted by Summerfield (1951), as the length of the helium line was increased, the preburner became more stable. Above a helium purge line length of about 1.0m, a large change in pipe length is necessary to accomplish a small change in frequency or the rate at which oscillations damp out. It was not possible to obtain solutions from TRNCHG for small helium purge line diameters. In general, small helium purge line diameters lead to reduced chamber pressures and greater stability. For a given helium line length, the volume of helium between the helium storage tank and the combustion chamber is important in determining whether fuelside preburner will be stable

Comparing the results generated by the non-linear model used in this study to the results generated by the linear model used by Lim (1986) to model the SSME fuelside preburner, the non-linear model showed the preburner's stability to be sensitive to engine parameters to which the linearized model predicted the preburner would be insensitive. One instance of the greater sensitivity of the non-linear model is that the inclusion of chemical kinetics in the calculation of reaction rates at full power level resulted in more

slowly damped pressure oscillations than for chemical kinetics being considered infinitely fast (figure 4.28, page 100). Lim assumed that chemical kinetics were infinitely fast. Reaction rate is a non-linear function of chamber temperature and the mole number of the species in the combustion chamber. A second instance in which the predictions of the non-linear and linearized models differ is in the effect that fuel mass flow rate has on chamber pressure oscillations. Lim stated that chug could not be eliminated by changing the mass flow rate. As shown in figure 4.18 (page 86), the non-linear model predicts a pronounced effect of fuel mass flow rate on the rate at which oscillations are damped. Chamber temperature, droplet vaporization rate and mean droplet diameter are all functions of the fuel mass flow rate.

Using a linearized model, Lim was able to predict the effect that a number of engine parameters had on the stability of the SSME fuelside preburner. The results of the linearized model were concise, required a relatively small amount of computer time and in most cases proved accurate. The non-linear model used in the current study was able to show that chemical kinetics and fuel mass flow rate play a greater role in determining whether or not the preburner undergoes stable operation than predicted by the linearized model. These predictions show that a non-linear model is necessary in a detailed study of chug and offset the greater computer time necessary to predict how the preburner operates.

5.2 POSSIBLE EXTENSIONS OF THIS RESEARCH

There are number of ways the fuelside preburner model could be changed to increase its accuracy and to enable it to be used to model different rocket engine phenomena.

To improve the accuracy of the fuelside preburner model, the oxidizer feed system could be more faithfully represented, adding pipes and an oxidizer manifold. A finer grid of pipes would also increase accuracy, although for most cases this is not necessary. Within the oxidizer feed system the compressibility of LOX could be taken into account.

In the combustion chamber, a droplet distribution, which, like Webber's (1972) could contain different sized droplets whose size is followed over time, could be added. Given temperature data for the combustion chamber walls, the rate of heat transfer from the combustion chamber walls to the chamber contents could be more accurately calculated.

Finally, if it were desired to study spatial variations in chamber pressure, temperature and composition, it would be possible to use multiple TSTR's to model the combustion chamber. TSTR's could be distributed longitudinally and radially throughout the combustion chamber. The exit mass flow rate from the face of one TSTR would be an inlet mass flow rate through the face of an adjacent TSTR. Such a scheme could prevent the mixture ratio from being overestimated

severely in sections of the combustion chamber that contain many liquid droplets.

It is reiterated here that the above alterations of the TSTR model were not necessary in the study of the SSME fuelside preburner chug and are presented as ways in which the fuelside preburner model can be extended to be used in different applications.

5.3 EVALUATION OF THE FUELSIDE PREBURNER MODEL

The TSTR model of the fuelside preburner combustion chamber is simple, yet has been shown capable of predicting low frequency combustion instability. With the proper assumptions, the model can be used over a wide domain of operating conditions and engine parameters.

Among the strengths of the fuelside preburner model are,

1. the frequency of pressure oscillations in the preburner is predicted to within 6% of typical measured frequencies,
2. the effect that various engine parameters and combinations of these parameters has on preburner operation was shown,
3. the presence of liquid in the combustion chamber is included,
4. chemical kinetics may be included for high temperatures and pressures and
5. the fuel preburner is predicted to maintain stable operation at full power level.

The preburner model's weaknesses are

1. chemical kinetics are not modelled during the SSME shutdown,
2. solutions cannot be generated when the diameter of the pipe connecting the helium storage tank to the helium check valve is too small,
3. accurate initial conditions are required and
4. long CPU times are required to generate solutions when large derivatives are encountered (e.g., when backflow of combustion chamber contents into the oxidizer feed system occurs).

Despite the model's limitations, the objectives of this research were basically met. The TSTR model was able to predict transient conditions in a rocket engine preburner. The model predicted that, during the SSME shutdown the fuelside preburner would not undergo unstable operation, yet when key engine parameters were changed by a small amount instability resulted. It is also possible, as a worst case, that the inclusion of chemical kinetics in the model for shutdown would result in unstable preburner operation. The frequency of the SSME preburner chug was accurately predicted, but the amplitude was not, since sustained oscillations were not predicted by TRNCHG. Finally, the model not only showed the influence that engine parameters and processes have on chug, but also pointed out, contrary to the predictions of a linearized model, that fuel mass flow rate and chemical kinetics are important.

The program, TRNCHG, was written for the SSME fuelside preburner. However, by altering the oxidizer feed system

calculations and changing the way that exit mass flow rate is calculated, TRNCHG could be applied to many other rocket engine combustion chambers to study low frequency combustion instability. Using such a program has been shown valuable in an in-depth study of chug.

LIST OF REFERENCES

Barrere, M. and Moutet, A., 1956, "Low Frequency Combustion Instability in Bipropellant Rocket Motors - Experimental Study," ARS Journal, Vol. 26, No. 1, pp. 9-19.

Coultas, T.A., 1972, "Combustion Instability," Liquid Propellant Rocket Combustion Instability, Harrje, D.T., and Reardon, F.H., eds., pp. 14-23.

Courtney, W.G., 1960, "Combustion Intensity in a Heterogeneous Stirred Reactor," ARS Journal, Vol. 30, No. 4, pp 356-357

Crocco, L., Grey, J., and Harrje, D.T., 1960, "Theory of Liquid Propellant Rocket Combustion Instability and its Experimental Verification," ARS Journal, Vol. 30, No. 2, pp.159-168.

Crocco, L., 1951, "Aspects of Combustion Instability in Liquid Propellant Rocket Systems," ARS Journal, Vol. 21, No. 6, pp. 163-178

Dykema, O.W., 1972, "Injector Pattern," Liquid Propellant Rocket Combustion Instability, Harrje, D.T., and Reardon, F.H., eds., pp 330-336

George, P.E., 1982, Gasification in Pulverized Coal Flames, Final Report (Part II), Department of Energy Report No. ME-TSPC-TR-82-12.

George, P.E., 1984, "An Investigation of Space Shuttle Main Engine Shutdown Chugging Instability," NASA/ASEE Summer Faculty Research Fellowship Program Report, Marshal Space Flight Center/ University of Alabama.

George, P.E., 1985, "Investigation and Modelling of Space Shuttle Main Engine Shutdown Transient Chugging," NASA/ASEE Summer Faculty Research Fellowship Program Report, Marshal Space Flight Center/ University of Alabama.

Heidmann, M.F., Sokolowski, D.E., and Diehl, L.A., 1967, "Study of Chugging Instability with Liquid-Oxygen and Gaseous-Hydrogen Combustors," NASA TN-4005, Lewis Research Center, Cleveland, OH.

Hersch, M., and Rice, E.J., 1967, "Gaseous Hydrogen-Liquid Oxygen Rocket Combustion at Supercritical Chamber Pressures", NASA TN D-4172, Lewis Research Center, Cleveland, OH.

Kuo, K.K., 1986, Principles of Combustion, John Wiley and Sons, NY.

Lawhead, R.B., and Combs, L.P., 1963, "Modelling Techniques for Liquid Propellant Rocket Combustion Processes," Ninth International Symposium on Combustion, Academic Press, NY, pp. 973-981.

Lim, K.C., 1986, A One-Dimensional Analysis of Low Frequency Combustion Instability in the Fuel Preburner of the Space Shuttle Main Engine, Master's Thesis, U. of Tennessee, Knoxville.

Nguyen, D.G., 1981, Engine Balance and Dynamic Model, Rockwell International Corp., Rocketdyne Division.

Penner, S.S., and Datner, P.P., 1955, "Combustion Problems in Liquid-Fuel Rocket Engines," Fifth International Symposium on Combustion, Reinhold, NY, pp. 11-28.

Pratt, D.T., and Radhakrishnan, K., 1986, "A Fast Algorithm for Calculation of Combustion Chemical Kinetics," Paper 8-A1, Central States Section Spring Tech. Meeting, The Combustion Institute, Lewis Research Center, Cleveland, OH.

Pratt, D.T. and Wormeck, 1976, "CREK, a Computer Program for the Calculation of Combustion Reaction Equilibrium and Kinetics in Turbulent and Laminar Flow," Thermal Energy Laboratory, Dept. of Mechanical Engr, Washington St. U., Pullman, WA.

Priem, R.J., 1966, "Combustion Process Influence on Stability," Aerospace Chemical Engineering, Vol. 62, pp. 103-112.

Rayliegh, J.W.S., 1945, The Theory of Sound, Vol. II, Dover Publications, NY.

Reardon, F.H., McBride, J.M., and Smith, A.J., 1966, "Effect of Injection Distribution on Combustion Instability," AIAA Journal, Vol. 4, No. 3.

Schoyer, H.F., and deBont, R.T.M., 1986, "Experimental Verification of Temperature Fluctuations During Combustion Instability," AIAA Journal, Vol. 24, No. 2, pp. 340-341.

Seymour, D., 1986, *personal correspondence.*

Summerfield, M., 1951, "A Theory of Unstable Combustion in Liquid Propellant Rocket Systems," ARS Journal, Vol. 21, No. 5, pp. 108-114.

Sutton, G.P., Rocket Propulsion Elements, John Wiley and Sons, N.Y.

VanOverbeke, T.J. and Claus, R.W., 1986, "SSME Fuelside Preburner Two-Dimensional Analysis," NASA Technical Memorandum 87299, Lewis Research Center, Cleveland, OH.

Webber, W.T., 1972, "Calculation of Low-Frequency Unsteady Behavior of Liquid Rockets From Droplet Combustion Parameters," J. of Spacecraft,, Vol. 9, No. 4, pp. 231-237.

White, F.M., 1979, Fluid Mechanics, McGraw-Hill, N.Y.

Williams, F.A., 1985, Combustion Theory, The Benjamin/Cummings Publishing Co. Inc., Menlo Park, CA.

Yang, V., and Culick, F.E., 1986, "Analysis of Low Frequency Combustion Instabilities in a Laboratory Ramjet Combustor," Comb. Sci. and Tech., Vol. 44, pp. 1-25.

APPENDIXES

APPENDIX A

COMBUSTION CHAMBER AND OXIDIZER FEED SYSTEM DERIVATIVES

A.1 DERIVATION OF THE TSTR GOVERNING EQUATIONS

The conservation of mass for the gas and the liquid phases is fully derived in Chapter III. The conservation of species and energy for a TSTR and the ideal gas law as used in the present study are derived below.

The Conservation of Species

Equation [3.6] can be written

$$\frac{d(\sigma_i \rho_c)}{dt} = \sum_{j=1}^{NSTRM} \left(\dot{m}^*_{jv}\sigma_{ij}\right) - \dot{m}_{gv}\sigma_i + \Gamma_{iv} \qquad [A.1]$$

for i=1,2,3 ...NS. The subscript v denotes a volumetric quantity. The derivative in [A.1] is expanded, giving

$$\rho_c \frac{d\sigma_i}{dt} + \sigma_i \frac{d\rho_c}{dt} = \sum_{j=1}^{NSTRM} \left(\dot{m}^*_{jv}\sigma^*_{ij}\right) - \dot{m}_{gv}\sigma_i + \Gamma_{iv} \qquad [A.2]$$

From equation [3.4],

$$\frac{d\rho_c}{dt} = \sum_{j=1}^{NSTRM} \left(\dot{m}^*_{jv}\right) - \dot{m}_{gv} \qquad [A.3]$$

[A.3] is substituted into [A.2] and the result is simplified, yielding

$$\frac{d\sigma_i}{dt} = \frac{1}{\rho_c} \sum_{j=1}^{NSTRM} \left[\dot{m}^*_{jv}(\sigma^*_{ij} - \sigma_i)\right] + \Gamma_{iv} \qquad [A.4]$$

For any variable, x,

$$\frac{d(\ln x)}{dt} = \frac{1}{x}\frac{dx}{dt} \qquad [A.5]$$

[A.5] is applied to [A.4], giving the conservation of species for the TSTR in its final form:

$$\frac{d(\ln \sigma_i)}{dt} = \frac{1}{\sigma_i \rho_c} \sum_{j=1}^{NSTRM} \left[\dot{m}^*_{jv}(\sigma^*_{ij} - \sigma_i)\right] + \Gamma_{iv} \qquad [A.6]$$

$$i=1,2,3 \ldots NS$$

Conservation of Energy

Conservation of energy is given by equation [3.7] as

$$\frac{dE}{dt} = \sum_{i=1}^{NS}\sum_{j=1}^{NSTRM}\left(\dot{m}^*_j \sigma^*_{ij} h^*_{ij}\right) - \sum_{i=1}^{NS}\left(\dot{m}_g \sigma_i h_i\right) - \dot{Q} \qquad [A.7]$$

assuming that changes in the kinetic and potential energies of the chamber contents are negligible,

$$\frac{dE}{dt} = \frac{dU}{dt} = \frac{d}{dt}\left(\sum_{i=1}^{NS} \rho_c V \sigma_i u_i\right) \qquad [A.8]$$

where E is the total energy (Joules) of the chamber contents, U is the internal energy (Joules) of the chamber contents and u_i is the

specific molar internal energy (J/kgmole) of species i. Expanding the derivative,

$$\frac{dE}{dt} = \frac{d\rho_c}{dt} V \sum_{i=1}^{NS} u_i\sigma_i + \rho_c V \sum_{i=1}^{NS} \frac{d\sigma_i}{dt} u_i + \rho_c V \sum_{i=1}^{NS} \sigma_i \frac{du_i}{dt} \qquad [A.9]$$

Assuming that the contents of the chamber behave as a mixture of perfect gases and that their specific heats at constant pressure, c_{pi} (J/kgmole·K) do not vary,

$$\frac{du_i}{dt} = \frac{d}{dt}\left(h_i - R_g T_c\right) = \frac{dT_c}{dt}\left(c_{pi} - R_g\right) \qquad [A.10]$$

Using [A.10], [A.9] becomes

$$\frac{dE}{dt} = \frac{d\rho_c}{dt} V \sum_{i=1}^{NS} \sigma_i u_i + \rho_c V \sum_{i=1}^{NS} \frac{d\sigma_i}{dt} u_i +$$

$$\rho_c V \frac{dT_c}{dt} \sum_{i=1}^{NS} \sigma_i (c_{pi} - R_g) \qquad [A.11]$$

[A.11] is substituted into [A.7] and [A.5] is applied, giving

$$\frac{d(\ln T_c)}{dt} = \left[\sum_{i=1}^{NS}\sum_{j=1}^{NSTRM} \dot{m}^*_{jv}\sigma^*_{ij}h^*_{ij} - \sum_{i=1}^{NS} \dot{m}_{gv}\sigma_i h_i - \frac{d\rho_c}{dt}\sum_{i=1}^{NS} \sigma_i u_i\right.$$

$$\left.\rho_c \sum_{i=1}^{NS} \frac{d\sigma_i}{dt} u_i - \dot{Q}/V\right] \Big/ \left[T_c \rho_c \sum_{i=1}^{NS} \sigma_i (c_{pi} - R_g)\right] \qquad [A.12]$$

The Ideal Gas Law

For the combustion chamber, the ideal gas law can be written

$$P_c = \rho_c \sigma_m R_g T_c$$

where $\sigma_m = \sum_{i=1}^{NS} \sigma_i$. Alternatively,

$$\frac{dP_c}{dt} = \sigma_m R_g T_c \frac{d\rho_c}{dt} + \rho_c \sigma_m R_g \frac{dT_c}{dt} + \rho_c R_g T_c \frac{d\sigma_m}{dt} \qquad [A.13]$$

Equation [A.5] is applied to [A.13], giving

$$\frac{d(\ln P_c)}{dt} = \frac{\sigma_m R_g T_c}{P_c} \frac{d\rho_c}{dt} + \frac{\rho_c \sigma_m R_g}{P_c} \frac{dT_c}{dt} + \frac{\rho_c R_g T_c}{P_c} \frac{d\sigma_m}{dt} \qquad [A.14]$$

or,

$$\frac{d(\ln P_c)}{dt} = \frac{1}{\rho_c} \frac{d\rho_c}{dt} + \frac{1}{T_c} \frac{dT_c}{dt} + \frac{1}{\sigma_m} \frac{d\sigma_m}{dt} \qquad [A.15]$$

A.2 DERIVATION OF THE REACTION RATE FROM ELEMENTARY KINETICS

The volumetric forward and reverse reaction rates for an elementary reaction, j, can be written (Pratt and Wormeck, 1976)

$$R'_{jv} = A'_j T_c^{N'_j} \exp\{-T'_{aj}/T_c\} (\rho_c \sigma_m)^{\nu'_m} \prod_{i=1}^{NS} (\rho_c \sigma_i)^{\nu'_{ij}} \qquad [A.16]$$

$$R''_{jv} = A''_j T_c^{N''_j} \exp\{-T''_{aj}/T_c\} (\rho_c \sigma_m)^{\nu''_m} \prod_{i=1}^{NS} (\rho_c \sigma_i)^{\nu''_{ij}} \qquad [A.17]$$

where A_j, N_j and T_{aj} are empirically determined coefficients, T_c is the combustion chamber temperature, ν_{ij} is the stoichiometric coefficient of species i in reaction j, ν_m is the stoichiometric coefficient for a third body, and the superscripts ' and " denote forward and reverse reaction, respectively. The overall rate of production of species i by a chain of NRXN elementary reactions is —

$$R_{iv} = \sum_{j=1}^{NRXN} (\nu''_{ij} R''_{jv} - \nu'_{ij} R'_{jv}) \qquad [A.18]$$

The following elementary reactions made up the overall conversion of H_2 and O_2 to water vapor in the TSTR model of the SSME fuelside preburner:

$$O_2 + H_2 \;\text{<---> OH + OH}$$
$$OH + H_2 \;\text{<---> } H_2O + H$$
$$O_2 + H \;\text{<---> OH + O}$$
$$O + H_2 \;\text{<---> OH + H}$$
$$O + H_2O \;\text{<---> OH + OH}$$
$$H + H + M \;\text{<---> } H_2 + M$$
$$O + O + M \;\text{<---> } O_2 + M$$
$$O + H + M \;\text{<---> OH + M}$$
$$H + OH + M \;\text{<---> } H_2O + M$$

Because the atoms O and H and the radical OH are so reactive, they are consumed nearly as soon as they are produced, so their mole

numbers were assumed to be constant at any given time, or

$$\frac{d\sigma_O}{dt} = \frac{d\sigma_H}{dt} = \frac{d\sigma_{OH}}{dt} = 0 \qquad [A.19]$$

Using equation [A.19], equation [A.4] can be written for O, H and OH, giving

$$f_H = \sum_{j=1}^{NSTRM} \dot{m}^*_{jv}(\sigma_{Hj} - \sigma_H) + R_{Hv} = 0$$

$$f_O = \sum_{j=1}^{NSTRM} \dot{m}^*_{jv}(\sigma_{Oj} - \sigma_O) + R_{Ov} = 0 \qquad [A.20]$$

$$f_{OH} = \sum_{j=1}^{NSTRM} \dot{m}^*_{jv}(\sigma_{OHj} - \sigma_{OH}) + R_{OHv} = 0$$

Since there are no radicals present in the inlet streams,

$$f_H = -\sigma_H(\Sigma\, \dot{m}^*_{jv}) + R_{Hv} = 0$$

$$f_O = -\sigma_O(\Sigma\, \dot{m}^*_{jv}) + R_{Ov} = 0 \qquad [A.21]$$

$$f_{OH} = -\sigma_{OH}(\Sigma\, \dot{m}^*_{jv}) + R_{OHv} = 0$$

At each time, values for σ_H , σ_O , $\sigma_{H\,O}$, T_c, P_c and $_c$ are known (these are the combustion chamber variables which are being integrated), so equations [A.21] constitute three equations in the three unknown mole numbers σ_H, σ_O and σ_{OH}.

The roots of equations [A.21] were found using a Newton iteration. The functions, f_i, were expanded in a Taylor series about the assumed solution and second order and higher terms were truncated (George, 1982), giving

$$f_i = f_{i,old} + \sum_{k=1}^{NRAD} \frac{\partial f_{i,old}}{\partial \sigma_k} \sigma_k \qquad i=1,NRAD \qquad [A.22]$$

where NRAD is the number of species whose mole number is assumed constant at each time step (Nrad=3 for the SSME TSTR model). If the correct values of the radical mole numbers are chosen, $f_i = 0$ for i=1,NRAD. [A.22] can then be written

$$\sum_{k=1}^{NRAD} \frac{\partial f_i}{\partial \sigma_k} \Delta\sigma_k = -f_{i,old} \qquad i=1,NRAD$$

or,

$$\begin{bmatrix} \partial f_H/\partial \sigma_H & \partial f_H/\partial \sigma_O & \partial f_H/\partial \sigma_{OH} \\ \partial f_O/\partial \sigma_H & \partial f_O/\partial \sigma_O & \partial f_O/\partial \sigma_{OH} \\ \partial f_{OH}/\partial \sigma_H & \partial f_{OH}/\partial \sigma_O & \partial f_{OH}/\partial \sigma_{OH} \end{bmatrix} \begin{Bmatrix} \Delta\sigma_H \\ \Delta\sigma_O \\ \Delta\sigma_{OH} \end{Bmatrix} = \begin{Bmatrix} -f_{H,old} \\ -f_{O,old} \\ -f_{OH,old} \end{Bmatrix} \qquad [A.23]$$

Equation [A.23] is solved for the correction variables $\Delta\sigma_i$, i=1,NRAD. New estimates for σ_i, i=1,NRAD, are

$$\sigma_{i,new} = \sigma_{i,old} + \Delta\sigma_i \qquad [A.24]$$

The results of [A.24] are successively substituted into [A.23] until

the condition

$$\sigma_i < \varepsilon_{ss} \qquad i=1,NRAD \qquad [A.25]$$

is met. ε_{ss} was set at $1.0x10^{-5}$ in the program TRNCHG.

When condition [A.25] was met, reaction rate for H_2O was calculated using the known values for mole numbers, temperature, pressure and density, the steady state values for the radical mole numbers and equations [A.16], [A.17] and [A.18]. By conservation of atoms,

$$R_{H_2v} \approx - R_{H_2Ov}$$
$$R_{O_2v} \approx - 0.5\, R_{H_2Ov} \qquad [A.26]$$

In all observed cases, the approximate values for R_{H_2v} and R_{O_2v} were close (within an estimated 5%) of the values calculated directly using [A.16], [A.17] and [A.18].

A.3 DERIVATION OF THE OXIDIZER FEED SYSTEM EQUATIONS

In integral form, the conservation of linear momentum for a control volume is (White, 1979)

$$\Sigma F = \frac{\partial}{\partial t} \left(\iiint_{CV} \rho\, v dV \right) + \iint_{CS} \rho v (v \cdot n)\, dA \qquad [A.27]$$

As shown in figure 3.6, using equations [3.15] and [3.16],

$$\Sigma F = (P_1 - P_2)A - fL\rho v^2 A \qquad [A.28]$$

For a pipe containing a liquid/vapor interface, [A.27] can be written

$$(P_1 - P_2)A - fL\rho v^2 A = \frac{d}{dt}(\rho_l V_l v + \rho_g V_g v) + \rho_l v^2 A - \rho_g v^2 A \quad [A.29]$$

Note that

$$\frac{dl_g}{dt} = -\frac{dl_l}{dt} = v \quad [A.30]$$

Divide by A and group terms for

$$P_1 - P_2 - fL\rho v^2 = (\rho_l l_l + \rho_g l_g)\frac{dv}{dt} + l_l v \frac{d\rho_l}{dt} + l_g v \frac{d\rho_g}{dt} \quad [A.31]$$

For each pipe node, k, equation [3.20] is written

$$\rho_k \sum_{n=1}^{NPN} A_n(dv_n/dt) + (d\rho_k/dt) \sum_{n=1}^{NPN} A_n v_n = 0 \quad [A.32]$$

Equations [A.31] and [A.32] constitute NN+NP linear equations in the NN+NP unknowns: dv_n/dt, n=1,2,3 ...NP, and $d\rho_k/dt$, k=1,2,3, ...NN. [A.31] and [A.32] can be expressed as the matrix equation [A] {X} = {B} where matrix [A] contains the coefficients of the unknowns, {X} contains the values of the unknowns and {B} contains $P_1 - P_2 - fL\rho v^2$ for rows 1,2,3 ...NP and zero for rows NP+1,NP+2,... NP+NN. In the program written for this study, {X} was found via a call to IMSL subroutine LEQT1F.

APPENDIX B

FLOWCHARTS, PROGRAM LISTING AND SAMPLE INPUT AND OUTPUT FILES FOR PROGRAM TRNCHG

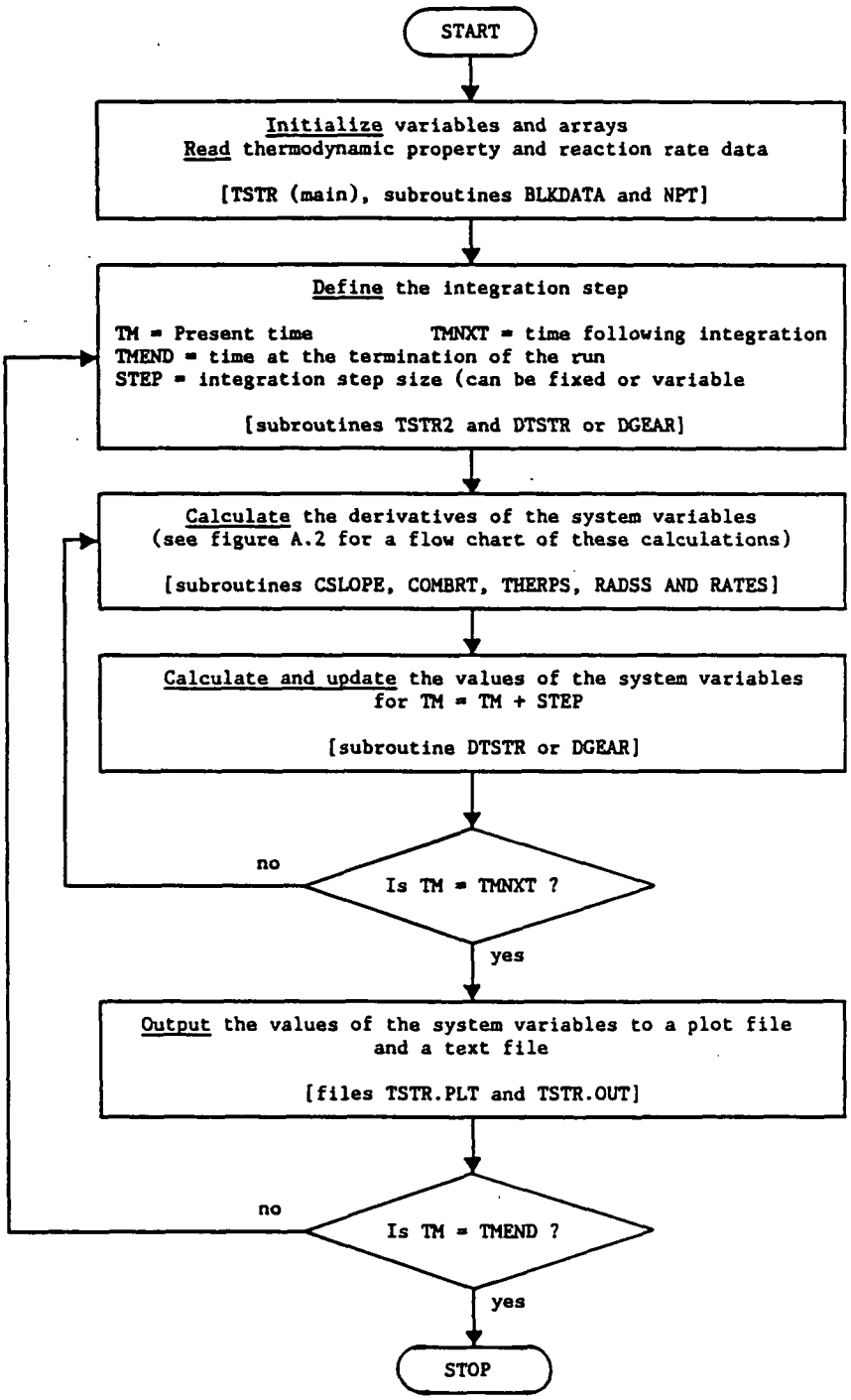

Figure B.1: Flowchart for Program TRNCHG

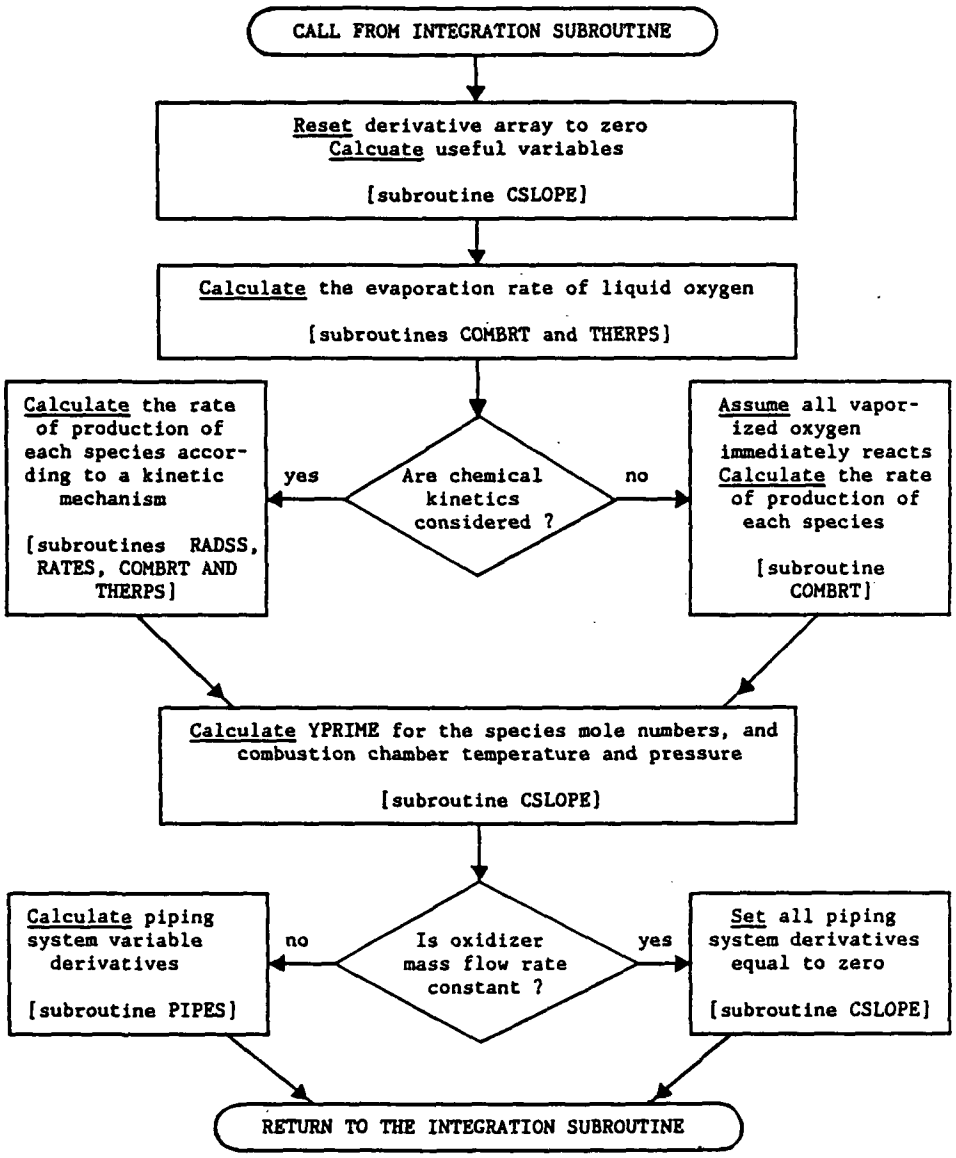

Figure B.2: Flowchart for the Calculation of Derivatives

```
C  TRNCHG:MAIN (AUGUST, 1987)
C
C  TRNCHG WAS WRITTEN TO PREDICT THE TRANSIENT BEHAVIOR OF THE
C  SPACE SHUTTLE MAIN ENGINE FUELSIDE PREBURNER DURING THE SHUT-
C  DOWN HELIUM PURGE. IT IS ALSO CAPABLE OF PREDICTING ENGINE BE-
C  HAVIOR DURING OPERATION AT FULL POWER LEVEL.
C
C  INITIAL PROGRAMMING FOR TRNCHG WAS BY DR. P. GEORGE II, CURRENT-
C  LY AT BATTELLE LAB, COLUMBUS, OH. SUBSEQUENT PROGRAMMING WAS BY
C  T. BARTRAND, MASTER'S CANDIDATE, U. OF TENNESSEE, KNOXVILLE.
C
C  THE PREBURNER COMBUSTION CHAMBER WAS MODELLED AS A STIRRED TANK
C  REACTOR. FUEL MASS FLOW RATE WAS TAKEN AS CONSTANT. OXIDIZER EN-
C  TERS THE COMBUSTION CHAMBER VIA A MULTI-PIPE MULTI-NODE FEED
C  SYSTEM WITH A CONSTANT PRESSURE AT THE FURTHEST UPSTREAM NODE.
C
C  THE TRNCHG SYSTEM VARIABLES, WHICH ARE INTEGRATED OVER TIME,
C  FALL INTO TWO CATEGORIES: THE CHAMBER VARIABLES AND THE OXI-
C  DIZER FEED SYSTEM VARIABLES.
C
C  CHAMBER VARIABLES INCLUDE:
C     S2(I) : MOLE NUNMBER OF SPECIES I (KGMOLES OF I/KG)
C     TK : TEMPERATURE (K)
C     PA : PRESSURE (PA)
C     DLIQ : LIQUID DENSITY IN THE COMBUSTION CHAMBER (KG/M**3)
C
C  FEED SYSTEM VARIABLES INCLUDE:
C     V(J) : VELOCITY IN PIPES J (M/S)
C     FVI(J) : POSITION OF THE LIQUID/VAPOR INTERFACE IN PIPE J
C            (% OF THE PIPE LENGTH)
C     RHO(K) : DENSITY AT NODE K (KG/M**3)
C     FVI2 : POSITION OF THE BACKFLOW INTERFACE IN THE LAST PIPE.
C            (% OF THE PIPE LENGTH)
C
C  EXECUTION OF TRNCHG INVOLVES 11 SUBROUTINES (WRITTEN FOR THE
C  PROGRAM) AND THE USE OF TWO IMSL SUBROUTINES: DGEAR, FOR NUMER-
C  ICAL INTEGRATION OF DIFFERENTIAL EQUATIONS AND LEQT1F, FOR SOLU-
C  TION OF MATRIX EQUATION A X = B FOR THE VECTOR X. A LISTING OF
C  THE SUBROUTINES USED IN THE EXECUTION OF TRNCHG AND A BRIEF
C  EXPLANATION OF THE FUNCTION THAT EACH PERFORMS FOLLOWS.
C
C  COMMONSS : COMMON BLOCK INCLUDED IN MOST OF THE SUBROUTINES
C     CALLED IN THE EXECUTION OF TRNCHG.
C  YCAL : USED TO CALL THE INTEGRATION ROUTINE AND CALL SUBROUTINE
C     OUTPT.
C  NPT: READS MOST OF THE NECESSARY DATA FOR EXECUTION. INITIAL-
C     IZES VARIABLES, CALCULATES THERMODYNAMIC PROPERTIES AND
C     FORMS REACTION RATE EXPRESSIONS.
C  DTSTR: RUNGE-KUTTA INTEGRATION SUBROUTINE TO BE USED IN THE
C     ABSENCE OF IMSL SUBROUTINE DGEAR. TO SELECT DTSTR THE VARI-
```

```
C     ABLE NDGEAR (NAMELIST ICONS) IS SET EQUAL TO 1. TO USE DGEAR
C     LET NDGEAR = 0.
C  CSLOPE: CALCULATES THE DERIVATIVES WITH RESPECT TO TIME FOR
C     THE SYSTEM VARIABLES ON A CALL FROM THE INTEGRATING ROUTINE.
C     CALLS SUBROUTINES COMBRT, PIPES AND THERPS.
C  THERPS: CALCULATES ENTHALPY, INTERNAL ENERGY AND SPECIFIC HEAT
C     AT CONSTANT PRESSURE FOR GASEOUS CONSTITUENTS WITHIN THE
C     COMBUSTION CHAMBER.
C  COMBRT: CALCULATES THE RATE OF PRODUCTION OF THE MAJOR SPECIES
C     IN THE COMBUSTION CHAMBER DUE TO VAPORIZATION AND COMBUSTION.
C     COMBRT CALLS BOTH RADSS AND THERPS.
C  PIPES: CALCULATES THE DERIVATIVES OF THE PIPING SYSTEM VARI-
C     ABLES ON A CALL FROM CSLOPE. ACCESSES IMSL SUBROUTINE LEQT1F.
C     INPUTS TO PIPES ARE FOUND IN NAMELIST INPIP AND COMMON BLOCK
C     CPIPE.
C  RADSS: CALCULATES THE RATE OF PRODUCTION OF THE MAJOR SPECIES IN
C     THE COMBUSTION CHAMBER DUE TO COMBUSTION. ASSUMES THE MOLE
C     NUMBERS OF THE VERY REACTIVE SPECIES (ATOMS AND RADICALS) ARE
C     CONSTANT AT ANY TIME. RADSS ACCESSES IMSL SUBROUTINE LEQT1F
C     AND SUBROUTINE RATES.
C  RATES: CALCULATES THE RATE OF PRODUCTION OF RADICALS AND ATOMS
C     AND THE DERIVATIVE OF THESE RATES. RATE FOR A GIVEN SPECIES
C     IS FOUND BY SUMMING THE CONTRIBUTIONS TO RATE BY EACH ELEMEN-
C     TARY REACTION.
C  OUTPT: OUTPUTS VALUES TO THE TEXT FILE TSTR.OUT AND THE PLOT
C     FILES TSTR.PLT1 AND TSTR.PLT2 ON RETURN FROM THE INTEGRATION
C     SUBROUTINE OR IF THE EXECUTION MUST BE STOPPED
C
C  OUTPUT IS CONTROLLED BY THE PARAMETER NDEBUG. FOR NDEBUG(I) EQUAL
C  TO 1 THE OUTPUT OF OUTPUT GROUP I IS PRINTED IN THE APPROPRIATE
C  FILE. OTHERWISE NDEBUG(I) SHOULD EQUAL 0.
C
C  OUTPUT GROUPS ARE:
C
C    NDEBUG(1) ---> PROBLEM PARAMETERS FROM NAMELISTS PARAM, ICONS,
C                   SSRXN AND PIPES.
C    NDEBUG(2) ---> THERMODYNAMIC PROPERTY DATA.
C    NDEBUG(3) ---> REACTION RATE DATA.
C    NDEBUG(4) ---> INITIAL CONDITIONS OF THE INLET STREAMS
C                   AND IN THE COMBUSTION CHAMBER.
C    NDEBUG(5) ---> INPUTS TO THE INTEGRATING ROUTINE.
C    NDEBUG(6) ---> OUTPUTS FROM THE INTEGRATING ROUTINE TO
C                   THE OUTPUT TEXT FILE (TSTR.OUT)
C    NDEBUG(7) ---> OUTPUTS FROM THE INTEGRATING ROUTINE TO
C                   THE OUTPUT PLOT FILE (TSTR.PLT)
C    NDEBUG(8) ---> TERMS USED IN THE CALCULATION OF DERIVATIVES
C                   TIVES IN SUBROUTINE CSLOPE.
C    NDEBUG(9) ---> DERIVATIVE ESTIMATES AT THE END OF
C                   SUBROUTINE CSLOPE.
C    NDEBUG(10) --> OUTPUTS VALUES OF TEMP, PRESS, AND MOLE NO. TO
```

```
C                    THE SCREEN IN CSLOPE (FOR INTERACTIVE USE)
C     NDEBUG(11) --> CONVERGENCE SUMMARY FOR SUBROUTINE RADSS
C     NDEBUG(12) --> SUMMARY OF THE DERIVATIVES CALCULATED IN
C                    SUBROUTINE PIPES.
C     NDEBUG(13) --> OUTPUTS FROM SUBROUTINE RATES, INCLUDING
C                    A LISTING OF THE RXNS WHOSE REACTION RATES
C                    ARE SMALL AND SET EQUAL TO ZERO.
C     NDEBUG(14) --> OUTPUTS VALUES OF TIME, STEP, TEMPERATURE
C                    AND MOLE NUMBERS OF THE MAJOR SPECIES TO
C                    THE SCREEN ON RETURN TO YCAL FROM THE INTEG-
C                    RATION SUBROUTINE.
C     NDEBUG(15) --> SUMMARY OF DERIVATIVE ESTIMATES, OLD AND
C                    NEW SYSTEM VARIABLE VALUES FROM THE RUNGE -
C                    KUTTA INTEGRATION SUBROUTINE DTSTR.
C
C  THREE SETS OF COMBUSTION CHAMBER CONSTITUENTS ARE
C  CONSIDERED IN TRNCHG:
C
C     (1) INLET STREAM CONSTITUENTS (REACTANTS) WHICH ARE
C         PRESENT IN SIGNIFICANT AMOUNTS IN THE COMBUSTION
C         CHAMBER,
C     (2) REACTION PRODUCTS WHICH ARE PRESENT IN SIGNIFICANT
C         AMOUNTS IN THE COMBUSTION CHAMBER AND
C     (3) RADICALS AND ATOMS, WHICH ARE CONSIDERED TO HAVE
C         SMALL CONCENTRATIONS RELATIVE TO REACTANTS AND
C         PRODUCTS AND WHOSE MOLE NUMBER IS TAKEN CONSTANT
C         AT ANY INSTANT OF TIME.
C
C
C  TRNCHG IS DOUBLE PRECISION FOR ALL REAL VARIBLES. THE MAXI-
C  MUM NUMBER OF SYSTEM VARIBLES IS 50, BUT CAN BE EASILY
C  INCREASED BY INCREASING THE DIMENSIONS OF ARRAYS Y, YPRIME,
C  WK AND IWK.
C
C  ***** TRNCHG USES SI FOR ALL CALCULATIONS *****
C
C      INCLUDE 'INIT.FOR/LIST'
C
      DIMENSION S2P(10),Y(50),IWK(50),WK(9000)
C
      INCLUDE 'COMMONSS.FOR/LIST'
C
      NAMELIST
     *  /RUNNO/ NMON,NDAY,NYR,NRUN,
     *  /PARAM/ VOL,Q,S2MIN,EMS,TKS,TMSD,RGMX,RHOGAS,RHOLIQ,
     *          RHOH2,AH2IN,AO2IN,FVI2MN,DLIQMN,DMMIN,DMC,
     *          CFTP,PHG,XPER,TMPER,CVR,
     *  /INITC/ XMASS,TK,PA,DM,
     *  /INDX1/ NDEBUG,MCON,KINET,
     *  /ICONS/ METH,MITER,NDGEAR,IER,STEP,TMI,TMPRNT,TMEND,
```

```
     *          INDEX,EPSI,
     *  /SSRRT/ EPSISS,RLX,RLX2,ITMAXS,IDGT,JER
     *  /INPIP/ V,FVI,RHO,FVI2,PL,AREA,RFLIQ,RFGAS,RFLHO,
     *          RFGHO,RFLV,RFGV,PS,CDIN,SM1MIN,
     *  /INDX2/ N1,N2,NP,NN,NHEO,NFVI
C
      DATA RGAS/ 8314.4 /,JJ/ 9 /,TENLN/ 2.302585093 /
C
      OPEN (UNIT=20,FILE='[BART.TSTR.WORK]TSTR.IN',READ ONLY,
     *      STATUS='OLD')
      OPEN (UNIT=30,FILE='[BART.TSTR.WORK]TSTR.OUT',STATUS='OLD')
      OPEN (UNIT=31,FILE='[BART.TSTR.WORK]TSTR.PLT1',STATUS='NEW')
      OPEN (UNIT=32,FILE='[BART.TSTR.WORK]TSTR.PLT2',STATUS='NEW')
C
C --- READ AND WRITE PROBLEM PARAMETERS FROM NAMELISTS.
C
      READ (20,RUNNO)
      READ (20,PARAM)
      READ (20,INITC)
      READ (20,INDX1)
      READ (20,ICONS)
      READ (20,SSRRT)
      READ (20,INPIP)
      READ (20,INDX2)
C
      WRITE (30,1000) NMON,NDAY,NYR,NRUN
C
      IF (NDEBUG(1)) THEN
         WRITE (30,1100) VOL,Q,S2MIN,XMASS,DM,DMMIN,CFTP,PHG,
     *                   NDEBUG
         WRITE (30,1150) DMC,AH2IN,AO2IN,MCON,KINET
         WRITE (30,1200) METH,MITER,NDGEAR,IER,EPSI,STEP,TMI,
     *                   TMPRNT,TMEND,TMSD
         WRITE (30,1300) EPSISS,RLX,ITMAXS,IDGT,JER
         WRITE (30,1400) NP,NN,NHEO,NFVI,RFLIQ,RFGAS,RFLHO,
     *                   RFGHO,RFLV,RFGV,CDIN,PS,FVI2
         WRITE (30,1500) (I,N1(I),N2(I),AREA(I),PL(I),I=1,NP)
         WRITE (30,1600) (I,V(I),FVI(I),I=1,NP)
         WRITE (30,1700) (I,RHO(I),I=1,NN)
      END IF
      S2MLG = DLOG(S2MIN)
      PAMAX = 1.0D+03 * PA
C
C --- ARATIO IS THE RATIO OF THE TOTAL AREA OF THE OXYGEN
C     INJECTORS TO THE AREA OF THE LAST PIPE IN THE OXIDIZER
C     FEED SYSTEM.
C
      ARATIO = 264.0 * AO2IN/AREA(NP)
      ARATSQ = ARATIO*ARATIO
C
```

```
C --- CALL NPT TO ESTABLISH INITIAL CONDITIONS FOR THE REACTANT
C     STREAMS AND COMBUSTION CHAMBER. NPT INDEXES SPECIES AND
C     FILLS S2 AND S1 ARRAYS AND INITIALIZES TEMPERATURE AND
C     PRESSURE.
C
      CALL NPT
C
C --- DEFINE THE ISIDE ARRAY. ISIDE(KK,LL) TELLS THE SIDE OF
C     RXN LL ON WHICH SPECIE KK IS FOUND. IF KK ON THE LHS,
C     ISIDE IS NEGATIVE. IF KK IS ON THE RHS, KK IS POSITIVE.
C     IF KK APPEARS TWICE, ISIDE=2. IF KK APPEARS ONCE,
C     ISIDE=1. FOR KK NOT PRESENT, ISIDE=0.
C
      DO 120 LL=1,JJ
      DO 110 KK=1,NSRATE
      DO 100 MM=1,4
         IF(KK.EQ.ID(MM,LL)) THEN
            IF(MM.LE.2.AND.ID(1,LL).EQ.ID(2,LL)) THEN
               ISIDE(KK,LL) = -2
            ELSE IF(MM.LE.2) THEN
               ISIDE(KK,LL) = -1
            ELSE IF(ID(3,LL).EQ.ID(4,LL)) THEN
               ISIDE(KK,LL) = 2
            ELSE
               ISIDE(KK,LL) = 1
            END IF
            GO TO 110
         END IF
  100 CONTINUE
      ISIDE(KK,LL) = 0
  110 CONTINUE
  120 CONTINUE
C
C --- WRITE THERMODYNAMIC AND REACTION RATE DATA TO THE OUTPUT
C     TEXT FILE.
C
      IF(NDEBUG(2)) THEN
         WRITE (30,1900) (I,ANAM(I),SMW(I),I=1,NS)
         WRITE (30,2000) (I,ANAM(I),SMW(I),I=NS+1,NSRATE)
         WRITE (30,2100) (ANAM(I),(Z(J),J=(I-1)*14+1,I*14),
     *                    I=1,NSRATE)
      END IF
      IF(NDEBUG(3)) THEN
         WRITE (30,2200) (J,(ID(K,J),K=1,4),J=1,JJ)
         WRITE (30,2300) (J,(ISIDE(K,J),K=1,NSRATE),J=1,JJ)
         WRITE (30,2400)
         DO 125 J=1,JJ
            TM1 = BX(J)/TENLN
            TM2 = BX2(J)/TENLN
            WRITE (30,2450) J,MODR(J),TM1,TEN(J),TACT(J),TM2,
```

```
     *                    TEN2(J),TACT2(J)
  125    CONTINUE
      END IF
C
C --- PUT MOLE NUMBER WITHIN THE PROBLEM DOMAIN
C     (S2MIN< S2 < 1/SMW), SUMMARIZE INPUTS AND WRITE INTIIAL
C     CONDITIONS TO THE PLOT AND TEXT OUTPUT FILES.
C
      SM = 0.0
      DO 130 I=1,NS
         IF(S2(I).LT.S2MIN) S2(I) = S2MIN
         SM = SM + S2(I)
  130 CONTINUE
C
C --- DEFINE USEFUL CONSTANTS
C
      TKINV = 1.0/TK
      SMINV = 1.0/SM
      RGASIN = 1.0/RGAS
      OMV = EMS(1)/VOL
      FMV = EMS(2)/VOL
      PMV = EMS(3)/VOL
      EMV = OMV + FMV + PMV
      RHOCC = PA*SMINV*RGASIN*TKINV
C
C --- WRITE INITIAL PIPE AND COMBUSTION CHAMBER CONDITIONS TO
C     THE TEXT FILE AND THE PLOT FILE.
C
      IF(NDEBUG(4)) THEN
         WRITE (30,2500) (I,ANAM(I),S2(I),ISTRM(I),S1(ISTRM(I),
     *                    I),AST(I),I=1,NSRATE)
         WRITE (30,2600) TK,PA,RHOCC,SM,VOL,(I,ANST(I),TKS(I),
     *                    EMS(I),SF(I),HS(I),SH(I),I=1,3)
      END IF
C
      IF(NDEBUG(7)) THEN
         TMP = TMI*1.0D+03
         PAP = PA*1.0D-06
         IF(DM.LT.DMMIN) DM = DMMIN
         DMP = DM * 1.0D+06
         DLIQ = XMASS/VOL
         DO 140 I=1,NSRATE
  140       S2P(I) = S2(I)*1.0D+03
         WRITE (31,2700)
         WRITE (31,2800) TMP,(S2P(I),I=1,NSRATE)
         WRITE (32,2750)
         WRITE (32,2850) TMP,TK,PAP,EMS(1),DLIQ,DMP,VR
      ENDIF
C
C --- SET PIPES INITIAL CONDITIONS AND INDICIES. NOTE THAT
```

```
C     THE LOG VARIABLE FORM IS NOT USED IN THE FORMULATION
C     OF THE PIPING SYSTEM OF EQUATIONS.
C
C     NN       NO. OF NODES
C     NP       NO. OF PIPES
C     NHEO     NO. OF PIPES THAT MAKE UP THE HELIUM PURGE
C              ORIFICE
C     NPV      INDEX FOR THE PIPE THAT ACTS AS THE HELIUM
C              CHECK VALVE
C     NFVI     INDEX FOR THE PIPE IN WHICH THE LIQUID/VAPOUR
C              INTERFACE IS LOCATED
C     NS4 --> NS5 INDICIES FOR PIPE FLUID VELOCITIES.
C     NS6 --> NS7 INDICIES FOR PIPE FLUID/VAPOUR INTERFACES.
C     NS8 --> NS9  INDICIES FOR NODAL DENSITIES
C     NS10     INDEX OF THE SYSTEM VARIABLE THAT FOLLOWS THE
C              PROGRESS OF A LIQUID/VAPOR INTERFACE THAT RE-
C              SULTS FROM BACKFLOW FROM THE COMBUSTION CHAM-
C              BER INTO THE OXIDIZER FEED SYSTEM.
C     NV       TOTAL NUMBER OF DEPENDENT (SYSTEM) VARIABLES
C              WHICH MUST BE INTEGRATED.
C
C     NODE 1 IS THE FURTHEST UPSTREAM NODE. PRESSURE FOR NODE
C     1 IS TAKEN AS CONSTANT. NODE NN IS THE FURTHEST DOWN-
C     STREAM NODE. IT IS THE JUNCTION OF THE PIPING SYSTEM WITH
C     THE COMBUSTION CHAMBER. ONLY ONE UPSTREAM AND ONE DOWN-
C     STREAM BOUNDARY ARE PROGRAMMED.
C
C     PIPE 1 IS TAKEN AS THE FURTHEST UPSTREAM PIPE. PIPE NP IS
C     THE FURTHEST DOWNSTREAM PIPE, CONNECTED TO THE COMBUSTION
C     CHAMBER VIA NODE NN.
C
      NS4 = NS3 + 1
      NS5 = NS3 + NP
      NS6 = NS5 + 1
      NS7 = NS5 + NP
      NS8 = NS7 + 1
      NS9 = NS7 + NN
      NS10 = NS9 + 1
      NV = NS10
      NPV = NHEO + 1
C
C --- N AND NWK ARE THE DIMENSIONS OF THE SYSTEM VARIABLES USED
C     IN THE INTEGRATION.
C
      N = NV
      IF(METH.EQ.1) NMETH = NV*13
      IF(METH.EQ.2) NMETH = NV*6
      IF(MITER.EQ.1.OR.MITER.EQ.2) NMITER = NV*(NV+1)
      IF(MITER.EQ.3) NMITER = NV
      IF(MITER.EQ.-1.OR.MITER.EQ.-2) MITER=NV*(2*NLC+NUC+3)
```

```
      IF(MITER.EQ.0) NMITER = 1
      NWK = 4*NV + NMETH + NMITER
C
C --- YCAL CARRIES OUT THE INTEGRATION AND OUTPUTS RESULTS TO A
C     PLOT FILE AND TEXT FILE ON RETURNS FROM THE INTEGRATION
C     ROUTINE.
C
      CALL YCAL(Y,WK,IWK,N,NWK)
C
      STOP
C
 1000 FORMAT(//2X,'***** TSTR OUTPUT TEXT FILE *****'/,
     * 12X,I2,2X,I2,2X,I4/,12X,'RUN NUMBER',2X,I3,//)
 1100 FORMAT(2X,'***** SOLUTION PARAMETERS *****'//,
     * 4X,'CC VOLUME  = ',1PD9.2,' M**3'/,
     * 4X,'CC HEAT TRANS. RATE    = ',1PD12.5,' J/S'/,
     * 4X,'MIN ALLOWABLE MOLE NO. = ',1PD12.5,' KGMOLE/KG'/,
     * 4X,'INITIAL MASS OF LIQ IN THE COMB CHAMBER = ',1PD12.5,
     * ' KG'/,4X,'INITIAL DROPLET DIAMETER = ',1PD12.5,' M'/,
     * 4X,'MIN ALLOWABLE DROPLET DIAMETER  = ',1PD10.3,' M'/,
     * 4X,'EXIT TURBINE FLOW RATE CONSTANT = ',1PD10.3/,
     * 4X,'HOT GAS MANIFOLD PRESSURE = ',1PD10.3,' PA'/,
     * /4X,'NDEBUG (1 FOR PRINITING, 0 FOR SUPRESSING OUTPUT)'
     * /,(8X,10(I1,2X)))
 1150 FORMAT(/4X,'DROPLET DIAMETER COEFFICIENT     = ',1PD11.4/,
     * 4X,'AREA OF HYDROGEN INJECTOR ANULUS = ',D11.4/,
     * 4X,'AREA OF THE OXIDIZER INJECTOR    = ',1PD11.4/,4X,
     * 'MCON (=0 FOR CONSTANT MASS FLOW; =1 FOR PIPING SYSTEM) ',
     * I1/,4X,'KINET (=0 FOR NO KINETICS; =1 FOR CALL TO RADSS) '
     * ,I1)
 1200 FORMAT(/4X,'INTEGRATION PARAMETERS:'/,
     * 6X,'MITER, METH, NDGEAR',2X,3(I1,3X)/,6X,'IER, EPSI',
     * 2X,I3,2X,1PD9.2/,6X,'INPUT STEP SIZE = ',1PD9.2,' SEC'/,
     * 6X,'INITIAL TIME = ',D9.2,' SEC'/,6X,'OUTPUT INTERVAL',
     * ' = ',D9.2,' SEC'/,6X,'FINAL TIME = ',D9.2,' SEC'/,
     * 6X,'TIME SHUTDOWN BEGINS = ',D9.2)
 1300 FORMAT(/4X,'FOR SS RATE APPROXIMATION:'/,6X,
     * 'CONVERGENCE CRITERION (MAX % CHANGE) = ',1PD9.2/,6X,
     * 'RELAXATION PARAMETER = ',0PF10.5/,6X,'MAX NO ITERATIONS',
     * '   = ',I7/,6X,'ERROR CHECK IDGT    = ',I2/,
     * 6X,'IMSL ERROR FLAG JER = ',I3)
 1400 FORMAT(/4X,'OXIDIZER FEED SYSTEM INPUTS:'/,
     * 6X,'NO. OF PIPES',2X,I2,2X,'NO. OF NODES',2X,I2/,
     * 6X,'NO. OF HELIUM ORIFICE PIPES',2X,I2/,
     * 6X,'PIPE IN WHICH THE INTERFACE IS INITIALLY LOCATED',
     * 2X,I2/,6X,'RFLIQ FOR THE OX PIPES  =  ',1PD10.3/,
     * 6X,'RFGAS FOR THE OX PIPES   = ',D10.3/,
     * 6X,'RFLIQ FOR THE HE ORIFICE = ',D10.3/,
     * 6X,'RFGAS FOR THE HE ORIFICE = ',D10.3/,
     * 6X,'RFLIQ FOR THE HE VALVE   = ',D10.3/,
```

```
     * 6X,'RFGAS FOR THE HE VALVE   = ',D10.3/,
     * 6X,'INJECTOR AND MANIFOLD CD = ',D10.3/,
     * 6X,'UPSTREAM SOURCE PRESSURE = ',D12.5,' PA'/,
     * 6X,'INITIAL BACKFLOW INTERFACE POSITION = ',1PD10.3)
1500 FORMAT(/4X,'PIPE GEOMETRY:'/,
     * 6X,'PIPE',2X,'NODE 1',2X,'NODE 2',2X,'AREA (M**2)',
     * 2X,'LENGTH (M)'/,(7X,I2,5X,I2,6X,I2,5X,1PD10.4,
     * 3X,0PF10.5))
1600 FORMAT(/4X,'PIPE INITIAL CONDITIONS:'/,6X,'PIPE',2X,
     * 'VELOCITY (M/SEC)',2X,'LIQUID/VAP INT. POSITION',
     * ' (% LENGTH)'/,(7X,I2,5X,1PD11.4,4X,1PD11.4))
1700 FORMAT(/4X,'INITIAL NODAL DENSITIES:'/,6X,'NODE',2X,
     * 'DENSITY (KG/M**3)'/,(7X,I2,6X,1PD11.4))
1800 FORMAT(12(A4,2X))
1900 FORMAT(/2X,'***** SPECIES PROPERTIES *****'//,
     * 4X,'MAJOR CONSTITUENTS:',/,6X,'INDEX',2X,'NAME',
     * 4X,'MOLEC. WT.',/,(8X,I2,3X,A4,4X,1PD11.4))
2000 FORMAT(/4X,'RATE DETERMINING RADICALS',/,
     * 6X,'INDEX',2X,'NAME',4X,'MOLEC. WT.',/,
     * (8X,I2,3X,A4,4X,1PD11.4))
2100 FORMAT(/2X,'***** "Z" ARRAY OF THERMO PROPERTY POLYNOMIAL '
     * 'COEFFICIENTS *****',//,6X,4HNAME,2X,12HCOEFFICIENTS,//,
     * (6X,A4,5(2X,1PD12.5)/,10X,5(2X,1PD12.5)/,10X,
     * 4(2X,1PD12.5)//))
2200 FORMAT(/2X'***** REACTION RATE INDICIES AND DATA *****'//,
     * 4X,'REACTION INDICIES',//,6X,7HRXN (J),4X,7HID(1,J),
     * 2X,7HID(2,J),2X,7HID(3,J),2X,7HID(4,J),/,
     * (9X,I2,8X,4(I2,7X)))
2300 FORMAT(/4X,'ISIDE ARRAY',//,6X,3HRXN,4X,12HISIDE(K,RXN),/,
     * (7X,I2,4X,7(2X,I2)))
2400 FORMAT(/4X,'REACTION RATE DATA IN SI UNITS',//,
     * 6X,3HRXN,2X,4HMODE,15X,2HBX,10X,3HTEN,8X,4HTACT,/)
2450 FORMAT(7X,I2,3X,I1,4X,3HFWD,2X,F11.3,2X,F11.3,2X,F11.3/,
     *  17X,3HREV,2X,F11.3,2X,F11.3,2X,F11.3)
2500 FORMAT(/2X,'***** CC AND INLET INITIAL CONDITIONS *****'//,
     * 4X,'SPECIE',2X,'NAME',2X,'S2 (KGMOLE/KG)',2X,'ISTRM',2X,
     * 'S1 (KGMOLE/KG)',2X,'STATE',/,
     * (6X,I2,4X,A4,3X,1PD12.5,5X,I1,5X,1PD12.5,4X,A4))
2600 FORMAT(/4X,'CC TEMPERATURE = ',0PF12.4,'  K'/,
     * 4X,'CC PRESSURE    = ',1PD12.4,' PA'/,
     * 4X,'CC DENSITY     = ',1PD12.5,' KG/M**3'/,
     * 4X,'AVG. MOL. WT.  = ',1PD12.5,' KG/KGMOLE'/,
     * 4X,'CC VOLUME      = ',1PD12.5,' M**3',//,
     * 4X,6HSTREAM,X,4HNAME,2X,4HTEMP,8X,4HMDOT,9X,2HSF,12X,2HHS,
     * 12X,2HSH/,18X,3H(K),6X,8H(KG/SEC),3X,12H(KGMOLE/SEC),3X,
     * 10H(J/KGMOLE),3X,7H(J/SEC)//,(6X,I1,4X,A4,2X,0PF6.2,2X,
     * 1PD11.5,2X,1PD11.5,2X,D12.5,2X,D12.5))
2700 FORMAT(2X,'TIME (MSEC)',2X,'MOLE NUMBER (KGMOLES/KG *1.0D+06)
     * ')
2800 FORMAT(2X,F8.3,7(X,1PD9.2))
```

```
2750 FORMAT(4X,'TIME',3X,'TEMPERATURE',X,'PRESSURE',X,' OX MDOT ',
    * 2X,'LIQ DEN',4X,'DROP DIAM ',2X,'VAP RATE'/,3X,'(MSEC)',6X,
    * '(K)',6X,'(MPA)',4X,'(KG/S)',4X,'(KG/M3)',4X,'(MICRONS)',2X,
    * '(KG/M3 S)')
2850 FORMAT(2X,F8.3,2X,F8.2,X,F8.3,2X,F8.4,3X,1PD9.2,3X,
    * 0PF8.3,3X,F8.2)
     END
```

```
C
C FILE INIT: INITIALIZATIONS OF VARIABLES
C
      IMPLICIT REAL*8 (A-H,P-Z)
      IMPLICIT INTEGER*4 (I-O)
      REAL*8 OMV
      CHARACTER*4 ANAM(20),AST(20),ASTNST(10),ANST(10),ALIQ,AGAS
C
```

```
COMMONSS.PROC
C
C
      COMMON
     * /CPARA/ SMW(10),AST,ANAM,RATE(10),YPP(10),OMV,FMV,PMV,
     *    EMV,SMEMV,RGAS,RGASIN,VOL,Q,S2MIN,S2MLG,SM,SMINV,
     *    TMSD,RGMX,ALIQ,AGAS,VR,RHOGAS,RHOLIQ,RHOH2,CPSUM,
     *    AH2IN,AO2IN,VH2,DM,DMMIN,DMC,CFTP,PHG,DPIN,RPX,
     *    DLIQMN,FVI2MN,XPER,TMPER,PAMAX,CVR,
     * /CSVAR/ S2(10),TK,TKINV,PA,RHOCC,RHINV,DLIQ,XMASS,
     * /CSTRM/ S1(3,30),ISTRM(10),TKS(3),EMS(3),DHF(10),
     *    INST(10),HS(3),ASTNST,ANST,SH(3),SF(3),
     * /CINTE/ TMEND,TMI,TMPRNT,STEP,EPSI,METH,MITER,INDEX,
     *    IER,NDGEAR,
     * /CIDX1/ NDEBUG(20),NREAC,NPROD,NRAD,NSRATE,JJ,NSTRM,
     *    NV,NS,NS1,NS2,NS3,NS4,NS5,NS6,NS7,NS8,NS9,NS10,MCON,
     *    KINET,
     * /CRATE/ ID(4,20),ISIDE(10,20),MODR(20),BX(20),BX2(20),
     *    TEN(20),TEN2(20),TACT(20),TACT2(20),ARR(10),RIP(10,10),
     *    X1(20),X2(20),
     * /CPROP/ Z(200),H(10),CP(10),U(10),S(10),DCP(10),H0(10),
     *    CP0(10),S0(10),
     * /CSSRR/ EPSISS,RLX,ITMAXS,IDGT,JER,
     * /CPIPE/ V(15),FVI(15),RHO(15),P(15),AREA(15),PL(15),
     *    PS,FVI2,CDIN,SM1MIN,RFLIQ,RFGAS,RFLV,RFGV,RFGHO,RFLHO,
     * /CIDX2/ N1(15),N2(15),NN,NP,NHEO,NFVI,NPV
C
```

```
      SUBROUTINE CSLOPE(N,T,Y,YPRIME)
C
C   CSLOPE CALCULATES THE DERIVATIVES WITH RESPECT TO TIME OF
C   THE SYSTEM VARIABLES.
C
C   N IS THE TOTAL NUMBER OF DEPENDENT VARIABLES.
C
C      YPRIME(1:NS)     --> D(LOG(S2(I))/DT
C      YPRIME(NS1)      --> D(DLIQ)/DT
C      YPRIME(NS2)      --> D(LOG(TK))/DT
C      YPRIME(NS3)      --> D(LOG(PA))/DT
C      YPRIME(NS4:NS5) --> D(V(J))/DT
C      YPRIME(NS6:NS7) --> D(FVI(J))/DT
C      YPRIME(NS8:NS9) --> D(RHO(K))/DT
C      YPRIME(NS10)     --> D(FVI2)/DT
C
C  SYSTEM VARIABLES INCLUDE COMBUSTION CHAMBER VARIABLES AND
C  FEED SYSTEM VARIABLES:
C
C      S2(I)  IS MOLE NUMBER OF SPECIES I (KGMOLES I/KG TOTAL)
C      DLIQ   IS THE COMBUSTION CHAMBER LIQUID DENSITY (KG/M**3)
C      TK     IS COMBUSTION CHAMBER TEMPERATURE (K)
C      PA     IS COMBUSTION CHAMBER PRESSURE (PA)
C      V(J)   IS FLUID VELOCITY IN PIPE J.
C      FVI(J) IS POSITION OF THE LIQUID/VAPOR INTERFACE IN PIPE J.
C      RHO(K) IS DENSITY OF NODE K.
C      FVI2   IS THE POSITION OF THE BACKFLOW INTERFACE (FROM THE
C             COMBUSTION CHAMBER INTO THE OXIDIZER FEED SYSTEM.
C
C  OTHER VARIABLES:
C
C      OMV = VOLUMETRIC MASS FLOW RATE THROUGH THE OXIDIZER
C            FEED SYSTEM
C      FMV = VOLUMETRIC MASS FLOW RATE THROUGH THE FUEL FEED
C            SYSTEM (CONSTANT)
C      PMV = VOLUMETRIC MASS FLOW RATE OF HELIUM INTO THE
C            COMBUSTION CHAMBER.
C      EMV = EXIT VOLUMETRIC MASS FLOW RATE (THE THE EXIT
C            TURBINE
C      SM  = AVERAGE MOLECULAR WEIGHT IN THE COMBUSTION CHAMBER
C            (DOES NO TAKE LIQUID SPECIES INTO ACCOUNT)
C
      INCLUDE 'INIT.FOR/LIST'
C
     DIMENSION Y(N),YPRIME(N),ALG(20)
C
     INCLUDE 'COMMONSS.FOR/LIST'
C
C --- RESET YPRIME ARRAY
C
```

```
      DO 100 I=1,N
  100 YPRIME(I) = 0.0
C
C --- IF THE HELIUM/OXYGEN INTERFACE IS AT THE LAST NODE STOP
C     EXECUTION
C
      IF(FVI(NP).GE.1.0) THEN
         WRITE (30,1000)
         CALL OUTPT(Y,TM,N,NSTEPS)
         STOP
      ENDIF
C
C --- COUNT ITERATIONS AT EACH TIME STEP
C
      IF(T.EQ.TMOLD) THEN
         ITER = ITER + 1
      ELSE
         ITER = 1
         TMOLD = T
      ENDIF
C
C --- COMPUTE MOLE NUMBERS. NO SPECIES MOLE NUMBER MAY EXCEED
C     1.0/SMW(I) (SMW(I) IS THE MOLECULAR WEIGHT OF SPECIES I)
C
      TMRAT = 0.0
      SM = 0.0
      DO 110 I=1,NS
         ALG(I) = DLOG(1.0/SMW(I))
         IF(Y(I).LT.ALG(I).AND.Y(I).GT.S2MLG) THEN
            S2(I) = DEXP(Y(I))
         ELSE IF(Y(I).GE.ALG(I)) THEN
            S2(I) = DEXP(ALG(I))
            Y(I) = ALG(I)
         ELSE
            S2(I) = S2MIN
            Y(I) = S2MLG
         ENDIF
         TMRAT = TMRAT + S2(I)*SMW(I)
  110 CONTINUE
C
C --- NORMALIZE MOLE NUMBERS
C
      DO 120 I=1,NS
         SM = SM + S2(I)
         S2(I) = S2(I)/TMRAT
  120 CONTINUE
      SMINV = 1./SM
C
C --- FIND TEMPERATURE, PRESSURE, DENSITY AND THE LIQUID DENSITY
C     FOR THE COMBUSTION CHAMBER AND BACKFLOW INTERFACE POSITION.
```

```
C
      DLIQ = Y(NS1)
      IF(DLIQ.LT.DLIQMN) THEN
         DLIQ = DLIQMN
      ENDIF
      TK = DEXP(Y(NS2))
      IF(TK.GT.1.0D+04) THEN
         TK = 1.0D+04
      ELSE IF(TK.LT.100.0) THEN
         TK = 90.0
      ENDIF
      PA = DEXP(Y(NS3))
      IF(PA.GT.PAMAX) THEN
         PA = PAMAX
      ELSE IF(PA.LT.1.0D+03) THEN
         PA = 1.0D+03
      ENDIF
      TKINV = 1.0 / TK
      FVI2 = Y(NS10)
      RHOCC = PA*RGASIN*SMINV*TKINV
      IF(RHOCC.LT.0.01) RHOCC = 0.01
      RHINV = 1.0/RHOCC
C
C --- FILL ARRAYS FOR V, RHO AND FVI
C
      DO 130 I=1,NP
         V(I) = Y(NS3+I)
         FVI(I) = Y(NS5+I)
  130 CONTINUE
      DO 140 I=1,NN
         RHO(I) = Y(NS7+I)
  140 CONTINUE
C
C --- DETERMINE MASS FLOW RATE IN THE OXIDIZER FEED SYSTEM AND
C     RATE OF ENERGY INFLUX TO THE CHAMBER FROM THE OXIDIZER
C     FEED SYSTEM.
C
      IF(FVI(NP).LT.1.0) THEN
         PMV = 0.0
         SF(3) = 0.0
         SH(3) = 0.0
         IF(V(NP).GT.0.0.AND.RHO(NN).GT.RGMX) THEN
            OMV = RHOLIQ * AREA(NP) * V(NP) / VOL
            SH(1) = OMV * HS(1) / SMW(3)
            SF(1) = 0.0
         ELSE
            OMV = RHOCC * AREA(NP) * V(NP) / VOL
            SH(1) = 0.0
            SF(1) = 0.0
            CALL THERPS(NS,TK)
```

```
            DO 150 I=1,NS
               SH(1) = SH(1) + OMV*S2(I)*H(I)
  150       CONTINUE
         ENDIF
      ELSE
         OMV = 0.0
         PMV = RHO(NN)*AREA(NP)*V(NP)/VOL
         SF(3) = PMV/SMW(1)
         SH(3) = SF(3)*HS(1)
      ENDIF
C
C --- DETERMINE THE VOLUMETRIC EXIT MASS FLOW RATE (EMV)
C
      PR = PHG/PA
      PB = PR**1.4286 - PR**1.7143
      IF(PB.LE.0.0) THEN
         EMV = 0.0
      ELSE
         EMV = CFTP*DSQRT(PA*PB/TK)
      ENDIF
      EMV = EMV/VOL
      IF (EMV.LT.0.0) EMV = 0.0
C
C --- COMBRT CALCULATES THE RATE OF PRODUCTION OF EACH SPECIES IN
C     THE CHAMBER DUE TO COMBUSTION AND VAPORIZATION.
C
      CALL COMBRT(T,Y,YPRIME)
C
C --- LOOPS TO CALCULATE YPRIMES C C --- YPP(I) ARE THE TERMS USED
C     TO FIND D(TEMP)/D(TIME)
C
       DO 160 IB = 1,10
  160    YPP(IB) = 0.0
C
C --- CALL THERPS FOR THE SPECIFIC MOLAR INTERNAL ENERGY AND
C     ENTHALPY FOR EACH SPECIES C
      CALL THERPS(NS,TK)
C
C --- CONSERVATION OF MASS FOR THE GAS PHASE
C
      IF(V(NP).GE.0.0.AND.RHO(NN).GE.RGMX) THEN
         SUMM = VR + FMV + PMV
      ELSE
         SUMM = VR + OMV + FMV + PMV
      ENDIF
      RPX = SUMM - EMV
C
C --- OUTPUT VALUES TO THE SCREEN IF NDEBUG(10) = 1
C
      IF(NDEBUG(10)) THEN
```

```
         WRITE (6,1100) T,V(NP),TK,VR,DM,DLIQ
      ENDIF
C
C --- CONSERVATION OF SPECIES
C
C     NOTE: IF THERE IS BACKFLOW INTO THE PIPES OR THERE IS
C     AN INTERFACE IN THE PIPES DUE TO BACKFLOW (FVI2>0.0),
C     OMV ACCOUNTS FOR THE INFLOW OR OUTFLOW OF CHAMBER CONTENTS.
C     CHAMBER GAS IN THE PIPES IS ASSUMED TO HAVE THE SAME
C     DENSITY AND TEMPERATURE AS THE CHAMBER CONTENTS.
C
      DO 170 I=1,NS
         IF(OMV.LT.0.0.AND.RHO(NN).LT.RGMX) THEN
            IF(ISTRM(I).GT.0) THEN
               YP = (SF(ISTRM(I))-(SUMM-OMV)*S2(I)+RATE(I))*RHINV
            ELSE
               YP = (-(SUMM-OMV)*S2(I)+RATE(I))*RHINV
            ENDIF
         ELSE
            IF(ISTRM(I).GT.0) THEN
               YP = (SF(ISTRM(I))-SUMM*S2(I)+RATE(I))*RHINV
            ELSE
               YP = (-SUMM*S2(I)+RATE(I))*RHINV
            ENDIF
         ENDIF
         YPRIME(I) = YP/S2(I)
         IF(Y(I).GE.ALG(I).AND.YP.GT.0.0) THEN
            YPRIME(I) = 0.0
            YP = 0.0
         ENDIF
         YPP(4) = YPP(4) + EMV*S2(I)*H(I)
         YPP(5) = YPP(5) + U(I)*S2(I)
         YPP(6) = YPP(6) + U(I)*YP
         YPP(8) = YPP(8) + S2(I)*(CP(I)-RGAS)
         YPP(9) = YPP(9) + YP
  170    CONTINUE
      YPP(1) = SH(1)
      YPP(2) = SH(2)
      YPP(3) = SH(3)
      YPP(5) = YPP(5)*RPX
      YPP(6) = YPP(6)*RHOCC
      YPP(7) = Q/VOL
      YPP(8) = YPP(8)*RHOCC
C
C --- CONSERVATION OF ENERGY
C
      TP = (YPP(1)+YPP(2)+YPP(3)-YPP(4)-YPP(5)-YPP(6)-YPP(7))/YPP(8)
      YPP(8) = YPP(8) * TK
      YPRIME(NS2) = TP/TK
C
```

```
C --- CONSERVATION OF MASS FOR THE LIQUID PHASE
C
      IF(ASTNST(1).EQ.AGAS) THEN
         YPRIME(NS1) = 0.0
      ELSE
         IF(V(NP).GE.0.0.AND.RHO(NN).GE.RGMX) THEN
            YPRIME(NS1) = OMV-VR-EMV*DLIQ/RHOCC
         ELSE
            YPRIME(NS1) = -VR-(EMV-OMV)*DLIQ/RHOCC
         ENDIF
      ENDIF
C
C --- THE IDEAL GAS LAW
C
      YPRIME(NS3) = YPRIME(NS2) + RPX * RHINV + YPP(9) * SMINV
C
C --- SUBROUTINE PIPES DETERMINES YPRIME FOR THE PIPING SYSTEM
C     DEPENDENT VARIABLES. PIPES IS CALLED IF MCON = 1. OTHERWISE
C     OXIDIZER FEED RATE REMAINS CONSTANT
C
      IF(MCON) CALL PIPES(Y,YPRIME,T)
C
C --- WRITE A SUMMARY OF THE TERMS USED TO CALCULATE DERIVATIVES
C
      IF(NDEBUG(8).EQ.1) THEN
         WRITE(30,1200) T,ITER,TK,PA,RHOCC,EMV,DLIQ,VR,
     *      (I,EMS(I),SF(I),SH(I),I=1,3)
         WRITE(30,1300) (IS,H(IS),U(IS),CP(IS),RATE(IS),IS=1,NS)
         WRITE(30,1400) ((IB,YPP(IB)),IB=1,9)
      ENDIF
C
C --- WRITE A SUMMARY OF YPRIME VALUES CALCULATED IN CSLOPE
C
      IF(NDEBUG(9).EQ.1) THEN
         WRITE(30,1500) T,ITER
         WRITE(30,1600)
         WRITE(30,1700) ((I,S2(I),Y(I),YPRIME(I)),I=1,NS),
     *         NS1,DLIQ,Y(NS1),YPRIME(NS1),NS2,TK,Y(NS2),
     *         YPRIME(NS2),NS3,PA,Y(NS3),YPRIME(NS3),NS10,
     *         FVI2,YPRIME(NS10)
         WRITE(30,1800) (J,V(J),YPRIME(NS3+J),FVI(J),
     *                  YPRIME(NS5+J),J=1,NP)
         WRITE(30,1900) (K,RHO(K),YPRIME(K+NS7),K=1,NN)
      ENDIF
C
      RETURN
C
 1000 FORMAT(2X,'***** INTERFACE HAS REACHED THE LAST NODE *****'//,
     * 2X,'*****          EXECUTION HALTED          *****'//)
 1100 FORMAT(X,'T ',1PD8.2,X,'V, TK, VR, DM, DLIQ ',D8.1,X,
```

```
     * 0PF6.1,3(X,1PD8.1))
 1200 FORMAT(/2X,'***** DEPENDENT VARIABLE DERIV. PARAMS *****'//,
     * 4X,'TIME = ',1PD12.5,2X,'ITERATION = ',I5/,4X,
     * 'TEMPERATURE = ',0PF15.4,2X,'PRESSURE = ',1PD12.5/,4X,
     * 'DENSITY = ',1PD12.5,2X,'EXIT VOLUMETRIC MASS FLOW = ',
     * 1PD12.5/,4X,'LIQ DENSITY = ',1PD12.5,' (KG/M**3)'/,4X,
     * 'VAPORIZATION RATE = ',1PD11.4,' KG/S M**3'//,4X,'STREAM',2X,
     * ' MASS FLOW ',2X,' MOLE FLOW ',2X,'ENTHALPY FLOW'/,14X,
     * '(KG/SEC)',2X,'(KGMOLE/SEC)',3X,'(JOULES/SEC)'//,
     * 3(7X,I1,4X,1PD11.4,2X,1PD11.4,2X,1PD11.4/))
 1300 FORMAT(/4X,'IN CSLOPE THERMO PROPS AND RXN RATES ARE:'/,
     * 4X,' I',2X,'     H     ',2X,'     U     ',2X,'    CP    ',
     * 4X,'     A    ' ,/,(4X,I2,4(2X,1PD12.5)))
 1400 FORMAT(/4X,'TEMPERATURE DERIVATIVE TERMS ARE: '/,
     * (4X,'YPP('I1,') = ',1PD12.5,2X,'YPP('I1,') = ',1PD12.5))
 1500 FORMAT(//2X,'***** CLSOPE YPRIME ESTIMATES *****'//,
     * 4X,'TIME = ',1PD12.5,2X,'ITERATION = ',I5,//)
 1600 FORMAT(4X,3H I ,2X,12H    S2(I)   ,2X,12H     Y(I)   ,2X,
     *       13H   YPRIME(I) ,//)
 1700 FORMAT(4X,I3,2X,1PD12.5,2X,1PD12.5,2X,1PD12.5)
 1800 FORMAT(/4X,'PIPE',2X,' VELOC. (M/S) ',2X,'D(VELOC.)/D(T)',
     * 2X,'FL/V INTERFACE',2X,'D(FVI)/D(TIME)'//,
     * (5X,I2,X,4(5X,1PD11.4)))
 1900 FORMAT(/4X,'NODE',2X,'DENSITY (M**3)',2X,'D(RHO)/D(TIME)'//,
     * (5X,I2,X,2(5X,1PD11.4)))
      END
C
```

```
      SUBROUTINE COMBRT(TM,Y,YPRIME)
C
C     COMBRT FINDS THE RATE OF PRODUCTION OF EACH OF THE SPECIES IN
C     THE COMBUSTION CHAMBER DUE TO REACTION RATE AND VAPORIZATION.
C
      INCLUDE 'INIT.FOR/LIST'
C
      DIMENSION Y(NV),YPRIME(NV)
C
      INCLUDE 'COMMONSS.FOR/LIST'
C
C --- FIND THE VAPORIZATION RATE, VR (KG/M**3 S) AND YPRIME(NS1)
C
C  CPSUM = THE AVERAGE SPECIFIC HEAT AT CONSTANT PRESSURE FOR
C          THE COMBUSTION CHAMBER GASES.
C     XK = THERMAL CONDUCTIVITY OF HYDROGEN (LEAST SQUARES LINEAR
C          FIT FOR XK AS A FUNCTION ONLY OF TEMPERATURE)
C    XMU = VISCOUSITY OF HYDROGEN (LEAST SQUARES LINEAR FIT FOR
C          XMU AS A FUNCTION ONLY OF TEMPERATURE)
C
      DATA PI/3.141592654/
C
      TAV = (TKS(1) + TK)/2.0
      CALL THERPS(NS,TAV)
      CPSUM = 0.0
      DO 100 I=1,NS
         CPSUM = CPSUM + CP(I)*S2(I)
  100 CONTINUE
      CALL THERPS(NS,TKS(1))
      XK = 5.282D-02 + 4.117D-04*TAV
      XMU = 5.0767D-06 + 1.4884D-08*TAV
C
C     (B) FIND THE AVBERAGE DROPLET DIAMETER, DM (M), THE RATE OF
C         VAPORIZATION, VR (KG/M3 S), AND THE TOTAL NUMBER OF
C         DROPLETS IN THE COMBUSTION CHAMBER, XNDR.
C
C         THE EXPRESSION USED TO CALCULATE EVAPORATION RATE WAS
C         ADAPTED FROM WEBBER (1972) (J. OF THE ARS)
C
      IF(ASTNST(1).EQ.AGAS) THEN
         VR = OMV
         GO TO 110
      ENDIF
      DM = DMC*OMV/FMV*DSQRT(SMW(2)*AH2IN*PA/RGAS/RHOLIQ/TKS(2))
      IF(DM.LT.DMMIN) DM = DMMIN
      DM3 = DM**3
      REN = RHOCC*VH2*DM/XMU
      ALPH = 1.0 + CVR * (TK-TKS(1))
      IF(ALPH.GT.1.0) THEN
         VRD = PI*XK*DM*(2.0+0.5*REN**0.5)*DLOG(ALPH)/CPSUM
```

```
      ELSE
         VRD = 0.0
      ENDIF
      XNDR = 6.0*DLIQ*VOL/RHOLIQ/DM**3/PI
      VR = 6.0*VRD*DLIQ/PI/RHOLIQ/DM3
      IF(VR.LE.0.0) THEN
         VR = 0.0
      ENDIF
  110 CONTINUE
C
C --- DETERMINE THE RATES OF PRODUCTION DUE TO COMBUSTION AND
C     VAPORIZATION
C     (A) IF KINET = 1, CHEMICAL KINETICS ARE CONSIDERED. REACTION
C         RATE IS CALCULATED IN RADSS ASSUMING THAT ATOM AND RADI-
C         CAL CONCENTRATIONS ARE STEADY STATE.
C     (B) IF KINET = 0, ALL OXYGEN WHICH VAPORIZES IS ASSUMED TO
C         IMMEDIATELY COMBUST.
C
      IF(KINET.EQ.1) THEN
         CALL RADSS
         RATE(3) = RATE(3) + VR/SMW(3)
      ELSE IF(KINET.EQ.0) THEN
         RATE(3) = 0.0
         RATE(4) = 2.0*VR/SMW(3)
         RATE(2) = -2.0*VR/SMW(3)
      ELSE IF(KINET.EQ.2) THEN
         CALL RATES
         DO 200 I=1,NS
            RATE(I) = ARR(I)
  200       CONTINUE
            RATE(3) = RATE(3) + VR/SMW(3)
      ENDIF
C
      IF(NDEBUG(15)) WRITE(30,1000) TM,TK,PA,DM,VRD,XNDR,REN,VR,
     *                              (ANAM(I),RATE(I),I=1,NS)
C
      RETURN
C
 1000 FORMAT(/,2X,'***** OUTPUT FROM COMBRT *****'//,4X,'AT TIME ',
     * 1PD11.5/,
     * 4X,'TEMPERATURE              = ',0PF10.3,' K '/,
     * 4X,'PRESSURE                 = ',1PD12.5,' PA'/,
     * 4X,'DROPLET DIAMETER         = ',D12.5,' M '/,
     * 4X,'DROPLET EVAPOATION RATE = ',D12.5,' KG/S/DROPLET'/,
     * 4X,'NO. OF DROPLETS          = ',D12.5,' DROPLETS'/
     * 4X,'REYNOLDS NO. OF DROPS    = ',D12.5/,
     * 4X,'TOTAL EVAPORATION RATE   = ',D12.5,' KG/M**3 S'//,
     * 4X,7HSPECIES,2X,'RATE OF PRODUCTION (KGMOLES/M**3 S)'//,
     * (5X,A4,5X,1PD12.5))
C
```

```
      END
C
```

```
      SUBROUTINE DTSTR(NV,CSLOPE,TM,STEP,Y,TMNXT,WK,NDEBUG)
C
C     THIS IS A RUNGE-KUTTA FOURTH ORDER INTEGRATING SUBROUTINE
C     WHICH ANSWERS A CALL MIMICKING A CALL TO IMSL SUBROUTINE
C     DGEAR. THE PURPOSE OF DGEAERX IS TO ALLOW DEBUGGING OF
C     THE TRANSIENT CHUGGING CODE AT MSFC, WHERE DGEAR IS NOT
C     AVAILABLE.
C
C     THE SIGNIFICANT VARIABLES ARE
C     NV=NUMBER OF VARIABLES
C     CSLOPE=NAME OF ROUTINE TO EVALUATE 1ST DERIVATIVE
C     TM=INDEPENDENT VARIABLE
C     STEP=DELTA TM
C     Y=ARRAY OF INDEPENDENT VARIABLES
C     SHOULD BE AN INTEGER
C     TMNXT=ENDING TM -(TMNXT-TM)/STEP
C     WK=WORK VECTOR OF 4*NV SIZE
C     OTHERS ARE UNUSED DUMMY PARAMETERS
C
C
      IMPLICIT REAL*8 (A-H,P-Z)
      DIMENSION Y(NV),WK(4,NV),YEND(100),F(100),NDEBUG(20)
C
C
      NSTEPS=(TMNXT-TM)/STEP
      IF(NSTEPS.LE.0) NSTEPS=1
C
C
      DO 100 J=1,NSTEPS
C
C     GET FIRST ESTIMATE OF THE DELTA X'S
C
         CALL CSLOPE (NV,TM,Y,F)
         DO 10 I=1,NV
            WK(1,I)=STEP*F(I)
            YEND(I)=Y(I)+WK(1,I)*0.5
 10      CONTINUE
C
C     GET SECOND ESTIMATE (USING YEND)
C
         NE=2
         TM2E=TM+STEP*0.5
         CALL CSLOPE (NV,TM2E,YEND,F)
         DO 20 I=1,NV
            WK(2,I)=STEP*F(I)
            YEND(I)=Y(I)+WK(2,I)*0.5
 20      CONTINUE
C
C     THIRD ESTIMATE
C
```

```
         NE=3
         CALL CSLOPE(NV,TM2E,YEND,F)
         DO 30 I=1,NV
            WK(3,I)=STEP*F(I)
            YEND (I)=Y(I)+WK(3,I)
 30      CONTINUE
C
C     LAST ESTIMATE
C
         NE=4
         TM2E=TM+STEP
         CALL CSLOPE(NV,TM2E,YEND,F)
         DO 40 I=1,NV
            WK(4,I)=STEP*F(I)
 40      CONTINUE
C
C     COMPUTE Y'S AT TM + STEP BY WEIGHTED AVERAGE
C
         DO 50 I=1,NV
            YEND(I)=Y(I)+(WK(1,I)+2*WK(2,I)+2*WK(3,I)+WK(4,I))/6.0
 50      CONTINUE
C
C     WRITE VALUES OF THE DERIVATIVE ESTIMATES AND "OLD" AND "NEW"
C     VALUE OF Y IF NDEBUG(15) = 1
C
         IF(NDEBUG(15)) THEN
            WRITE(30,1000) TM,STEP
            WRITE(30,1100) (K,(WK(I,K),I=1,4),Y(K),YEND(K),K=1,NV)
         ENDIF
C
C     ADVANCE Y&TM FOR NEXT STEP
C
         DO 60 I=1,NV
            Y(I)=YEND(I)
 60      CONTINUE
         TM=TM+STEP
C
 100  CONTINUE
C
      RETURN
C
C FORMATS
C
 1000 FORMAT(//,2X,'***** DTSTR OUTPUT *****'//,
     * 6X,'TIME = ',1PD12.5,' SEC',2X,'STEP = ',D12.5,' SEC'//,
     * 4X,'INDEX',X,'ESTIMATE 1',X,'ESTIMATE 2',X,'ESTIMATE 3',
     * X,'ESTIMATE 4',X,'  Y OLD  ',X,'  Y NEW   '//)
 1100 FORMAT(6X,I2,2X,1PD10.3,X,D10.3,X,D10.3,X,D10.3,X,D10.3,
     * X,D10.3)
C
```

```
      END
C
```

```
      SUBROUTINE NPT
C
C --- DEFINITION OF INPUT VARIABLES.
C
C      ANAM(I)    = HOLERITH NAME OF SPECIES I
C      S2(I)      = MOLE NUMBER OF SPECIES I (KGMOLES OF I/
C                   KG (TOTAL))
C      XIN(I)     = INLET MOLE FRACTION OF SPECIES I
C      XCC(I)     = INITIAL MOLE FRACTION OF SPECIES I.
C      AST(I)     = PHASE OF SPECIES I
C      ISTRM(I)   = NUMBER OF THE INLET STREAM CONTAINING SPECIES I
C      INST(J)    = NUMBER OF THE SPECIES CONTAINED IN REACTANT
C                   STREAM J
C      ANST(J)    = HOLERITH NAME OF THE SPECIES IN STREAM J
C      ASTNST(J)  = PHASE OF REACTANT STREAM J
C      DHF(J)     = LATENT HEAT OF VAP. OF LIQUID IN STREAM J
C      HS(J)      = ENTHALPY OF THE INCOMING FLUID IN STREAM J
C      TKS(J)     = TEMPERATURE OF STREAM J (ASSUMED CONSTANT)
C      SF(J)      = MOLE FLOW (KGMOLE/M^3 SEC) INTO THE CC
C      SH(J)      = ENTHALPY FLOW (J/M^3 SEC) INTO THE CC
C
      INCLUDE 'INIT.FOR/LIST'
C
      CHARACTER*4 AXP(10),AXR(10),ASTP(10),DATA(12),ASTR(10),
     *            AT(7),CMNT,PHAZ,DT1,DT2,ATYP,AX,ASTX,BLANK,
     *            AREAC,APROD,ARADI,ACOMM,AREVE,AGLOB,AHETE,
     *            APYRO,ACGS,THIRD
C
      DIMENSION SMWR(10),XIN(20),XCC(20),SMWP(10),XCCP(10),
     *            TX(50),TY(50)
C
      INCLUDE 'COMMONSS.FOR/LIST'
C
      DATA BLANK/'    '/,AREAC/'REAC'/,APROD/'PROD'/,ARADI/'RADI'/,
     *     S2/ 10*0.0/,S1/90*0.0/,XIN/20*0.0/,XCC/20*0.0/,
     *     ISTRM/10*0/,NREAC/0/,NPROD/0/,NRADI/0/,NS/0/,NSRATE/0/,
     *     ALIQ/'L   '/,AGAS/'G   '/,LSI/ 1 /,ACOMM/'COMM'/,
     *     AREVE/'REVE'/,AGLOB/'GLOB'/,AHETE/'HETE'/,APYRO/'PYRO'/,
     *     ACGS/'CGS '/,THIRD/'M   '/,XMAX/0.00125/,XMIN/0.0005/,
     *     TENLN/2.302585093/
C
C --- READ RELEVANT SPECIES AND ASSIGN THEM AS REACTANT, PRODUCT OR
C     RATE DETERMINING RADICAL.
C
  100 READ(20,1000) ATYP,AX,SMWX,ISTRMX,XINX,XCCX,ASTX,DHFX,HNSTRM
      IF(ATYP.EQ.BLANK) GO TO 110
      IF(ATYP.EQ.AREAC) THEN
         NREAC = NREAC + 1
         ANAM(NREAC) = AX
         ANST(ISTRMX) = AX
```

```
            SMW(NREAC) = SMWX
            ISTRM(NREAC) = ISTRMX
            XIN(NREAC) = XINX
            XCC(NREAC) = XCCX
            AST(NREAC) = ASTX
            ASTNST(ISTRMX) = ASTX
            DHF(ISTRMX) = DHFX
            HS(ISTRMX) = HNSTRM
            INST(ISTRMX) = NREAC
         ELSE IF(ATYP.EQ.APROD) THEN
            NPROD = NPROD + 1
            AXP(NPROD) = AX
            SMWP(NPROD) = SMWX
            XCCP(NPROD) = XCCX
            ASTP(NPROD) = ASTX
         ELSE
            NRAD = NRAD + 1
            AXR(NRAD) = AX
            SMWR(NRAD) = SMWX
            ASTR(NRAD) = ASTX
         END IF
         GO TO 100
  110 CONTINUE
C
C --- PUT ALL SPECIES INTO THE S2 AND OTHER ASSOCIATED ARRAYS.
C     ORDER IS: FIRST REACTANTS, SECOND PRODUCTS AND THIRD
C     RADICALS.
C
      NS = NREAC + NPROD
      NSRATE = NS + NRAD
      NS1 = NS + 1
      NS2 = NS1 + 1
      NS3 = NS1 + 2
      DO 120 I=1,NPROD
         II = NREAC + I
         ANAM(II) = AXP(I)
         SMW(II) = SMWP(I)
         XCC(II) = XCCP(I)
         AST(II) = ASTP(I)
  120 CONTINUE
      DO 130 I=1,NRAD
         II = NS + I
         ANAM(II) = AXR(I)
         SMW(II) = SMWR(I)
         AST(II) = ASTR(I)
  130 CONTINUE
      DO 140 I=1,NSRATE
         S2(I) = XCC(I)/SMW(I)
         IF(S2(I).LT.S2MIN) S2(I) = S2MIN
  140 CONTINUE
```

```
      DO 150 I=1,NREAC
  150 S1(ISTRM(I),I) = XIN(I)/SMW(I)
C
C --- DEFINE THE ONE DIMENSIONAL Z ARRAY WHICH HOLDS THE COEFFI-
C     CIENTS OF THE POLYNOMIALS THAT GIVE THERMODYNAMIC PROPERTIES.
C
  160 READ (20,1100) (DATA(I),I=1,3)
      DO 170 I=1,NSRATE
         IF(DATA(1).EQ.ANAM(I)) THEN
            READ (20,1200) (Z(J),J=(I-1)*14+1,I*14)
            GO TO 160
         ENDIF
  170 CONTINUE
      IF(DATA(1).EQ.BLANK) THEN
         READ (20,1350)
         GO TO 180
      ENDIF
      READ (20,1300)
      GO TO 160
  180 CONTINUE
C
C --- SET INITIAL MOLE AND ENERGY FLOWS (SF AND SH)
C
      DO 190 J=1,3
         SF(J) = EMS(J)/VOL/SMW(INST(J))
         SH(J) = SF(J) * HS(J)
  190 CONTINUE
C
C --- READ AND DETERMINE CONSTANTS USED IN DETERMINING
C     CHEMICAL REACTION RATES.
C
C --- READ MECHANISM/RATE DATA CARDS
C     COLUMNS 13 THROUGH 48 OF THE MECHANISM CARD ARE USED
C     AS A LABEL TO IDENTIFY THE KINETIC MECHANISM USED ON
C     THE SOLUTION OUTPUT.
C
C  THE VARIABLE DT1 (COLUMNS 73/76) IS USED AS A FLAG:
C
C  CGS  ---> CGS UNITS, RATE CONSTANTS IN GM-MOLES, CM,
C            SEC AND EACT IN (KCAL/GM-MOLE) OTHERWISE
C            THE SI UNITS (KG-MOLES,M,SEC) ARE ASSUMED.
C  COMM ---> COMMENT CARD, FIRST 48 CHARACTERS PRINTED
C  REVE ---> REVERSE RATE DATA, IN SAME UNITS AS FORWARD
C            DATA
C  GLOB ---> GLOBAL RATE EXPRESSION DATA IN SI UNITS
C  PYRO ---> HETEROGENEOUS PYROLYSIS REACTIONS
C  HETE ---> HETEROGENEOUS CHAR REACTIONS
C
C  THE HETEROGENEOUS REACTIONS ARE PROGRAMED IN CHAPTERS
C  1 & 2 OF SUBROUTINE CORECT.  BX(J), TEN(J), AND TACT(J)
```

```
C  ARE READ AS BX(J), ALPHA(1 OR 2), AND TACT(J) FOR PYROLY-
C  SIS AND BX(J), TEN(J) AND TACT(J) FOR THE CHAR REACTIONS.
C
C  DT1 AMD DT2 (COL 73/80) CAN HAVE ANYTHING (COMMENTS) IF
C  ABOVE SIX WORDS ARE NOT REQUIRED.
C  TACT IS ACTIVATION TEMPERATURE, = EACT/GASCON, DEG K
C
      IF(NDEBUG(3)) WRITE (30,1500)
      DO 200 I=1,20
         TEN2(I)=0.
         BX2(I)=0.
  200 CONTINUE
C
      JJ=1
      NPYROL=0
      NGLOB=0
      NHETER=0
C
  210 READ (20,1600) (DATA(I),I=1,12),BX(JJ),TEN(JJ),
     *               TACT(JJ),DT1,DT2
      IF (DATA(1).EQ.BLANK.AND.DT1.NE.ACOMM) GO TO 400
C
C --- CHECK FOR COMMENT CARD
C
      IF (DT1.NE.ACOMM) GO TO 220
      IF (NDEBUG(3)) WRITE (30,1700) (DATA(I),I=1,12)
      GO TO 210
C
C --- SCAN TO INSURE ALL REACTANTS IN SPECIES LIST
C
  220 DO 240 IR=1,6
         I=2*IR-1
         IF (DATA(I).EQ.BLANK.OR.DATA(I).EQ.THIRD) GO TO 240
     DO 230 IS=1,NSRATE
            IF (DATA(I).EQ.ANAM(IS)) GO TO 240
  230    CONTINUE
         IF (NDEBUG(3).NE.1) GO TO 210
         WRITE (30,1800)
         WRITE (30,1900) (DATA(IDD),IDD=1,12)
         WRITE (30,2000) DATA(I)
         GO TO 210
  240 CONTINUE
C
C --- CHECK FOR REVERSE RATE DATA.  NOTE:
C
C     (1) ORDER OF CARDS MUST BE CORRECT
C     (2) UNITS OF REVERSE DATA ASSUMED SAME AS FORWARD DATA
C
      IF (DT1.NE.AREVE) GO TO 250
      J = JJ-1
```

```
      BX2(J) = BX(JJ)
      TEN2(J) = TEN(JJ)
      TACT2(J) = TACT(JJ)
      IF (NDEBUG(3)) WRITE (30,2100) BX2(J),TEN2(J),
     *               TACT2(J),DT1,DT2
C
C --- CONVERT BX2 FOR INTERNAL CALCULATIONS
C
      BX2(J) = BX2(J)*TENLN
      IF (LSI) GO TO 210
      BX2(J) = BX2(J)-TENLN*3.0
      TACT2(J) = TACT2(J)*1000.0/1.987
      IF (MODR(J).EQ.2) BX2(J) = BX2(J)-TENLN*3.0
      GO TO 210
C
C --- CHECK FOR UNITS
C
  250 LSI = 1
      IF (DT1.EQ.ACGS) LSI = 0
      IF (LSI.EQ.0) TACT(JJ)=TACT(JJ)*1000./1.987
      IF (NDEBUG(3)) WRITE (30,2200) JJ,(DATA(I),I=1,12),
     *               DT1,DT2,BX(JJ),TEN(JJ),TACT(JJ)
      IF (DT1.NE.APYRO) GO TO 260
      NPYROL = NPYROL+1
      IF (NPYROL.GT.2) WRITE (30,2300)
      NHETER = NHETER+1
      NGLOB = NGLOB+1
  260 CONTINUE
      IF (DT1.NE.AHETE) GO TO 270
      NGLOB = NGLOB+1
      NHETER = NHETER+1
  270 CONTINUE
      IF (DT1.EQ.AGLOB) NGLOB=NGLOB+1
C
C --- CONVERT BX FOR INTERNAL CALCULATIONS
C
      BX(JJ) = BX(JJ)*TENLN
C
C --- ID(I,J) IS THE INDEX NUMBER OF THE I-TH DISTINCT SPECIES
C     IN REACTION J ... I=1,4 AS NO DISTINCT THIRD BODIES ARE
C     CONSIDERED
C
      DO 280 I=1,4
  280 ID(I,JJ) = 0
C
      ND = 1
      DO 330 N=1,6
         K = N*2 - 1
         IF (DATA(K).EQ.BLANK) GO TO 330
         IF (DATA(K).NE.THIRD) GO TO 290
```

```
            DATA(K) = BLANK
            GO TO 330
  290       CONTINUE
            DO 300 I=1,NSRATE
               IF (DATA(K).NE.ANAM(I)) GO TO 300
               II = I
               GO TO 310
  300       CONTINUE
  310       IF (K.GT.3) GO TO 320
            ID(ND,JJ) = II
            ND = ND+1
            GO TO 330
  320       IF (ND.EQ.2) ND = 3
            ID(ND,JJ) = II
            ND = ND+1
  330 CONTINUE
C
C
C --- STORE THE TYPE OF REACTION...THREE TYPES
C     MODR 1 ... A + B ---> C + D
C     MODR 2 ... AB + M ---> A + B + M
C     MODR 3 ... A + B + M ---> AB + M
C
      MODR(JJ)=1
      IF (ID(2,JJ).EQ.0) MODR(JJ)=2
      IF (ID(4,JJ).EQ.0) MODR(JJ)=3
C
C --- THE FOLLOWING SECTION, UP TO STATEMENT 355 INCLUSIVE,
C     MAY BE ELIMINATED IF REVERSE (AS WELL AS FORWARD) RATE
C     DATA IS SUPPLIED FOR  ** ALL ** REACTIONS.
C
C     THIS SECTION CALCULATES REVERSE RATE CONSTANTS FROM
C     EQUILIBRIUM CONSTANTS AND FORWARD RATE CONSTANTS FOR
C     TWENTY POINTS OVER THE TEMPERATURE RANGE 1000K TO 4000K
C
      IF (DT1.EQ.AGLOB) GO TO 390
      IF (DT1.EQ.AHETE) GO TO 390
      IF (DT1.EQ.APYRO) GO TO 390
      DX=(XMAX-XMIN)/19.0
      SUMX=0.0
      SUMY=0.0
      IHCPS=2
      DO 360 N=1,20
         TX(N)=XMIN + DX*DFLOAT(N-1)
         SUMX=SUMX+TX(N)
         XTKINV=TX(N)
         XTK=1.0/XTKINV
         TLN=DLOG(XTK)
         CALL THERPS(NSRATE,XTK)
         RTKINV = 1./(XTK * RGAS)
```

```
         SUM1=0.0
         DO 350 ND=1,4
            K=ID(ND,JJ)
            IF (K.EQ.0) GO TO 350
            GF = HO(K) - SO(K)
            IF (ND.LT.3) SUM1=SUM1+GF
            IF (ND.GE.3) SUM1=SUM1-GF
  350    CONTINUE
         TM1=0.0
         IF (ID(2,JJ).EQ.0) TM1=TLN-2.50034
         IF (ID(4,JJ).EQ.0) TM1=2.50034-TLN
C
C --- -2.50034=LN(RGAS) RGAS IN UNITS ATM M**3/KGMOLE K HERE ONLY
C
         TY(N)=TM1-SUM1+TEN(JJ)*TLN-TACT(JJ)*XTKINV+BX(JJ)
         SUMY = SUMY+TY(N)
  360 CONTINUE
      XBAR = SUMX/20.0
      YBAR = SUMY/20.0
      SUMX = 0.0
      SUM1 = 0.0
      SUMY = 0.0
      DO 370 N=1,20
         SUMX = SUMX+TY(N)*(TX(N)-XBAR)
         SUM1 = SUM1+(TX(N)-XBAR)**2
         SUMY = SUMY+(TY(N)-YBAR)**2
  370 CONTINUE
      TEN2(JJ) = 0.0
      TACT2(JJ) = -SUMX/SUM1
      BX2(JJ) = (YBAR+TACT2(JJ)*XBAR)/TENLN
      SUMX = 0.0
      DO 380 N=1,20
         SUMX=SUMX+(TY(N)+TACT2(JJ)*TX(N)-TENLN*BX2(JJ))**2
  380 CONTINUE
      SUMY = DSQRT(1.0-SUMX/SUMY)
      SUMX = DSQRT(SUMX/19.0)
      DATAT = TACT2(JJ)
      IF (LSI.NE.1) DATAT=TACT2(JJ)*1.987*0.001
      IF (NDEBUG(3)) WRITE (30,2400) SUMX,SUMY,BX2(JJ),
     *                               TEN2(JJ),TACT2(JJ)
C
C --- CONVERT BX2 FOR INTERNAL CALCULATIONS
C
      BX2(JJ) = BX2(JJ)*TENLN
C
  390 JJ = JJ+1
C
C --- CONVERT ALL RATE DATA TO SI UNITS
C
      IF (LSI) GO TO 210
```

```
      J = JJ-1
      BX(J) =BX(J)-TENLN*3.0
      BX2(J)=BX2(J)-TENLN*3.0
      IF (MODR(J).EQ.2) BX2(J)=BX2(J)-TENLN*3.0
      IF (MODR(J).EQ.3) BX(J)=BX(J)-TENLN*3.0
     GO TO 210
C
  400 JJ=JJ-1
      NPYROP=NPYROL+1
      NGLOBP=NGLOB+1
      NHETRP=NHETER+1
C
C --- SET CONTACT INDEXES TO UNITY
C
      DO 410 J=1,JJ
         X1(J)=1.0
         X2(J)=1.0
  410 CONTINUE
C
C --- RETURN TO TSTR
C
      RETURN
 1000 FORMAT(A4,X,A4,X,F7.4,X,I1,X,1PD11.5,X,D11.5,X,A4,X,
     * D11.4,X,D11.4)
 1100 FORMAT(3A4)
 1200 FORMAT(5D15.8/,5D15.8/,4D15.8/)
 1300 FORMAT(///)
 1350 FORMAT(/)
 1400 FORMAT((A4,5(X,1PD11.4)))
 1500 FORMAT(/2X,'***** REACTION RATE DATA FROM NPT *****'//)
 1600 FORMAT(12A4,3F8.3,2A4)
 1700 FORMAT(6X,3H***,12A4,3H***)
 1800 FORMAT(/4X,26HFOLLOWING REACTION IGNORED)
 1900 FORMAT(8X,6A4,5H---->,6X,6A4)
 2000 FORMAT(4X,9HREACTANT ,A4,26H NOT FOUND IN SPECIES LIST)
 2100 FORMAT(/14X,17HREVERSE RATE DATA,28X,3F15.3,2A4)
 2200 FORMAT(/4X,9HREACTION ,I2,3X,6A4,5H---->,3X,6A4/,
     * 6X,14HDATA COMMENT: ,2A4/,6X,21HFWD RATE DATA: BX  = ,
     * F10.3,X,7HTEN  = ,F10.3,X,8HTACT  = ,F10.3)
 2300 FORMAT(2X,'***** TOO MANY PYROLYSIS REACTIONS *****')
 2400 FORMAT(6X,33HCALCULATED REVERSE RATE CONSTANTS/,
     * 6X,16HSTD DEVIATION = ,1PD11.3,X,13HCORR COEFF = ,D11.3/,
     * 6X,21HREV RATE DATA : BX2 = ,0PF10.3,X,7HTEN2 = ,F10.3,X,
     * 8HTACT2 = ,F10.3)
 2500 FORMAT(2X,'***** KINETIC REACTION RATE DATA IN SI UNITS '
     * '*****'//,
     * 7X,1HJ,6X,4HMODR,12X,2HID,19X,2HBX,10X,3HTEN,9X,4HTACT,13X,
     * 3HBX2,9X,4HTEN2,9X,5HTACT2/)
 2600 FORMAT((5X,I2,1H.,I8,3X,4I5,2(3X,3F13.3)))
      END
```

```
      SUBROUTINE PIPES(Y,YPRIME,TM)
C
C
      INCLUDE 'INIT.FOR/LIST'
C
      DIMENSION Y(NV),YPRIME(NV),DV(15),DRH(15),FVIC(15),
     *   SUM1(15),SUM2(15),RF(15),ALEQ(50,50),BLEQ(50),
     *   WKAREA(100)
C
      INCLUDE 'COMMONSS.FOR/LIST'
C
C --- SHUTDOWN IS BEGUN BY SETTING THE DENSITY OF THE FURTHEST
C     UPSTREAM NODE IN THE PIPING SYSTEM EQUAL TO THE DENSITY
C     OF THE HELIUM AT THE HELIUM SOURCE PRESSURE AND TEMPERA-
C     TURE. THIS IS DONE AT TIME = TMSD (TIME OF SHUTDOWN).
C
      IF(TM.GT.TMSD) THEN
         RHO(1) = RHOGAS
         Y(NS8) = RHOGAS
      ENDIF
      IF(NDEBUG(12)) THEN
         WRITE(30,1000)
      ENDIF
C
C --- FIND THE LIQUID/VAPOR INTERFACE POSITION AND VELOCITY IN
C     EACH PIPE. NOTE:
C
C     (1) POSITION IS FIXED USING POSITION AND NODAL DENSITIES
C         (0.0 < FVI < 1.0).
C     (2) IF A NODE HAS JUST BECOME GASEOUS (THE INTERFACE HAS
C         JUST PASSED THROUGH) ITS DENSITY IS RECALCULATED USING
C         THE PREVIOUS NODAL PRESSURE AND THE IDEAL GAS RELATION.
C     (3) D(FVI(J))/DT IS EITHER ZERO (IF THERE IS NO INTERFACE
C         IN THE PIPE) OF EQUAL TO THE FLUID VELOCITY IN THE PIPE.
C     (4) AN INTERFACE CAN ENTER THE PIPE VIA BACKFLOW FROM THE
C         COMBUSTION CHAMBER. THIS OCCURS WHEN THE VELOCITY IN THE
C         LAST PIPE IS NEGATIVE. THE INTERFACE THAT RESULTS FROM
C         BACKFLOW IS NEVER ALLOWED TO PROCEED PAST THE UPSTREAM
C         NODE OF THE LAST PIPE.
C
       DO 100 J=1,NP
         ND1 = N1(J)
         ND2 = N2(J)
         IF(J.LE.NHEO) THEN
            RFLX = RFLHO
            RFGX = RFGHO
         ELSE IF(J.EQ.NPV) THEN
            RFLX = RFLV
            RFGX = RFGV
         ELSE
```

```
            RFLX = RFLIQ
            RFGX = RFGAS
         ENDIF
C
C --- BOTH PIPE NODES ARE GASEOUS
C
         IF(RHO(ND1).LT.RGMX.AND.RHO(ND2).LT.RGMX) THEN
            YPRIME(NS5+J) = 0.0
            FVI(J) = 1.0
            FVIC(J) = 0.0
            RFJ = RFGX*PL(J)*V(J)*V(J)*RHO(ND2)
            RF(J) = DSIGN(RFJ,V(J))
            Y(NS5+J) = 1.0
C
C --- ONLY THE UPSTREAM NODE IS GASEOUS. THREE CASES:
C          (1) 0 < FVI < 1.0: THERE IS AN INTERFACE IN THE PIPE
C          (2) FVI > 1.0: THE INTERFACE HAS JUST LEFT THE PIPE.
C              THE DOWNSTREAM NODE IS MADE GASEOUS AND FVI IS SET
C              AT 1.0.
C          (3) FVI < 1.0: THE INTERFACE HAS RETURNED TO THE UP-
C              STREAM PIPE. DENSITY OF NODE ND1 RETURNS TO THE
C              CONSTANT LIQUID DENSITY (RHOLIQ). FVI IS RESET TO
C              0.0 AND FVI AND ITS VELOCITY ARE RECALCULATED FOR
C              THE UPSTREAM PIPE.
C
         ELSE IF(RHO(ND1).LT.RGMX) THEN
C
C   THE INTERFACE HAS JUST LEFT THE PIPE
C
            IF(FVI(J).GE.1.0) THEN
               YPRIME(NS5+J) = 0.0
               FVI(J) = 1.0
               FVIC(J) = 0.0
               RFJ = RFGX*PL(J)*V(J)*V(J)*RHO(ND2)
               RF(J) = DSIGN(RFJ,V(J))
               Y(NS5+J) = 1.0
               RHO(ND2) = P(ND2)*SMW(1)/RGAS/TKS(3)
               Y(NS7+ND2) = RHO(ND2)
C
C   THE INTERFACE IS MOVING WITHIN THE PIPE
C
            ELSE IF(FVI(J).GE.0.0) THEN
               NFVI = J
               YPRIME(NS5+J) = V(J)/PL(J)
               FVIC(J) = 1.0 - FVI(J)
               RFJ = PL(J)*V(J)*V(J)*(FVI(J)*RFGX*RHO(ND1) +
     *               FVIC(J)*RFLX*RHO(ND2))
               RF(J) = DSIGN(RFJ,V(J))
C
C   THE INTERFACE IS RETURNING UPSTREAM
```

```
C
            ELSE IF(FVI(J).LT.0.0) THEN
               IF(J.EQ.1) THEN
                  FVI(J) = 0.0
                  YPRIME(NS5+J) = 0.0
                  FVIC(J) = 1.0
                  RFJ = PL(J)*V(J)*V(J)*RHOLIQ*RFLX
                  RF(J) = DSIGN(RFJ,V(J))
               ELSE
                  FVI(J-1) = 1.0 + FVI(J)
                  FVIC(J-1) = 1.0 - FVI(J-1)
                  RFJ = PL(J-1)*V(J-1)*V(J-1)*(FVI(J-1)*RFGX*
     *                  RHO(ND1-1)+FVIC(J-1)*RFLX*RHO(ND1))
                  RF(J-1) = DSIGN(RFJ,V(J-1))
                  Y(NS5+J-1) = FVI(J-1)
                  YPRIME(NS5+J-1) = V(J-1)/PL(J-1)
                  RHO(ND1) = RHOLIQ
                  Y(NS7+ND1) = RHOLIQ
                  FVI(J) = 0.0
                  FVIC(J) = 1.0
                  RFJ = PL(J)*V(J)*V(J)*RFLX*RHOLIQ
                  RF(J) = DSIGN(RFJ,V(J))
                  Y(NS5+J) = 0.0
                  YPRIME(NS5+J) = 0.0
               ENDIF
            ENDIF
C
C --- BOTH NODES ARE LIQUID
C
         ELSE
            YPRIME(NS5+J) = 0.0
            FVI(J) = 0.0
            FVIC(J) = 1.0
            RFJ = PL(J)*V(J)*V(J)*RFLX*RHOLIQ
            RF(J) = DSIGN(RFJ,V(J))
         ENDIF
  100 CONTINUE
C
C --- IF THE VELOCITY OF THE FURTHEST DOWNSTREAM PIPE (NP) IS
C     NEGATIVE, AN INTERFACE PASSES INTO THE PIPE. THE SYSTEM
C     VARIABLE Y(NS10)=FVI2 FOLLOWS THE PROGRESS OF THE INTER-
C     FACE UPSTREAM IN THE SAME WAY FVI(J) FOLLOWS THE OXYGEN/
C     HELIUM INTERFACE. NOTE:
C
C     (1) THE INTERFACE THAT ENTERS THE PIPES FROM THE COMBUS-
C         TION CHAMBER CAN ONLY GO AS FAR AS THE UPSTREAM NODE
C         OF THE FURTHEST DOWNSTREAM PIPE.
C     (2) FVI2 IS VIEWED BACKWORD: AS THE INTERFACE GOES UP THE
C         PIPE, FVI2 RANGES FROM 0 TO 0.9999.
C
```

```
      IF((V(NP).LE.0.0).OR.(RHO(NN).LE.RGMX).OR.
     *         (FVI2.GT.FVI2MN)) THEN
          IF(FVI2.GT.1.0) THEN
             FVI2 = 0.9999
             YPRIME(NS10) = 0.0
             RHO(NN) = RHOCC
             Y(NS7+NN) = RHOCC
          ELSE IF(FVI2.GT.FVI2MN.OR.V(NP).LT.0.0) THEN
             YPRIME(NS10) = -V(NP)/PL(NP)
             RHO(NN) = RHOCC
             Y(NS7+NN) = RHOCC
          ELSE IF(FVI(NP).GE.1.0) THEN
             FVI2 = 0.0
             Y(NS10) = 0.0
             YPRIME(NS10) = 0.0
             RHO(NN) = PA*RGASIN/TKS(3)/SMW(1)
             Y(NS7+NN) = RHO(NN)
          ELSE
             FVI2 = 0.0
             YPRIME(NS10) = 0.0
             RHO(NN) = RHOLIQ
             Y(NS7+NN) = RHOLIQ
          ENDIF
       ELSE
          YPRIME(NS10) = 0.0
       ENDIF
C
C --- FIND PRESSURE AT EACH NODE.
C
C          (1) IF A NODE IS GASEOUS, PRESSURE IS FOUND USING THE
C              PERFECT GAS RELATION.
C          (2) IF A NODE IS LIQUID, PRESSURE IS FOUND BY CALCU-
C              LATING THE PRESSURE LOSSES FROM UPSTREAM PIPES AND
C              SUBTRACTING FROM FURTHEST UPSTREAM PRESSURE.
C          (3) SOURCE NODE PRESSURES ARE FIXED. PRESSURE AT NODE
C              NN (WHICH CONNECTS THE PIPING SYSTEM TO THE COMBUS-
C              TION CHAMBER) IS ALSO FIXED.
C
       P(1) = PS
       XDPIN = 0.5*OMV*OMV*VOL*VOL/(AO2IN*AO2IN*264.0*264.0*
     *         CDIN*CDIN)
       IF(FVI(NP).LT.1.0) THEN
          IF(FVI2.GT.FVI2MN.OR.V(NP).LT.0.0) THEN
             DPIN = XDPIN / RHOCC
          ELSE
             DPIN = XDPIN / RHOLIQ
          ENDIF
       ELSE
          DPIN = XDPIN / RHOGAS
       ENDIF
```

```
      DPIN = DSIGN(DPIN,V(NP))
      P(NN) = PA + DPIN
      DO 110 J=2,NP
         ND1 = N1(J)
         IF(RHO(ND1).LT.RGMX) THEN
            P(ND1) = RHO(ND1) * RGAS * TKS(3) / SMW(1)
         ELSE
            SRF = 0.0
            RHLSM = 0.0
            DO 120 JX=J-1,NP
               SRF = SRF + RF(JX)*AREA(JX)
               RHLSM = RHLSM + RHOLIQ * FVIC(JX) * PL(JX)
  120       CONTINUE
            RHLSM = RHLSM + FVI2*PL(NP)*(RHOCC-RHOLIQ)+
     *              FVI(J)*PL(J)*RHO(ND1)
            DELP1 = P(ND1-1) - P(NN)
            IF(DABS(SRF).LT.1.0D-04) THEN
               P(ND1) = P(ND1-1)
            ELSE
               P(ND1) = P(ND1-1) - RF(J-1)*AREA(J-1)*DELP1/SRF
            ENDIF
            DELP2 = P(ND1) - P(NN)
            DELPP = DELP2/DFLOAT(NN-ND1)
            DO 130 KX = ND1+1,NN-1
               P(KX) = P(KX-1) - DELPP
  130       CONTINUE
            GO TO 140
         ENDIF
  110 CONTINUE
  140 CONTINUE
C
C --- THE EQUATIONS FOR DRH(K) AND DV(J) ARE LINEAR FOR THE
C     DERIVATIVES. A MATRIX EQUATION IS SET UP WITH THE COEF-
C     FICIENTS OF DRH AND DV IN MATRIX ALEQ AND THE RHS IN
C     VECTOR BLEQ. IMSL SUBROUTINE LEQT1F IS CALLED TO SOLVE
C     THE MATRIX EQUATION  [ALEQ]*{D} = {BLEQ}. VALUES FOR DV
C     AND DRH ARE RETURNED IN BLEQ.
C
C --- CALCULATE THE COEFFICIENTS ALEQ(NP+K,NP+K) = SUM1(K)
C
C --- RESET SUM1
C
      DO 150 K=1,NN
  150 SUM1(K) = 0.0
C
C --- CALCULATE SUM1
C
      DO 160 J=1,NP
         SUM1(N1(J)) = SUM1(N1(J)) - AREA(J)*V(J)
         SUM1(N2(J)) = SUM1(N2(J)) + AREA(J)*V(J)
```

```
  160 CONTINUE
      DO 161 K=1,NN
         IF(DABS(SUM1(K)).LT.SM1MIN) SUM1(K)=DSIGN(SM1MIN,
     *          SUM1(K))
  161 CONTINUE
C
C --- RESET ALEQ AND BLEQ
C
      NVP = NN + NP
      DO 170 I=1,NVP
         BLEQ(I) = 0.0
      DO 180 J=1,NVP
         ALEQ(I,J) = 0.0
  180 CONTINUE
  170 CONTINUE
C
C --- FILL ALEQ AND BLEQ
C
      MLIQ = 0
      DO 190 J=1,NP-1
         ND1 = N1(J)
         ND2 = N2(J)
C
C --- BOTH NODES ARE GASEOUS
C
         IF(RHO(ND2).LT.RGMX) THEN
            ALEQ(J,J) = 0.5*PL(J)*(RHO(ND1) + RHO(ND2))
            ALEQ(J,NP+ND1) = 0.5 * PL(J) * V(J)
            ALEQ(J,NP+ND2) = 0.5 * PL(J) * V(J)
            BLEQ(J) = P(ND1) - P(ND2) - RF(J)
            ALEQ(NP+ND1,NP+ND1) = SUM1(ND1)
            ALEQ(NP+ND1,J) = - RHO(ND1) * AREA(J)
            ALEQ(NP+ND2,J) = RHO(ND2) * AREA(J)
C
C --- ONLY THE UPSTREAM NODE IS GASEOUS
C
         ELSE IF(MLIQ.LT.1) THEN
            MLIQ = 1
            JHE = J
            ALEQ(J,J) = RHLSM
            ALEQ(J,NP+ND1) = PL(J) * FVI(J) * V(J)
            ALEQ(J,NP+NN) = PL(NP) * FVI2 * V(NP)
            BLEQ(J) = P(ND1)-AREA(NP)*P(NN)/AREA(J)-SRF/AREA(J)-
     *                RHOLIQ*V(J)*V(J)-RHO(NN)*V(NP)*V(NP)*AREA(NP)/
     *                AREA(J)
            ALEQ(NP+ND1,NP+ND1) = SUM1(ND1)
            ALEQ(NP+ND1,J) = - RHO(ND1) * AREA(J)
C
C --- BOTH NODES ARE LIQUID
C
```

```
         ELSE
            ALEQ(J,J) = 1.0
            ALEQ(J,J-1) = -AREA(J-1)/AREA(J)
            ALEQ(NP+ND1,NP+ND1) = 1.0
         ENDIF
  190 CONTINUE
C
C --- THE FURTHEST DOWNSTREAM PIPE IS HANDLED SEPARATELY BECAUSE
C     OF THE POSSIBILTY OF A BACKFLOW INTERFACE.
C
C --- THE UPSTREAM NODE IS LIQUID
C
      IF(RHO(NN-1).GT.RGMX) THEN
         ALEQ(NP,NP) = 1.0
         ALEQ(NP,NP-1) = -AREA(NP-1)/AREA(NP)
         ALEQ(NP+NN-1,NP+NN-1) = 1.0
         ALEQ(NP+NN,NP+NN) = 1.0
C
C --- THE FURTHEST DOWNSTREAM NODE IS LIQUID
C
         IF(FVI2.LE.0.0) THEN
            BLEQ(NP+NN) = 0.0
C
C --- A BACKFLOW INTERFACE EXISTS
C
         ELSE
            BLEQ(NP+NN) = RPX
         ENDIF
C
C --- BOTH NODES ARE HELIUM
C
      ELSE IF(FVI(NP).GE.1.0) THEN
         ALEQ(NP,NP) = 0.5*PL(NP)*(RHO(NN-1) + RHO(NN))
         ALEQ(NP,NP+NN-1) = 0.5 * PL(NP) * V(NP)
         ALEQ(NP,NP+NN) = 0.5 * PL(NP) * V(NP)
         BLEQ(NP) = P(NN-1) - P(NN) - RF(NP)
         ALEQ(NP+NN-1,NP+NN-1) = SUM1(NN-1)
         ALEQ(NP+NN-1,NP) = -RHO(NN-1) * AREA(NP)
         ALEQ(NP+NN,NP+NN) = 1.0
         BLEQ(NP+NN) = YPRIME(NS3) * RHO(NN)
C
C --- AN HELIUM/OXYGEN INTERFACE EXISTS IN THE PIPE
C
      ELSE IF(FVI2.LE.0.0) THEN
         ALEQ(NP,NP)=PL(NP)*(RHO(NN-1)*FVI(NP) + RHOLIQ*FVIC(NP))
         ALEQ(NP,NP+NN-1) = PL(NP) * V(NP) * FVI(NP)
         BLEQ(NP) = P(NN-1) - P(NN) - RF(NP)
         ALEQ(NP+NN-1,NP+NN-1) = SUM1(NN-1)
         ALEQ(NP+NN-1,NP) = -RHO(NN-1) * AREA(NP)
         ALEQ(NP+NN,NP+NN) = 1.0
```

```
C
C --- TWO INTERFACES EXIST IN THE LAST PIPE (BACKFLOW AND HE/OX)
C
      ELSE
         ALEQ(NP,NP) = PL(NP)*(RHO(NN-1)*FVI(NP)+(FVIC(NP)-FVI2)
     *                  * RHOLIQ + RHOCC * FVI2)
         ALEQ(NP,NP+NN-1) = PL(NP) * FVI(NP) * V(NP)
         ALEQ(NP,NP+NN) = PL(NP) * FVI2 * V(NP)
         BLEQ(NP) = P(NN-1) - P(NN) - RF(NP)
         ALEQ(NP+NN-1,NP+NN-1) = SUM1(NN-1)
         ALEQ(NP+NN-1,NP) = -RHO(NN-1) * AREA(NP)
         ALEQ(NP+NN,NP+NN) = 1.0
         BLEQ(NP+NN) = YPRIME(NS3) * RHOCC
      ENDIF
      ALEQ(NP+1,NP+1) = 1.0
      ALEQ(NP+1,1) = 0.0
      IERP = 10
      CALL LEQT1F(ALEQ,1,NVP,50,BLEQ,0,WKAREA,IERP)
      IF(IER.GT.100) THEN
         WRITE (30,1300) IERP,TM,TK,PA,RHOCC,FVI2,YPRIME(NS10)
         WRITE (30,1310) (J,FVI(J),YPRIME(NS5+J),V(J),DV(J),
     *                    J=1,NP)
         WRITE (30,1320) (K,RHO(K),P(K),DRH(K),K=1,NN)
         STOP
      ENDIF
      DO 800 J=1,NP
         DV(J) = BLEQ(J)
         YPRIME(NS3+J) = DV(J)
  800 CONTINUE
      DO 900 K=1,NN
         DRH(K) = BLEQ(NP+K)
         YPRIME(NS7+K) = DRH(K)
  900 CONTINUE
      IF(NDEBUG(12)) THEN
         WRITE (30,1400) FVI2,YPRIME(NS10),SRF
         WRITE (30,1500) (J,V(J),DV(J),RF(J),J=1,NP)
         WRITE (30,1600) (K,RHO(K),DRH(K),P(K),K=1,NN)
      ENDIF
      RETURN
 1000 FORMAT(//2X,'***** OUTPUT FROM SUBROUTINE PIPES *****'//)
 1300 FORMAT(//2X,'***** CONVERGENCE OF PIPING SYSTEM FAILED',
     * ' *****'//,4X,'LEQT1F RETURNED WITH IER = ',I4,
     * ', EXECUTION HALTED'/,4X,'TIME = ',1PD11.4,
     * 4X,'CHAMBER TEMPERATURE = ',0PF10.2,' K'/,
     * 4X,'CHAMBER PRESSURE    = ',1PD11.4,' PA'/,
     * 4X,'CHAMBER DENSITY     = ',D11.4,' KG/M**3'/,
     * 4X,'FVI2                = ',D11.4/,
     * 4X,'YPRIME(FVI2)        = ',D11.4)
 1310 FORMAT(//,4X,4HPIPE,5X,3HFVI,4X,9HD(FVI)/DT,2X,8HVELOCITY,
     * 5X,7HD(V)/DT//,(6X,I1,2X,1PD10.3,X,1PD10.3,X,1PD10.3,X,
```

```
     * 1PD10.3))
1320 FORMAT(//4X,4HNODE,3X,7HDENSITY,3X,8HPRESSURE,4X,
     * 9HD(RHO)/DT//,(6X,I1,2X,1PD10.3,X,1PD10.3,X,1PD10.3))
1400 FORMAT(/4X'PIPES DERIVATIVE ESTIMATE SUMMARY'//,
     * 4X,'POSITION OF THE BACKFLOW INTERFACE (FVI2) = ',
     * 1PD11.4/,4X,'D(FVI2)/DT    = ',D11.4,4X,'SRF           = ',
     * D11.4)
1500 FORMAT(/4X,'PIPE',2X,'    V      ',2X,'  D(V)/DT  ',2X,
     * '     RF    '//,(5X,I2,3X,1PD11.4,2X,D11.4,2X,D11.4))
1600 FORMAT(/4X,'NODE',2X,'    RHO    ',2X,' D(RHO)/DT ',2X,
     * '    P      '//,(5X,I2,3X,1PD11.4,2X,D11.4,2X,D11.4))
      END
```

```
      SUBROUTINE RADSS
C
      INCLUDE 'INIT.FOR/LIST'
      DIMENSION G1(20),BLEQ(10),WKAREA(10),ALEQ(10,10),S2I(10)
C
      INCLUDE 'COMMONSS.FOR/LIST'
C
      ITER = 0
C
      SMNS = 0.0
      DO 100 I=1,NS
         SMNS = SMNS + S2(I)
  100 CONTINUE
      DO 110 I=NS1,NSRATE
         S2I(I) = S2(I)
  110 CONTINUE
C
C --- DEFINE THE G1 ARRAY: G1(I) = MASS INFLOW OF SPECIES I FROM
C     THE PIPES.
C
      G1(2) = FMV / SMW(2)
      G1(3) = OMV / SMW(3)
C
C --- ITERATION BEGINS
C
  120 CALL RATES
      ICHK = 0
      ITER = ITER + 1
      DO 140 I=NS1,NSRATE
         BLEQ(I-NS) = - G1(I) - ARR(I) + EMV * S2(I)
         DO 130 K=NS1,NSRATE
            ALEQ(I-NS,K-NS) = RIP(I,K)
  130    CONTINUE
         ALEQ(I-NS,I-NS) = ALEQ(I-NS,I-NS) - EMV
  140 CONTINUE
C
C --- LEQT1F SOLVES THE MATRIX EQUATION : [ALEQ]{DS2}={BLEQ} AND
C     RETURNS THE ANSWER IN THE VECTOR {BLEQ}.
C
      CALL LEQT1F(ALEQ,1,NRAD,10,BLEQ,IDGT,WKAREA,JER)
C
C --- INCREMENT ALL S2 BY DS2 AND KEEP THE RESULT WITHIN THE BOUNDS
C     ( S2MIN < S2(I) < 1.0/SMW(I) )
C
      SM = SMNS
      DO 150 I=NS1,NSRATE
         ALG = 1.0/SMW(I)
         SCHK = DABS(BLEQ(I-NS)/S2(I))
         IF(SCHK.GT.EPSISS) ICHK = 1
         S2(I) = S2(I) + RLX*BLEQ(I-NS)
```


C-3

```
            IF(S2(I).LT.S2MIN) S2(I) = S2MIN
            IF(S2(I).GT.ALG) S2(I) = ALG
            SM = SM + S2(I)
  150    CONTINUE
         SMINV = 1.0/SM
C
C --- STOP THE ITERATION IF ITERATION COUNTER ITER IS GREATER
C     THAN ITMAXS. IF THE SPECIES MOLE NUMBERS FALL BELOW THE
C     MINIMUM ALLOWABLE MOLE NUMBER THE ITERATION CANNOT CON-
C     VERGE. IF THIS TAKES PLACE THE MOLE NUMBERS ARE SET TO
C     MINIMUM ALLOWABLE MOLE NUMBER AND EXECUTION IS ALLOWED
C     TO CONTINUE.
C
         IF(ITER.GT.ITMAXS) THEN
            ISTOP = 0
            S2CHK = S2MIN*100.0
            DO 160 I = NS1,NSRATE
               IF(S2(I).LE.S2CHK) THEN
                  ISTOP = 1
                  S2(I) = S2MIN
               ENDIF
  160       CONTINUE
            IF (ISTOP.EQ.1) GO TO 170
            WRITE (30,1000) ITMAXS,TM,TK,PA,RHOCC,DLIQ,VR
            WRITE (30,1100) (ANAM(I),S2(I),I=1,NS)
            WRITE (30,1200) (ANAM(I),S2(I),BLEQ(I-NS),I=NS1,NSRATE)
            WRITE (30,1300)
            STOP
         ENDIF
C
C --- IF ICHK = 1 THE CONVERGENCE CRITERION WAS NOT MET
C
         IF(ICHK) GO TO 120
C
C --- CALCULATE THE RATE OF PRODUCTION OF THE PRODUCTS AND INFER
C     THE RATE OF CONSUMPTION OF THE REACTANTS FROM THE CONSERVATION
C     OF ATOMS


C
  170    RATE(4) = ARR(4)
         RATE(2) = -RATE(4)
         RATE(3) = -RATE(4)*0.5
         RATE(1) = 0.0
C
C --- OUTPUT FOR NDEBUG(11) = 1
C
         IF(NDEBUG(11)) THEN
            WRITE (30,1400) ITER,RLX,EPSISS
            WRITE (30,1500) TK,PA,RHOCC,OMV,FMV,PMV
```

```
         WRITE (30,1600)
         WRITE (30,1700) (ANAM(I),S2I(I),I=NS1,NSRATE)
         WRITE (30,1800)
         WRITE (30,1900) (ANAM(I),S2(I),ARR(I),RATE(I),I=1,NSRATE)
       ENDIF
C
       RETURN
C
 1000 FORMAT(/2X,'***** IN RADSS, ITMAX = ',I7,' EXCEEDED *****'//,
     * 4X,'RADICAL MOLE NUMBER ITERATION DID NOT CONVERGE FOR:'//,
     * 4X,'TIME = ',1PD11.4,' SEC'/,
     * 4X,'CC TEMPERATURE    = ',0PF10.3,' K'/,
     * 4X,'CC PRESSURE       = ',1PD11.4,' PA'/,
     * 4X,'CC DENSITY        = ',D11.4,' KG/M**3'/,
     * 4X,'CC LIQUID DENSITY = ',D11.4,' KG/M**3'/,
     * 4X,'CC VAPOR. RATE    = ',D11.4,' KG/M**3 SEC'//)
 1100 FORMAT(4X,'MAJOR SPECIES  MOLE NUMBER (KGMOLES/KG)'//,
     * (8X,A4,13X,D11.4))
 1200 FORMAT(//4X,'SPECIES  MOLE NUMBER (KGMOLES/KG)  INCREMENT'//,
     * (5X,A4,7X,D11.4,13X,D11.4))
 1300 FORMAT(//2X,'***** EXECUTION HALTED *****')
 1400 FORMAT(/2X,'***** OUTPUT FROM SSRATE *****',//,
     * 4X,'SSRATE SUCCEEDED AFTER ',I4,' ITERATIONS.'/,
     * 4X,'RELAXATION FACTOR = ',1PD8.2/,
     * 4X,'PERCENT TOLERANCE = ',D8.2)
 1500 FORMAT(4X,'TEMPERATURE   = ',F8.2/,
     *       4X,'PRESSURE      = ',1PD12.4/,
     *       4X,'DENSITY       = ',D12.4/,
     *       4X,'OMV, FMV, PMV = ',3(D12.4,2X))
 1600 FORMAT(/4X,'SPECIES',2X,'INITIAL MOLE NO.'//)
 1700 FORMAT(5X,A4,3X,D12.5)
 1800 FORMAT(/4X,'CONVERGED SOLUTION:'//,
     * 4X,'SPECIES',2X,'EFFECTIVE S2',2X,'SS RXN RATE ',2X,
     * 'EFFECTIVE RXN
RATE'/,12X,'KGMOLE(I)/KG',X,'KGMOLE/M^3*SEC',X,
     * 'KGMOLE/M^3*SEC'//)
 1900 FORMAT(5X,A4,3X,1PD12.5,2X,D12.5,2X,D12.5)
       END
```

```
      SUBROUTINE RATES
C
C --- CALCULATES RATE OF PRODUCTION OF EACH SPECIES, ARR(I),
C     AND THE DERIVATIVE OF THE RATE OF PRODUCTION OF EACH
C     SPECIES, I, WITH RESPECT TO THE MOLE NUMBER OF EACH
C     SPECIES, K , RIP(I,K).
C
      INCLUDE 'INIT.FOR/LIST'
C
      DIMENSION RFP(20,20),RRP(20,20),RF2(20),RR(20)
C
      INCLUDE 'COMMONSS.FOR/LIST'
C
      DATA BIG/46.051/
C
C
C --- DETERMINE DENSITY AND OFTEN USED CONSTANTS
C
      TLN = DLOG(TK)
      TKSQ = TK * TK
      TKSQIN = 1.0/TKSQ
      RHSM = PA * RGASIN * TKINV
      RHOP = RHSM * SMINV
      RHSQ = RHOP * RHOP
      RHINV = 1.0 / RHOP
C
C --- FIND THE FORWARD AND REVERSE RATES OF EACH OF THE ELEMENTARY
C     REACTIONS, J, FOR J=1,JJ (JJ = NO. OF ELEM RXNS)
C
      DO 10 J=1,JJ
         RF2(J) = 0.0
         RR(J)  = 0.0
         I = ID(1,J)
         K = ID(2,J)
         M = ID(3,J)
         N = ID(4,J)
         MODE = MODR(J)
         R1 = 0.0
         R2 = 0.0
         TX1 = TACT(J)*TKINV - BX(J) - TEN(J)*TLN
         TX2 = TACT2(J)*TKINV - BX2(J) - TEN2(J)*TLN
         R1 = DEXP(-TX1)
         R2 = DEXP(-TX2)
C
C --- SECTION FOR FORWARD REACTION RATES
C
         IF(DABS(TX1).GT.BIG) THEN
            IF(NDEBUG(13))WRITE(30,1000) ITER,J
            GO TO 50
         ENDIF
```

```
         R1 = R1 * X1(J)
         IF(MODE-2) 20,30,40
   20       RF2(J) = R1 * S2(I) * RHSQ * S2(K)
            GO TO 60
   30       RF2(J) = R1 * RHSM * S2(I) *RHOP
            GO TO 60
   40       RF2(J) = R1 * RHSM * S2(I) * RHOP
            IF(K.NE.0) RF2(J) = RF2(J) * S2(K) * RHOP
            GO TO 60
   50    RF2(J) = 0.0
   60    CONTINUE
C
C --- SECTION FOR REVERSE RATES
C
         IF(DABS(TX2).GT.BIG) THEN
            IF(NDEBUG(13)) WRITE(30,1100) ITER, J
            GO TO 100
         ENDIF
         R2 = X2(J) * R2
         IF(MODE-2) 70,80,90
   70       RR(J) = R2 * S2(M) * RHSQ * S2(N)
            GO TO 10
   80       RR(J) = R2 * RHSM * S2(M) * RHSQ * S2(N)
            GO TO 10
   90       RR(J) = R2 * RHSM * RHOP * S2(M)
            GO TO 10
  100       RR(J) = 0.0
   10 CONTINUE
C
C --- FIND THE RATE OF PRODUCTION OF EACH SPECIES I, ARR(I).
C
      DO 110 I=1,NSRATE
         ARR(I) = 0.0
      DO 120 J=1,JJ
         ARR(I) = ARR(I)+DFLOAT(ISIDE(I,J))*(RF2(J)-RR(J))
  120 CONTINUE
  110 CONTINUE
C
C --- FIND THE DERIVATIVES OF THE FWD AND REV RXN RATES OF EACH
C     ELEMENTARY RXN WITH RESPECT TO EACH MOLE NO. (I.E.
C     RFP(J,K)=D(RF2(J))/D(S2(K)) AND RRP(J,K)=D(RR(J))/D(S2(K)))
C
      DO 130 J=1,JJ
      DO 140 K=1,NSRATE
         RFP(J,K) = 0.0
         RRP(J,K) = 0.0
         IF(ISIDE(K,J).LT.0)
RFP(J,K)=-DFLOAT(ISIDE(K,J))*RF2(J)/S2(K)
         IF(ISIDE(K,J).GT.0) RRP(J,K)= DFLOAT(ISIDE(K,J))*
RR(J)/S2(K)
```

```
  140 CONTINUE
  130 CONTINUE
C
C --- FIND THE DERIVATIVE OF THE RATE OF PRODUCTION OF EACH SPECIES
WITH
C     RESPECT TO THE MOLE NO. OF EACH SPECIES
(RIP(I,K)=D(ARR(I))/D(S2(K))
C
      DO 150 I=1,NSRATE
      DO 160 K=1,NSRATE
         RIP(I,K) = 0.0
      DO 170 J=1,JJ
         RIP(I,K) = RIP(I,K)+DFLOAT(ISIDE(I,J))*(RFP(J,K)-RRP(J,K))
  170 CONTINUE
  160 CONTINUE
  150 CONTINUE
      RETURN
 1000 FORMAT(4X,'IN RATES, FOR ITERATION ',I4,'FWD RATE = 0 FOR J =
',
     * I2)
 1100 FORMAT(4X,'IN RATES, FOR ITERATION ',I4,'REV RATE = 0 FOR J =
',
     * I2)
      END
```

```
      SUBROUTINE YCAL(Y,WK,IWK,N,NWK)
C
C     TSTR2 RUNS THE CALLING OF THE INTEGRATION ROUTINE AND
C     THE OUTPUTTING OF DATA TO THE OUTPUT AND PLOT FILES
C
      INCLUDE 'INIT.FOR/LIST'
C
      REAL*4 SDUMMY(4)
C
      EXTERNAL CSLOPE
C
      DIMENSION Y(N),IWK(N),WK(NWK),WK2(4,100),S2P(10),CHG(50)
C
      INCLUDE 'COMMONSS.FOR/LIST'
      COMMON / GEAR / DUMMY(48),SDUMMY,IDUMMY(38)
C
C --- PUT MOLE NUMBERS, TEMPERATURE AND DENSITY INTO LOG VARIABLE
C     FORM AND INSERT THEM INTO THE VECTOR Y. DENSITY OF LIQUID IN
C     THE COMBUSTION CHAMBER IS LEFT IN NON-LOG FORM.
C
      DO 100 I=1,NS
  100 Y(I) = DLOG(S2(I))
      Y(NS1) = XMASS/VOL
      Y(NS2) = DLOG(TK)
      Y(NS3) = DLOG(PA)
      VH2 = EMS(2)/AH2IN/RHOH2/264.0
C
C --- PLACE THE PIPING SYSTEM VARIABLES INTO THE VECTOR Y.
C
      DO 110 I=1,NP
         Y(NS3+I) = V(I)
         Y(NS5+I) = 0.0
         IF(N2(I).EQ.NN) OMV = OMV + RHO(NN)*AREA(I)*V(I)
  110 CONTINUE
      DO 120 I=1,NN
         Y(NS7+I) = RHO(I)
  120 CONTINUE
C
C --- GET GOOD INTITIAL ESTIMATES FOR ATOM AND RADICAL MOLE
C     NUMBERS VIA A CALL TO RADSS
C
      IF(KINET.EQ.1) THEN
         CALL RADSS
      ENDIF
C
C --- BEGIN THE INTEGRATION LOOP
C
      NSTEPS = JIDINT((TMEND-TMI)/TMPRNT)
      DO 150 NX = 1,NSTEPS
         TMNXT = TMNXT + TMPRNT
```

```
            IF(TMNXT.GT.TMEND) TMNXT = TMEND
            IF(NDEBUG(5)) WRITE (30,1000) NX,NSTEPS,TM,TMNXT
            IF(NDGEAR) THEN
               CALL DTSTR(N,CSLOPE,TM,STEP,Y,TMNXT,WK2,NDEBUG)
            ELSE
               CALL DGEAR (N,CSLOPE,CHGJ,TM,STEP,Y,TMNXT,EPSI,METH,
     *                     MITER,INDEX,IWK,WK,IER)
               IF(IER.GE.128) THEN
                  WRITE (30,1100) IER,TM
                  DO 140 I=1,NV
  140             -    CHG(I) = WK(IDUMMY(11)+I)/WK(I)
                  WRITE (30,1200) (I,Y(I),CHG(I),I=1,NV)
                  CALL OUTPT(Y,TM,N,NSTEPS)
                  STOP
               END IF
            END IF
         IF (NDEBUG(14))
     *    WRITE (6,1300) TM,STEP,TK,PA,RHOCC,(V(J),J=1,3),
     *       (RHO(K),K=1,3),(FVI(J),J=NP-2,NP),V(NP),FVI2,
     *       (S2(I),I=1,4)
C
C --- ON RETURN FROM THE INTEGRATION ROUTINE OUTPUT DEPENDENT
C     VARIABLES AND SIGNIFICANT PROBLEM PARAMETERS TO THE TEXT
C     AND PLOT OUTPUT FILES.
C
      CALL OUTPT(Y,TM,N,NSTEPS)
      IF(TM.GT.TMPER.AND.IPER.LT.1) THEN
         IPER = 1
         DMCX = DMC
         DMC = XPER * DMC
      ELSE IF(TM.GT.TMPER.AND.IPER.LE.5) THEN
         IPER = IPER + 1
      ELSE IF(IPER.GT.5) THEN
         DMC = DMCX
      ENDIF
  150 CONTINUE
C
      RETURN
 1000 FORMAT(/2X,'***** INTEGRATING ROUTINE CALLED *****'//,
     * 4X,'CALL FOR STEP ',I7,' OUT OF ',I12,' STEPS'/,
     * 4X,'STEP BEGINS AT TIME = ',1PD12.5,
     * ' AND ENDS AT TIME = ',1PD12.5)
 1100 FORMAT(2X,'***** ERROR CONDITION ON RETURN FROM DGEAR
*****'//,
     * 4X,'EXECUTION STOPPED. IER = ',I4,X,'TIME = ',1PD12.5//,
     * 2X,'VARIABLE',2X,'VALUE AT HALT',2X,'RELATIVE CHANGE'//)
 1200 FORMAT(5X,I2,5X,1PD12.5,4X,D12.5)
 1300 FORMAT(/2X,'ON RETURN TO YCAL: TIME = ',1PD8.2,' STEP =
',D8.2/,
     * 2X,'TEMP = ',0PF10.2,X,'PRESS = ',1PD8.2,X,'DENS  = ',D8.2/,
```

```
     * 2X,'V(1:3)        = ',3D9.2/,
     * 2X,'RHO(1:3)      = ',3D9.2/,
     * 2X,'FVI(NP-2:NP) = ',3D9.2/,
     * 2X,'V(NP) = ',D9.2,2X,'FVI2  = ',D9.2/,
     * 2X,'S2(1:4)  = ',4D9.2)
      END
```

```
      SUBROUTINE THERPS(NS,XTK)
C
C  THERPS CALCULATES THE SPECIFIC MOLAR INTERNAL ENERGY,
C  ENTHALPY AND SPECIFIC HEAT AT CONSTANT PRESSURE FOR EACH
C  SPECIES, I=1,NS.
C
C  H(I)  = ENTHALPY (J/KGMOLE)
C  U(I)  = INTERNAL ENERGY (J/KGMOLE)
C  CP(I) = SPECIFIC HEAT AT CONSTANT PRESSURE (J/KGMOLE K)
C
C  THERPS IS MODELLED AFTER SUBROUTINE HCPS USED BY DR. PAUL
C  GEORGE II (PHD DISERTATION, PURDUE UNIVERSITY, 1982).
C
      IMPLICIT REAL*8 (A-H,P-Z)
      IMPLICIT INTEGER*4 (I-O)
C
      DIMENSION H1(20),H2(20),HO1(20),HO2(20),CP1(20),CP2(20),
     * CPO1(20),CPO2(20),S1(20),S2(20),SO1(20),SO2(20),U1(20),
     * U2(20)
C
      COMMON
     * / CPROP / Z(200),H(10),CP(10),U(10),S(10),DCP(10),HO(10),
     *            CPO(10),SO(10)
C
C
      DATA ICIT/14/,RGAS/8314.4/
      IT=0
      IF (XTK.LT.950.0) THEN
         IT=7
      ELSE IF(XTK.GT.1050.0) THEN
         IT = 0
      ELSE
         GO TO 70
      ENDIF
C
      XTKSQ=XTK**2
      XTKCU=XTKSQ*XTK
      XTK4=XTKCU*XTK
      XTKINV=1./XTK
      XTLN=DLOG(XTK)
      RTK=RGAS*XTK
C
C --- H(I), U(I), CP(I), DCP(I) REQUIRED
C
      DO 60 I=1,NS
         K=IT+ICIT*(I-1)
         CP1X=Z(K+1)
         CP2X=XTK*Z(K+2)
         CP3X=XTKSQ*Z(K+3)
         CP4X=XTKCU*Z(K+4)
```

```
      CP5X=XTK4*Z(K+5)
      HO(I)=0.2*CP5X+0.25*CP4X+0.33333333*CP3X+0.5*CP2X+CP1X
     *       +XTKINV*Z(K+6)
      SO(I)=0.25*CP5X+0.33333333*CP4X+0.5*CP3X+CP2X+CP1X*XTLN
      CPO(I) = CP1X + CP2X + CP3X + CP4X + CP5X
      H(I) = HO(I) * RTK
      U(I) = H(I) - RTK
      S(I) = SO(I) * RGAS
      CP(I) = CPO(I)*RGAS
   60 CONTINUE
C
      RETURN
C
   70 XTKSQ=XTK**2
      XTKCU=XTKSQ*XTK
      XTK4=XTKCU*XTK
      XTKINV=1./XTK
      XTLN=DLOG(XTK)
      RTK=RGAS*XTK
C
C --- H(I), U(I), CP(I), DCP(I) REQUIRED
C
      DO 80 ITK = 1,2
         IT = 0
         IF(ITK.EQ.2) IT = 7
         DO 90 I=1,NS
            K=IT+ICIT*(I-1)
            CP1X=Z(K+1)
            CP2X=XTK*Z(K+2)
            CP3X=XTKSQ*Z(K+3)
            CP4X=XTKCU*Z(K+4)
            CP5X=XTK4*Z(K+5)
            HO(I)=0.2*CP5X+0.25*CP4X+0.33333333*CP3X+0.5*CP2X+CP1X
     *         +XTKINV*Z(K+6)
            SO(I)=0.25*CP5X+0.33333333*CP4X+0.5*CP3X+CP2X+CP1X*XTLN
            CPO(I) = CP1X + CP2X + CP3X + CP4X + CP5X
            H(I) = HO(I) * RTK
            U(I) = H(I) - RTK
            S(I) = SO(I) * RGAS
            CP(I) = CPO(I)*RGAS
            IF(ITK.EQ.1) THEN
               HO1(I) = HO(I)
               SO1(I) = SO(I)
               CPO1(I) = CPO(I)
               H1(I) = H(I)
               CP1(I) = CP(I)
               U1(I) = U(I)
               S1(I) = S(I)
            ELSE
               HO2(I) = HO(I)
```

```
                S02(I) = S0(I)
                CP02(I) = CP0(I)
                H2(I) = H(I)
                CP2(I) = CP(I)
                U2(I) = U(I)
                S2(I) = S(I)
             ENDIF
   90     CONTINUE
   80 CONTINUE
      FR1 = (XTK - 950.0)/100.0
      FR2 = (1050.0 - XTK)/100.0
      DO 100 I=1,NS
         H0(I) = FR1*H01(I) + FR2*H02(I)
         S0(I) = FR1*S01(I) + FR2*S02(I)
         CP0(I) = FR1*CP01(I) + FR2*CP02(I)
         H(I) = FR1*H1(I) + FR2*H2(I)
         U(I) = FR1*U1(I) + FR2*U2(I)
         CP(I) = FR1*CP1(I) + FR2*CP2(I)
  100 CONTINUE
C
      RETURN
C
      END
```

```
INPUT FILE TSTR.IN
&RUNNO NMON=06,NDAY=11,NYR=1987,NRUN=1 &END
&PARAM VOL=0.013,Q=-5.5D+07,S2MIN=1.0D-18,EMS=0.0,
  18.00,0.0,TKS=120.0,120.0,200.0,TMSD=0.00E+03,
  RGMX=65.5,RHOGAS=12.4435,RHOLIQ=990.70,RHOH2=9.86784,
  AH2IN=1.329D-05,AO2IN=1.09682D-05,FVI2MN=1.0D-08,
  DLIQMN=1.0D-07,DMMIN=1.5D-06,DMC=0.585,CFTP=0.96738,
  PHG=1.03393D+06,TMPER=5.0D+02,XPER=20.0,CVR=1.23045D-02
  &END
&INITC XMASS=1.00D-15,TK=550.00,PA=5.16964D+06,
  DM=1.0D-07 &END
&INDX1 NDEBUG=0,0,0,0,0,0,1,0,0,0,0,0,0,0,0,0,0,0,0,0,
  MCON=1,KINET=0 &END
&ICONS METH=2,MITER=2,NDGEAR=0,IER=10,STEP=1.0D-12,
  TMI=0.0,TMPRNT=5.0D-04,TMEND=1.0D-01,INDEX=1,
  EPSI=1.0D-05 &END
&SSRRT EPSISS=1.0D-06,ITMAXS=25,IDGT=0,JER=10 &END
&INPIP V=9*0.001,FVI=5*1.0,4*0.0,RHO=6*12.4435,
  4*990.70,FVI2=0.0,PL=5*0.30,0.005,3*0.040,
  AREA=5*4.29085D-05,4*2.02683D-03,RFLIQ=0.130294,
  RFGAS=0.182725,RFLHO=0.836663,RFGHO=1.14483,
  RFLV=1.72000D+04,RFGV=1.82725D+04,PS=5.16964D+06,
  CDIN=0.50,SM1MIN=0.0D-08 &END
&INDX2 N1=1,2,3,4,5,6,7,8,9,N2=2,3,4,5,6,7,8,9,10,
  NP=9,NN=10,NHEO=5,NFVI=6 &END
REAC HE    4.0026 3 1.00000D+00 0.00000D+00 G    0.00000D+00 -3.5416D+06
REAC H2    2.0160 2 1.00000D+00 9.99999D-01 G    0.00000D+00 -3.1432D+06
REAC O2   32.0000 1 1.00000D+00 1.00000D-09 L    2.00000D+05 -2.7300D+05
PROD H2O  18.0160 0 0.00000D+00 1.00000D-09 G    0.00000D+00  0.0000D+00
RADI H     1.0080 0 0.00000D+00 0.00000D-00 G    0.00000D+00  0.0000D+00
RADI O    16.0000 0 0.00000D+00 0.00000D-08 G    0.00000D+00  0.0000D+00
RADI OH   17.0080 0 0.00000D+00 0.00000D-08 G    0.00000D+00  0.0000D+00

HE               L 5/66HE 1.00 0.00 0.00 0.G   300.000  5000.000             1
 0.25000000D+01 0.00000000D+00 0.00000000D+00 0.00000000D+00 0.00000000D+00    2
-0.74537498D+03 0.91534888D+00 0.25000000D+01 0.00000000D+00 0.00000000D+00    3
 0.00000000D+00 0.00000000D+00-0.74537498D+03 0.91534884D+00                   4
        0    2.7080   37.0000     298.0    1200.0    6000.0          HE       5
AR               L 5/66AR  1              G   300.000  5000.000
 0.25000000E+01 0.0           0.0           0.0           0.0
-0.74537502E+03 0.43660006E+01 0.25000000E+01 0.0           0.0
 0.0           0.0          -0.74537498E+03 0.43660006E+01
        0    3.4180   124.000     300.0    1200.0    5000.0
CH4              J 3/61C   1H   400  000  0G   300.000  5000.000             1
 0.15027072E 01 0.10416798E-01-0.39181522E-05 0.67777899E-09-0.44283706E-13    2
-0.99787078E 04 0.10707143E 02 0.38261932E 01-0.39794581E-02 0.24558340E-04    3
-0.22732926E-07 0.69626957E-11-0.10144950E 05 0.86690073E 00                  4
       0.   3.8220  137.0000
CH3              J 6/69C   1H   3    0    0G   300.000  5000.000             1
```

```
 2.84003270E+00 6.08690860E-03-2.17403380E-06 3.60425760E-10-2.27253000E-14    2
 1.64498130E+04 5.50567510E+00 3.46663500E+00 3.83018450E-03 1.01168020E-06    3
-1.88592360E-09 6.68031820E-13 1.63131040E+04 2.41721920E+00                   4

CHO                     C   1H   1O   1    0G   300.000  5000.000             1
 3.61363839E+00 3.26359808E-03-1.29355163E-06 2.38238898E-10-1.64668247E-14    2
 3.18113141E+03 5.22165078E+00 4.07467474E+00-2.20831318E-03 1.12814616E-05    3
-1.07609505E-08 3.39297805E-12 3.33218275E+03 4.03515416E+00                   4

CH2O              J 3/61C   1H   2O   1    0G   300.000  5000.000             1
 2.83642490E+00 6.86052980E-03-2.68826470E-06 4.79712580E-10-3.21184060E-14    2
-1.52360310E+04 7.85311690E+00 3.79637830E+00-2.57017850E-03 1.85488150E-05    3
-1.78691770E-08 5.55044510E-12-1.50889470E+04 4.75481630E+00                   4

CH3O                    C   1H   3O   1    0G   300.000  5000.000             1
 5.23759870E+00 7.99608790E-03-3.96765581E-06 8.31862800E-10-6.26533814E-14    2
 1.09662525E+03-5.89948723E+00 2.04832571E+00 1.15498951E-02-3.75331995E-06    3
 2.54155659E-13 1.69432993E-24 2.63293614E+03 1.27359509E+01                   4

CO                J 9/65C   1O   100  000  0G   300.000  5000.000             1
 0.29840696E 01 0.14891390E-02-0.57899684E-06 0.10364577E-09-0.69353550E-14    2
-0.14245228E 05 0.63479156E 01 0.37100928E 01-0.16190964E-02 0.36923594E-05    3
-0.20319674E-08 0.23953344E-12-0.14356310E 05 0.29555351E 01                   4
        0    3.5900  110.0000     298.0    1200.0    6000.0           CO       1
CO2               J 9/65C   1O   200  000  0G   300.000  5000.000             1
 0.44608041E 01 0.30981719E-02-0.12392571E-05 0.22741325E-09-0.15525954E-13    2
-0.48961442E 05-0.98635982E 00 0.24007797E 01 0.87350957E-02-0.66070878E-05    3
 0.20021861E-08 0.63274039E-15-0.48377527E 05 0.96951457E 01                   4
        0    3.9960  190.0000     298.0    1200.0    6000.0           CO2      1
CO2-              J12/66C  1.0  2.E  1.00 0.G   300.000  5000.000             1
 0.45454636E+01 0.26054317E-02-0.10928734E-05 0.20454421E-09-0.14184542E-13    2
-0.54761969E+05 0.18317366E+01 0.34743738E+01 0.16913805E-02 0.73533802E-05    3
-0.99554249E-08 0.36846715E-11-0.54249051E+05 0.83834333E+01                   4
        0.        0.        0.                                                 5
N                 J 3/77N  1.   0.   0.   0.G   300.000  5000.000             1
 0.24370813E+01 0.13233886E-03-0.90907747E-07 0.22864058E-10-0.13762291E-14    2
 0.56128586E+05 0.45211115E+01 0.25000000E+01-0.31078153E-08 0.83216099E-11    3
-0.94278291E-14 0.38108037E-17 0.56106977E+05 0.41806431E+01                   4
        0.        3.       71.                                                5
NO2               J 9/64N  1.0  2.00 0.00 0.G   300.000  5000.000             1
 0.46240768E+01 0.25260332E-02-0.10609501E-05 0.19879239E-09-0.13799383E-13    2
 0.22899900E+04 0.13324137E+01 0.34589233E+01 0.20647063E-02 0.66866069E-05    3
-0.95556736E-08 0.36195881E-11 0.28152266E+04 0.83116980E+01                   4
        0.        0.        0.                                                 5
HCN               L12/69H  1.C  1.N  1.0  0.G   300.000  5000.000             1
 0.37068119E+01 0.33382804E-02-0.11913316E-05 0.19992917E-09-0.12826451E-13    2
 0.14962637E+05 0.20794907E+01 0.24513559E+01 0.87208375E-02-0.10094203E-04    3
 0.67255712E-08-0.17626959E-11 0.15213004E+05 0.80830088E+01                   4
        0.        0.        0.                                                 5
```

```
NH3               J 9/65N  1.H  3.00 0.00 0.G   300.000  5000.000              1
 0.24165173E+01 0.61871223E-02-0.21785136E-05 0.37599079E-09-0.24448857E-13    2
-0.64747187E+04 0.77043486E+01 0.35912771E+01 0.49388665E-03 0.83449322E-05    3
-0.83833385E-08 0.27299092E-11-0.66717148E+04 0.22520962E+01                  4
       0.        0.        0.                                                 5
C2H6                    C   2H   6    0    0G   300.000  5000.000              1
 1.49270752E+00 1.90694888E-02-7.11984782E-06 1.19069803E-09-7.37266162E-14    2
-1.13918457E+04 1.36588993E+01 3.06380013E+00 8.59581465E-03 1.64679051E-05    3
-2.00919579E-08 6.52385805E-12-1.15878959E+04 6.93085386E+00                  4
        0    4.4180  230.0000                                                 5
C2H4                    C   2H   4          G   300.000  5000.000
 0.34552152E 01 0.11491803E-01-0.43651750E-05 0.76155095E-09-0.50123200E-13
 0.44773119E 04 0.26987959E 01 0.14256821E 01 0.11383140E-01 0.79890006E-05
-0.16253679E-07 0.67491256E-11 0.53370755E 04 0.14621819E 02
        0    4.2320  205.0000
FUEL OIL (LIQUID)       C   1H 1.8          G   300.000  5000.000
 0.27797000E 01
-0.37392400E 04-0.15651223E 02 0.27797000E 01
                               -0.37392400E 04-0.15651223E 02
                                                    NO TRANSPORT
C3H8                    C   3H   8    0    0G   300.000  5000.000              1
 3.07371055E+00 2.52859519E-02-9.12630575E-06 1.46940810E-09-8.73487271E-14    2
-1.45316354E+04 7.48445307E+00 3.21459483E+00 1.63977335E-02 1.68421811E-05    3
-2.16111737E-08 5.77092196E-12-1.42864159E+04 8.64456968E+00                  4
        0    5.0610  254.0000                                                 5
C6H6                    C   6H   6    0    0G   300.000  5000.000              1
 9.66494563E+00 2.12364775E-02-7.09034255E-06 1.01513328E-09-5.14055768E-14    2
 5.17497547E+03-3.07774861E+01 3.01886004E+00 1.22221561E-02 6.87572729E-05    3
-9.93386474E-08 4.01152941E-11 8.10080315E+03 9.63207440E+00                  4
        0    5.27    440.
C8H18                   C   8H  18    0    0G   300.000  5000.000              1
 1.14954126E+01 6.35313436E-02-2.71361101E-05 4.80764212E-09-3.02563294E-13    2
-3.35887669E+04-3.30429513E+01 2.27071846E+01-1.27549696E-02 1.04233714E-04    3
-6.08467720E-08-9.43552892E-13-3.39058757E+04-7.78443415E+01                  4
             7.451    320.
H                  J 3/77H   1    0    0    0G   300.000  5000.000              1
 0.25000000E+01 0.00000000E 00 0.00000000E 00 0.00000000E 00 0.00000000E 00    2
 0.25474390E+05-0.45989841E+00 0.25000000E+01 0.00000000E 00 0.00000000E 00    3
 0.00000000E 00 0.00000000E 00 0.25474390E+05-0.45989841E+00                   4
        0    2.7080   37.0000     298.0    1200.0    6000.0          H         1
H2                 J 3/61H   2    0    0    0G   300.000  5000.000              1
 0.31001883E 01 0.51119458E-03 0.52644204E-07-0.34909964E-10 0.36945341E-14    2
-0.87738013E 03-0.19629412E 01 0.30574446E 01 0.26765198E-02-0.58099149E-05    3
 0.55210343E-08-0.18122726E-11-0.98890430E 03-0.22997046E 01                  4
        0    2.9150   38.0000     300.0    1200.0    5000.0          H2        1
H2O                J 3/61H   20   100  000  0G   300.000  5000.000              1
 0.27167633E 01 0.29451374E-02-0.80224374E-06 0.10226682E-09-0.48472145E-14    2
-0.29905826E 05 0.66305671E 01 0.40701275E 01-0.11084499E-02 0.41521180E-05    3
-0.29637404E-08 0.80702103E-12-0.30279722E 05-0.32270046E 00                  4
```

```
    1.2000    2.7100  506.0000     298.0    1200.0    6000.0          H2O       1
H02               J 3/64H   10   200  000  0G   300.000  5000.000              1
 0.37866280E 01 0.27885404E-02-0.10168708E-05 0.17183946E-09-0.11021852E-13    2
 0.11888500E 04 0.48147611E 01 0.35094850E 01 0.11499670E-02 0.58784259E-05    3
-0.77795519E-08 0.29607883E-11 0.13803331E 04 0.68276325E 01                   4
       0    3.4700   107.000     298.0    1200.0    6000.0          H02E      1
H2O2              L 2/69H   20   20   00   0G   300.000  5000.000              1
 0.45731667E 01 0.43361363E-02-0.14746888E-05 0.23489037E-09-0.14316536E-13    2
-0.18006961E 05 0.50113696E 00 0.33887536E 01 0.65692260E-02-0.14850126E-06    3
-0.46258055E-08 0.24715147E-11-0.17663147E 05 0.67853631E 01                   4
                                                                   UNKNOWN
N                 J 3/77N   1    0    0    0G   300.000  5000.000              1
 0.24370811E+01 0.13233886E-03-0.90907754E-07 0.22864054E-10-0.13762291E-14    2
 0.56128585E+05 0.45211111E+01 0.25000004E+01-0.31078154E-08 0.83216097E-11    3
-0.94278278E-14 0.38108039E-17 0.56106975E+05 0.41806431E+01                   4
       0.    3.2980   71.4000     300.0    1200.0    5000.0          N         1
NO                J 6/63N   10   100  000  0G   300.000  5000.000              1
 0.31890000E 01 0.13382281E-02-0.52899318E-06 0.95919332E-10-0.64847932E-14    2
 0.98283290E 04 0.67458126E 01 0.40459521E 01-0.34181783E-02 0.79819190E-05    3
-0.61139316E-08 0.15919076E-11 0.97453934E 04 0.29974988E 01                   4
       0    3.4700  119.0000     298.0    1200.0    6000.0          NO        1
N2                J 3/77N   2    0    0    0G   300.000  5000.000              1
 0.28532899E+01 0.16022128E-02-0.62936893E-06 0.11441022E-09-0.78057465E-14    2
-0.89008093E+03 0.63964897E+01 0.37044177E+01-0.14218753E-02 0.28670392E-05    3
-0.12028885E-08-0.13954677E-13-0.10640795E+04 0.22336285E+01                   4
       0    3.6810   91.5000     300.0    1200.0    5000.0          N2        1
O                 J 3/77O   1    0    0    0G   300.000  5000.000              1
 0.25342961E+01-0.12478170E-04-0.12562724E-07 0.69029862E-11-0.63797095E-15    2
 0.29231108E+05 0.49628591E+01 0.30309401E+01-0.22525853E-02 0.39824540E-05    3
-0.32604921E-08 0.10152035E-11 0.29136526E+05 0.26099342E+01                   4
       0    3.0500  106.7000     298.0    1200.0    6000.0          O         1
OH                J12/70O   1H   10   00   0G   300.000  5000.000              1
 0.29131230E+01 0.95418248E-03-0.19084325E-06 0.12730795E-10 0.24803941E-15    2
 0.39647060E+04 0.54288735E+01 0.38365518E+01-0.10702014E-02 0.94849757E-06    3
 0.20843575E-09-0.23384265E-12 0.36715807E+04 0.49805456E+00                   4
    .7540    2.6620  506.0000     300.0    1200.0    5000.0          OH        1
O2                J 9/65O   2    0    0    0G   300.000  5000.000              1
 0.36219521E 01 0.73618256E-03-0.19652219E-06 0.36201556E-10-0.28945623E-14    2
-0.12019822E 04 0.36150942E 01 0.36255980E 01-0.18782183E-02 0.70554543E-05    3
-0.67635071E-08 0.21555977E-11-0.10475225E 04 0.43052769E 01                   4
       0    3.4670  106.7000     300.0    1200.0    5000.0          O2        1
H2O(L)            J11/65H   20   100  000  0L   273.150  1000.000              1
 0.0            0.0            0.0            0.0            0.0               2
 0.0            0.0            0.12712782E 02-0.17662790E-01-0.22556661E-04    3
 0.20820908E-06-0.24078614E-09-0.37483200E 05-0.59115345E 02                   4
                                                NO TRANSPORT                   5


C2H6    O2              C2H4    H2              14.41   0.0      25000.GLOBAL
```

C3H8	O2		C2H4	H2		14.41	0.0	25000.	GLOBAL
C8H18	O2		C2H4	H2		14.41	0.0	25000.	GLOBAL
C2H4	O2		CO	H2		12.57	0.0	25200.	GLOBAL
C6H6	O2		CO	H2		7.720	1.0	19650.	GLOBAL
FUEL OIL	O2		CO	H2		7.720	1.0	19650.	GLOBAL
H2O(L)			H2O			13.90	0.0	25900.	SUUBERG
O2	H2		OH	OH		11.903	0.0	22661.	PRATT
OH	H2		H2O	H		11.439	0.0	5187.	PRATT
O2	H		OH	O		11.677	0.0	8712.	PRATT
O	H2		OH	H		9.352	0.0	3903.	PRATT
O	H2O		OH	OH		11.095	0.0	9115.	PRATT
H	H	M	H2		M	12.699	-1.15	0.0	PRATT
O	O	M	O2		M	9.672	-0.278	0000	PRATT
O	H	M	OH		M	10.627	-0.0	-1400.	PRATT
H	OH	M	H2O		M	10.778	-0.00	-252.0	PRATT
H	O2	M	HO2		M	9.186	0.0	503.5	WALD7
CO	OH		H	CO2		8.336	0.0	300.	PRATT
CO	O	M	CO2		M	8.000	0.0	1259.	PRATT
CO2	O		CO	O2		10.279	0.0	27268.	PRATT
CH4	O		CH3	OH		13.300	0.0	9.000	CGS
CH4	H		CH3	H2		14.1	0.0	11.900	CGS
CH4	OH		CH3	H2O		13.500	0.0	5.000	CGS
CH3	CHO		CH4	CO		11.5	0.50	0.0	CGS
CH3	CH2O		CHO	CH4		10.00	0.5	6.000	CGS
CH3	O		CH2O	H		14.41	0.0	2.000	CGS
CH3	OH		CH2O	H2		12.6	0.0	0.0	CGS
CH3	H	M	CH4		M	26.86	-3.0	0.0	CGS
CH3	O2		CH3O	O		13.380	0.0	28.810	CGS
CH3O		M	CH2O	H	M	13.700	0.0	21.000	CGS
CH2O		M	CHO	H	M	16.700	0.0	72.000	CGS
CH2O	O		CHO	OH		13.700	0.0	4.600	CGS
CH2O	H		CHO	H2		13.130	0.0	3.760	CGS
CH2O	OH		CHO	H2O		10.5	1.0	0.0	CGS
CHO		M	CO	H	M	14.160	0.0	19.000	CGS
CHO	H		CO	H2		14.300	0.0	0.0	CGS
CHO	OH		CO	H2O		14.000	0.0	0.0	CGS
CHO	O		CO	OH		14.000	0.0	0.0	CGS

```
***** TSTR OUTPUT TEXT FILE *****
          6  11  1987
         RUN NUMBER    1


***** SOLUTION PARAMETERS *****

  CC VOLUME  =  1.30D-02 M**3
  CC HEAT TRANS. RATE    = -6.50000D+07 J/S
  MIN ALLOWABLE MOLE NO. =  1.00000D-18 KGMOLE/KG
  INITIAL MASS OF LIQ IN THE COMB CHAMBER =  1.00000D-15 KG
  INITIAL DROPLET DIAMETER =  1.00000D-07 M
  MIN ALLOWABLE DROPLET DIAMETER  =  5.000D-07 M
  EXIT TURBINE FLOW RATE CONSTANT =  9.233D-01
  HOT GAS MANIFOLD PRESSURE =  1.723D+06 PA

  NDEBUG (1 FOR PRINITING, 0 FOR SUPRESSING OUTPUT)
     1  1  1  1  1  1  1  0  0  0
     0  0  0  1  0  0  0  0  0  0

  DROPLET DIAMETER COEFFICIENT     =  4.8500D-01
  AREA OF HYDROGEN INJECTOR ANULUS =  1.3290D-05
  AREA OF THE OXIDIZER INJECTOR    =  1.0968D-05
  MCON (=0 FOR CONSTANT MASS FLOW; =1 FOR PIPING SYSTEM) 1
  KINET (=0 FOR NO KINETICS; =1 FOR CALL TO RADSS) 0

  INTEGRATION PARAMETERS:
    MITER, METH, NDGEAR  2   2   0
    IER, EPSI   10   5.00D-07
    INPUT STEP SIZE =  1.00D-12 SEC
    INITIAL TIME =  0.00D+00 SEC
    OUTPUT INTERVAL =  5.00D-04 SEC
    FINAL TIME =  1.00D-01 SEC
    TIME SHUTDOWN BEGINS =  0.00D+00

  FOR SS RATE APPROXIMATION:
    CONVERGENCE CRITERION (MAX % CHANGE) =  1.00D-06
    MAX NO ITERATIONS   =      25
    ERROR CHECK IDGT    =  0
    IMSL ERROR FLAG JER =  10

  OXIDIZER FEED SYSTEM INPUTS:
    NO. OF PIPES  11  NO. OF NODES  12
    NO. OF HELIUM ORIFICE PIPES   7
    PIPE IN WHICH THE INTERFACE IS INITIALLY LOCATED   8
    RFLIQ FOR THE OX PIPES  =   1.303D-01
    RFGAS FOR THE OX PIPES   =  1.827D-01
```

RFLIQ FOR THE HE ORIFICE = 1.367D-01
RFGAS FOR THE HE ORIFICE = 5.283D-01
RFLIQ FOR THE HE VALVE = 1.720D+04
RFGAS FOR THE HE VALVE = 1.827D+03
INJECTOR AND MANIFOLD CD = 5.000D-01
UPSTREAM SOURCE PRESSURE = 5.16964D+06 PA
INITIAL BACKFLOW INTERFACE POSITION = 0.000D+00

PIPE GEOMETRY:

PIPE	NODE 1	NODE 2	AREA (M**2)	LENGTH (M)
1	1	2	8.1073D-05	0.30000
2	2	3	8.1073D-05	0.30000
3	3	4	8.1073D-05	0.30000
4	4	5	8.1073D-05	0.30000
5	5	6	8.1073D-05	0.30000
6	6	7	8.1073D-05	0.30000
7	7	8	8.1073D-05	0.30000
8	8	9	2.0268D-03	0.00500
9	9	10	2.0268D-03	0.04000
10	10	11	2.0268D-03	0.04000
11	11	12	2.0268D-03	0.04000

PIPE INITIAL CONDITIONS:

PIPE	VELOCITY (M/SEC)	LIQUID/VAP INT. POSITION (% LENGTH)
1	1.0000D-03	1.0000D+00
2	1.0000D-03	1.0000D+00
3	1.0000D-03	1.0000D+00
4	1.0000D-03	1.0000D+00
5	1.0000D-03	1.0000D+00
6	1.0000D-03	1.0000D+00
7	1.0000D-03	1.0000D+00
8	1.0000D-03	0.0000D+00
9	1.0000D-03	0.0000D+00
10	1.0000D-03	0.0000D+00
11	1.0000D-03	0.0000D+00

INITIAL NODAL DENSITIES:

NODE	DENSITY (KG/M**3)
1	2.0739D+01
2	2.0739D+01
3	2.0739D+01
4	2.0739D+01
5	2.0739D+01
6	2.0739D+01
7	2.0739D+01
8	2.0739D+01
9	9.9070D+02
10	9.9070D+02
11	9.9070D+02

```
   12       9.9070D+02

****** REACTION RATE DATA FROM NPT ******


 FOLLOWING REACTION IGNORED
     C3H8    O2              ---->      C2H4    H2
 REACTANT C3H8 NOT FOUND IN SPECIES LIST

 FOLLOWING REACTION IGNORED
     C8H18   O2              ---->      C2H4    H2
 REACTANT C8H1 NOT FOUND IN SPECIES LIST

 FOLLOWING REACTION IGNORED
     C2H4    O2              ---->      CO      H2
 REACTANT C2H4 NOT FOUND IN SPECIES LIST

 FOLLOWING REACTION IGNORED
     C6H6    O2              ---->      CO      H2
 REACTANT C6H6 NOT FOUND IN SPECIES LIST

 FOLLOWING REACTION IGNORED
     FUEL OIL02              ---->      CO      H2
 REACTANT FUEL NOT FOUND IN SPECIES LIST

 FOLLOWING REACTION IGNORED
     H2O(L)                  ---->      H2O
 REACTANT H2O( NOT FOUND IN SPECIES LIST

 REACTION  1   O2      H2              ---->   OH      OH
   DATA COMMENT: PRATT
   FWD RATE DATA: BX  =     11.903 TEN  =      0.000 TACT  =  22661.000
   CALCULATED REVERSE RATE CONSTANTS
   STD DEVIATION =   2.428D+00 CORR COEFF =   9.475D-01
   REV RATE DATA : BX2 =     19.489 TEN2 =      0.000 TACT2 =  30793.276

 REACTION  2   OH      H2              ---->   H2O     H
   DATA COMMENT: PRATT
   FWD RATE DATA: BX  =     11.439 TEN  =      0.000 TACT  =   5187.000
   CALCULATED REVERSE RATE CONSTANTS
   STD DEVIATION =   4.078D-01 CORR COEFF =   9.939D-01
   REV RATE DATA : BX2 =     14.133 TEN2 =      0.000 TACT2 =  15784.008

 REACTION  3   O2      H               ---->   OH      O
   DATA COMMENT: PRATT
   FWD RATE DATA: BX  =     11.677 TEN  =      0.000 TACT  =   8712.000
   CALCULATED REVERSE RATE CONSTANTS
   STD DEVIATION =   1.892D+00 CORR COEFF =   8.664D-01
```

```
  REV RATE DATA : BX2 =    17.639 TEN2 =      0.000 TACT2 =  14056.891

REACTION  4   O       H2              ---->   OH      H
  DATA COMMENT: PRATT
  FWD RATE DATA: BX  =      9.352 TEN  =      0.000 TACT  =   3903.000
  CALCULATED REVERSE RATE CONSTANTS
  STD DEVIATION =   5.361D-01 CORR COEFF =   9.459D-01
  REV RATE DATA : BX2 =    10.976 TEN2 =      0.000 TACT2 =   6690.385

REACTION  5   O       H2O             ---->   OH      OH
  DATA COMMENT: PRATT
  FWD RATE DATA: BX  =     11.095 TEN  =      0.000 TACT  =   9115.000
  CALCULATED REVERSE RATE CONSTANTS
  STD DEVIATION =   1.283D-01 CORR COEFF =   9.217D-01
  REV RATE DATA : BX2 =    10.025 TEN2 =      0.000 TACT2 =   1305.377

REACTION  6   H       H       M       ---->   H2              M
  DATA COMMENT: PRATT
  FWD RATE DATA: BX  =     12.699 TEN  =     -1.150 TACT  =      0.000
  CALCULATED REVERSE RATE CONSTANTS
  STD DEVIATION =   1.051D-01 CORR COEFF =   1.000D+00
  REV RATE DATA : BX2 =    11.955 TEN2 =      0.000 TACT2 =  51707.198

REACTION  7   O       O       M       ---->   O2              M
  DATA COMMENT: PRATT
  FWD RATE DATA: BX  =      9.672 TEN  =     -0.278 TACT  =      0.000
  CALCULATED REVERSE RATE CONSTANTS
  STD DEVIATION =   1.274D+00 CORR COEFF =   9.941D-01
  REV RATE DATA : BX2 =     7.667 TEN2 =      0.000 TACT2 =  50190.523

REACTION  8   O       H       M       ---->   OH              M
  DATA COMMENT: PRATT
  FWD RATE DATA: BX  =     10.627 TEN  =      0.000 TACT  =  -1400.000
  CALCULATED REVERSE RATE CONSTANTS
  STD DEVIATION =   6.110D-01 CORR COEFF =   9.988D-01
  REV RATE DATA : BX2 =    15.564 TEN2 =      0.000 TACT2 =  54467.238

REACTION  9   H       OH      M       ---->   H2O             M


  DATA COMMENT: PRATT
  FWD RATE DATA: BX  =     10.778 TEN  =      0.000 TACT  =   -252.000
  CALCULATED REVERSE RATE CONSTANTS
  STD DEVIATION =   4.828D-01 CORR COEFF =   9.995D-01
  REV RATE DATA : BX2 =    16.785 TEN2 =      0.000 TACT2 =  63424.861

FOLLOWING REACTION IGNORED
    H       O2      M       ---->       HO2             M
REACTANT HO2  NOT FOUND IN SPECIES LIST
```

1	2.1829D+01	1.0000D+00
2	2.1829D+01	1.0000D+00
3	2.1829D+01	1.0000D+00
4	2.1829D+01	1.0000D+00
5	2.1829D+01	1.0000D+00
6	2.1829D+01	1.0000D+00
7	2.1829D+01	1.0000D+00
8	8.7429D-01	1.0216D-01
9	8.7429D-01	0.0000D+00
10	8.7429D-01	0.0000D+00
11	8.7429D-01	0.0000D+00

NODAL DENSITIES AND PRESSURES:

NODE	DENSITY (KG/M**3)	PRESSURE (PA)
1	2.0739D+01	5.1696D+06
2	2.0253D+01	5.0484D+06
3	1.9775D+01	4.9292D+06
4	1.9306D+01	4.8123D+06
5	1.8845D+01	4.6976D+06
6	1.8395D+01	4.5853D+06
7	1.7954D+01	4.4753D+06
8	1.7522D+01	4.3677D+06
9	9.9070D+02	4.2120D+06
10	9.9070D+02	4.2119D+06
11	9.9070D+02	4.2119D+06
12	9.9070D+02	4.2119D+06

```
     5        1.8900D+01   4.7112D+06
     6        1.8472D+01   4.6045D+06
     7        1.8056D+01   4.5007D+06
     8        1.7651D+01   4.3999D+06
     9        9.9070D+02   4.2855D+06
    10        9.9070D+02   4.2855D+06
    11        9.9070D+02   4.2855D+06
    12        9.9070D+02   4.2855D+06

***** INTEGRATING ROUTINE CALLED *****

  CALL FOR STEP       3 OUT OF          200 STEPS
  STEP BEGINS AT TIME =  1.00000D-03 AND ENDS AT TIME =  1.50000D-03

***** CC AND INLET CONDTNS ON RETURN  *****
***** FROM THE INTEGRATING SUBROUTINE *****

  TIME FOLLOWING INTEGRATION =  1.50000D-03 SEC
  FINAL STEP SIZE =  1.75435D-05 SEC
  ERROR FLAG, IER =    0

  SPECIES NAME  S2 (KGMOLE/KG)  ISTRM  S1 (KGMOLE/KG)  STATE
     1    HE      1.00944D-18     3      2.49838D-01    G
     2    H2      4.82805D-01     2      4.96032D-01    G
     3    O2      1.03397D-11     1      3.12500D-02    L
     4    H2O     1.48005D-03     0      0.00000D+00    G
     5    H       1.00000D-18     0      0.00000D+00    G
     6    O       1.00000D-18     0      0.00000D+00    G
     7    OH      1.00000D-18     0      0.00000D+00    G

  DENSITY OF LIQUID IN THE CC =  5.07032D-03 KG
  BACKFLOW INTERFACE POSITION =  0.00000D+00
  CC TEMPERATURE =     465.0223  K
  CC PRESSURE    =  4.21058D+06 PA
  CC DENSITY     =  2.24873D+00 KG/M**3
  AVG. MOL. WT.  =  4.84285D-01 KG/KGMOLE
  CC VOLUME      =  1.30000D-02 M**3
  OMV, FMV, PMV, EMV =   1.350D+02  1.615D+03  0.000D+00  1.694D+03 KG/M3/S
  UPSTREAM PRESSURE  =  5.1696D+06 PA
  INJECTOR PRESSURE DROP =  7.4206D+02 PA

  STREAM      TEMP (K)      MDOT (KG/SEC)   SF (KGMOLE/SEC)  SH (JOULES/SEC)
    1          120.000       1.75556D+00     0.000000D+00     -1.152083D+06
    2          160.000       2.10000D+01     8.012821D+02     -2.518590D+09
    3          120.000       0.00000D+00     0.000000D+00      0.000000D+00

  PIPE CONDITIONS:

    PIPE  VELOCITY (M/SEC)  LIQUID/VAP INT. POSITION (% LENGTH)
```

SPECIES	NAME	S2 (KGMOLE/KG)	ISTRM	S1 (KGMOLE/KG)	STATE
1	HE	1.00027D-18	3	2.49838D-01	G
2	H2	4.90960D-01	2	4.96032D-01	G
3	O2	1.51292D-11	1	3.12500D-02	L
4	H2O	5.67428D-04	0	0.00000D+00	G
5	H	1.00000D-18	0	0.00000D+00	G
6	O	1.00000D-18	0	0.00000D+00	G
7	OH	1.00000D-18	0	0.00000D+00	G

DENSITY OF LIQUID IN THE CC = 1.11943D-03 KG
BACKFLOW INTERFACE POSITION = 0.00000D+00
CC TEMPERATURE = 467.4076 K
CC PRESSURE = 4.28538D+06 PA
CC DENSITY = 2.24344D+00 KG/M**3
AVG. MOL. WT. = 4.91528D-01 KG/KGMOLE
CC VOLUME = 1.30000D-02 M**3
OMV, FMV, PMV, EMV = 7.201D+01 1.615D+03 0.000D+00 1.698D+03 KG/M3/S
UPSTREAM PRESSURE = 5.1696D+06 PA
INJECTOR PRESSURE DROP = 2.1102D+02 PA

STREAM	TEMP (K)	MDOT (KG/SEC)	SF (KGMOLE/SEC)	SH (JOULES/SEC)
1	120.000	9.36176D-01	0.000000D+00	-6.143656D+05
2	160.000	2.10000D+01	8.012821D+02	-2.518590D+09
3	120.000	0.00000D+00	0.000000D+00	0.000000D+00

PIPE CONDITIONS:

PIPE	VELOCITY (M/SEC)	LIQUID/VAP INT. POSITION (% LENGTH)
1	1.1627D+01	1.0000D+00
2	1.1627D+01	1.0000D+00
3	1.1627D+01	1.0000D+00
4	1.1627D+01	1.0000D+00
5	1.1627D+01	1.0000D+00
6	1.1627D+01	1.0000D+00
7	1.1627D+01	1.0000D+00
8	4.6623D-01	3.3539D-02
9	4.6623D-01	0.0000D+00
10	4.6623D-01	0.0000D+00
11	4.6623D-01	0.0000D+00

NODAL DENSITIES AND PRESSURES:

NODE	DENSITY (KG/M**3)	PRESSURE (PA)
1	2.0739D+01	5.1696D+06
2	2.0260D+01	5.0501D+06
3	1.9793D+01	4.9339D+06
4	1.9340D+01	4.8210D+06

STREAM	TEMP (K)	MDOT (KG/SEC)	SF (KGMOLE/SEC)	SH (JOULES/SEC)
1	120.000	2.71235D-01	0.000000D+00	-1.779982D+05
2	160.000	2.10000D+01	8.012821D+02	-2.518590D+09
3	120.000	0.00000D+00	0.000000D+00	0.000000D+00

PIPE CONDITIONS:

PIPE	VELOCITY (M/SEC)	LIQUID/VAP INT. POSITION (% LENGTH)
1	3.3503D+00	1.0000D+00
2	3.3503D+00	1.0000D+00
3	3.3503D+00	1.0000D+00
4	3.3503D+00	1.0000D+00
5	3.3503D+00	1.0000D+00
6	3.3503D+00	1.0000D+00
7	3.3503D+00	1.0000D+00
8	1.3508D-01	4.6974D-03
9	1.3508D-01	0.0000D+00
10	1.3508D-01	0.0000D+00
11	1.3508D-01	0.0000D+00

NODAL DENSITIES AND PRESSURES:

NODE	DENSITY (KG/M**3)	PRESSURE (PA)
1	2.0739D+01	5.1696D+06
2	2.0427D+01	5.0918D+06
3	2.0121D+01	5.0156D+06
4	1.9822D+01	4.9410D+06
5	1.9529D+01	4.8681D+06
6	1.9243D+01	4.7967D+06
7	1.8962D+01	4.7268D+06
8	1.8688D+01	4.6583D+06
9	9.9070D+02	4.5941D+06
10	9.9070D+02	4.5941D+06
11	9.9070D+02	4.5941D+06
12	9.9070D+02	4.5941D+06

****** INTEGRATING ROUTINE CALLED ******

CALL FOR STEP 2 OUT OF 200 STEPS
STEP BEGINS AT TIME = 5.00000D-04 AND ENDS AT TIME = 1.00000D-03

****** CC AND INLET CONDTNS ON RETURN ******
****** FROM THE INTEGRATING SUBROUTINE ******

TIME FOLLOWING INTEGRATION = 1.00000D-03 SEC
FINAL STEP SIZE = 1.02457D-05 SEC
ERROR FLAG, IER = 0

```
    5    H       1.00000D-18     0       0.00000D+00    G
    6    O       1.00000D-18     0       0.00000D+00    G
    7    OH      1.00000D-18     0       0.00000D+00    G

  CC TEMPERATURE =     550.0000  K
  CC PRESSURE    =   5.1696D+06 PA
  CC DENSITY     =  2.27907D+00 KG/M**3
  AVG. MOL. WT.  =  4.96031D-01 KG/KGMOLE
  CC VOLUME      =  1.30000D-02 M**3

  STREAM NAME  TEMP        MDOT         SF            HS            SH
               (K)      (KG/SEC)   (KGMOLE/SEC)   (J/KGMOLE)    (J/SEC)

    1    O2    120.00  0.00000D+00  0.00000D+00  -2.73000D+05   0.00000D+00
    2    H2    160.00  2.10000D+01  8.01282D+02  -3.14320D+06  -2.51859D+09
    3    HE    120.00  0.00000D+00  0.00000D+00  -3.54160D+06   0.00000D+00

****** INTEGRATING ROUTINE CALLED ******

  CALL FOR STEP       1 OUT OF          200 STEPS
  STEP BEGINS AT TIME =  0.00000D+00 AND ENDS AT TIME =  5.00000D-04

****** CC AND INLET CONDTNS ON RETURN  ******
****** FROM THE INTEGRATING SUBROUTINE ******

  TIME FOLLOWING INTEGRATION =  5.00000D-04 SEC
  FINAL STEP SIZE =  3.17799D-06 SEC
  ERROR FLAG, IER =    0

  SPECIES NAME  S2 (KGMOLE/KG)  ISTRM  S1 (KGMOLE/KG)  STATE
     1    HE      1.00146D-18     3      2.49838D-01    G
     2    H2      4.95236D-01     2      4.96032D-01    G
     3    O2      2.18638D-11     1      3.12500D-02    L
     4    H2O     8.90040D-05     0      0.00000D+00    G
     5    H       1.00000D-18     0      0.00000D+00    G
     6    O       1.00000D-18     0      0.00000D+00    G
     7    OH      1.00000D-18     0      0.00000D+00    G

  DENSITY OF LIQUID IN THE CC =  4.84393D-05 KG
  BACKFLOW INTERFACE POSITION =  0.00000D+00
  CC TEMPERATURE =     493.6106  K
  CC PRESSURE    =  4.59581D+06 PA
  CC DENSITY     =  2.26077D+00 KG/M**3
  AVG. MOL. WT.  =  4.95325D-01 KG/KGMOLE
  CC VOLUME      =  1.30000D-02 M**3
  OMV, FMV, PMV, EMV =   2.086D+01  1.615D+03  0.000D+00  1.681D+03 KG/M3/S
  UPSTREAM PRESSURE  =  5.1696D+06 PA
  INJECTOR PRESSURE DROP =  1.7713D+01 PA
```

5	6	4	7	7
6	5	5	2	0
7	6	6	3	0
8	6	5	7	0
9	5	7	4	0

ISIDE ARRAY

RXN	ISIDE(K,RXN)						
1	0	-1	-1	0	0	0	2
2	0	-1	0	1	1	0	-1
3	0	0	-1	0	-1	1	1
4	0	-1	0	0	1	-1	1
5	0	0	0	-1	0	-1	2
6	0	1	0	0	-2	0	0
7	0	0	1	0	0	-2	0
8	0	0	0	0	-1	-1	1
9	0	0	0	1	-1	0	-1

REACTION RATE DATA IN SI UNITS

RXN	MODE		BX	TEN	TACT
1	1	FWD	11.903	0.000	22661.000
		REV	19.489	0.000	30793.276
2	1	FWD	11.439	0.000	5187.000
		REV	14.133	0.000	15784.008
3	1	FWD	11.677	0.000	8712.000
		REV	17.639	0.000	14056.891
4	1	FWD	9.352	0.000	3903.000
		REV	10.976	0.000	6690.385
5	1	FWD	11.095	0.000	9115.000
		REV	10.025	0.000	1305.377
6	3	FWD	12.699	-1.150	0.000
		REV	11.955	0.000	51707.198
7	3	FWD	9.672	-0.278	0.000
		REV	7.667	0.000	50190.523
8	3	FWD	10.627	0.000	-1400.000
		REV	15.564	0.000	54467.238
9	3	FWD	10.778	0.000	-252.000
		REV	16.785	0.000	63424.861

****** CC AND INLET INITIAL CONDITIONS ******

SPECIE	NAME	S2 (KGMOLE/KG)	ISTRM	S1 (KGMOLE/KG)	STATE
1	HE	1.00000D-18	3	2.49838D-01	G
2	H2	4.96031D-01	2	4.96032D-01	G
3	O2	3.12500D-11	1	3.12500D-02	L
4	H2O	5.55062D-11	0	0.00000D+00	G

****** "Z" ARRAY OF THERMO PROPERTY POLYNOMIAL COEFFICIENTS ******

NAME	COEFFICIENTS				
HE	2.50000D+00	0.00000D+00	0.00000D+00	0.00000D+00	0.00000D+00
	-7.45375D+02	9.15349D-01	2.50000D+00	0.00000D+00	0.00000D+00
	0.00000D+00	0.00000D+00	-7.45375D+02	9.15349D-01	
H2	3.10019D+00	5.11195D-04	5.26442D-08	-3.49100D-11	3.69453D-15
	-8.77380D+02	-1.96294D+00	3.05744D+00	2.67652D-03	-5.80991D-06
	5.52103D-09	-1.81227D-12	-9.88904D+02	-2.29970D+00	
O2	3.62195D+00	7.36183D-04	-1.96522D-07	3.62016D-11	-2.89456D-15
	-1.20198D+03	3.61509D+00	3.62560D+00	-1.87822D-03	7.05545D-06
	-6.76351D-09	2.15560D-12	-1.04752D+03	4.30528D+00	
H2O	2.71676D+00	2.94514D-03	-8.02244D-07	1.02267D-10	-4.84721D-15
	-2.99058D+04	6.63057D+00	4.07013D+00	-1.10845D-03	4.15212D-06
	-2.96374D-09	8.07021D-13	-3.02797D+04	-3.22700D-01	
H	2.50000D+00	0.00000D+00	0.00000D+00	0.00000D+00	0.00000D+00
	2.54744D+04	-4.59898D-01	2.50000D+00	0.00000D+00	0.00000D+00
	0.00000D+00	0.00000D+00	2.54744D+04	-4.59898D-01	
O	2.53430D+00	-1.24782D-05	-1.25627D-08	6.90299D-12	-6.37971D-16
	2.92311D+04	4.96286D+00	3.03094D+00	-2.25259D-03	3.98245D-06
	-3.26049D-09	1.01520D-12	2.91365D+04	2.60993D+00	
OH	2.91312D+00	9.54182D-04	-1.90843D-07	1.27308D-11	2.48039D-16
	3.96471D+03	5.42887D+00	3.83655D+00	-1.07020D-03	9.48498D-07
	2.08436D-10	-2.33843D-13	3.67158D+03	4.98055D-01	

****** REACTION RATE INDICIES AND DATA ******

REACTION INDICIES

RXN (J)	ID(1,J)	ID(2,J)	ID(3,J)	ID(4,J)
1	3	2	7	7
2	7	2	4	5
3	3	5	7	6
4	6	2	7	5

```
    CH3O            M       ---->      CH2O    H       M
 REACTANT CH3O NOT FOUND IN SPECIES LIST

 FOLLOWING REACTION IGNORED
    CH2O            M       ---->      CHO     H       M
 REACTANT CH2O NOT FOUND IN SPECIES LIST

 FOLLOWING REACTION IGNORED
    CH2O    O               ---->      CHO     OH
 REACTANT CH2O NOT FOUND IN SPECIES LIST

 FOLLOWING REACTION IGNORED
    CH2O    H               ---->      CHO     H2
 REACTANT CH2O NOT FOUND IN SPECIES LIST

 FOLLOWING REACTION IGNORED
    CH2O    OH              ---->      CHO     H2O
 REACTANT CH2O NOT FOUND IN SPECIES LIST

 FOLLOWING REACTION IGNORED
    CHO             M       ---->      CO      H       M
 REACTANT CHO  NOT FOUND IN SPECIES LIST

 FOLLOWING REACTION IGNORED
    CHO     H               ---->      CO      H2
 REACTANT CHO  NOT FOUND IN SPECIES LIST

 FOLLOWING REACTION IGNORED
    CHO     OH              ---->      CO      H2O
 REACTANT CHO  NOT FOUND IN SPECIES LIST

 FOLLOWING REACTION IGNORED
    CHO     O               ---->      CO      OH
 REACTANT CHO  NOT FOUND IN SPECIES LIST

***** SPECIES PROPERTIES *****

 MAJOR CONSTITUENTS:
   INDEX  NAME    MOLEC. WT.
      1   HE       4.0026D+00
      2   H2       2.0160D+00
      3   O2       3.2000D+01
      4   H2O      1.8016D+01

 RATE DETERMINING RADICALS
   INDEX  NAME    MOLEC. WT.
      5   H        1.0080D+00
      6   O        1.6000D+01
      7   OH       1.7008D+01
```

```
FOLLOWING REACTION IGNORED
    CO      OH              ---->      H       CO2
REACTANT CO   NOT FOUND IN SPECIES LIST

FOLLOWING REACTION IGNORED
    CO      O       M       ---->      CO2             M
REACTANT CO   NOT FOUND IN SPECIES LIST

FOLLOWING REACTION IGNORED
    CO2     O               ---->      CO      O2
REACTANT CO2  NOT FOUND IN SPECIES LIST

FOLLOWING REACTION IGNORED
    CH4     O               ---->      CH3     OH
REACTANT CH4  NOT FOUND IN SPECIES LIST

FOLLOWING REACTION IGNORED
    CH4     H               ---->      CH3     H2
REACTANT CH4  NOT FOUND IN SPECIES LIST

FOLLOWING REACTION IGNORED
    CH4     OH              ---->      CH3     H2O
REACTANT CH4  NOT FOUND IN SPECIES LIST

FOLLOWING REACTION IGNORED
    CH3     CHO             ---->      CH4     CO
REACTANT CH3  NOT FOUND IN SPECIES LIST

FOLLOWING REACTION IGNORED
    CH3     CH2O            ---->      CHO     CH4
REACTANT CH3  NOT FOUND IN SPECIES LIST

FOLLOWING REACTION IGNORED
    CH3     O               ---->      CH2O    H
REACTANT CH3  NOT FOUND IN SPECIES LIST

FOLLOWING REACTION IGNORED
    CH3     OH              ---->      CH2O    H2
REACTANT CH3  NOT FOUND IN SPECIES LIST

FOLLOWING REACTION IGNORED
    CH3     H       M       ---->      CH4             M
REACTANT CH3  NOT FOUND IN SPECIES LIST

FOLLOWING REACTION IGNORED
    CH3     O2              ---->      CH3O    O
REACTANT CH3  NOT FOUND IN SPECIES LIST

FOLLOWING REACTION IGNORED
```

OUTPUT FROM TSTR.PLT1

TIME (MSEC) MOLE NUMBER (KGMOLES/KG*1.0D+06)

0.000	1.00D-15	4.96D+02	3.13D-08	5.55D-08	1.00D-15	1.00D-15	1.00D-15
0.500	1.00D-15	4.95D+02	2.19D-08	8.90D-02	1.00D-15	1.00D-15	1.00D-15
1.000	1.00D-15	4.91D+02	1.51D-08	5.67D-01	1.00D-15	1.00D-15	1.00D-15
1.500	1.01D-15	4.83D+02	1.03D-08	1.48D+00	1.00D-15	1.00D-15	1.00D-15
2.000	1.00D-15	4.72D+02	7.01D-09	2.65D+00	1.00D-15	1.00D-15	1.00D-15
2.500	1.01D-15	4.61D+02	4.75D-09	3.88D+00	1.00D-15	1.00D-15	1.00D-15
3.000	1.01D-15	4.52D+02	3.24D-09	4.98D+00	1.00D-15	1.00D-15	1.00D-15
3.500	1.01D-15	4.44D+02	2.23D-09	5.86D+00	1.00D-15	1.00D-15	1.00D-15
4.000	1.02D-15	4.38D+02	1.56D-09	6.47D+00	1.00D-15	1.00D-15	1.00D-15
4.500	1.01D-15	4.36D+02	1.11D-09	6.77D+00	1.00D-15	1.00D-15	1.00D-15
5.000	1.01D-15	4.35D+02	7.98D-10	6.78D+00	1.00D-15	1.00D-15	1.00D-15
5.500	1.00D-15	4.38D+02	5.83D-10	6.52D+00	1.00D-15	1.00D-15	1.00D-15
6.000	1.01D-15	4.42D+02	4.31D-10	6.03D+00	1.00D-15	1.00D-15	1.00D-15
6.500	1.00D-15	4.48D+02	3.21D-10	5.41D+00	1.00D-15	1.00D-15	1.00D-15
7.000	1.00D-15	4.54D+02	2.40D-10	4.73D+00	1.00D-15	1.00D-15	1.00D-15
7.500	1.00D-15	4.59D+02	1.79D-10	4.11D+00	1.00D-15	1.00D-15	1.00D-15
8.000	1.00D-15	4.64D+02	1.33D-10	3.63D+00	1.00D-15	1.00D-15	1.00D-15
8.500	1.00D-15	4.66D+02	9.83D-11	3.34D+00	1.00D-15	1.00D-15	1.00D-15
9.000	1.01D-15	4.67D+02	7.21D-11	3.27D+00	1.00D-15	1.00D-15	1.00D-15
9.500	1.00D-15	4.66D+02	5.25D-11	3.41D+00	1.00D-15	1.00D-15	1.00D-15
10.000	1.00D-15	4.63D+02	3.80D-11	3.69D+00	1.00D-15	1.00D-15	1.00D-15
10.500	1.01D-15	4.60D+02	2.74D-11	4.05D+00	1.00D-15	1.00D-15	1.00D-15
11.000	1.01D-15	4.57D+02	1.98D-11	4.42D+00	1.00D-15	1.00D-15	1.00D-15
11.500	1.01D-15	4.54D+02	1.43D-11	4.74D+00	1.00D-15	1.00D-15	1.00D-15
12.000	1.00D-15	4.52D+02	1.03D-11	4.98D+00	1.00D-15	1.00D-15	1.00D-15
12.500	1.01D-15	4.50D+02	7.53D-12	5.10D+00	1.00D-15	1.00D-15	1.00D-15
13.000	1.01D-15	4.50D+02	5.50D-12	5.11D+00	1.00D-15	1.00D-15	1.00D-15
13.500	1.00D-15	4.51D+02	4.03D-12	5.01D+00	1.00D-15	1.00D-15	1.00D-15
14.000	1.00D-15	4.53D+02	2.97D-12	4.84D+00	1.00D-15	1.00D-15	1.00D-15
14.500	1.01D-15	4.55D+02	2.19D-12	4.62D+00	1.00D-15	1.00D-15	1.00D-15
15.000	1.00D-15	4.57D+02	1.62D-12	4.40D+00	1.00D-15	1.00D-15	1.00D-15
15.500	1.00D-15	4.58D+02	1.19D-12	4.20D+00	1.00D-15	1.00D-15	1.00D-15
16.000	1.00D-15	4.60D+02	8.76D-13	4.07D+00	1.00D-15	1.00D-15	1.00D-15
16.500	1.00D-15	4.60D+02	6.43D-13	4.00D+00	1.00D-15	1.00D-15	1.00D-15
17.000	1.01D-15	4.60D+02	4.71D-13	4.01D+00	1.00D-15	1.00D-15	1.00D-15
17.500	1.00D-15	4.60D+02	3.44D-13	4.08D+00	1.00D-15	1.00D-15	1.00D-15
18.000	1.01D-15	4.59D+02	2.50D-13	4.19D+00	1.00D-15	1.00D-15	1.00D-15
18.500	1.00D-15	4.57D+02	1.82D-13	4.32D+00	1.00D-15	1.00D-15	1.00D-15
19.000	1.00D-15	4.56D+02	1.33D-13	4.45D+00	1.00D-15	1.00D-15	1.00D-15
19.500	1.00D-15	4.55D+02	9.67D-14	4.56D+00	1.00D-15	1.00D-15	1.00D-15
20.000	1.00D-15	4.55D+02	7.06D-14	4.63D+00	1.00D-15	1.00D-15	1.00D-15
20.500	1.01D-15	4.54D+02	5.16D-14	4.66D+00	1.00D-15	1.00D-15	1.00D-15
21.000	1.01D-15	4.54D+02	3.77D-14	4.65D+00	1.00D-15	1.00D-15	1.00D-15
21.500	1.00D-15	4.55D+02	2.77D-14	4.60D+00	1.00D-15	1.00D-15	1.00D-15
22.000	1.01D-15	4.56D+02	2.03D-14	4.53D+00	1.00D-15	1.00D-15	1.00D-15
22.500	1.01D-15	4.56D+02	1.49D-14	4.45D+00	1.00D-15	1.00D-15	1.00D-15

23.000	1.00D-15	4.57D+02	1.09D-14	4.38D+00	1.00D-15	1.00D-15	1.00D-15
23.500	1.01D-15	4.57D+02	8.01D-15	4.32D+00	1.00D-15	1.00D-15	1.00D-15
24.000	1.00D-15	4.58D+02	5.87D-15	4.28D+00	1.00D-15	1.00D-15	1.00D-15
24.500	1.00D-15	4.58D+02	4.30D-15	4.27D+00	1.00D-15	1.00D-15	1.00D-15
25.000	1.01D-15	4.58D+02	3.14D-15	4.28D+00	1.00D-15	1.00D-15	1.00D-15

OUTPUT FROM TSTR.PLT2

TIME (MSEC)	TEMPERATURE (K)	PRESSURE (MPA)	OX MDOT (KG/S)	LIQ DEN (KG/M3)	DROP DIAM (MICRONS)	VAP RATE (KG/M3 S)
0.000	550.00	5.170	0.0000	7.69D-14	0.500	0.00
0.500	493.61	4.596	0.2712	4.84D-05	1.914	20.35
1.000	467.41	4.285	0.9362	1.12D-03	6.382	66.55
1.500	465.02	4.211	1.7556	5.07D-03	11.863	119.96
2.000	477.70	4.308	2.4446	1.15D-02	16.710	165.78
2.500	497.47	4.515	2.9397	1.79D-02	20.582	202.48
3.000	518.24	4.780	3.1864	2.19D-02	22.964	225.56
3.500	535.86	5.063	3.2084	2.26D-02	23.795	234.25
4.000	547.72	5.328	3.0371	2.02D-02	23.114	228.56
4.500	552.48	5.541	2.7347	1.59D-02	21.207	210.73
5.000	549.80	5.679	2.3266	1.09D-02	18.262	182.44
5.500	540.22	5.726	1.8799	6.44D-03	14.813	148.46
6.000	525.28	5.679	1.4397	3.38D-03	11.296	113.41
6.500	507.36	5.555	1.0855	1.68D-03	8.423	84.80
7.000	489.16	5.382	0.8521	9.15D-04	6.508	65.86
7.500	473.24	5.196	0.7644	6.99D-04	5.736	58.41
8.000	461.60	5.028	0.8243	8.46D-04	6.086	62.20
8.500	455.41	4.905	1.0086	1.40D-03	7.354	75.07
9.000	454.85	4.838	1.2706	2.47D-03	9.202	93.38
9.500	459.14	4.830	1.5540	4.06D-03	11.246	113.27
10.000	466.86	4.871	1.8115	5.93D-03	13.166	131.76
10.500	476.31	4.949	2.0109	7.62D-03	14.734	146.86
11.000	485.81	5.047	2.1227	8.72D-03	15.707	156.37
11.500	493.91	5.151	2.1455	8.98D-03	16.039	159.79
12.000	499.56	5.243	2.0899	8.44D-03	15.758	157.29
12.500	502.19	5.311	1.9692	7.35D-03	14.947	149.53
13.000	501.76	5.349	1.8173	6.04D-03	13.840	138.74
13.500	498.68	5.352	1.6559	4.80D-03	12.615	126.72
14.000	493.71	5.325	1.5095	3.82D-03	11.470	115.43
14.500	487.85	5.275	1.3982	3.17D-03	10.574	106.59
15.000	482.09	5.213	1.3378	2.83D-03	10.058	101.52
15.500	477.31	5.150	1.3287	2.79D-03	9.929	100.29
16.000	474.12	5.096	1.3684	2.99D-03	10.172	102.73
16.500	472.83	5.059	1.4435	3.42D-03	10.692	107.84
17.000	473.38	5.042	1.5411	4.00D-03	11.395	114.72
17.500	475.46	5.045	1.6382	4.66D-03	12.117	121.76
18.000	478.54	5.065	1.7237	5.27D-03	12.774	128.15
18.500	482.02	5.096	1.7833	5.73D-03	13.257	132.84
19.000	485.32	5.133	1.8125	5.97D-03	13.522	135.46
19.500	487.95	5.169	1.8108	5.95D-03	13.556	135.82
20.000	489.61	5.199	1.7825	5.73D-03	13.383	134.17
20.500	490.15	5.219	1.7334	5.37D-03	13.041	130.83
21.000	489.64	5.227	1.6764	4.94D-03	12.621	126.75
21.500	488.27	5.224	1.6207	4.54D-03	12.197	122.60

22.000	486.36	5.211	1.5724	4.22D-03	11.819	118.88
22.500	484.28	5.191	1.5397	4.01D-03	11.551	116.24
23.000	482.36	5.169	1.5259	3.92D-03	11.423	114.99
23.500	480.88	5.148	1.5302	3.94D-03	11.432	115.07
24.000	480.02	5.131	1.5495	4.07D-03	11.558	116.31
24.500	479.83	5.120	1.5800	4.27D-03	11.773	118.41
25.000	480.25	5.117	1.6153	4.50D-03	12.032	120.95

VITA

Timothy A. Bartrand was born in [redacted] on [redacted]. In June, 1979, he received a diploma from Rogers High School, Wyoming, Michigan and in August, 1979, began studies at the University of Notre Dame, Notre Dame, Indiana. He received a Bachelor of Science degree in Aerospace Engineering from Notre Dame in May, 1983.

In June, 1983, Mr. Bartrand joined the United States Peace Corps and, after an intensive language, technical and cross cultural training, taught secondary school Mathematics and Physics in Bachuo Akagbe, a rural village in the Southwest Province of Cameroon.

After completing his Peace Corps service, Mr. Bartrand began study toward a Master of Science degree in Mechanical Engineering at the University of Tennessee, Knoxville. This degree will be awarded in December, 1987.

The author will work toward a Ph.D. in Mechanical Engineering at Purdue University, beginning in August, 1987.